

56472

LONG RANGE TRANSPORT OF AEROSOLS

**A THESIS SUBMITTED TO
THE GRADUATE SCHOOL OF NATURAL AND APPLIED SCIENCES
OF
THE MIDDLE EAST TECHNICAL UNIVERSITY**

BY

GÜLEN GÜLLÜ

**IN PARTIAL FULFILLMENT OF THE REQUIREMENTS FOR THE DEGREE OF
DOCTOR OF PHILOSOPHY
IN
THE DEPARTMENT OF ENVIRONMENTAL ENGINEERING**


SEPTEMBER 1996

Approval of the Graduate School of Natural and Applied Sciences



Prof. Dr. Tayfur Öztürk
Director

I certify that this thesis satisfies all the requirements as a thesis for the degree of Doctor of Philosophy.



Prof. Dr. Aysel Atımtay
Head of Department


This is to certify that we have read this thesis and that in our opinion it is fully adequate, in scope and quality, as a thesis for the degree of Doctor of Philosophy.



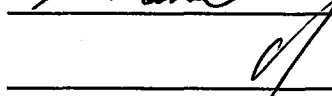
Prof. Dr. Gürdal Tuncel
Supervisor

Examining Committee Members

Prof. Dr. Namık Kemal Aras



Prof. Dr. Gürdal Tuncel



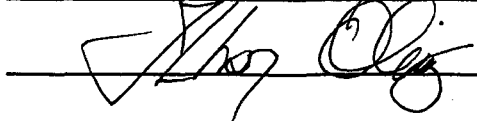
Prof. Dr. Yavuz O. Ataman



Prof. Dr. Cemal Saydam



Assoc. Prof. Dr. İlhan Olmez



ABSTRACT

LONG RANGE TRANSPORT OF AEROSOLS

Güllü, Gülen

Ph.D., Department of Environmental Engineering

Supervisor: Prof. Dr. Gürdal Tuncel

September 1996, 256 pages

Concentrations of elements and ions measured in aerosol samples collected between March 1992 and December 1993 were investigated to understand general features of elemental concentration, sources and source regions affecting chemical composition of aerosols in the eastern Mediterranean atmosphere. Collected samples were analyzed by atomic absorption spectrometry, instrumental neutron activation analysis, ion chromatography and colorimetry for about 40 elements and major ionic species. Back trajectories were calculated and used to determine locations of sources of aerosols. Various statistical methods like factor analysis, factor analysis-absolute factor score method and potential source contribution function were applied on the data to determine the sources, source compositions and source regions of atmospheric particles.

In order to understand air mass transport patterns and to explain observed seasonal variations of the measured concentrations, 4-day back

trajectories ending at the Antalya station were calculated daily for the years 1992, 1993 and 1995. The classification of trajectories indicates that most frequent air mass movements occur from north, northwest, west and northeast sectors.

Concentrations of elements were found to vary greatly in time scales ranging from days to seasons. The local and distant rain event are the determining factors for the observed variations in elemental concentrations.

Calculation of enrichment factors have revealed four general source groups, namely a crustal source, a marine source, an anthropogenic source and an unknown source which has small but observable contribution on the concentrations of some ultra trace elements. Factor analysis identifies two crustal components, one marine component, one local pollution component and one distant pollution component. The most promising marker elements to distinguish Saharan dust from local soil were found to be Cr, Nd, Mg and Cs as they have significantly different compositions in the local soil and Saharan dust.

Potential Source Contribution Function (PSCF) technique show that there are two principal components in the eastern Mediterranean. The main source regions of crustal elements is eastern Turkey and central and eastern parts of the north Africa whereas the anthropogenic components usually originates from the countries surrounding Mediterranean, Balkan countries and former USSR countries lying to the north of the station.

Scavenging ratios of elements in the eastern Mediterranean are higher than corresponding ratios reported in literature due to the non linear temporal variability between deposition fluxes and atmospheric aerosols resulting from low precipitation frequency and different cloud properties. Although there are some variations for some species within the groups, in

general the order of SRs is determined as sea salt elements > crustal elements > anthropogenic elements.

Keywords: Aerosols, Eastern Mediterranean, Ions, Trace Elements, Enrichment Factors, Factor Analysis, Back Trajectory, Potential Source Contribution Function, INAA, AAS, Long Range Transport



ÖZ

AEROSOLLERİN UZUN VADELİ TAŞINIMI

Güllü, Gülen

Doktora, Çevre Mühendisliği Bölümü

Tez Yöneticisi: Prof. Dr. Gürdal Tuncel

Eylül 1996, 256 sayfa

Doğu Akdeniz atmosferinde Mart 1992, Aralık 1993 tarihleri arasında toplanan aerosol örneklerinin elemental ve iyon konsantrasyonları irdelenmiştir. Doğu Akdeniz bölgesindeki aerosollerin kimyasal konsantrasyonlarına etki eden kaynakların ve kaynak bölgelerinin belirlenmesine çalışılmıştır. Toplanan örnekler atomik absorpsiyon spektrometrisi, enstrümental nötron aktivasyon analizi, iyon kromatografisi ve kolorimetri kullanılarak yaklaşık olarak 40 element ve iyonlar için analiz edilmiştir. Elde edilen verilere faktör analizi, korelasyon matrisi ve potansiyel kaynak katkı fonksiyonları gibi birçok değişik istatistiksel metotlar uygulanarak kaynakların, kaynak kompozisyonlarının ve kaynak bölgelerinin bulunmasına çalışılmıştır.

Hava kütlesi taşınım yolunu anlamak ve gözlemlenen mevsimsel değişimleri açıklayabilmek için 1992, 1993 ve 1995 yılları için günlük back trajektoriler hesaplanmıştır. Trajektörilerin gruplanması sonucu, hava

kütlesinin sıklıkla kuzey, kuzeybatı, batı ve kuzeydoğu yönlerinden geldiği bulunmuştur.

Elementlerin konsantrasyonlarının günlük ve mevsimlik zaman aralıklarında önemli ölçüde değişim gösterdiği bulunmuştur. Yörel ve bölgesel yağmur, elemental konsantrasyon değişimlerinde belirleyici faktördür.

Zenginleşme faktörleri dört ana grubu göstermiştir. Bunlar, toprak kaynağı, deniz kaynağı, antropojenik kaynak ve bazı eser elementlerin içinde bulunduğu bilinmeyen bir kaynaktır. Faktör analizi, iki toprak kaynağı, bir deniz kaynağı, bir bölgesel kirlenici kaynağı ve bir uzak kirlilik kaynağı belirlemiştir. İki toprak kaynağının kompozisyonları belirlendiğinde, Sahra çölü tozunun, yerel toprak'dan ayrılması için en belirleyici iz elementlerin Cr, Nd, Mg ve Cs olduğu bulunmuştur.

Potansiyel Kaynak Katkı Fonksiyonu (PKKF) tekniği, Doğu Akdeniz'de iki ana bileşenin olduğunu göstermiştir. Toprak kaynaklı elementler için, doğu Türkiye ve kuzey Africa'nın orta ile doğu kısmı ana kaynak olarak gözükürken antropojenik elementler için Akdenizi çevreleyen ülkelerin, balkan ülkelerinin ve istasyonun kuzeyinde yer alan eski SSCB ülkerinin ana kaynak olduğu belirlenmiştir.

Çökme akıları ve atmosferik aerosollerin zamana bağlı olarak değişimlerinde düşük yağmur miktarı ve değişik bulut özellikleri nedeni ile lineer olmayan bir değişim gözlemlendiğinden, Doğu Akdeniz bölgesinde literatürde ki değerlerden yüksek 'scavenging' oranları bulunmuştur. Gruplar içinde bazı değişimler gözlemlense de, hesaplanan scavenging oranları sırasıyla deniz tuzu elementleri>toprak elementleri>antropojenik elementler olarak bulunmuştur.

Anahtar Kelimeler: Aerosol, Dođu Akdeniz, Iyonlar, Eser Elementler, Zenginleşme Faktörleri, Faktör Analizi, Geri Trajektöri, Potansiyel Kaynak Katkı Fonksiyonu, INAA, AAS, Uzun Mesafeli Taşınım





To Ali and Sera...

ACKNOWLEDGEMENTS

I am deeply grateful to my supervisor Prof. Dr. Gürdal TUNCEL for his guidance, endless encouragement, supervision, suggestions in the every phases of this work.

I wish to express my appreciation to Assoc.Prof.Dr. İlhan Olmez in the Nuclear Reactor Laboratory, Massachusetts Institute of Technology, for his supervision during my a year laboratory work at MIT. I would like also to thank the Environmental Research and Radiochemistry Group of the MIT for their helpfulness and friendship.

Thanks are also due to the TÜBİTAK and International Atomic Energy Agency for my one year stay in Boston, USA.

I extend my sincere thank to Esra Kulođlu and Engin Güven for calculating backtrajectories, Turan Karakaş, Habibe Yiđit, Güven Kaya, Ayfer Esen and Ramazan Demir for performing Atomic Absorption Spectrometry analyses and all my friends in the Environmental Engineering Department.

I would like to express my deepest appreciation to my husband, Ali Sait GÜLLÜ, and my little daughter S. Sera GÜLLÜ for their endless support, understanding and patience during these years. I am grateful to my parents, Nimet-Hilmi Hacısalıhođlu for their endless support and encouragement.

TABLE OF CONTENTS

ABSTRACT	iii
ÖZ	vi
ACKNOWLEDGEMENTS	x
TABLE OF CONTENTS	xi
LIST OF TABLES	xv
LIST OF FIGURES	xvii

CHAPTER

I. INTRODUCTION	1
2. BACKGROUND	6
2.1. Atmospheric Trace Elements, Ionic Species and Their Sources	6
2.1.1. Sources of Trace Elements	8
2.1.2. Sources of Sulfur and Nitrogen Compounds	10
2.2. Long-Range Transport of Trace Elements	12
2.3. Long-Range Transport of Mineral Aerosols	14
2.4. Long-Range Transport of Sulfur and Nitrogen Compounds	16
2.5. Long-Range Transport of Pollutants to the Mediterranean Sea	17
2.6. Receptor Models	20
2.6.1. Factor Analysis	22
2.6.2. FA-AFS Method	24
2.6.3. Theory of PSCF Analysis	27

2.7.	Meteorological Regimes and Transport Processes in the Mediterranean Sea	29
2.7.1.	Back-trajectory Analysis	32
3.	MATERIAL AND METHODS	38
3.1.	Sampling Site Description	38
3.2.	PM-10 High Volume Air Sampler	41
3.3.	Sample Handling	44
3.3.1.	Preparation of Pure Nitric Acid	46
3.4.	Analytical Techniques	47
3.4.1.	Determination of Major Anions by Ion Chromatography	47
3.4.1.1.	Preparation of Samples for Cl ⁻ , NO ₃ ⁻ and SO ₄ ⁼ Analysis	50
3.4.2.	Determination of NH ₄ ⁺ by Colorimetry	50
3.4.2.1.	Preparation of Samples	51
3.4.3.	Trace Element Determination by Atomic Absorption Spectrometry	51
3.4.3.1.	Flame Atomic Absorption (FAAS) and Emission Spectrometry (ES)	51
3.4.3.2.	Graphite Furnace Atomic Absorption Spectrometry (GFAAS)	52
3.4.3.3.	Preparation of Samples for AAS Analysis	53
3.4.3.4.	Analysis of Standard Reference Materials	54
3.4.4.	Instrumental Neutron Activation Analysis	55
3.4.4.1.	Trace Element Determination by Instrumental Neutron Activation Analysis	57
3.4.4.2.	Preparation of Samples	58
3.4.4.3.	“Short” Irradiations and Counting	60
3.4.4.4.	Long Irradiations of Samples	61
3.4.4.5.	Analysis of the Gamma-Ray Spectra	64
3.5.	Data Quality Assurance	66

3.5.1.	Blanks	66
3.5.2.	Detection Limits of the Analytical Methods.....	70
3.5.3.	Error Propagation	72
3.5.4.	Participation to Intercalibration Studies	78
3.5.5.	Comparison of INAA and AAS Techniques	81
4.	RESULTS AND DISCUSSION	82
4.1.	General Characteristics of Data	82
4.1.1.	Distribution Characteristics of the Eastern Mediterranean Aerosols	84
4.1.2.	Comparison with other data	92
4.2.	Analysis of Back Trajectories of the Eastern Mediterranean.....	101
4.2.1.	Comparison of Back Trajectories, Climatologies at Eastern and Western Mediterranean Basins .	108
4.3.	Temporal Variations in Aerosol Composition.....	113
4.3.1.	Regional Background Concentrations of the Eastern Mediterranean Atmosphere.....	114
4.3.2.	Short-term (Daily) Variations of Aerosol Concentrations in the Eastern Mediterranean Atmosphere	116
4.3.3.	Long-term (Seasonal) Variations of Aerosol Concentrations in the Eastern Mediterranean Atmosphere	128
4.3.4.	Factors Affecting Temporal Variations of Aerosols	138
4.3.4.1.	Influence of Local Rain Events	138
4.3.5.	Variations of the Sectorial Elemental Concentrations	150
4.3.5.1.	Dust Storms Observed at the Eastern Mediterranean	162
4.4.	Sources of Pollutants in the Eastern Mediterranean	171

4.4.1.	Correlations between Species	172
4.4.2.	Enrichment Factors	176
4.4.2.1.	Crustal Enrichment Factors	178
4.4.2.2.	Marine Enrichment Factors	187
4.4.3.	Crustal and Marine Contribution of Elements ..	192
4.5.	Source Apportionment and Quantification	197
4.5.1.	Principal Component Factor Analysis (FA)	198
4.5.1.1.	Treatment of Values Below Detection Limit ...	198
4.5.1.2.	Extraction of Factors	200
4.5.2.	The Use of Absolute Factor Score Method (FA-AFS)	204
4.6.	Geographical Locations of Potential Source Regions	212
4.6.1.	Potential Source Contribution Function (PSCF)	213
4.7.	The Temporal Variability of Scavenging Ratios over the Eastern Mediterranean Basin	225
5.	CONCLUSIONS	236
6.	RECOMMENDATIONS FOR FUTURE RESEARCH	241
	REFERENCES	243
	VITA.....	256

LIST OF TABLES

TABLE

2.1	Main anthropogenic emission sources of trace elements in Europe.....	11
2.2.	Worldwide atmospheric trace metal emissions of enriched trace elements.....	12
2.3.	Monthly average temperature and total precipitation amounts observed during the years 1992 and 1993 and long term averages for the Antalya Meteorological Station.....	30
3.1.	Performance Specifications for PM-10 Sampler.....	42
3.2.	Analytical techniques of measured species.....	48
3.3.	Ion chromatographic parameters.....	49
3.4.	Working parameters used in Flame atomic absorption and emission measurements.....	52
3.5.	Working instrumental parameters in GFAAS.....	53
3.6.	Graphite furnace temperature programs.....	55
3.7.	γ -ray energies used in the determination of concentrations.....	59
3.8.	Average Filter Blank Concentrations and Standard Deviations.....	67
3.9.	Calculated detection limits for the elements observed by INAA.....	73
3.10	Calculated detection limits for the elements observed by AAS.....	74
3.11	Elements observed by INAA, frequency of observation and Average Percent Statistical Uncertainty.....	76
3.12.	Elements observed by AAS, frequency of observation and Average Percent Statistical Uncertainty.....	77
4.1.	Summary of Eastern Mediterranean Aerosol Data: Arithmetic and geometric means and standard deviations, median and mode values.....	86

4.2	Skewness, Kolmogorov-Smirnov statistic (K-S DN) for fitted variables.....	89
4.3.	Concentrations of trace elements and major ions in aerosols over various regions.....	97
4.4.	The Calculated Regional Background Concentrations of Trace Elements in the Eastern Mediterranean Atmosphere.....	117
4.5.	Seasonal Elemental Concentrations	137
4.6.	Contribution of rain events on the summer, winter annual average concentrations of anthropogenic elements.....	149
4.7.	Average Contributions of Elements from Different Sectors.....	151
4.8.	Concentrations of elements in Saharan dust and non-Saharan Dust data subsets.....	168
4.9.	Element to Al ratios in Saharan and non-Saharan dust data subsets.....	170
4.10	Correlation Coefficients among the measured species.....	173
4.11	Seasonal mean crustal enrichment factors (EF _c) and winter to summer EF _c ratios.....	186
4.12	Crustal and marine contribution on the observed concentrations.....	196
4.13	Varimax rotated factor loading and corresponding probable source type.....	201
4.14	Varimax rotated factor analysis for crustal elements only.....	206
4.15	Mean source contributions.....	208
4.16	Mean source contributions of Local soil and Saharan Dust	211
4.17	Summary of annual average aerosol concentrations and precipitation composition and scavenging ratios.....	227

LIST OF FIGURES

FIGURES

2.1	Idealized mass size distribution of suspended particles.....	8
2.2	Synoptic weather pattern type A.....	33
2.3	Synoptic weather pattern type B.....	33
2.4	Synoptic weather pattern type C.....	34
2.5	Synoptic weather pattern type D.....	34
2.6	Synoptic weather pattern type E.....	35
3.1	The location of the sampling station and topography of the region.....	40
3.2	A picture of the sampling platform.....	41
3.3	The cross-sectional view of PM-10 Size Selective High Volume Air Sampler	43
3.4	A typical γ -ray spectra for Short-1 counts.....	62
3.5	A typical γ -ray spectra for Short-2 counts	63
3.6	A typical γ -ray spectra for Long Irradiations	65
3.7	Plot of percent blank subtraction and percent of observance of samples analysed by INAA.....	68
3.8	Plot of percent blank subtraction and percent of observance of samples analysed by AAS	69
3.9	Percent of laboratory blank to field blank for AAS Analyses.....	71
3.10	Calculated average percent statistical uncertainty and average frequency of observance of the elements measured by INAA.....	75
3.11	Atmospheric concentrations of coarse fraction Al and V measured by different laboratories.....	79
3.12	Atmospheric concentrations of coarse fraction As and Fe measured by different laboratories.....	80
3.13	Comparison of INAA and AAS results for the elements measured with both methods.....	81

4.1	The frequency histograms and associated distribution curves for V and Ti.....	93
4.2	The frequency histograms and associated distribution curves for Cu and Ni.....	94
4.3	Locations of the particulate aerosol samples.....	99
4.4	Average concentrations of some trace elements in the Mediterranean Sea coastal locations.....	100
4.5	The sectoring technique to classify trajectories.....	102
4.6	The seasonal flow patterns at Antalya station.....	104
4.7	Annual frequencies of air mass transport from wind sectors.....	105
4.8	Monthly variation of percent contribution of major wind sectors.....	107
4.9	The mean frequency of air mass transport at different sites in the Mediterranean.....	109
4.10	Annual frequencies of air mass transport from wind sectors at Corsica, Amasra and Antalya.....	111
4.11	Seasonal frequencies of air mass transport from wind sectors at Corsica, Amasra and Antalya.....	112
4.12	Histogram for calculation of most frequently occurring value.....	115
4.13	Temporal variations of Na.....	119
4.14	Temporal variations of Cl.....	119
4.15	Temporal variations of Al.....	120
4.16	Temporal variations of Fe.....	120
4.17	Temporal variations of Zn.....	121
4.18	Temporal variations of nss-SO ₄	121
4.19	Temporal variations of Pb.....	122
4.20	Temporal variations of As.....	122
4.21	Examples of back trajectories corresponding to high Al and high SO ₄ concentration days.....	126
4.22	Monthly variation of Al and Sc.....	131
4.23	Monthly variation of Fe and La.....	132
4.24	Monthly variation of Cr and Ni.....	133
4.25	Monthly variation of nss-SO ₄ and Se.....	134

4.26	Monthly variation of Na and Cl.....	135
4.27	Monthly variation of As and Mo.....	136
4.28	The ratio of elemental concentrations in non-raining days-to- average concentrations in raining days.....	140
4.29	The ratio of elemental concentrations measured at the raining day to those measured two days before the rain event.....	141
4.30	Variation of Al concentration as a function of number of non-raining days.....	143
4.31	Variation of Sb concentration as a function of number of non-raining days.....	143
4.32	Average concentration of elements measured between 3 days before and 10 days after rain event.....	144
4.33	Representative trajectories for each sector.....	154
4.34	Average contribution of Na and Cl from different sectors.....	157
4.35	Average contribution of Al, Sc, Co and Dy from different sectors ...	157
4.36	Average contribution of Cr, Ni, Pb, nss-SO ₄ , As and Mo from different sectors.....	159
4.37	Bulk data of Al concentration together with Saharan dust episodes indicated with shaded regions.....	164
4.38	Back trajectories of 28-29 March 1992.....	165
4.39	A sequence of METEOSAT vis images from 25 to 31 March 1992 .	167
4.40	Crustal enrichment factors.....	179
4.41	EF diagrams of Sc and La.....	181
4.42	EF diagrams of K, Mn, V and Ti.....	184
4.43	EF diagrams of Fe, Tb, Ce and Dy.....	185
4.44	Marine enrichment factors.....	189
4.45	The Cl/Na-ncr ratio.....	190
4.46	Relation between Cl/Na-ncr and nss-SO ₄	191
4.47	The Br/Na-ncr ratio.....	192
4.48	Temporal variation of % crustal Na and Al concentrations.....	194
4.49	Temporal variation of % ss-SO ₄ and Na concentrations.....	194
4.50	Time series plot of Factor Scores.....	203

4.51	Factor score plot of Factor 2 and back trajectories corresponding to peak days.....	205
4.52	X-to-Al ratios in local soil and Saharan dust.....	212
4.53	Crustal Enrichment Factors of local soil and Saharan dust compositions.....	213
4.54	The subregions used in the source apportionment of aerosol data.	215
4.55	The Potential Source Contribution Function of Al, Fe, Nd and Ca..	218
4.56	The Potential Source Contribution Function of As, Se, Sb and Pb..	220
4.57	The Potential Source Contribution Function of NO ₃ and nss-SO ₄ ..	222
4.58	Examples of backtrajectories corresponding to high As concentration days.....	223
4.59	The monthly SRs for Al, Ca and Fe and the arithmetic mean of aerosol composition and volume weighted mean precipitation composition at Antalya station.....	231
4.60	The monthly SRs for Na, Cl and Mg and the arithmetic mean of aerosol composition and volume weighted mean precipitation composition at Antalya station.....	232
4.61	The monthly SRs for Pb, Sb and Zn and the arithmetic mean of aerosol composition and volume weighted mean precipitation composition at Antalya station.....	233
4.62	The monthly SRs for nss-SO ₄ , NO ₃ and NH ₄ and the arithmetic mean of aerosol composition and volume weighted mean precipitation composition at Antalya station.....	234

CHAPTER 1

INTRODUCTION

Major issues concerning environmental protection today carry global dimensions. Many countries around the world are concerned for the increasing atmospheric levels of greenhouse gases that threaten to change the climate, chemicals that reduce the ozone layer and pollutants that cause acid rain. Pollutants often travel long distances crossing national borders through the atmosphere to cause damage on land and water. The magnitude of damage is severe especially for the semi-closed seas such as the Mediterranean and the Black Sea.

There is an enormous pressure on the Mediterranean environment as a result of intensive industrial development, rising population at coastal locations, and a continual increase in wastes of all kinds. In 1975, UNEP convened a conference in Barcelona at which a historic Mediterranean Action Plan (MAP) was adopted by 16 Mediterranean States and the EEC in order to address their common problem -a troubled sea on which they all depend. The MAP has three components, namely:

- * Management component, which involves, integrated planning of the development and management of the resources of the Mediterranean Basin
- * Assessment component which includes coordinated program for research, monitoring and exchange of information and assessment of the state of pollution and of protection measures,

- * Legal component which includes, framework convention and related protocols with their technical annexes for the protection of the Mediterranean environment.

The complexity of physical and chemical atmospheric processes, combined with the enormity of the global atmosphere, make results from comprehensive trace species measurement programs difficult to interpret without a clear conceptual model of the workings of the atmosphere. Measurements alone cannot be used directly by policy makers to form balanced and cost-effective strategies for dealing with these problems: an understanding of individual processes within the atmosphere does not automatically imply an understanding of the system as a whole. On the other hand, a model developed without continual comparison against actual data is nothing more than a collection of mathematical formulae. Solution of the complex environmental problems can be possible only with the close integration of models and experimental measurements. With the realization of this fact, monitoring programs like MED POL in order to collect actual data all over the world has been initiated and encouraged.

In May 1988, despite a limited data base existing for the region, with the realization of importance of atmospheric pollution transport on marine ecosystems especially for the semi-closed seas, airborne pollution studies were initiated within the framework of national MED POL monitoring program with the coordination of World Meteorological Organization (WMO). Within the MED-POL national monitoring program, an airborne pollution study was initiated in 1992 at south of Turkey. In this study, results obtained from daily aerosol collections between March 1992 and December 1993 at a Mediterranean coastal site were studied extensively. Collected samples were analyzed for a range of inorganic species including major ions and approximately 40 trace elements. The results of these analyses were discussed in terms of the atmospheric processes controlling the aerosol concentrations and source regions affecting concentrations of these species in the eastern Mediterranean

basin. The data set generated in this work is the most extensive one. In general data are extremely limited in the eastern Mediterranean basin. Although there had been few works in which inorganic species were measured, they are limited either in temporal coverage or in the parameters included in the measurements. The data generated in this work includes the largest set of parameters in the whole Mediterranean basin which is invaluable to identify types and locations of sources affecting the eastern Mediterranean basin. The importance of our data lie not only in the improved data base of concentrations of a number of components in aerosols also, more importantly it allows for the first time a clear evaluation of the meteorological control of the aerosol composition regime to be considered in the eastern part of the basin.

The main objectives of the work are summarized below:

- * To determine atmospheric concentrations of major ions and trace elements in aerosols. Most of the aerosol studies at Mediterranean region were concentrated on Western of the basin (e.g. Buat-Menard and Arnold, 1978; Arnold et al., 1982; Dulac et al., 1987) Except few studies performed on eastern part of the basin (Chester et al., 1984; Kubilay, 1996) there are no data available for the eastern part of the Mediterranean basin. Due to the expected spatial variability of atmospheric concentrations and fluxes of contaminants, results of a monitoring program which run continuously for several years will be very beneficial to predict atmospheric contaminant inputs and to identify the sources and source regions for atmospheric contaminants.

- * To determine background concentrations at the Eastern Mediterranean region. In source apportionment studies, difficulty is encountered due to the uncertainties in the assessment of background concentrations of chemical species at a specific receptor site.

- * To understand long-range transport patterns of pollutants to the Eastern Mediterranean region. Measured concentrations of about 40 trace elements and ions such as SO_4^{2-} , NO_3^- , NH_4^+ in each daily sample for a two year period enabled us to apply multivariate statistical techniques to determine source types and regions of pollutants.
- * To characterize the Saharan dust component of the Mediterranean aerosols. The Saharan dust flux to the Eastern Mediterranean region is not well known. One of the purposes of the study was to obtain a chemical signature for the Saharan dust component.
- * Calculation of Scavenging Ratios (SR) for the eastern Mediterranean Basin. SR's have been frequently used to estimate wet deposition fluxes on marine locations when actual wet deposition data are absent (e.g. Duce et al., 1983; 1991). Since average SR may vary significantly from one geographical region to another, it is very crucial to determine the SRs calculated from a multi-year data set on aerosol and precipitation composition to explore the temporal variability of SRs over the eastern Mediterranean. As the first time, the simultaneous measurements of aerosol and precipitation for almost 2-year period will enable us to determine the SRs at the eastern Mediterranean.

In the following chapter of this thesis one can find a survey of existing works relevant to the global atmosphere, and specifically to the Mediterranean region after a brief review of sources of trace elements in the atmosphere. This chapter also reviews the receptor modeling techniques that are commonly used for source apportionment purposes and climatology and meteorology of the Mediterranean basin.

Sampling techniques, instrumentation and used analytical techniques were discussed in the third chapter of the study. Within this study, a total of 600

daily aerosol samples were analyzed with a combination of Instrumental Neutron Activation Analysis (INAA), Atomic Absorption Spectrometry (AAS) and Ion Chromatography (IC) techniques. The results of data quality assurance, blank values, detection limits of the analytical methods used are also given in the third chapter.

The results obtained are extensively discussed in the fourth chapter. A discussion on the source regions and signatures of pollutants which were determined through application of various receptor modeling techniques are also presented in chapter four.

In the fifth chapter of the study, concluding remarks, some suggestions for further research on this subject were given.



CHAPTER 2

BACKGROUND

2.1. Atmospheric Trace Elements, Ionic Species and Their Sources

Aerosols in the atmosphere originate from both natural and anthropogenic sources. Global aerosol production estimates suggest that since they interact with solar radiation and affect micro-meteorological processes, aerosols may affect radiative transfer and affect Earth's energy balance and hence the climate (Cunningham and Zoller, 1981; Charlson et al., 1992). Therefore accurate data on the quantity and characteristics of pollutants at source and receptor sites are required in order to assess perturbations in the biogeochemical cycles of trace elements.

The particulate material in the atmosphere contains 80-90% of inorganic material. The remainder consist of organic compounds and biological debris (Cawse, 1987). Aerosols and associated elements are emitted from their sources and transported in the zonal circulation before deposition to land and water surfaces. Major and minor elemental composition of particles are used as a tracer to determine sources of particles in ambient aerosols (Hopke et al., 1976; Thurston and Spengler, 1985). Tracers from particular source regions have been used to document the dispersal caused by atmospheric transport (Ondov and Kelly, 1991). Trace elements whose sources are well documented would be the ideal tracers.

The primary sources of particulate material in the atmosphere are the resuspension of soil by wind, sea-spray, high temperature combustion processes, forest fires, decomposition of plants and animals and volcanic activity. In addition, transformation of gaseous species such as volatile metals, SO₂ and nitrogen oxides to particulate forms by photochemical and gas phase reactions also contributes to the atmospheric burden of aerosols .

Figure 2.1 shows an idealized mass distribution of particle sizes found in the atmosphere. The "nucleation" range consists of particles with diameters less than ~0.08 μm that are emitted directly from combustion sources or secondary aerosols formed from gaseous species. In polluted areas, the lifetimes of particles in the nucleation range are usually less than one hour, because they rapidly coagulate with larger particles or serve as nuclei for cloud or fog droplets (Watson and Chow, 1994). Particles in this size range are detected only when emission sources are close to the measurement site. The "accumulation" range consists of particles with diameters between 0.08 and ~2 μm. These particles result from the coagulation of smaller particles emitted from combustion sources, from condensation of volatile species, and from finely ground dust particles. The nucleation and accumulation ranges comprise the fine particle, or "PM_{2.5}" size fraction (Watson and Chow, 1994). Particles larger than 2.5 μm are called coarse particles. Coarse particles result from grinding activities and are dominated by material of geological origin (Watson and Chow, 1994). Pollen and spores, ground-up trash and leaves are also included in the coarse fraction. An upper limit of 10 μm is often attached to the coarse range to correspond to the US health standard for suspended particles. The mass concentration of all particles with diameter less than 10 μm is often termed the "PM₁₀" size fraction. The coarse size fraction is practically limited by gravitational settling, since most particles larger than ~30 μm fall out of the atmosphere very close to the point at which they were emitted (Watson and Chow, 1994).

The Figure 2.1 shows the accumulation range which consists of at least two modes. Recent measurements of size distributions show this detail in

several different urban areas (Wall et al., 1988; Bassett and Seinfeld, 1983). The peak centered at $\sim 0.2 \mu\text{m}$ is interpreted as "condensation" mode including gas-phase reaction products, and the $\sim 0.7 \mu\text{m}$ peak is interpreted as a "droplet" mode that results from reactions taking place in water droplets (Watson and Chow, 1994).

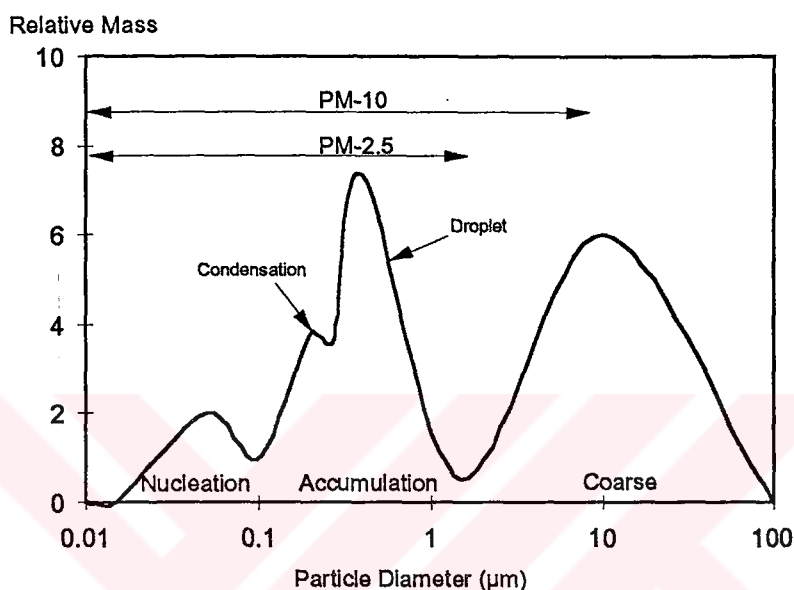


Figure 2.1. Idealized mass size distribution of suspended particles (Watson and Chow, 1994)

2.1.1. Sources of Trace Elements

Trace elements are introduced into the atmosphere from both natural and anthropogenic sources. Wind-blown resuspension of crustal material, bubble bursting over the ocean, forest fires, volcanic activity and biogenic emissions are the most common natural sources of particles in the atmosphere. Among these, wind-blown crustal dust is particularly important. Arid and semiarid areas are major continuous sources of the crustal material. Volcanoes seem to be dominant natural source of chalcophilic elements at remote locations (Cunningham and Zoller, 1981). Buat-Menard and Arnold (1978) estimated that

about 10 t yr^{-1} Cd was discharged into the atmosphere from Mount Etna. However, there is no recent volcanic activity in the Mediterranean Sea. Among the natural sources, biogenic processes are considered as a principal contributor of the trace metals into the atmosphere. Volatile and particulate material of biogenic origin account 30-50% of the As, Cd, Cu, Mn, Pb, Sb and Zn and for over 50% of the Se and Mo emitted annually from natural sources (Nriagu, 1989). High biogenic outputs have been recognized in recently published models of the global atmospheric cycles of selenium (Ross, 1985; Mosher and Duce, 1988), arsenic (Chivers and Peterson, 1987) and mercury (Fitzgerald, 1986).

Anthropogenic sources of trace elements are the combustion of fossil fuels, roasting of ores for refining metals, processing of crustal material for manufacturing cement, and burning of wastes. Combustion of fossil fuels to produce electricity and heat is the main source for anthropogenic emissions of Be, Co, Hg, Mo, Ni, Sb, Se, Sn, and V (Nriagu and Pacyna, 1988). Combustion processes are also important sources of atmospheric As, Cr, Cu, Mn, and Zn (Pacyna et al., 1984). Large amounts of As, Cd, Cu, In, and Zn also come from the pyrometallurgical processes in the production of lead, copper and zinc. Contribution of various sources in the total anthropogenic emission of trace elements in Europe is presented in Table 2.1. Coal combustion is the main source of Be, Co, Mo, Sb, and in the atmosphere, while Ni, and V are released mainly from oil combustion. Smelters and secondary non-ferrous metal plants are the most important sources of As, Cd, Cu and Zn. Iron and steel and ferro-alloy industries accounts for approximately 80% of total Cr and Mn emissions in Europe.

Global atmospheric emissions (10^6 kg/yr) of selected chalcophilic elements are given in Table 2.2. For all of the elements listed in the table anthropogenic emissions exceeds natural emissions by a large margin.

2.1.2. Sources of Sulfur and Nitrogen Compounds

The main man-made sulfur sources include combustion of coal and oil in stationary combustion sources like power plants, boilers, ore processing, roasting and heating of non-metallic minerals, sulfuric acid plants, fertilizer manufacturing, plastics, paints and varnish manufacturing, oxidation towers and motor vehicle emissions. Natural sources of sulfur include sea-spray, eolian weathering of soils, volcanoes, biomass burning, and biogenic emissions from soils, plants, wetlands and the ocean. Few reliable estimates of natural emission exist worldwide and these estimates vary widely. Often natural emissions have been derived to balance either regional or global budgets. According to the Katsoulis and Whelpdale's (1990) work, natural emissions of sulfur is between 10 and 30% of anthropogenic emissions.

There are four basic natural processes by which nitrogen oxides and ammonia enter the atmosphere these include transformations of nitrogen during nitrification and denitrification, volatilization of ammonia, combustion of fossil fuels and lightning (Katsoulis and Whelpdale, 1990). Anthropogenic sources of nitrogen oxides and ammonia on the other hand include combustion of fossil fuels, transportation, nitric acid production, fertilizer production and domestic animals.

In the atmosphere, nitrogen oxides undergo a complex series of reactions. Although products of these reactions can be transported over long distances only the ones that are stable can be measured at distant receptor sites. The stable nitrogen species that survive long-range transport include HNO_3 , NH_4^+ , and NO_3^- . Due to complex surface exchange processes of nitrogen species which are highly dependent on cover at a given location, extrapolation to a large region by using past few measurements are quite uncertain. However, the evidence is that the contribution of NO_x to environmental acidification is significant and growing. The role of nitrogen species on the

Table 2.1. Main anthropogenic emission sources of trace elements in Europe (Pacyna et al., 1984).

Metal	Main sources (% contribution to the total emission)
As	Cu-Ni smelters (68), Zn-Cd smelters (14), combustion of fuels (10)
Be	coal combustion (100)
Cd	Zn-Cd smelters (60), Cu-Ni smelters (23), combustion of fuels (10), refuse incinerators (3)
Co	combustion of fuels (100)
Cr	iron, steel and ferro-alloy making (80), combustion of fuels (15)
Cu	Cu-Ni smelters (50), combustion of fuels (22), iron, steel and ferro-alloy making (11), wood combustion (11)
Mn	iron, steel and ferro-alloy making (84), coal combustion (11)
Mo	combustion of fuels (100)
Ni	oil combustion (60), coal combustion (17), mining and refining (10)
Pb	gasoline combustion (60), non-ferrous metal production (22), iron, steel and ferro-alloy making (12)
Sb	coal combustion (74), refuse incinerators (25)
Se	combustion of fuels (100)
V	oil combustion (100)
Zn	zinc-cadmium smelters (60), iron, steel and alloy manufacturing (13), refuse incinerators (17), wood combustion (6)

Table 2.2. Worldwide atmospheric trace metal emissions (10^6 kg/yr) of enriched trace elements (Bewers et al., 1988; Pacyna, 1986).

Element	Sources	
	Natural	Anthropogenic
As	7.8	24
Cd	0.96	7.3
Cu	19	56
Ni	26	47
Pb	19	449
Se	0.4	1.1
Zn	4	314

acidification of the environment have increased particularly after regional protocols to reduce SO_x emissions became affective.

2.2. Long-Range Transport of Trace Elements

It is well established that, particles bearing trace elements emitted by natural and anthropogenic activities of travel beyond regional boundaries and contribute to atmospheric particle loading on a global scale. To estimate the significance of such transport, background concentrations and the amount of material transported as well as the residence times of the particles in atmosphere must be known. It is believed that submicrometer aerosols (particles with diameters ranging between $0.01 - 0.1 \mu\text{m}$) from various sources escape to the free troposphere and form a globally uniform aerosol mass which is called "global background aerosol". The concept of background aerosol was first introduced by Junge (1963), then found widespread acceptance. Understanding composition and components of background aerosol is important to understand the role of aerosols on long-term climatic changes. Studies of

aerosol composition and sources in pristine sites have started in late 1960's in an attempt to understand background particles. Such studies gained momentum in early 1970's with the development of contamination free sampling systems and sensitive analytical techniques. To study background aerosols, sampling stations were established on locations which are not affected from anthropogenic sources such as mountaintops (Dams and De Jonge, 1979; Adams et al., 1977; 1980; 1983), and remote islands (Duce et al., 1983; Arimato et al., 1987). However, although mountain top stations were build above timberline and at altitudes where surface is under permanent snow cover, the influence of local soil and anthropogenic particles are clearly visible in the generated data sets (Ram et al., 1983). Similarly, island-based stations are always under the influence of marine aerosols (Duce et al., 1983).

Polar regions in both Northern and Southern hemispheres appear to be ideal locations for remote aerosol studies. However, the Arctic region is shown to be under the influence of pollution-derived aerosols originated mainly from Eurasia, especially during spring and winter seasons (Rahn and McCaffrey, 1979; Heidam, 1985; Barrie, 1989; Heintzenberg et al., 1991). The Antarctic, on the other hand, is free from such transport of anthropogenic emissions and hence offers the best location on earth to study the composition of background aerosol (Robinson et al., 1988; Sterns and Wendler, 1988).

There are number of studies to determine trace element composition of Antarctic aerosols (Duce et al., 1973; Zoller et al. 1974; Maenhout et al., 1979; Cunningham and Zoller, 1981; Tuncel et al., 1989; Radlein and Heumann, 1992). These studies showed that, crustal dust, sea salt, sulfate particles, meteoritic particles, volcanic particles and biogenic emissions are the main components of Antarctic aerosol. In Antarctic snow, Boutron and Lorius (1979) found enrichments of heavy metals as high in 1914 as the ones observed in 1974, which indicated that in the Southern Hemisphere background aerosols are not significantly influenced by anthropogenic emissions, but are linked with natural phenomena.

The use of trace elements as tracers of long-range transport of air pollutants have been demonstrated (Rahn and Lowenthal, 1984; Pacyna et al., 1984; Olmez and Gordon, 1985).

Studies where trace element tracers were used at several locations on the Pacific Ocean provide most dramatic evidence supporting the long-range atmospheric transport of natural and anthropogenic trace elements to the remote areas of the world's oceans. The long-range transport of natural and anthropogenic trace elements from Asia to the mid-Pacific was first documented during experiments at Enewetak Atoll as part of SEAREX program (Arimoto et al., 1985; Duce et al., 1980; 1983) and at the Mauna Loa Observatory in Hawaii (Parrington et al., 1983; Shaw, 1980). These studies indicated that, even though the atmospheric loading of aerosols and gases are lower over the Pacific compared to continental regions, pollution derived and mineral aerosols are transported deep into the Pacific Ocean from Asia.

2.3. Long-Range Transport of Mineral Aerosols

Mineral dust is one of the oldest and longest studied example of long-range transport. Beginning 200 years ago, descriptions of dust events have appeared with increasing frequency in the scientific literature. In 1833, Darwin, in Cape Verde Island, experienced a Saharan dust outbreak. Due to the extent and severity of the event, he speculated that this mechanism of transport might be significant source of material in ocean sediments which is shown to be correct 150 years later (Darwin, 1846).

Wind-induced mobilization of eolian material is the main natural aerosol production mechanism (e.g. Prospero et al., 1983). Geochemical studies of deep sea sediments suggest that soil material transported from arid regions by wind is responsible for distribution of certain clay minerals in oceanic sediments (Chester et al., 1979, Prospero, 1981).

Extensive documentation of spatial and temporal variability of Saharan mineral aerosol over the tropical North Atlantic, Western and Eastern Mediterranean has been obtained in last 20 years (Prospero and Carlson, 1970; Chester et al., 1977; Chester et al., 1979; Savoie and Prospero, 1977, 1980). Similar transport of eolian dust from Asian deserts to the Pacific have also been reported (Parrington et al., 1983; Duce et al., 1993). These studies have demonstrated that, the arid regions of Africa and Asia is an important source of mineral aerosol on the global atmosphere (Duce et al., 1980; Uematsu et al., 1983; Parrington et al., 1983; Duce et al., 1993).

Mineral aerosols are important because they reduce visibility (Joseph and Manes, 1971); they affect cloud physics and chemistry, local meteorological conditions and scavenges gases such as, $\text{SO}_2 + \text{NO}_2$. But the most important function of aerosols on a global scale is their potential role in the modification of global climate. The 90% of aerosols on the global scale consist of SO_4^{2-} and sea salt particles. Since these species are transparent to IR radiation, they were not considered as greenhouse species. But if the concentration of opaque particles produced by anthropogenic sources increased on a global scale, particles increases the short-wave radiative scattering which causes cooling (Ackerman and Chung, 1992). On the other hand, the presence of dust decreases the observed long-range radiation more vigorously on desert areas. This effect of dust on radiation led us to consider the link between dust and climate. Although the ultimate radiative effects of dust are uncertain, there is sufficient evidence to suggest that the effects of mineral dust must be considered when modeling the radiation balance. These effects should be estimated for the lower latitudes, which are the major areas of intense dust production and transport. These regions are also the location of the major energy exchanges of the earth's climate system (Schutz et al., 1990).

There are several studies to obtain geological and chemical composition of Saharan origin desert aerosols in various regions (Ganor et al., 1991; Tschiersch, et al., 1990; Lavi et al., 1992; Coude-Gaussen et al., 1987; Talbot et al., 1986). The studies on Saharan dust have mostly concerned from the Sahelian belt to either the Gulf of Guinea (Bertrand et al., 1974; Domergue, 1980) or the Caribbean Sea (Carlson and Prospero, 1972; Glaccum and Prospero, 1980; Morales, 1979).

The overall amount of mineral aerosol (dust) reaching the Mediterranean basin is large compared to the atmospheric impact on other oceans and since the desert dust intrusions to the basin occur in the form of pulses, these can impose intermittent, non-steady state conditions on the mixed layer in the Mediterranean (Chester, 1986; Chester et al., 1989; Quetel, 1993). The assessment of such an influence demands quantitative knowledge of the atmospheric concentrations and fluxes of the particles over the marine environment.

Knowledge of the dust concentration over the eastern Mediterranean has been limited by ship time (Chester et al., 1977; 1981; 1984) though long term assessments of dust deposition have been provided by the Israeli scientists. According to these measurements, about 25 million tons of desert dust annually reach the eastern Mediterranean (Yaalon and Ganor, 1989; Ganor and Mamane, 1982). This addition contributes to the characteristics of the typical Mediterranean soil (Yaalon and Ganor, 1973).

2.4. Long-Range Transport of Sulfur and Nitrogen Compounds

Although the residence time of nitrogen oxides in the atmosphere is less than the residence time of the sulfur oxides, the oxides of nitrogen and of sulfur on the atmosphere could undergo similar degrees of dispersion when transported over great distances (Galloway, 1993). Because of the diffuse

nature of sulfur and nitrogen emissions, the long-range transport of S and NO_x is most likely from highly populated areas at North America, Europe, or Asia.

Andrea et al., (1988) have studied the possibility of material being transported from Asia to North America by examining the composition of the atmospheric aerosol and gases over the western North Pacific Ocean. They have concluded that dimethylsulfide (DMS) concentration over the Pacific ocean is controlled by marine rather than continental processes. The vertical profiles of SO₂ and nss-SO₄²⁻ from the work of Andrea et al. (1988) suggest that, significant amounts of SO₂ and nss-SO₄²⁻ are produced by the oxidation of DMS within the boundary layer. These authors also concluded that the concentrations of NO₃⁻ are influenced by the long-range transport of pollutant nitrogen, presumably from Asia.

2.5. Long-Range Transport of Pollutants to the Mediterranean Sea

Over the last decade significant progress has been made in understanding the atmospheric transport and removal processes of natural and anthropogenic pollutants over the western Mediterranean region (e.g. Arnold et al., 1982; Chester et al., 1984; Dulac et al., 1987). The impact of atmospheric transport and fluxes of pollutants are important particularly in semi enclosed seas such as the Mediterranean Sea which is under the antagonistic influence of the industrialized North European belt and of the Saharan belt at the south.

In late 70's and 80's, considerable amount of work has been carried out in the Mediterranean atmosphere to define the chemical character of aerosols (Ganor and Mamane, 1982; Chester et al., 1977; 1981; Migon and Caccia, 1990; Tomadin et al., 1984; Bergametti et al., 1989; Simo et al., 1991; Ganor, 1991) rainwater (Loye-Pilot and Morelli, 1988; Glavas, 1988; Migon et al., 1993; Loye-Pilot et al., 1986) and to estimate the atmospheric inputs of particulate and dissolved phases into the Mediterranean Sea (e.g. Dulac et al., 1987; Remoudaki et al., 1991; Migon et al., 1989; 1991; Loye-Pilot et al., 1991; Migon

and Caccia, 1993; Al-Momani et al., 1995). Major conclusion of these studies is that a substantial fraction of the contamination entering the Mediterranean Sea originate from sources located on surrounding land and transported to the region through the atmosphere. Deposition of elements and ions from atmosphere to the Mediterranean sea can play an important role in the geochemistry of these species (see e.g. Boyle et al., 1985; GESAMP, 1985; Martin et al., 1989).

Although, the region is well studied, particularly in last 20 years, most of the studies were performed on western part of the basin. Although there are some short term studies on eastern basin (Chester et al., 1984), data are not yet available for long term aerosol collections over the eastern Mediterranean.

Since the eleventh session of GESAMP, at the request of UNEP, the Working Group on the Interchange of Pollutants Between the Atmosphere and the Oceans (INTERPOLL) focused on the description of transport processes towards and into the Mediterranean region. Since, deposition of the transuranic elements derived from atmospheric weapons tests over the Pacific was detectable over the Mediterranean, it was concluded that; long range atmospheric transport of contaminants is likely to the Mediterranean basin (GESAMP, 1985). Based on trajectory climatology, the group concluded that: (1) long-range contaminant flow from the north to the western Mediterranean takes place at least 30% of the time, with no detectable seasonal variation, (2) transport to the eastern Mediterranean is mainly from the north and north-west, where industrial sources could contribute to contamination loadings, (3) flow patterns vary significantly from year to year.

In GESAMP's (1985) report, it has been shown that the concentrations and deposition of certain atmospheric contaminants like Pb and Cd, over the Mediterranean were comparable to those over the Baltic and the North Seas. For Pb, Zn, Cu and Hg, atmospheric input to the Mediterranean sea was shown to be in the same order of magnitude as the input from rivers.

The variability of atmospheric trace metal concentrations in the Western Mediterranean aerosol was studied by Dulac et al., (1987). The Al, Br, Cd, Na, Pb and ^{210}Po concentrations from bulk filters and cascade impactor samples collected during 5 cruises between 1980 and 1983 have been used to characterize possible aerosol sources. Soil mobilization, anthropogenic emissions, and volcanism were suggested to be the main sources of aerosols over the western Mediterranean. By using three-dimensional air mass trajectory analysis, Authors have shown that the short-term (daily) variability of atmospheric concentrations of elements reflects both changes in continental source strengths and airflow patterns. Authors also showed that, although southwestern Europe was responsible for the largest Pb and Cd inputs (30-40%), due to prevailing westerly flow, inputs from North Africa were also significant (20-25%). Dulac et al. (1987) concluded that a continuous sampling strategy is needed due to strong seasonal changes in pollution source strengths and intense but sporadic soil dust transport.

Seasonal variability of the elemental composition of atmospheric aerosol particles over the northwestern Mediterranean has been studied by Bergametti et al. (1989). The results of a continuous monitoring study on a Corsican coastal site showed that seasonal changes in the chemical composition of aerosols is due to the variations in local precipitation rate rather than changes of airflow patterns or source strengths. A 10 year climatological study of airflow's (1975-1984) in the northwestern Mediterranean region by Miller et al. (1987) indicating little or no seasonal variations of the frequency of airflow patterns at the 850 hPa barometric level also support the conclusion.

Recently, a review paper has been published by Chester et al., (1993) to define the chemical character of aerosols from the atmosphere of the Mediterranean Sea and surrounding regions. Chester et al., (1993) combined a number of data sets given in the literature related with the Mediterranean atmosphere and environs and tried to characterize the Mediterranean aerosol.

They found that aerosol composition over the Mediterranean Sea is a mixture of urban and crustal components. Due to lack of available long term data for the eastern Mediterranean, Red Sea and Arabian aerosol data were used to define chemical character. They conclude that with the available aerosol data, the Eastern Mediterranean aerosols are mainly perturbed by crustal material from the surrounding desert regions. They also concluded that, this conclusion must be verified using long-term aerosol results. The results of this thesis will verify the reached conclusion for the eastern Mediterranean basin.

2.6. Receptor Models

Receptor oriented models have been employed to identify possible sources of pollution, to resolve the elemental composition of the sources and to determine the contribution of each source to the total pollution level (Cooper and Watson, 1980; Hopke, 1985). In air pollution studies, among all multivariate statistical approaches, Principal Component Analysis (PCA) (Thurston and Spengler, 1985) Factor Analysis (FA) (Hopke, 1985), Chemical Mass Balance (CMB) (Friedlander, 1973; Gordon, 1980) have been most commonly applied to arrays of pollution variables, to aerosol elemental composition data, or to spatial pollution distributions in order to derive information about pollution sources influencing the data.

The first environmental receptor modeling application of classical factor analysis was done by Blifford and Meeker (1967). They applied rotated FA to both particle elemental composition and mass data from 30 US cities, thereby identifying independent components of particle variance as due to specific source classes. The factor analysis was then re-used by Hopke et al. (1976) for their analysis of particle composition data from Boston. Hopke et al. (1976) applied FA to Boston total suspended particle elemental composition data in order to identify particle contributors in that city. The CMB model was first suggested by Miller et al. (1972). By assuming that the number of sources and their compositions at the receptor site are known, Miller et al., (1972) derived the

mass contribution of each source to particular sample. In 1979, Watson suggested a mathematical formalism called effective variance weighting that included the uncertainty in the measurement of the source composition profiles as well as the uncertainties in the ambient concentrations.

While receptor modeling techniques have been repeatedly shown to be useful in quantifying the sources of urban and rural aerosols, studies in order to estimate the contributions from distant pollution sources have been started by Thurston and Spengler (1985) and Hopke (1985). Thurston and Spengler (1985) presented a new source apportionment technique to identify and quantify the major particle pollution source classes affecting a monitoring site in metropolitan Boston. The technique is basically dependent on calculation of Absolute Principal Component Scores and the subsequent regression of daily mass and elemental concentrations on these scores. Hopke (1985) have developed target transformation factor analysis (TTFA) to determine the number of independent sources that contribute to the system, to identify the elemental source profiles and to calculate the contribution of each source to each sample.

All of the receptor models mentioned above use the chemical measurements of the aerosol samples collected from receptor site and identify the possible sources in terms of their chemical nature and estimate the importance of contribution of these sources. First generated receptor models like PCA, FA and CMB have limited abilities to locate regional sources of air pollutants because only chemical information is used and the regional pollutants are often secondary in their chemical nature and these receptor models can not determine the specific location of sources. To overcome these shortcomings, meteorological information needs to be incorporated into the receptor model. Malm et al., (1986) presented the potential source contribution technique (PSCF) to identify geographical regions that may have a higher probability of being source areas of pollutants.

Brief theory of three most commonly used multivariate statistical methods which will also be used in the data analysis part of this work are given in the following sections.

2.6.1. Factor Analysis

Factor analysis provides preliminary information about the possible sources that may influence the sampling locations. In principle, it indicates groups of elements where concentrations fluctuate together from one sample to another and separates these elements into "factors" (Henry, 1984). Ideally, each extracted factor represents a source affecting the samples.

The major goals of factor analysis are (1) to determine, the number of factors needed to describe the experimental data satisfactorily and (2) to determine the matrix of factor loadings, (A).

If a data set of elemental concentrations determined at N observations for a total of n elements. The concentration of the j -th element ($j=1\dots n$) at the i -th sampling duration ($i=1\dots N$) is denoted by x_{ji} . It is convenient to transform the data set to the standardized variables z_{ji} by

$$z_{ji} = \frac{(x_{ji} - \bar{x}_j)}{\sigma_j} \quad (1)$$

As a result, the z_{ji} have a mean of zero and a variance of unity. In the factor model, the z_{ji} are assumed to be a linear sum of m common factors (in our particular case to be interpreted as emission sources) with $m \leq r$, which account for the correlations between the variables and a unique contribution which is specific for each individual sample

$$z_{ji} = \left(\sum_{k=1}^m a_{jk} f_{ki} \right) + d_j u_{ji} \quad (2)$$

The coefficients a_{jk} , representing the correlation of element j with factor k , are indicative for the relative elemental composition of the factor k . These coefficients are often called the loadings of the factors. The m coefficients f_{ki} are usually called the factor scores. They represent the contribution of factor k to sample i . The product $d_j u_{ji}$ represents the residual error for variable j in sample i , which is not accounted for by the m common factors. For a given sample i , the z_{ji} can be conceived as a column vector with the standardized element concentrations as its components. Equation (2) can then be written as

$$\begin{pmatrix} z_{1i} \\ z_{2i} \\ \vdots \\ z_{ni} \end{pmatrix} = f_{1i} \begin{pmatrix} a_{11} \\ a_{21} \\ \vdots \\ a_{n1} \end{pmatrix} + f_{2i} \begin{pmatrix} a_{12} \\ a_{22} \\ \vdots \\ a_{n2} \end{pmatrix} + \dots + f_{mi} \begin{pmatrix} a_{1m} \\ a_{2m} \\ \vdots \\ a_{nm} \end{pmatrix} + \begin{pmatrix} d_1 u_{1i} \\ d_2 u_{2i} \\ \vdots \\ d_n u_{ni} \end{pmatrix} \quad (3)$$

where the m column vectors

$$\bar{a}_k = \begin{pmatrix} a_{1k} \\ a_{2k} \\ \vdots \\ a_{nk} \end{pmatrix} \quad (k=1, \dots, m) \quad (4)$$

contain the loadings of the corresponding factor k .

For the complete data set, equation (2) can be expressed in matrix form,

$$Z = AF + DU \quad (5)$$

where Z is an $n \times N$ matrix with components z_{ji} ; A an $n \times m$ matrix with components a_{jk} ; F an $m \times N$ matrix with components f_{ki} ; D a diagonal $n \times n$ matrix with components d_j on the diagonal; and U an $n \times N$ matrix with components u_{ji} .

In factor analysis the number of factors m is decided by the eigenvalue cutoff. As the cutoff value decreases, m is increases. One of the serious drawbacks in factor analysis is the selection of this cutoff value which in turn

governs the value of m . On the selection of the cutoff value, Henry (1984) pointed out that there is no universally applicable method for establishing m and it is necessary to discard a number of small eigenvalues. Generally, eigenvectors with eigenvalues greater than 1 are more signal than noise and should be kept in the model. Those eigenvectors with eigenvalues less than 0.5 have more than twice as much noise as signal and should be eliminated from the model. For eigenvalues between 1 and 0.5, the associated eigenvectors are more noise than signal, but they may be important enough to kept in the model.

By definition, multivariate analysis requires several observations, the more the better. If there are too few samples, the results of a multivariate model are not likely to be reliable. Experience has shown that 100 samples or more is generally acceptable and that 20 or 30 is usually too few. A simple rule of thumb was developed by Henry and reported in Henry et al., (1984). In a typical multivariate receptor model with N observations of V variables, there will be V means and $V(V-1)/2$ variances and correlations. The total number of degrees of freedom in the data set is NV . Thus, the degrees of freedom are reduced to $NV - V - V(V-1)/2$. This is now divided by V to get the number of degrees of freedom per variable in the analysis:

$$N - 1 - \frac{(V - 1)}{2} \quad (6)$$

Experience has show that this number should be at least 30 and preferably 60 or greater to obtain reliable results.

2.6.2. FA-AFS Method

Factor Analysis-Absolute Factor Score is a method which allows the estimation of source particle characteristics for an unconventional source category: transported (coal combustion related) aerosols. This approach first developed by Thurston and Spengler (1985). In their work, Principal

Component Analysis (PCA) was applied to fine and coarse elemental concentration data collected in Watertown, Massachusetts over a two year period. Based upon these PCA results, fine and coarse particle pollution sources affecting the monitoring site were identified. The particle mass contribution of each identifies source was then estimated using PCA-Absolute Principal Component Scores (APCS) technique: the technique was based on the computation of APCS's for each sample, followed by the regression of sample particle mass concentrations on these APCS to derive each identified source's estimated mass contribution. By using Factor Analysis instead of PCA, this method was then used by Tuncel et al., (1985). By performing a multiple linear regression of the concentration of each element vs. the absolute scores of the factors, Tuncel et al. (1985) determined the regional sulfate component at Shenandoah Valley.

In this method, after the Varimax rotated Factor Analysis has been applied to the data set, the factor scores (f_{kj}) are computed. The factor scores are correlated with their respective pollution sources having an impact on the site (i.e. higher factor score implies a higher pollution impact by the pollution source j during observation k). However, because they are computed from the normalized elemental concentrations, z_{ik} , they too are normalized. To solve this problem a component derived by initializing a correlation about origin and normalizing the data to the mean of all elements in each Sample instead of to the mean of all samples for each element.

The 'absolute zero' factor score (FS) has been estimated for each factor score by separately scoring an extra day wherein all elemental concentrations are zero. This is accomplish by deriving the z-score for absolute zero concentrations,

$$(z_o)_i = \frac{0 - \bar{x}_j}{\sigma_i} = -\frac{\bar{x}_j}{\sigma_i} \quad (7)$$

and then calculating the rotated absolute zero FS scores, F_o , for each of m components,

$$F_{om} = \sum_{l=1}^n A_{ml}(z_o) \quad (8)$$

These estimates of the FS scores for each component at absolute zero are then used to estimate Absolute Factor Scores (AFS) for each component on each day as follows

$$[AFS]_{mxj} = [F]_{mxj} - [F_o]_{mxj} \quad (9)$$

where the j columns of $[F_o]$ are all identical equal to the values calculated in (8). It can be proved that the calculation of $[AFS]$ according to equation (9) gives the exact score which would be achieved had the original scoring been executed using unnormalized data.

Regressing daily concentration data on these AFS gives estimates of the coefficients which convert the AFS into pollutant source contributions (in mg/m^3) for each sampling day as follows

$$M_k = \zeta_o + \sum_{j=1}^m \zeta_j AFS_{jk} \quad (10)$$

where M_k is the particle mass recorded (in mg/m^3) during observation k ; AFS_{jk} is the rotated absolute factor score for component j on observation k ; $\zeta_j AFS_{jk}$ is the particle mass contribution (in mg/m^3) made by the pollution source identified with component j ; and ζ_o is the particle mass contribution made by sources unaccounted for in the FA. If the FA is successful, z_o should tend toward zero.

For each of the pollution sources identified in the FA, it is possible to derive information regarding the elemental composition of particles from that source. The individual weighted regression of each element's recorded daily concentrations on the predicted mass contributions from all sources during

those days yields estimates of the content of that element in each source's mass, as follows

$$C_k = a_o + \sum_{j=1}^m a_j S_{jk} \quad (11)$$

where C_k is the concentration of an element i during observation k ; S_j is the mass concentration of source j on day k ; and a_j is the mean mass fraction of source j 's particles represented by the element. Repeating this weighted least square regression for each of the $i=1,2,\dots,n$ elements considered in this analysis, by size fraction, allows an estimation of the elemental source profiles of each pollution source identified in each particle size category (a_{ij}). Moreover, the product of these estimates of the mean elemental mass fractions and the prior estimates of the mean component mass impacts yields estimates of the contribution by the j th source to the ambient concentrations of element i during observation k . Thus, estimates can be derived for both the elemental composition of the identified source particles and their contributions to the ambient elemental concentrations.

2.6.3. Theory of PSCF Analysis

The PSCF is a new receptor-oriented method which is able to incorporate the meteorological information into an analysis. The concept of PSCF was introduced to identify geographical regions that may have a higher probability of being source areas of potential harmful substances like sulfate in the study area. The results of a PSCF analysis may then be useful in tracing atmospheric constituents.

Trajectories are related to the composition of collected material by selectively matching the time of arrival of each trajectory at the receptor site to sampling interval of filter sample. The value of PSCF for a single grid cell of 5° long by 5° latitude is calculated by counting each 3 hr trajectory segment endpoint that terminates within that grid cell. Suppose N represent the total

number of trajectory segment endpoints for the whole study period, T . If the number of endpoints that fall in the ij -th cell is n_{ij} , the probability of an event at the receptor site is related to that cell, A_{ij} , over entire study period T is given by,

$$P[A_{ij}] = \frac{n_{ij}}{N} \quad (12)$$

If, for the same cell, there are m_{ij} endpoints whose times of arrival of air parcels correspond to events with pollutant concentrations higher than an arbitrarily given value, the probability of this "matched" event, B_{ij} is given by

$$P[B_{ij}] = \frac{m_{ij}}{N} \quad (13)$$

The PSCF for the ij -th cell is then defined as:

$$PSCF_{ij} = \frac{P[B_{ij}]}{P[A_{ij}]} = \frac{m_{ij}}{n_{ij}} \quad (14)$$

The PSCF value can be interpreted as the conditional probability that concentrations larger than a given criterion value are related to the passage of air parcels through the ij -th cell during transport to the receptor site.

Cells for which high PSCF values are calculated result from the arrival of air parcels at a receptor site with pollutant concentration higher than a given value observed at the site. These cells are indication of areas of "high potential" contributions to the pollution at a receptor site. It is important to note that the exact location of the source(s) within the high-potential areas is unknown in the present analysis because of (1) the fundamental limitation of the PSCF methodology that cells must be large enough to have a reasonable number of counts in them, and (2) the uncertainty involved in calculating the backward air parcel trajectories.

2.7. Meteorological Regimes and Transport Processes in the Mediterranean Sea

The Mediterranean Sea is known throughout the world for its distinctive climate. To understand the transport of both natural and anthropogenic materials to the Mediterranean Sea from major sources, the flow climatology of the basin must be well described and understood.

In the Mediterranean basin, winter rainfall is at least three times the summer rainfall. Indeed over much of the basin, the summer rainfall is virtually zero. This strong summer-winter rainfall contrast is echoed by a pronounced seasonal cycle in almost all climate variables.

The rainy season starts in mid-October and continues around the end of April. In July, August and September the region experiences warm, dry conditions linked to the presence of a strong high-pressure ridge extending eastwards from the Azores subtropical anticyclone. Winter is characterized by cyclic disturbances and low mean pressure in the Mediterranean, with higher pressure to the east associated with the Siberian high. For the years 1992 and 1993 and long term monthly average temperature and total precipitation amount for the Antalya station are given in Table 2.3.

The topography behind the coastline of the Mediterranean is complex and provides barriers and channels for air flow that bring extremely different air masses to the region. Strong winds, which are tunneled through gaps in the mountain ranges that surround the Mediterranean Basin, are among the best known meteorological features of the region: (1) the north-westerly mistral through the Alps-Pyrenees gap; (2) the northeasterly bora through the Trieste gap; (3) the easterly lavender and the westerly vendaval through the Strait of Gibraltar, and (4) the warm southeasterly to southwesterly scirocco, ghibli, or Khamsin from Africa (UNEP/WMO, 1989).

Table 2.3. Monthly average temperature and total precipitation amounts observed during the years 1992 and 1993 and long term averages for the Antalya Meteorological Station.

	1992		1993		Long Term Ave.	
	Temp (°C)	Tot. Prec. (mm)	Temp (°C)	Tot. Prec. (mm)	Temp (°C)	Tot. Prec. (mm)
January	8.29	–	7.6	264.7	9.8	255.8
February	7.06	81.5	8.5	116.0	10.2	164.56
March	10.96	182.1	10.9	129.3	12.6	89.35
April	15.19	34.0	15.0	29.6	15.9	43.72
May	19.13	19.6	18.3	120.5	19.7	29.79
June	24.00	3.0	24.9	20.0	24.4	6.65
July	27.06	1.0	28.3	–	28.1	3.97
August	28.22	0.1	28.1	–	27.9	4.27
September	24.24	2.2	23.7	–	24.7	13.77
October	20.77	0.6	21.2	74.8	19.7	62.22
November	13.9	194.4	12.9	100.9	15.3	111.47
December	8.1	176.0	11.6	80.0	11.8	269.76

Synoptic weather patterns are essential as a first tool to understand the overall flow configurations. For evaluation of the pathways of contaminants to the Mediterranean region five main synoptic weather patterns were determined and a brief description of the five main synoptic weather patterns are given below (Dayan and Miller, 1989).

Type A: An anticyclone or ridge of high pressure lies over the northeastern Atlantic or the British isles. During the presence of this blocking anticyclone, a quasi-permanent low pressure trough in the midtroposphere (about 500 hpa) extends along the axis of the Mediterranean basin. This trough line leads to cyclogenesis when voracity maxima move into its region of influence to form cyclogenesis. This major synoptic feature occurs especially during the winter period (Miller et al., 1987) (Figure 2.2).

Type B: Northern Europe is dominated by an anticyclone. Pressure is relatively low over the whole Mediterranean (Figure 2.3).

Type C: Westerly type. A deep depression (or a sequence of depressions) dominates the middle latitudes of Europe, and westerly winds prevail over most of the Mediterranean (Figure 2.4). Types A, B and C are the most common types of winter in the Mediterranean Basin.

Type D: Easterly type. An anticyclone dominates central and southern Europe giving easterly winds over most of the Mediterranean. Pressure is relatively low over northern Europe (Figure 2.5).

Type E: Anticyclonic type. An anticyclone or ridge of high pressure covers the greater part of the Mediterranean area, giving generally light winds, mainly westerly in the north, easterly in the south, and northerly in the east. Pressure is relatively low over central or northern Europe (Figure 2.6).

Types A, B, and C are the most common types during winter whereas types D and E most frequently observed during summer. When types D and E prevail, the high pressure over the Mediterranean decreases toward the east, northwesterly wind prevails and warm weather occur. These easterly pattern are almost continuous in July and August, but very infrequently from November to April. Although these classifications are very useful to get the overall picture, each individual weather system has its own unique characteristics and may greatly influence the transport of pollutants to the region.

2.7.1. Back-trajectory Analysis

The backward trajectory models were developed to study the origin and history of air during its travel over the previous three or four days before arriving at sampling locations. The trajectories were deduced from geostrophic winds determined from the pressure gradients in the developing synoptic scale features of the meteorological situation. Since the geostrophic wind is the most important factor affecting the transport of pollutants, flow climatologies based on backward trajectories represent seasonal transport paths in the various parts of the defined region.

There are numerous studies for long range transport of pollutants using Lagrangian models in the literature (Fisher, 1983; Eliassen, 1984). Such studies have been performed in the past for remote sites such as the Bermuda island, Alaska, Mauna Loa, Hawaii (Miller, 1981a,b; Miller and Harris, 1985) and for some receptor locations within the Mediterranean region (Dayan, 1986; Miller et al., 1987).

In this study, among the available pressure and height models, the Air Resources Laboratories Branching Atmospheric Transport (ARL-BAT) model was chosen mainly because of its wide acceptance in the literature and its readily available software. The ARL-BAT model (Heffter et al., 1983) has been developed to compute long-distance trajectories in understanding atmospheric

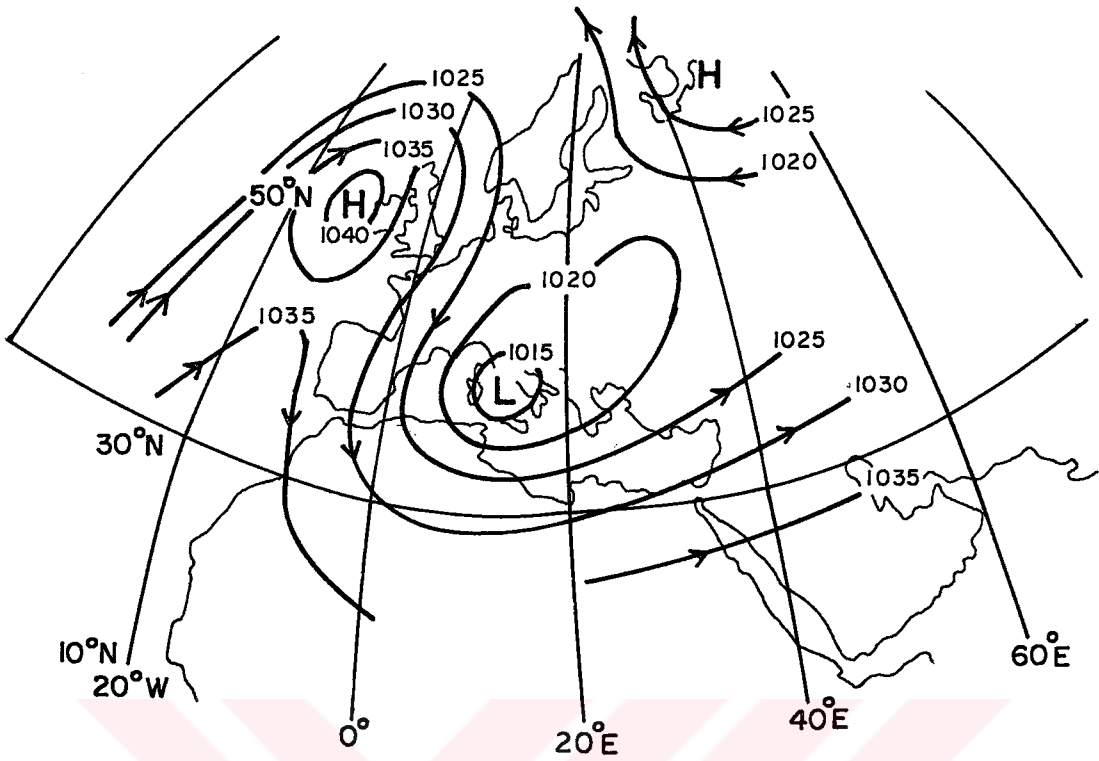


Figure 2.2. Syroptic weather pattern type A

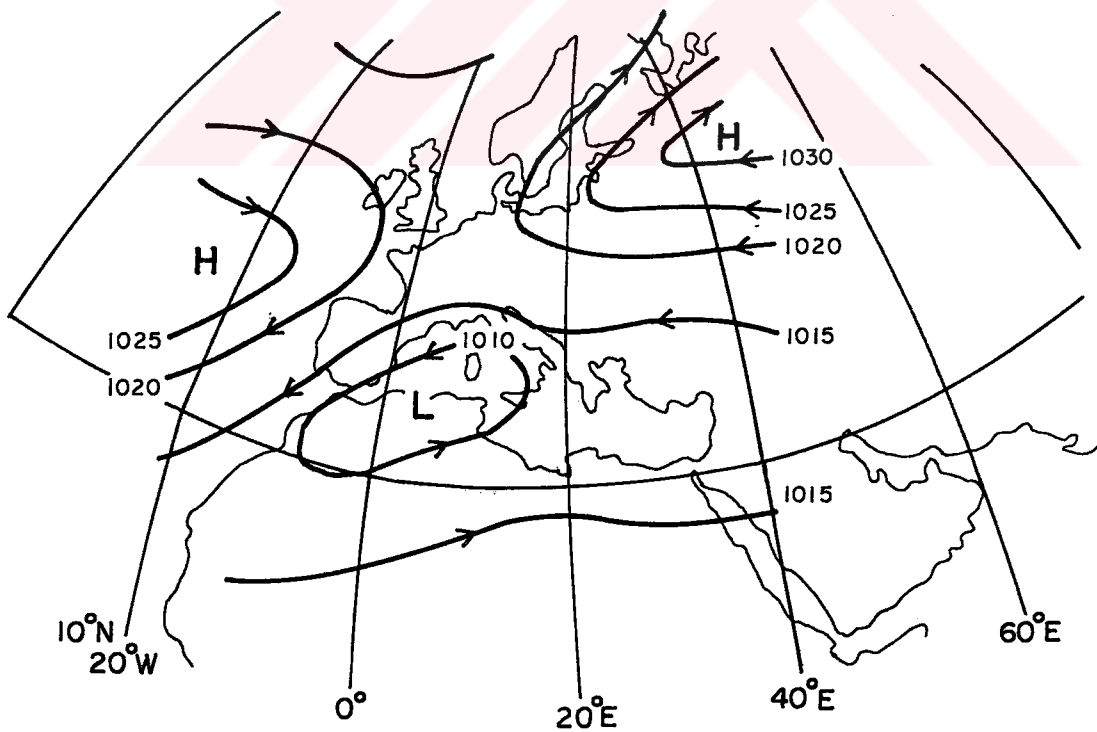


Figure 2.3. Syroptic weather pattern type B

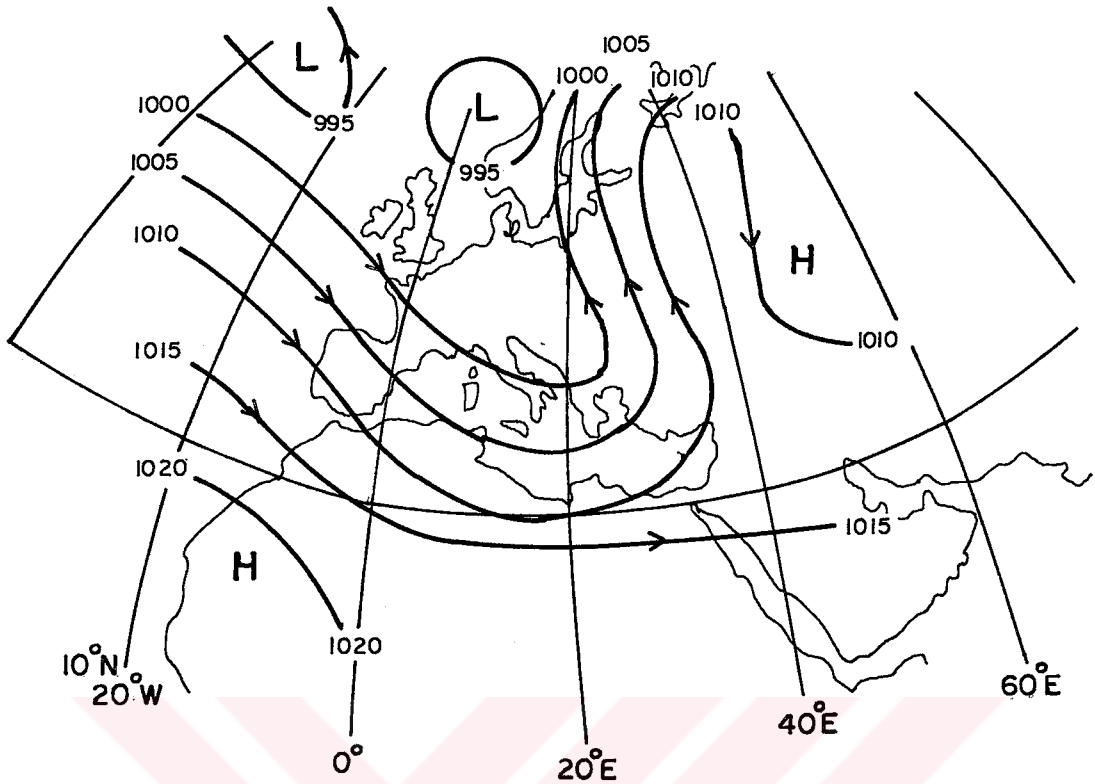


Figure 2.4. Synoptic weather pattern type C

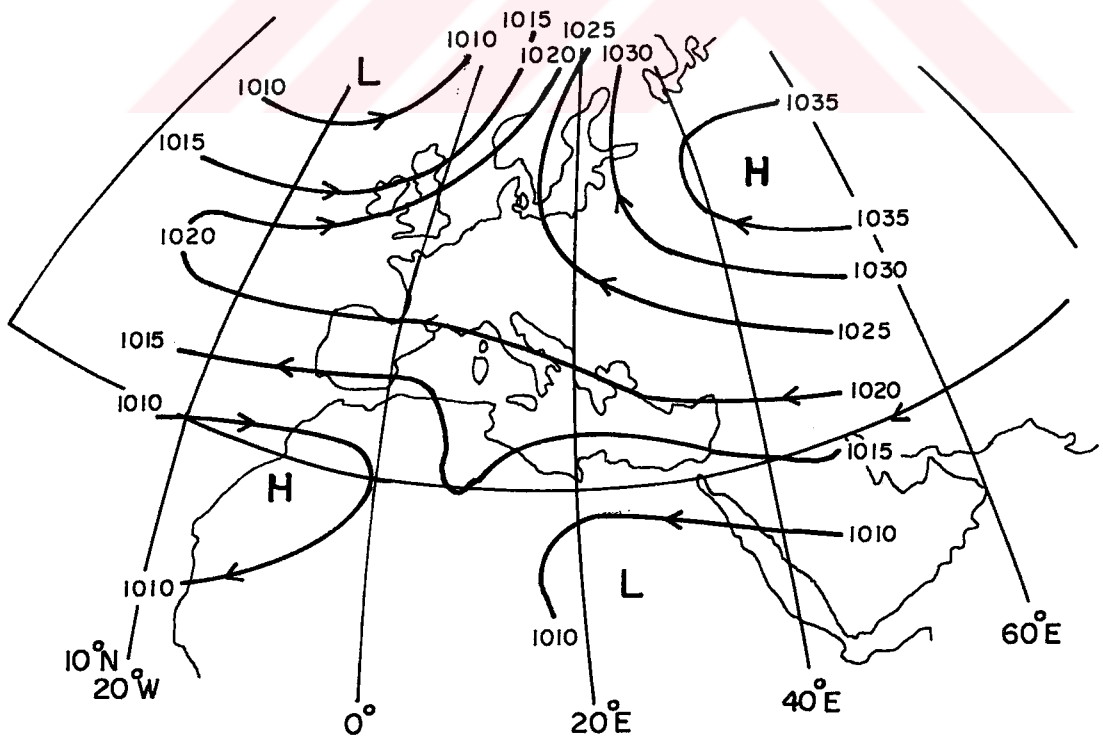


Figure 2.5. Synoptic weather pattern type D

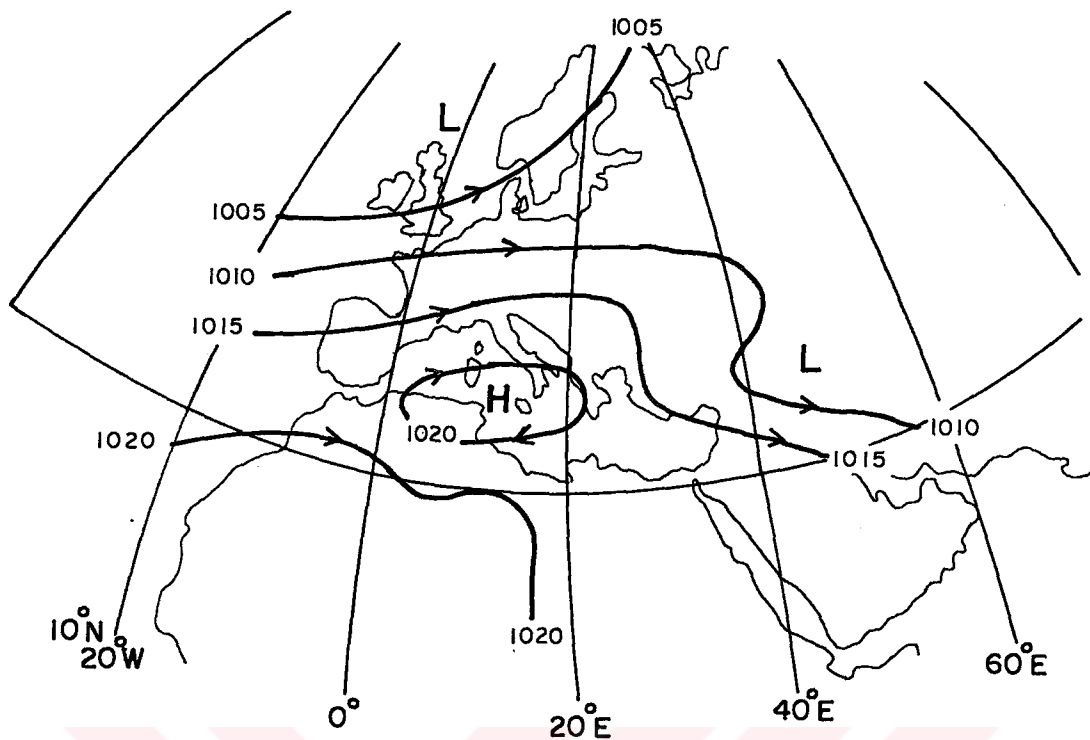


Figure 2.6 Synoptic weather pattern type E

transport. It is a purely kinematic model which computes the air mass backward or forward trajectories on the basis of wind-field data. The model inputs are latitude-longitude data grids (2.5 degrees) of wind analysis, every 6 hours, at several standard pressure levels.

trajectories are computed by three-hour segments through an averaged wind in a layer (50m to 3000m) from the winds linearly weighted according to the height,

$$V_i = \frac{\sum H_j V_j}{\sum H_j} \quad (15)$$

The BAT model divides the lower troposphere into 3 layers. The layers are determined according to whether it is day or night and from the vertical temperature profile at each rawinsonde station. The first layer is assumed to

have a constant height of 300 m above the surface. The second layer, boundary layer extends from the top of the surface layer at night, or from the surface during the day, to the boundary layer height determined from a critical inversion. The third layer, the upper layer, extends from the critical inversion to a fixed height of 3000 m. The criteria for the critical inversion are:

- 1) $\Delta\theta / \Delta Z \geq 0.005 \text{ } ^\circ\text{K/m}$
- 2) $\theta_T - \theta_B \geq 2 \text{ } ^\circ\text{K}$

where $\Delta\theta / \Delta Z$ is the change of potential temperature (θ) with height (Z) and θ_T and θ_B are defined at the top and base of the inversion. When no critical inversion exists, the boundary layer height is assumed to be 3000 m, and no upper layer is defined.

The trajectory of a puff is calculated for 4 days duration (32 three hour segments) using the modified Euler advection technique (Heffter et al., 1983) for each segment. A step in the technique is calculated as follows:

$$\text{step} = \frac{\sum_{I=1}^N w_I \cdot \Delta t \cdot d_I^{-2}}{\sum_{I=1}^N d_I^{-2}} \quad (16)$$

where,

N = number of rawinsonde stations within a 1° latitude scan radius. If $N=0$, the scan radius is increased by 1° steps, and at 5° , if $N=0$, the trajectory calculation is terminated.

w_I = vertically averaged wind at station I (average of the observed winds through the layer in which the trajectory is being calculated)

Δt = advection step time interval (3 hours)

d_i =distance from station i to step origin (inverse distance squared weighting).

Average winds are assumed to persist from 3 hours before to 3 hours after observation time. For a more complete transport wind network, missing average values at a station are linearly interpolated, whenever possible, from average values 6 hours before and 6 hours after observation time.

The model requires user supplied input data for each run. These requirements are the source location, start date, number of days that trajectories are required, and geographic boundaries for meteorological input data and output maps. The required upper-air meteorological data are the observed upper-air winds and temperatures at all mandatory and significant levels from all rawinsonde and pibal stations located on Europe, Turkey and North Africa (-10° to 40°N longitude and 25° to 60°E latitude). The meteorological data from all stations located within the geographic boundary are written in time sequence on computer at the Turkish Meteorological Office and each month they are routinely copied and sent to our department. Data from 1992 through 1995 are presently archived and transformed to backward in time series.

CHAPTER 3

MATERIAL AND METHODS

3.1. Sampling Site Description

Atmospheric sampling station was implemented at a coastal site at the Mediterranean coast of Turkey, at approximately 20 km to the east of from the town of Antalya (31.0 longitude east of Greenwich and 36.8 latitude north of Equator). The station is located on a rock structure at a height of 20 meters above the sea level.

Site selection was an important step in establishing reference stations where sampling is performed to study long range transport. The sampling site should not be under the influence of any local point and area sources to be able to detect low levels of pollutants which are being advected from upper atmosphere. However, three additional requirements were dictated by the logistics of sampling.

- (1) Station must be located at a site where power is available,
- (2) station must be on the grounds of a government property so that it can be protected against potential vandalism and
- (3) there must be capable people to change samples.

One difficulty to establish a "reference station" on the Mediterranean coast was the extensive domestic and foreign tourism in the region. Most of the

Mediterranean coast is covered by either holiday resorts or summer houses. Finding a site far from all activities proved difficult.

After visiting all possible sites along the Mediterranean coast, a rest area owned by the Ministry of Forestry, 20 km's to the east of the city of Antalya was selected as the site where the station to be established. The area was under protection throughout the year and power was available. The nearest population center was the city of Antalya which was approximately 20 km away. There were no point sources which can effect the station site. The location of the sampling station and topography of the region are given in Figure 3.1.

The station was consist of two components, namely the platform and the field laboratory. The platform was built on the rock structure near the sea approximately 20 m above the sea level. It was consist of a 4 m x 4 m concrete base and surrounded by a 2 m high fence. The wiring of the fence was covered by polyethylene to avoid contamination of collected samples by metal particles which can result from the corrosion of metal. The equipments including a wet only precipitation sampler, a wet and dry deposition sampler, a Hi-Vol sampler and a Hi-Vol impactor were anchored to the concrete base of the platform. No sockets were placed on the platform to avoid short circuiting due to sea spray, particularly during winter months. Power to the equipments was controlled from the field laboratory. A picture of the platform is given in Figure 3.2.

The field laboratory consisted of a container with dimensions of 3 m x 2 m x 2 m. The power was distributed from the container to equipments on the platform. The field laboratory included a storage area, a refrigerator to store samples until they were shipped to the central laboratory in Ankara and a sample change area. The sample change area consisted of a table where certain precautions were taken to reduce the possibility of contamination to a minimum. The table was lined with a sheet of polyethylene. A small plate of plexiglas with dimension of 50 cm x 50 cm was placed on the polyethylene sheet. All sampling handling in the field laboratory was carried out on this

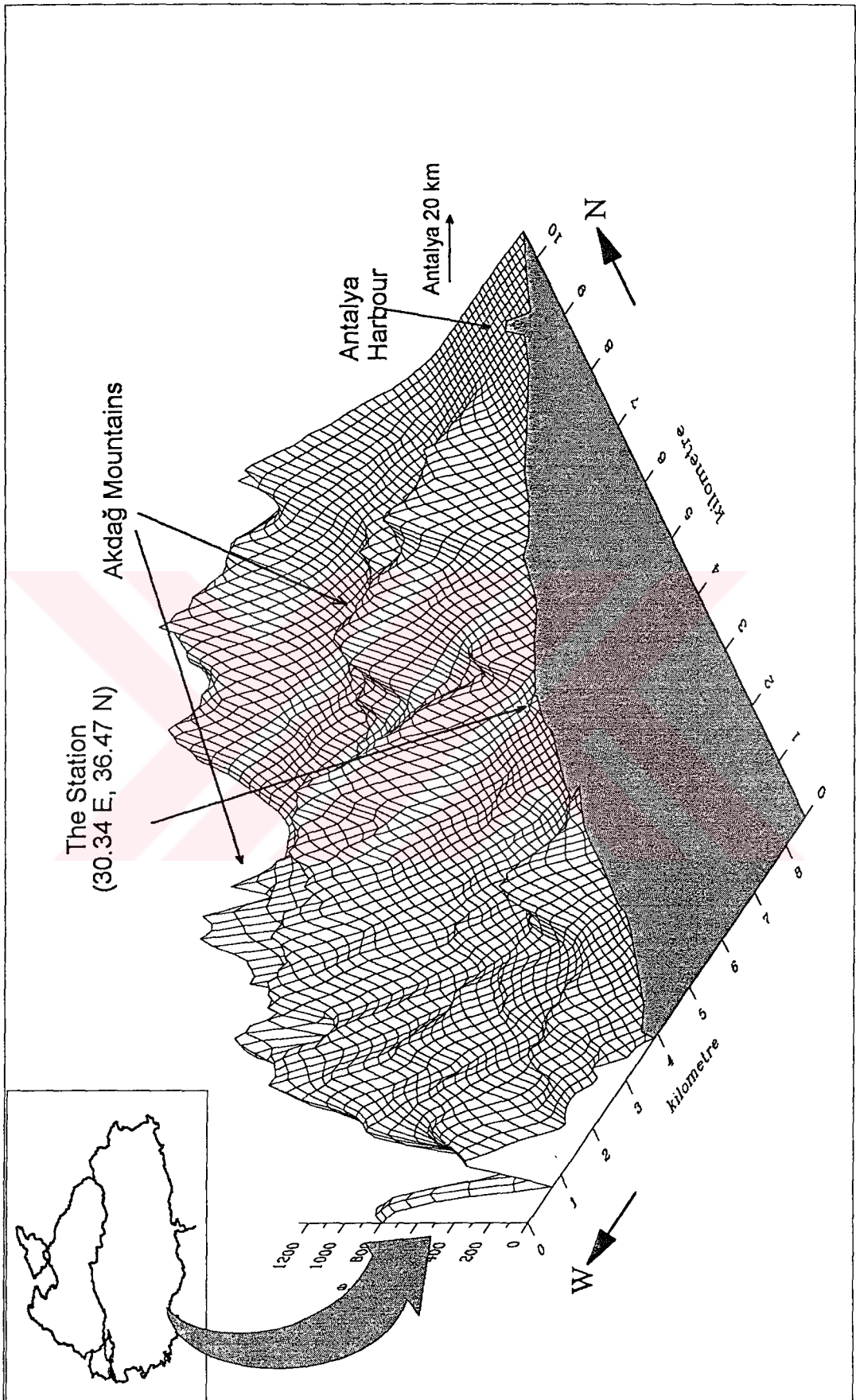


Figure 3.1. The topography of the Antalya Station

plexiglas board. The plexiglas was first wiped with a damp tissue paper and then with a dry tissue paper before it was used to change samples. It was covered with a sheet of polyethylene when it was not used.



Figure 3.2. A picture of the sampling platform

The sampling in the station was started in December 1991 and continued until now. In this study, results of 1992 and 1993 aerosol samples will be discussed extensively. During this period, a total of 600 daily aerosol samples were collected.

3.2. PM-10 High Volume Air Sampler

The most widely used airborne particle sampler in rural studies is the high volume sampler. With the advent of new air pollution guidelines in the USA on July, 1987, new air samplers which separate the particles with 50% efficiency at $10\ \mu\text{m}$ (PM-10) were built by companies. In this study, PM-10 aerosol sampling was done with a SIERRA-ANDERSEN Model SAUV-10H PM-10 High Volume Air Sampler, using 20 x 28 cm Whatman 41 cellulose filter. The

PM-10 performance specifications of the sampler are summarized in Table 3.1. The size selective inlet attached to the Hi-Vol sampler (Figure 3.3) separates particles smaller than 10 microns aerodynamic diameter from the larger particles. Only the particles pass through the preimactor are collected by the filter.

With the particular model of Hi-Vol sampler used in this study suspended particles in the air were sampled at a flow rate of $1.35 \text{ m}^3 \text{ min}^{-1}$ through the circumferential inlet of the Size Selective Inlet. The symmetrical design insure wind-direction insensitivity, and the inlet design and internal configuration make the collection efficiency independent of wind speed from 0 to 36 kilometers per hour. The particles are then accelerated through multiple circular impactor nozzles. By virtue of their larger momentum, particles greater than the $10 \text{ }\mu\text{m}$ impactor cut-point impact onto the greased impaction surface. The PM-10 (particles smaller than $10 \text{ }\mu\text{m}$) are carried vertically upward by the air flow and down multiple vent tubes on the $20 \times 28 \text{ cm}$ filter, where they are collected (Figure 3.3). The large particles which settle out in the impaction chamber on the collection shim are removed during maintenance periods.

Table 3.1. Performance Specifications for PM-10 Sampler

Parameter	Specifications
Flow-rate	45 cubic feet per minute, 1.35 cubic meters per minute
Flow-rate stability	Over 24 hours, average flow rate within $\pm 5\%$ of initial
Filter media	8 in x 10 in (20 cm x 28 cm) Whatman-41 cellulose filter
Inlet collection efficiency	The inlet has a cut-point of 9.7 ± 0.5 microns over a wind speed of 0 to 36 km h^{-1}

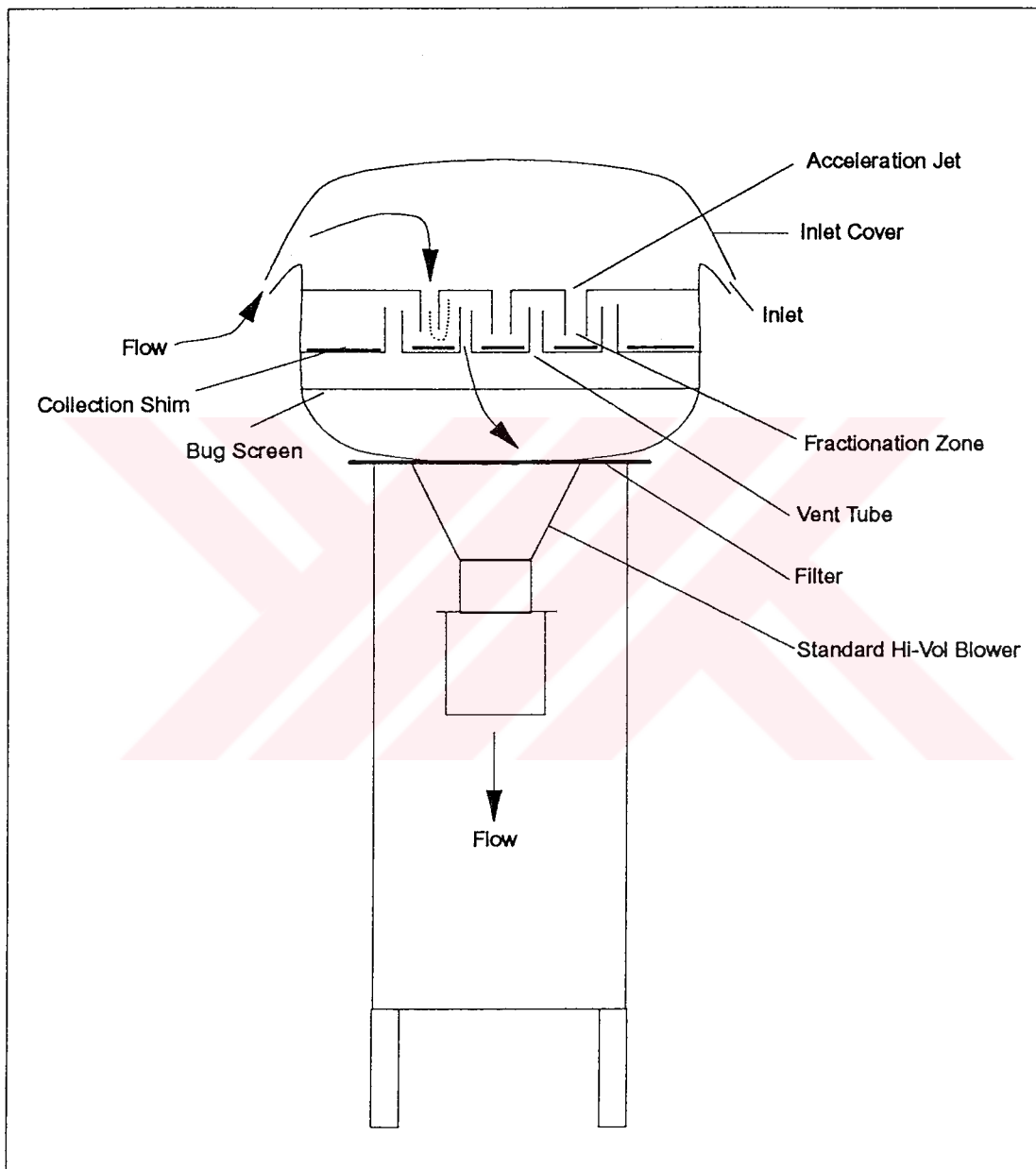


Figure 3.3. The cross-sectional view of PM-10 Size Selective High Volume Air Sampler

Whatman-41 cellulose filters were used to be able to operate the sampler at high flow rate without significant pressure drop due to particle loading,.

Flow was controlled by a venturi device. The orifice in the flow controller was a specially machined nozzle designed to react to a specific pressure ratio expressed in absolute term. When air reaches the speed of sound in the throat (smallest diameter) of the orifice, a sound-pressure barrier is set up that will not allow more air through under the existing temperature and pressure conditions.

3.3. Sample Handling

Filters were changed at 10:00 am every day. To change the filter, the sampler was stopped, the flow was recorded from the dry-gasmeter. The filter cassette on the sampler was covered, placed in a polyethylene bag and carried to the field laboratory. In the field laboratory, the filter was removed from the cassette on the precleaned plexiglas board and heat sealed in an acid-washed polyethylene bag. After it was labeled with permanent non-vanishing ink, it was placed in another polyethylene bag together with sampling information sheet in which sampling conditions like sample ID, date of sampling, flow recorded, temperature, precipitation events, were logged and the circular chart which recorded changes in the flow during sampling. The second bag was also heat-sealed and the sample was stored at 4°C in a refrigerator in the container until it was shipped to the main laboratory in Ankara. The filter cassette was wiped with damp tissue paper, an unused Whatman-41 filter was placed in the cassette, cassette was carried to the sampling platform in a polyethylene bag, placed on the sampler and the cover was removed. Using flow controller chart recorder, the air flow through the filter was determined and recorded to the sample information sheet which was prepared for each sample. The indicator reading on flow dry-gasmeter was also recorded. The difference between the flows calculated using calibrated flow charts and gas meter was always less than 5%. Every month, flow of the pump was calibrated by calibration kit, and after each calibration a blank sample was taken. To obtain blank filters, all manipulations carried out on the real samples were performed except air was

pulled through blank filters for only 1 minute. Collected filter and blank samples were sent from the station at approximately every month. Samples were kept in the refrigerator at 4°C, for approximately 3 months prior to analysis.

Since the concentrations of ions and trace elements are expected to be very low in aerosol samples, a great care was taken to minimize contamination during sampling. The cleaning procedure for the plastic equipment consisted, of consecutive washes in 10% reagent grade nitric acid followed by several rinses with distilled deionized water. During sample handling processes, all sample manipulations were done using teflon coated tweezers. Samples were never touched directly by hand, and powder-free disposable polygloves were used to prevent contamination of tweezers. All personnel involved with sampling wore clean room garb, particle-free polyethylene gloves and hair covers, while working with them in the laboratory.

All sample handling processes after receiving the samples from the field were performed in a clean area in the Environmental Engineering Department. The room consisted of two parts connected to each other with a door. The outer part of the room was used as a laboratory for storage of refrigerated samples, and HPLC analysis. Inner part of the room was used to prepare samples. There are five High Efficiency Particulate (HEPA) Filters in inner room to remove particles with a size range of less than 0.1 μm . Particle measurements have shown that, particle number concentration in the room is approximately 50 times smaller than the particle concentrations outside the room.

Selection of collection material is an important consideration to obtain a useful sample for the purpose. The filter should retain particles but permit air flow through it. It should provide the sample in a manner that makes it easy to quantify both the total mass of collected material and the chemical composition of the aerosol. Neustadler et al. (1975) found that cellulose filter materials such as Whatman 41 could be employed in ambient monitoring with insignificantly lower collected mass if proper care were taken in the humidity equilibration that must be conducted before weighting exposed or unexposed filter. Cellulose

filters have been found to have somewhat lower retention when sampling begins but their collection efficiency improves as the filter become loaded with particles (Lowenthal and Rahn, 1987). Whatman 41 filters are popular for aerosol sampling in rural areas due to their high loading capacity and have low blank values (Dams et al., 1972).

The cellulose filters were weighted before and after sampling. The filters were left overnight in the clean room where the room temperature and humidity were almost constant throughout the year to obtain constant weight. The uncertainty associated with mass measurements were about 5%.

Filters were divided into four equal parts which was separately weighted and recorded. One fourth of the total exposed filter was used for the analysis of trace elements using neutron activation analysis, the second quarter filter was used for analysis of ions, including $\text{SO}_4^{=}$, NO_3^- Cl^- by IC and NH_4^+ by colorimetry. The third quarter filter was used for analysis of heavy metals by atomic absorption spectrometry and the last quarter was archived for any potential future use.

3.3.1 Preparation of Pure Nitric Acid

The only reagents, that were added to samples for metal analysis by AAS and digestion of filters, were nitric acid HF and H_2O . One of the most important features of the analytical reagents should be pure in order to avoid contamination of the samples. Ultrapure HNO_3 , HF and water were used through the study. The pure nitric acid was obtained from two different sources; commercial supra pure grade (MERCK) was used in the beginning of the study. But, pure HNO_3 produced by subboiling distillation of analytical grade HNO_3 was used to avoid the high cost of large volumes of commercial suprapure grade HNO_3 . The HF used in the digestion of samples was commercial suprapure grade (MERCK) acid. The pure water used was produced by deionization of double distilled water using a NANOpure, Series 550, ULTRApure water system manufactured by Barnstead/Thermolyne Corporation, deionizer equipped with

two ion exchange cartridges (Barnstead, G-01505-26) to remove cations, one cartridge (Barnstead, G-01505-24) to remove anions, and one cartridge (Barnstead, G-99257-00) to remove organic and a particulate filter. The HF used through analysis was supra-pure grade (MERCK). Supra pure nitric acid was prepared from lower grade nitric acid in a quartz sub-boiling distillation unit. In this unit, commercial analytical grade nitric acid was heated slowly with two quartz rods equipped with an electrical heater. Then the produced nitric acid vapor was condensed on a cooled quartz rode.

3.4. Analytical Techniques

A variety of sensitive instruments have been developed in recent years to measure a wide range of species at nanogram levels or less. Considerations such as compatibility of the technique to filter matrix, extend of sample processing necessary, speed of analysis the extend of training needed for operators availability of instruments, cost per analysis play important role in addition to sensitivity and precision of the proposed method. In this study, for choosing the analytical method, the factors like, sensitivity, accuracy and precision obtainable with the analytical technique, and availability to the instrument were taken into account. Based on the above criteria instrumental neutron activation analysis (INAA) and atomic absorption spectrometry (AAS) techniques were used for trace element measurements and Ion Chromatography (IC) was used for determination of SO_4^{2-} , NO_3^- and Cl.

A summary of analytical techniques used for trace elements and ions are presented in Table 3.2.

3.4.1. Determination of Major Anions by Ion Chromatography

Ion Chromatography was used to determine major anion concentrations in aerosol samples. The method has been a widely used for the simultaneous analysis of inorganic ions present in different matrixes such as natural waters, rain samples, aerosol samples etc. (Wang et al., 1983; Small et al., 1975).

Table 3.2. Analytical techniques of measured species.

Measured species	Analysis techniques
Pb, Cu, Cd, Ni, V, Cr	GFAAS (Perkin Elmer 1100B spectrophotometer coupled with HGA 700)
Na, Mg, Al, Cl, K, Sc, Ti, V, Cr, Mn, Fe, Co, Zn, Ga, As, Se, Br, Rb, Sr, Mo, Cd, In, Sb, Cs, Ba, La, Ce, Nd, Sm, Eu, Gd, Tb, Dy, Yb, Lu, Hf, Au, Hg, Th, U	INAA
Al, Zn, Fe, Ca, Mg	FAAS (Perkin Elmer 1100B spectrophotometer)
K, Na	FAES (Perkin Elmer 1100B spectrophotometer)
Cl ⁻ , NO ₃ ⁻ , SO ₄ ²⁻	HPLC (Vydac column with Jasco 875 UV-VIS detector)
NH ₄ ⁺	Colorimetric (Nessler's method)

It was essentially a high performance liquid chromatographic method (HPLC) using specific stationary and mobile phases that are suitable for the separation of ions.

Aerosol samples were analyzed for anions Cl^- , NO_3^- and SO_4^{2-} by using a Varian model 2010 HPLC coupled with a VYDAC 302 IC anion exchange column and it connected to the JASCO UV-VIS 875 detector. This system was connected to a Peak 2 software to calculate peak areas. Table 3.3 lists the operating conditions of the ion chromatography used during the experimental work.

One quarter of filter samples were placed into 100 mL polyethylene beakers containing 50 mL double distilled dieionized water. Beakers were placed into an ultrasonic shaker and sonicated for approximately 40 minutes. Then, the solution was filtered through 0.22 μm pore size cellulose acetate filter. A 100 μL portion of filtrates were directly injected to the IC..

The mobile phase was 1 mM phthalic acid adjusted to a pH of 4.95 with sodium tetraborate solution. This mobile phase was degassed for approximately 30 min prior to analysis to expel dissolved gases. Calibration curves were prepared with 0.5, 1.0, 2.0, 4.0, 5.0, 10.0 M solutions of NaCl , K_2SO_4 and NaNO_3 .

Table 3.3. Ion chromatographic parameters

Eluent	3 mM phytalic acid	Flow rate x mL min^{-1}
Separator column type	302 IC	2.46 x 25 cm
Injection volume	100 μL	
pH of mobile phase	4.95	
Flow rate	3 mL/min	

3.4.1.1. Preparation of Samples for Cl^- , NO_3^- and SO_4^{2-} Analysis

A quarter filter was placed into 100 mL beaker containing 50 mL deionized water. Beakers were placed into ultrasonic shaker and shaken 40 minutes. The solution was then filtered through 0.22 μm pore size cellulose filter and filtrate was directly used for ion analysis. If filtrates were not analyzed immediately, the cups containing filtrates were covered with parafilm, and they were kept at -4°C in the freezer until the day of analysis to avoid sample loss due to evaporation. It had been experienced in the early phases of the study that, significant amount of samples can be lost even when the filtrates were kept at refrigerator at 4°C if extreme precautions were not taken to minimize evaporation.

3.4.2. Determination of NH_4^+ by Colorimetry

Ammonium ion was determined spectrophotometrically using a Unicam 8625 UV-VIS Spectrometer. Direct Nesslerization method was used (Standard Methods, 1990), in this method Nessler's reagent which is a alkaline solution of mercuric iodide (K_2HgI_4) combines with NH_3 to form a yellowish-brown colloidal dispersion which intensity is directly proportional to the amount of NH_3 originally present. The reaction can be represented by the equation:



The absorbance of the colored solution was measured at 425 nm in a glass cell with an optical path length of 1 cm. Standard ammonium solutions were prepared from ammonium sulfate after drying it at 100°C for about 1 hour.

A new calibration curve was prepared each time when Nessler's reagent was changed.

3.4.2.1. Preparation of Samples

Filtered solution that was prepared for ion analysis was also used for determination of NH_4^+ . First, prepared samples were used for ion chromatography then the rest of the samples were used for ammonia determination.

3.4.3 Trace Element Determination by Atomic Absorption Spectrometry

Total amount of 310 daily collected PM-10 aerosol samples were analyzed by either flame atomic absorption (FAAS) and emission spectrometry (ES) or graphite furnace atomic absorption spectrometry (GFAAS).

3.4.3.1. Flame atomic absorption (FAAS) and emission spectrometry (ES)

The aerosol filter samples collected at the year 1992 were analyzed for major cations namely Al, K, Na, Mg, Fe, Zn and Ca by Flame atomic absorption and or emission spectrometry. A Perkin-Elmer 1100B model atomic absorption spectrophotometer connected to a Epson L-850 printer was used for the absorption measurements and recording. Major ions, including Na, K and Ca were analyzed by flame atomic emission spectrometry (ES). Magnesium, Fe and Zn were analyzed by flame atomic absorption spectrometry. Working instrumental parameters for these analyses are summarized in Table 3.4. With exception of Al, all elements were determined in air-acetylene flame. Al was determined in nitrous oxide-acetylene flame since this element may form some stable oxides and its atomization occurs at higher temperatures.

Before the analysis, the instrument was allowed to warm up for about 20 minutes. Position of burner and Hollow Cathode Lamp (HCL) were optimized to obtain maximum sensitivity. The solutions were directly aspirated to burner with 7-8 mL/min flow rate. Standard solutions used in calibration were prepared by necessary dilutions of commercially available 1000 mg/L stock solutions (Aldrich). Method of standard additions was used throughout the study.

3.4.3.2. Graphite Furnace Atomic Absorption Spectrometry (GFAAS)

Graphite furnace atomic absorption spectrometry was used to determine concentrations of Pb, Cu, Cd, Ni, V, and Cr, whose concentrations in collected samples were too low to be detected by flame AAS. A Perkin Elmer 1100B spectrophotometer coupled to Perkin Elmer HGA 700 electrothermal atomization system was used for GFAAS measurements. Deuterium lamp was used to correct for nonspecific background absorption. Argon was used as the purge gas. During the analysis, internal gas flow rate through the graphite tube was 300 mL/min; however gas flow was interrupted during atomization. Instrumental settings and temperature programs for each element are listed in Table 3.5 and Table 3.6, respectively.

Table 3.4. Working parameters used in Flame atomic absorption and emission measurements

Elements	Al	Zn	Fe	Ca	Mg	K	Na
Technique	FAAS	FAAS	FAAS	ES	FAAS	ES	ES
Wavelength, nm	309.3	213.9	459.4	422.7	285.2	766.5	589.0
Slit width, nm	0.7	0.7	0.7	0.7	0.7	0.7	0.7
Air, mL/min.	-	10.1	9.8	7.7	8.0	8.5	8.7
Acetylene, mL/min	7.0	2.2	2.2	2.1	2.0	1.6	1.4
N. Oxide, mL/min	5.0	-	-	-	-	-	-

Sample volume, ashing, atomization temperature, ramp and hold times were optimized before analysis to obtain maximum absorbance and minimum background. If it was possible, the average absorbance value was held about 0.4 to 0.6 and if the absorbance value exceeds the maximum absorbance value of the standards, the samples were diluted with distilled-deionized water.

Physical interference caused by the scattering of source radiation by the NaCl was reported for aerosol samples collected at marine sites (Sturgeon et al., 1979; Lindahl et al., 1984). The use of NH_4NO_3 and HNO_3 had been recommended to minimize such interference (Ediger et al., 1974; Sturgeon et al., 1979; Lindahl et al., 1984). Although the samples analyzed in this study were collected at a coastal station and they all contained high concentrations of Na and Cl which formed NaCl upon drying, light scattering did not cause a significant problem for most of the elements except Cr and Ni. The background problem in these two elements were solved by careful adjustment of temperature program. The addition of matrix was avoided as they increased the blank levels significantly.

During the analysis of refractory elements such as Cr, memory effect from the graphite tube was detected. Especially in samples with high concentration of Cr, some of the Cr deposited in the colder regions of the tube and appeared in the subsequent injections. This problem was solved by adding additional cleaning step to temperature program. The efficiency of the cleaning steps was tested by injecting high concentrations of Cr. The cleaning cycle was tuned until no Cr signal appeared in subsequent heatings.

Table 3.5. Working instrumental parameters in GFAAS

	Pb	Cr	V	Ni	Cu	Cd
tube	u ^a	p ^b	p	p	p	u
Wavelength, nm	283.3	357.9	318.4	232.0	324.8	228.8
Slit width, nm	0.7	0.7	0.7	0.2	0.7	0.7
Lamb current, mA	9	16	18	25	13	3
Sample volume, μL	25	20	100	25	20	25

^a. uncoated ^b pyrolytic coated

3.4.3.3. Preparation of Samples for AAS Analysis

In order to determine elemental concentrations in air particulates by atomic absorption spectrometry, it is necessary to bring the material into solution

which can be accomplished by acid digestion. For digestion and handling of samples, procedures developed in the WMO/UNEP Expert Meeting on Quality Assurance for the MED POL Airborne Pollution Measurements (27-30 May 1993) were followed.

One fourth of the aerosol filters transferred into a 250 mL teflon beakers, 30 mL of sub-boiled HNO_3 was added and beakers were closed with a teflon cover. Samples were refluxed for 10-12 hours at 130 ± 10 °C in a sand bath. After refluxing the clearness of the solutions were checked, if the solution were not clear enough some more acid (up to a total of 20 mL) was added and refluxing was continued for 6-8 more hours. Then the covers were removed from the beakers and HNO_3 was evaporated until its volume decreased to 10 μL . Then, 5 mL of supra pure HF acid was added to destroy the silicate matrix. The beakers were covered and acid was refluxed for 6-8 hour on a sand bath. At the end of refluxing, the covers were removed and heating was resumed until samples reached to near dryness. About 5 mL of concentrated HNO_3 were added and evaporation was repeated until the white fumes of HF was no longer be visible. The evaporation was repeated to ensure that the all of the added HF which can damage the nebulizer and other parts of the spectrometer was completely removed. When all HF was evaporated, samples were removed from the hot bath and allowed to cool. The residue was redissolved with 1% nitric acid in a 50 mL volumetric flask and made up to 50 mL with the same 1% HNO_3 solution and transferred to 100 mL acid washed teflon bottles.

Special attention was paid to avoid contamination of samples during handling. All labware and glassware were soaked in 30% HNO_3 overnight and rinsed several times with double distilled-deionized water.

3.4.3.4. Analysis of Standard Reference Materials

The accuracy of the AAS analyses flame and graphite furnace were tested by analysing standard reference materials (SRM) on a daily basis. Three different SRM's from NIST (GSP-1, SRM-1646 and SRM-2704) were digested

and analysed along with the samples. The reference materials were analysed every morning before starting the analysis and results were compared with the certified values. One of the SRM's and one of the standard's were selected and injected several times during a day to check the variations in the slope of the calibration line. If the results are close to the certified values, the analysis was resumed. All elements were analysed by standard addition method to eliminate the matrix effect. In general, very good agreement with the certified values was obtained for most of the elements.

Table 3.6. Graphite furnace temperature programs

	Step No	1	2	3	4	5	6	7
Pb	Furnace Temp. °C	90	130	800	2000	2200		
	Ramp Time, Sec.	5	10	10	0	1		
	Hold Time, Sec	15	18	15	5	2		
Cr	Furnace Temp. °C	90	130	1650	2500	2650		
	Ramp Time, Sec.	5	10	10	0	1		
	Hold Time, Sec	15	20	15	5	3		
V	Furnace Temp. °C	90	130	60	90	130	1400	2650
	Ramp Time, Sec.	5	10	0	5	10	9	0
	Hold Time, Sec	22	25	5	25	25	10	8
Ni	Furnace Temp. °C	90	130	1400	2500	2650		
	Ramp Time, Sec.	5	10	10	0	1		
	Hold Time, Sec	15	18	20	5	3		
Cd	Furnace Temp. °C	90	130	700	2000	2300		
	Ramp Time, Sec.	5	10	10	0	1		
	Hold Time, Sec	15	18	15	5	3		

3.4.4. Instrumental Neutron Activation Analysis

Highly sensitive nuclear methods of analysis have been developed for measuring concentrations of up to fifty elements in individual samples of many types of environmental samples. With the introduction of high resolution Ge(Li)

γ -ray detector in the mid-sixties the instrumental neutron activation analysis (INAA) became one of the most widely used analytical technique for the analysis of airborne particulate matter, and it still holds its position (e.g. Zoller and Gordon, 1970; Tuncel et al., 1989; Ondov et al., 1990; Hacisalihoglu et al., 1992).

Neutron activation analysis uses the production of radionuclides from the elements present in the sample for the identification and quantitative determination of these elements. The samples to be analysed are irradiated with thermal neutrons in a nuclear reactor. As a result of nuclear reactions, i.e.(n, γ) reactions, between these neutrons and the stable isotopes of the elements, radionuclides may be produced. The radiation emitted by the decaying radionuclides is measured with a γ -ray detector. Decay corrected activity can be calculated by the formula:

$$A_o = \frac{A\lambda e^{-\lambda t_1}}{1 - e^{-\lambda(t_2 - t_1)}} \quad (1)$$

where, A_o : decay corrected count rate at the end of the irradiation

A : measured activity

t_1 : time out of the reactor to beginning of counting

t_2 : time out of the reactor to end of counting.

Concentrations of elements in each sample are then determined by comparing the activities of isotopes in samples with those in standard materials which are irradiated together with samples. The unknown element concentrations in the sample can be calculated by using the following formula:

$$m_x = m_s \frac{A_s}{A_x} \quad (2)$$

where, m_x : mass of the element in the sample

m_s : mass of the element in the standard

A_x : decay corrected activity of the sample

A_s : decay corrected activity of the standard.

There are sufficiently developed software's for identification of γ -ray peaks and determination of their area. These programs mainly consist of a search for statistically significant γ -ray peaks, and the resolutions of pairs of unresolved peaks and the calculation of the net counting rate due to the isotopes present in the complex spectra. The γ -ray spectra obtained at the end, are processed by computer packages for each energy line and are compared with that of standards irradiated with the sample.

3.4.4.1. Trace Element Determination by Instrumental Neutron Activation Analysis

All of the aerosol filters collected in 1993 were analysed by instrumental neutron activation analysis using a procedure developed by Ölmez (1989). The INAA facilities at Massachusetts Institute of Technology, Nuclear Reactor Laboratory (MITR-II) were used. The aerosol filters were irradiated twice in the 5 MW MITR-II research reactor at a neutron flux of $8 \times 10^{12} \text{ n cm}^{-2} \text{ s}^{-1}$. For analysis of short lived isotopes, samples were irradiated for 1 min and immediately counted for 5 minutes. At the end of so called "short-l" count, samples were recounted for 20 min to determine the γ -activity from isotopes with half-lives ranging between 2.25 minutes (Al) and 14.96 hours (Na). Samples were then allowed to decay 7-10 days. After activities of short lived isotopes decrease sufficiently, they were re irradiated at the same neutron flux for 12 hours and counted for 12 hours with high purity Ge detectors. γ -rays emitted from the irradiated samples were collected with high purity germanium γ -ray detectors coupled to a 8192-channel pulse-height analysers (Canberra, CT). The spectra were analysed using computer programs (ND 9900 Genie system run on VMS 200, Canberra, CT) to search for the γ -peak(s) of each isotope. The concentrations of elements are determined by comparing the activities of

isotopes in standard material, SRM #1633 (flyash). γ -ray energies used for the determination of elemental concentrations are given in Table 3.7. Accuracy of the analytical technique was checked by analysing NIST Standard Reference Material # 1571 (orchard leaves) along with samples.

A pneumatic tube facility in the research reactor shorten the sample transfer time down to 3-4 sec which was crucial in this study, particularly in the analysis of short-lived isotopes, since the irradiation time was only 1 min, the decay time would be significant for very short lived elements such as Al if the transfer time between reactor and counting system were long.

3.4.4.2 Preparation of Samples

All sample handling prior to analysis were done in clean area. When collected filters were delivered from the station, they were divided into four equal parts in the clean area available in the METU Environmental Engineering Department taking all necessary precautions to protect the sample from contamination during sample handling. One quarter of the filters were placed in acid washed polyethylene bags, heat sealed and carried to the MIT Nuclear Reactor Laboratory for INAA. Samples were reopened at the Massachusetts Institute of Technology (MIT) reactor laboratory in a laminar flow clean hood. Since the concentrations were expected to be very low in these samples, all tools used to prepare filters for irradiation were acid-washed with diluted nitric acid, rinsed with deionized water and air dried on the clean workbench under laminar HEPA filtered air flow. When not in use, cleaned tools stored in a closed polyethylene container.

Using clean tools, one fourth of the quarter filters were cut. Each one of the cut piece was folded with the sample side facing inward. Since the geometry of samples and blanks are very important in INAA, all of the samples and the blanks were folded to the exactly same size.

Table 3.7. γ -ray energies used in the determination of concentrations

Element	Half-life	Key Energy (keV)	Scanning Stage	Element	Half-life	Key Energy (keV)	Scanning Stage
Al	2.25 m	1779.0	Short-1	Te	1.35 d	149.8	Long-1
Cu	5.10 m	1039.3	"	W	0.99 d	479.6	"
Mg	9.45 m	843.8	"	U	2.36 d	106.4	"
Ti	5.76 m	320.1	"	Yb	4.19 d	393.3	"
V	3.76 m	1434.1	"	Ce	0.09 y	145.4	Long-2
Ba	1.39 m	165.9	Short-2	Cs	2.07 y	795.9	"
Cl	0.62 h	1642.4	"	Cr	0.08 y	320.1	"
Dy	2.33 h	94.7	"	Co	5.27 y	1173.2	"
Ga	14.1 h	834.1	"	Eu	13.5 y	1408.0	"
In	0.90 h	417.0	"	Gd	0.66 y	97.4	"
I	0.42 h	442.9	"	Hf	0.12 y	482.1	"
Mn	0.58 h	846.8	"	Ir	0.20 y	316.5	"
Na	14.96h	1368.6	"	Fe	0.12 y	1099.2	"
Sr	0.29 h	388.4	"	Lu	0.02 y	208.4	"
Sb	2.70 d	564.1	Long-1	Nd	0.03 y	91.1	"
As	1.09 d	559.1	"	Rb	0.05 y	1076.7	"
Br	1.47 d	554.3	"	Sc	0.23 y	889.3	"
Cd	2.23 d	336.3	"	Se	0.33 y	264.7	"
Au	2.70 d	411.8	"	Ta	0.31 y	1221.4	"
La	1.48 d	487.0	"	Tb	0.19 y	298.6	"
Mo	2.75 d	140.5	"	Th	0.07 y	311.9	"
K	0.52 d	1524.6	"	Zn	0.67 y	1115.5	"
Sm	1.93 d	103.2	"	Zr	0.18 y	724.2	"

After folding, samples and blanks were placed in ultra thin, acid washed polyethylene bags and each bag was clearly labelled according to the sample identification number. After irradiation, filters were removed from the polybags they were irradiated in and placed into polybags for counting. It is well known that cellulose filters become brittle and flaky upon proton irradiation with thermal neutrons. Although this characteristics of the filters may result in loss of sample during their transfer from polyethylene bags to vials, with the exception of few sample, this problem was not observed in this study.

In order to determine the variability of trace elements concentrations in filters used, several blank filters were analysed together with the samples. As trace elements may also be introduced to samples as a result of improper sample handling, unclean bags used in transportation, handling of sample at the field and the sampling apparatus itself, field blank samples were also analysed in addition to filter blanks. Same sample preparation procedures were applied to those blank filters. Handling of blank filters in the field and laboratory was similar to handling of samples.

National Institute of Standards (NIST) Standard Reference Material SRM-1571 orchard leaves was routinely used to check the accuracy of the analysis and SRM 1633 was used as standard material. A known amount of SRM was weighed to the nearest 0.01 mg in a temperature controlled room. The weighted SRMs was transferred into precleaned, ultra thin polyethylene bags and heat sealed. One of each SRM standards were included to each set of samples irradiated.

3.4.4.3 “Short” Irradiations and Counting

Since γ -rays emitted from the irradiated samples were counted using four high purity germanium γ -ray detectors, four filters one for each detector that were folded and heat sealed into precleaned and labelled polyethylene bag and four SRM's (both flyash and orchard leaves) which were carefully weighted (4-5

mg) and heat sealed in polybags were inserted in a prewashed pneumatic tube sample carriers called "rabbits".

Using pneumatic tube system available in the reactor laboratory, rabbits were transferred to 5 MW MITR-II research reactor which had a thermal neutron flux of $8 \times 10^{12} \text{ n cm}^{-2} \text{ s}^{-1}$ and irradiated for 1 min. At the end of irradiation rabbit was transferred back from the reactor to the sample processing area. In the sample processing area rabbits were opened behind a lead shield and irradiated samples and standards were taken out. Irradiated polyethylene bags containing samples were replaced with unirradiated one to avoid unnecessary blank and samples and standards were counted immediately twice; first for 5 min (Short-1) and then for 20 min (Short-2). The first γ -ray spectrum which was collected for 5 minutes was analysed for the determination of ^{27}Mg , ^{51}Ti , ^{49}Ca , ^{52}V , ^{66}Cu and ^{28}Al . Then samples were allowed to decay for 10 minutes and a second γ -ray spectrum was acquired from each sample by counting for 20 minutes. This second spectrum was analysed for ^{24}Na , ^{38}Cl , ^{42}K , ^{56}Mn , $^{69\text{m}}\text{Zn}$, $^{116\text{m}}\text{In}$, ^{128}I , and $^{87\text{m}}\text{Sr}$ isotopes. Typical γ -ray spectra for Short-1 and Short-2 counts are given in Figures 3.4 and 3.5, respectively.

3.4.4.4 Long Irradiations of Samples

Upon completion of the short irradiation, irradiated samples, blanks and standards were set aside to decay for two to three weeks. After short lived isotopes decayed completely, approximately 40 previously irradiated samples, blanks and SRM's were placed into a new prewashed rabbit. Besides SRM's which were normally used as standards, a synthetic standard was also prepared for mercury determination. A known amount of mercury standard (4 to 5 mg) was placed into precleaned polyethylene bag and to eliminate any loss of mercury from the standard, the standard was encapsulated into a clean quartz tube. In the MIT's reactor, irradiation port is cooled to room temperature, therefore fast neutron beam intensity was kept at minimum. This unique property of the reactor effectively eliminates any loss of mercury due to the

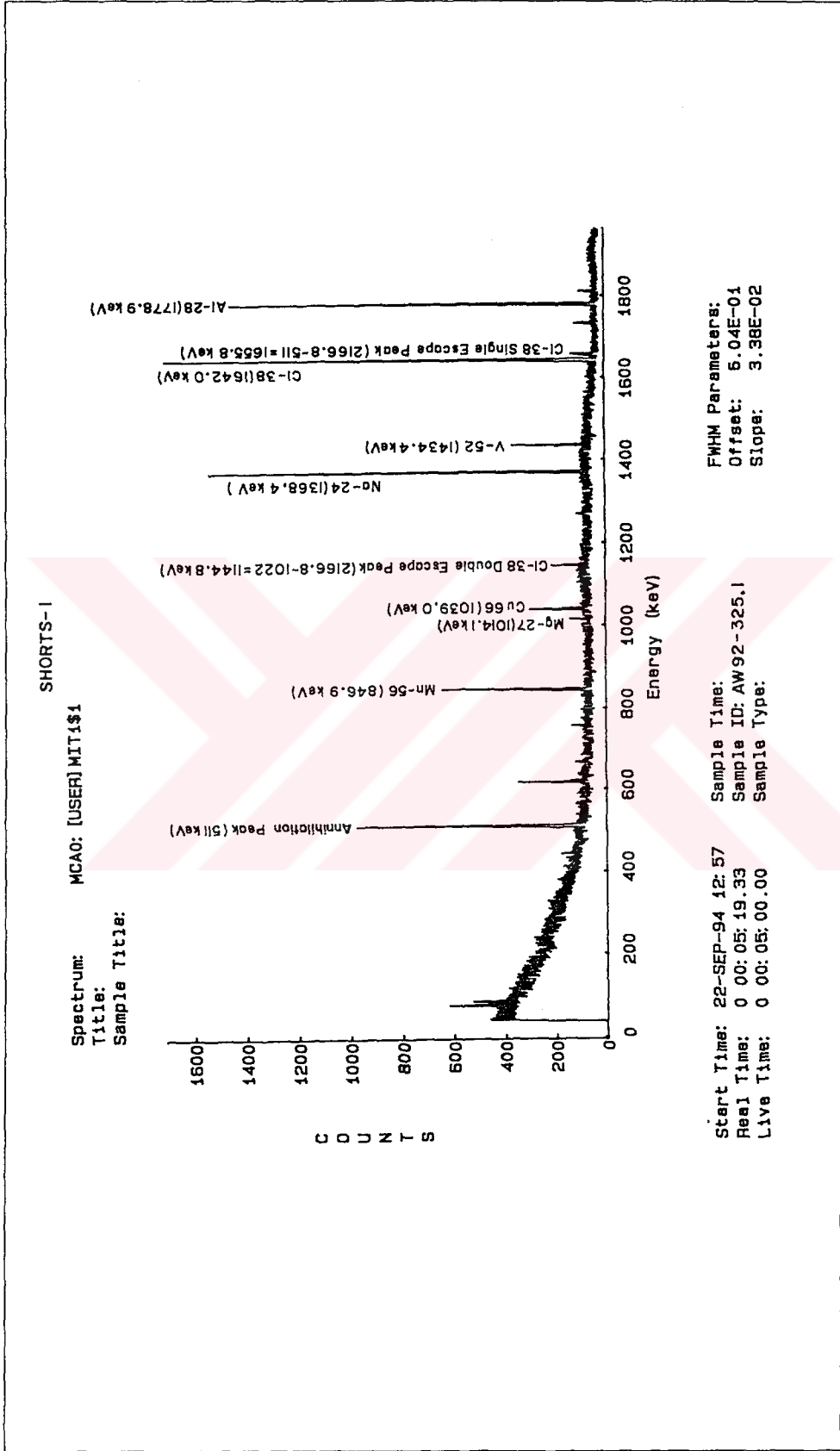


Figure 3.4 A typical gamma-ray spectra for Short-1 counts

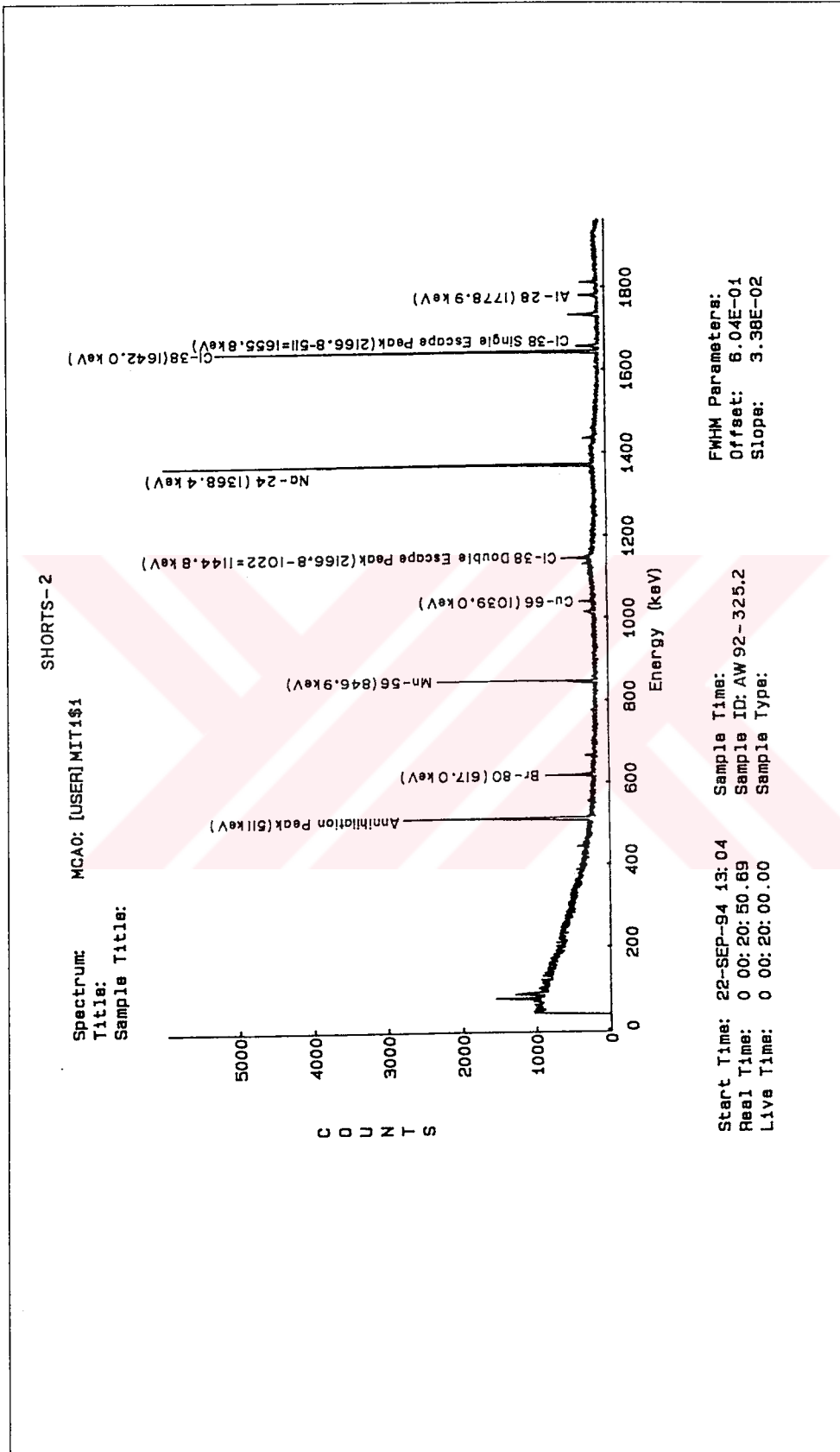


Figure 3.5 A typical gamma-ray spectra for Short-2 counts

sample heating, so that except mercury standard there was no need to encapsulate samples in quartz tubes which saved time and money.

For long irradiation, prepared rabbit was transferred to the reactor and irradiated for 12 hours. After irradiation, rabbits were allowed to decay for 3 to 4 days after which they were cooling rabbit transferred from the reactor, they were opened behind a lead shield and irradiated sample containing polyethylene bags were replaced with clean one and counted for 6 hours. The γ -ray emission from the samples was measured with a high purity Germanium detector with FWHM of about 1.75 keV for the 1332 keV line of Co-60. Samples were counted for 6 hours approximately three days after irradiation for the determination of ^{24}Na , ^{42}K , ^{68}Zn , ^{72}Ga , ^{76}As and ^{83}Br , ^{99}Mo , ^{115}Cd , ^{122}Sb , ^{140}La , ^{153}Sm , ^{175}Yb , ^{177}Lu , ^{187}W , ^{198}Au , ^{48}Sc , ^{51}Cr , ^{59}Fe , ^{60}Co , ^{65}Zn , ^{75}Se , ^{95}Zr , ^{86}Rb , ^{110}Ag , ^{124}Sb , ^{131}Ba , ^{134}Cs , ^{141}Ce , ^{147}Nd , ^{152}Eu , ^{160}Tb , ^{177}Lu , ^{181}Hf , ^{182}Ta , and ^{192}Ir isotopes. A typical γ -ray spectra for Long Irradiations is given in Figure 3.6.

3.4.4.5 Analysis of the γ -Ray Spectra

The spectra obtained at the end of short and long Irradiations were analysed using computer programs, ND 9900 Genie system run on VMS 200 to search for the γ -peak(s) of each isotope.

Before spectra of samples were collected, the detector was calibrated for energy using isotopes with known γ -peaks. The ^{22}Na (511 and 1274.4 keV), ^{60}Co (1173.2 and 1332.5 keV) and ^{137}Cs (661.6 keV) were used in the energy calibration. All parameters describing the samples (sample ID, irradiation time, counting time, etc.) were entered and saved with the spectra.

Computer program uses peak shape parameters which can be calibrated using actual peaks in samples to improve the accuracy, consistency and speed of fitting. The peak shape function consists of a Gaussian centre

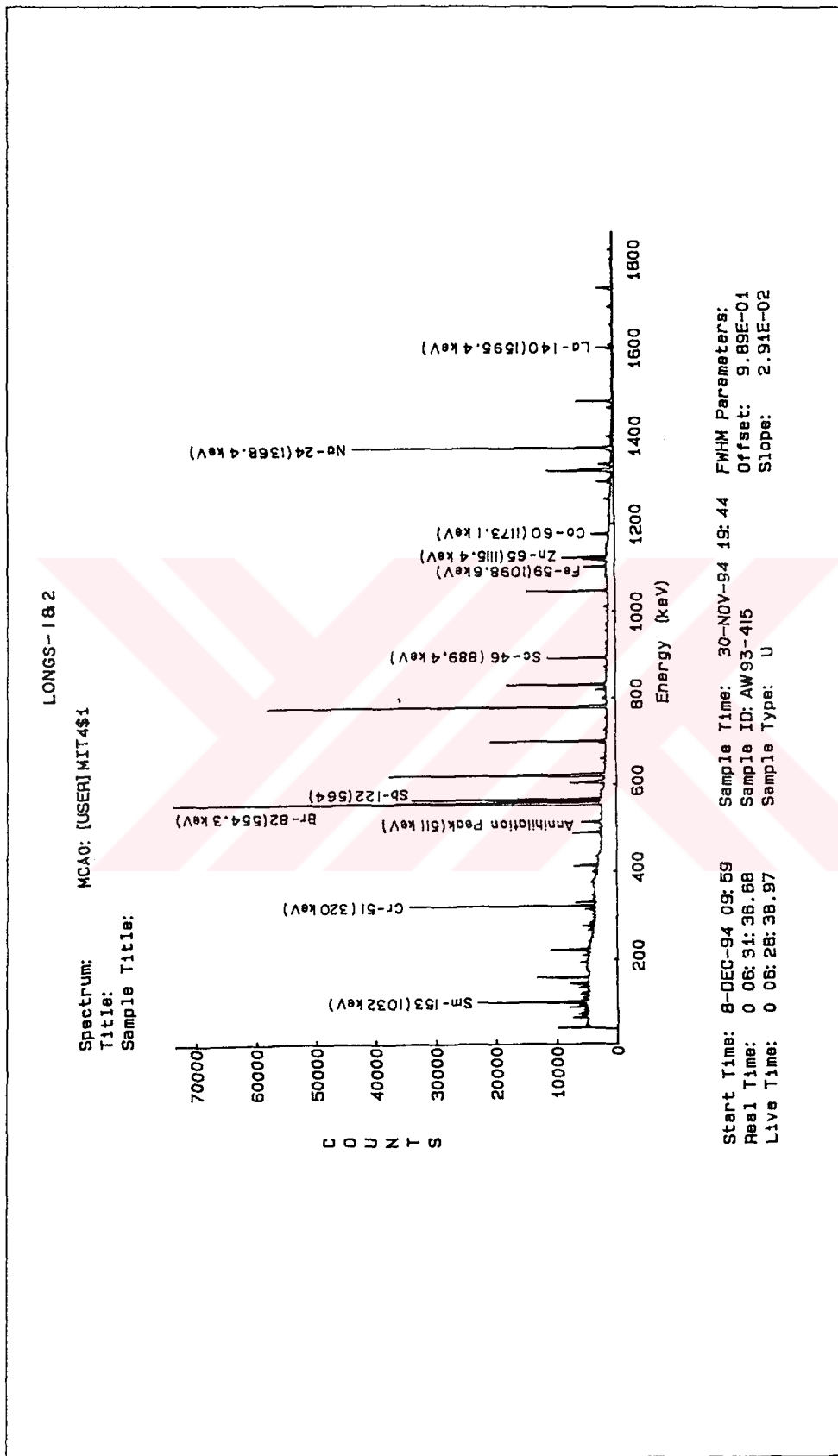


Figure 3.6 A typical gamma-ray spectra for Long counts

part and exponential upper and lower tails which are joined smoothly to the Gaussian part. The fitting intervals are determined automatically by the program but they can be changed by the user.

The program uses the available library which includes for each nuclide; its label, proton and neutron number, half-life, number of gamma lines and their energies and branching ratio. Since the library provided by the software includes too many isotopes which are not normally observed in aerosol samples, separate dedicated libraries were prepared for the analysis of first and second counts long spectra.

The nuclide identification procedure is started by comparing the energy of each spectrum peak with the energies of the gamma lines of the nuclides in the gamma library. If the energies match with a given tolerance for a gamma line nuclide, it is possible that this nuclide is present and its other peaks are checked.

3.5. Data Quality Assurance

3.5.1. Blanks

Since the concentrations of measured species were expected to be low in measured samples due to the sampling location, contamination from every source tried to be kept under control as much as possible. In order to determine degree of contamination in aerosol samples, field and laboratory blanks were prepared.

Field blanks were prepared in the same way as the samples were taken from the samplers. Field blanks for aerosol samples were treated similarly with sample filters, except air was pulled through blanks for only one minute. Average concentrations of eight field blank samples were given in Table 3.8.

Table 3.8. Average Filter Blank Concentrations and Standard Deviations (ng/100cm² filter)

Element	Avg. Blank Conc.	STD	Element	Avg. Blank Conc.	STD
Na	20520	5300	Cd	9.2	12.2
Mg	8500	2750	In	0.67	0.37
Al	5400	1900	Sb	3	0.5
Cl	60000	5800	Cs	1.5	0.7
K	4800	3300	Ba	890	400
Sc	0.56	0.11	La	2.6	1.1
Ti	820	260	Ce	5.2	1.9
V	14	7	Nd	12	6
Cr	1000	260	Sm	0.37	0.04
Mn	100	30	Eu	0.44	0.19
Fe	3400	520	Gd	0.3	0.2
Co	3.7	1.1	Tb	0.28	0.07
Zn	215	80	Dy	3.7	0.6
Ga	480	190	Yb	0.25	0.09
As	2.96	1.48	Lu	0.05	0.03
Se	3.7	0.7	Hf	0.5	0.3
Br	300	75	Au	0.37	0.3
Rb	9	2	Hg	4.26	0.75
Sr	410	20	Th	0.52	0.11
Mo	20	7	U	5.6	2.6

In order to have an idea of the blank contributions, percent blank subtraction were calculated and results are given in Figure 3.7 for INAA technique. Figure 3.7 also shows percent of observance of an element above blank level. An inverse correlation has been found between percent blank contribution and percent observance of an element above blank level. As the blank contribution increases, after blank subtraction more samples have concentrations below detection limit. Higher blank contribution (greater than 30%) were observed for the elements Ba, Cd, U, Cr, Ga and Au, for these elements frequency of observance is around 60% for Ba, Cd, U and Cr and for Au and Ga only 20% of the total samples have concentration values above blank level. For the rest of the elements blank contribution is less than 20% which means that most of the measured species can be determined reliably using the mentioned sampling and analytical procedure and contribution of blank subtraction on the uncertainties are small.

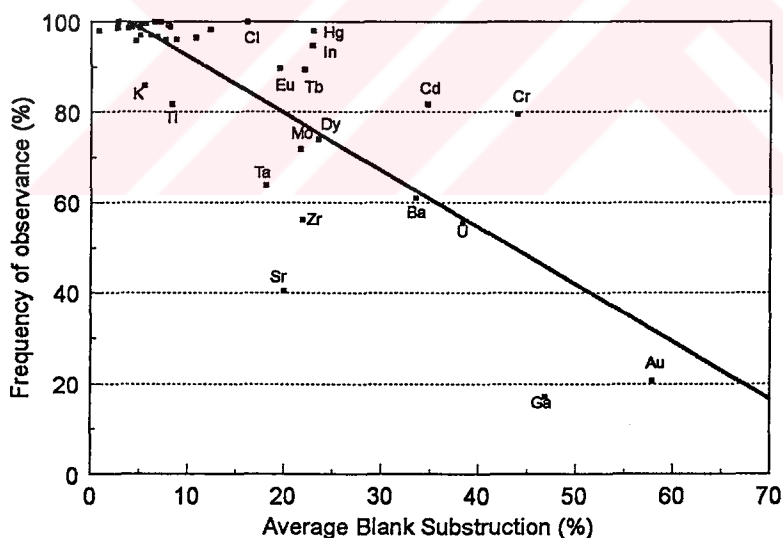


Figure 3.7. Plot of percent blank subtraction and percent of observance of samples analyzed by INAA

For AAS analysis, percent blank subtraction were calculated and results are given in Figure 3.8 together with percent of observance of an element above blank level. Similar inverse correlation as observed in INAA analysis has been

found between percent blank contribution and percent observance of an element above blank level. Around 50% blank contribution was observed for Cd in which frequency of observance is around 60%. High blank subtraction was also found for Pb. The reason of high blank contribution is probably due to low ambient concentration Cd and Pb in the sampling region. Although for Pb, around 50% blank contribution was found, 85% of the total samples have Pb concentration values above blank level. For Ni and Zn, above 30% blank contribution was found, however, only 5% of the samples have below detection limit for Ni and Zn. For these elements and the elements having blank contribution less than 20% while frequency of observance is around 95%, it can be said that, measured species were determined reliably using the mentioned sampling and analytical procedure and contribution of blank subtraction are small.

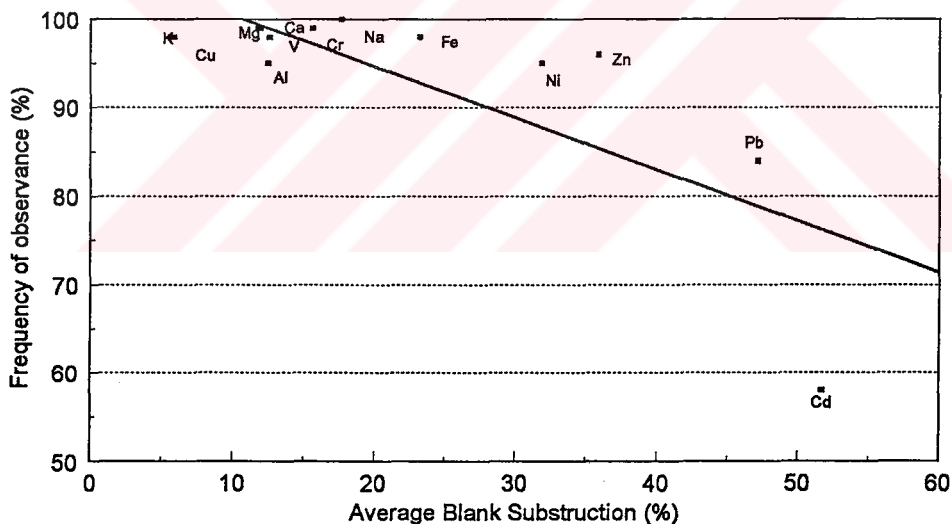


Figure 3.8. Plot of percent blank subtraction and percent of observance of samples analyzed by AAS

In addition to field blanks, laboratory blanks were also prepared in order to determine source of contamination observed in field blanks. For the INAA analysis, laboratory blanks consist of unused Whatman 41 filter paper. However, for the AAS analysis, laboratory blanks did contain only used reagents

and deionized water. During acid digestion procedure, several laboratory blanks were prepared parallel to the real samples. Therefore it is possible to find the contamination contribution of used reagents. All these blank samples were analysed along with the analysis of samples. To determine the source of contamination the results of field blanks and laboratory blanks for the INAA analysis were compared, and it has been found that almost 95% of the contamination arise from filter itself. Since in the INAA analysis, sample pre-treatment before analysis is minimum, contamination during sample handling is only contribute 5% as an average. However, for the AAS analysis, different contamination sources for each element were found. Since in the AAS analysis, during sample pre-treatment a number of contamination sources exist like used reagents, deionized water etc., for each element different ratios of laboratory blank to field blank were observed. Percent of laboratory blank to field blank is given in Figure 3.9. As it is shown in Figure 3.9, for V, Zn, Al, and Mg contribution of filter as a contamination source is less than 10%. For Na and Cu, only 50% of contamination are attributed to laboratory blank, rest of the contamination is arises due to sample handling and from filter itself. For the rest of the elements, contribution of filter as a contamination source is around 20-25%, 75-80% of contamination are attributed to the used reagents.

3.5.2. Detection limits of the analytical methods

As investigating trace substances in the air a serious effort has been spend to measure a true state of nature. However, many of the today's air quality problems are associated with chemical levels too low to be measured precisely. Therefore, for the data set with so many values below detection limit, determination of detection level should be the first step of data analysis for the used analytical technique.

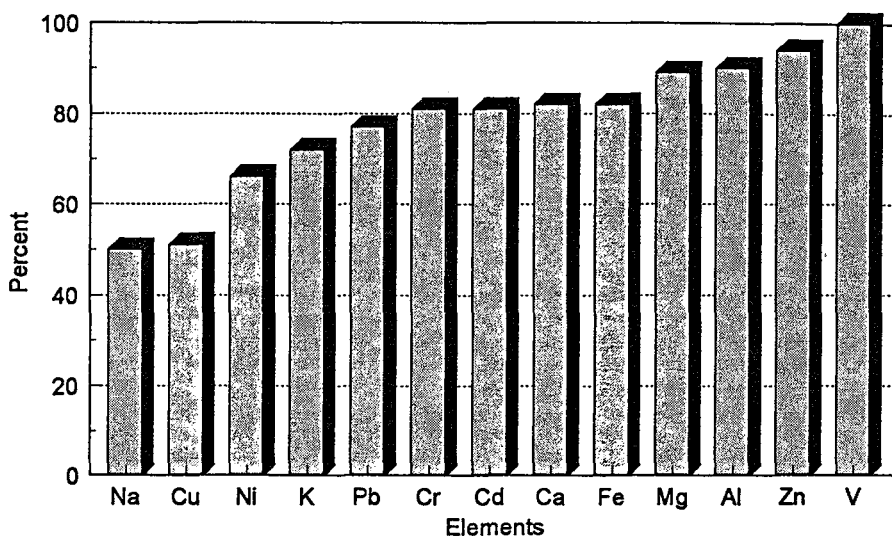


Figure 3.9. Percent of laboratory blank to field blank for AAS Analysis

The detection limits in analytical methods depend upon the sensitivity of the technique and on the composition of the sample. In INAA technique, the detection limit is determined by several factors; intensity of neutron flux, background in the g-ray spectrum, experimental parameters and composition of the sample. That is, detection limits are unique to each sample and determined by both element concentrations and the presence of other individual elements. A high concentration of a single element yields high background levels in the spectra and may result in poor signal-to-noise ratios. The result is a higher detection limit in that sample for the rest of the elements. For these reasons, generally valid detection limits cannot be provided for the INAA technique.

The detection limits in AAS are also influenced by many factors, but are ultimately determined by the sensitivity and by the fluctuation of the background.

In practice, the detection limits are determined by the variability of the blank value for the analytical method.

In analysis of atmospheric aerosol, commonly used definition of detection limit is "twice the standard deviation of a number of replicates analysis of a field blanks" (Galasyn et al., 1987; Dzubay and Stevens, 1984). Calculated detection

limits according to the above definition for INAA results and AAS are given in Table 3.9 and 3.10, respectively.

As shown in Tables 3.9 and 3.10, all detection limits at both INAA and AAS technique are much smaller than corresponding observed concentrations.

3.5.3. Error Propagation

The analytical errors were quantified by considering all possible error sources and by calculating the propagation of each error using the error propagation law. The error analysis covers, the preparation of filter (weighing of filter before and after sampling), the determination of elemental concentrations using analytical techniques (INAA, Ion Chromatography, AAS), the blank values of elemental concentrations in filters, volumetric errors from the chemicals used for digestion and all volumetric flasks, teflon digestion vessels. The systematic errors such as bounce-off the particles, differences between the collection characteristics and sampling efficiencies of the high volume pump when flow rate changes could not be quantified exactly.

For the INAA results, average percent statistical uncertainty in sampling and analysis were calculated using error propagation law. In error propagation, statistical errors in γ -ray counting were coupled with the uncertainties in volume determination, weighing of filters etc. The errors in volume and weighing were assumed to be 5% although it might probably be smaller than this value, a conservative value was assumed to avoid bias in calculations. The magnitudes of propagated errors are mostly determined by the statistical uncertainty in γ -ray counting, which changes from element to element, and which also depends on composition of the sample. Calculated average percent statistical uncertainty is given in Figure 3.10 together with frequency of observance of the element during entire analysis. For the elements having average statistical uncertainty greater than 50% and the elements observed less than 70% of the samples were not considered as reliable elements and were not included in the discussions. As can be seen in Figure 3.10, In, Cd, Ba, Ta, Au, U, Sr, Ga, and Ir

Table 3.9 Calculated detection limits for the elements observed by INAA
(ng/27 cm² filter)

Element	Detection Limit	Average Conc.	Element	Detection Limit	Average Conc.
Na	2.9 •10 ³	1.8•10 ⁵ ±2.3•10 ⁵	Cd	6.6	13.5±25.1
Mg	1.5 •10 ³	5.5•10 ⁴ ±4.3•10 ⁴	In	0.2	1.12±0.72
Al	1.04•10 ³	6.5•10 ⁴ ±8.0•10 ³	Sb	0.22	42.3±23.9
Cl	3.1•10 ³	2.6•10 ⁵ ±4.0•10 ⁵	Cs	0.4	11.7±8.8
K	1.8•10 ³	4.4•10 ⁴ ±3.9•10 ⁴	Ba	220	960±960
Sc	0.06	12.9±16.8	La	0.6	42.1±45.2
Ti	1.4•10 ²	5050±5050	Ce	1	82.1±114.1
V	3.8	275±210	Nd	3.2	73.2±110.9
Cr	1.4•10 ²	660±470	Sm	0.02	6.14±8.81
Mn	16	1100±910	Eu	0.1	1.46±1.87
Fe	2.8•10 ²	4.5•10 ⁴ ±5.8•10 ⁴	Gd	0.1	5.94±9.21
Co	0.6	30.2±41.7	Tb	0.04	0.75±1.04
Zn	42	1400±1300	Dy	0.3	7.44±7.73
Ga	1 •10 ²	3.7 •10 ² ±4.8 •10 ²	Yb	0.05	2.52±3.37
As	0.8	190±160	Lu	0.016	0.43±0.59
Se	0.4	35.9±22.9	Hf	0.16	3.71±5.35
Br	40	2300±2700	Au	0.16	0.09±0.12
Rb	1	110±115	Hg	0.4	12.7±19.7
Sr	10	880±830	Th	0.06	11.9±15.1
Mo	4	100±160	U	1.4	6.94±9.73

Table 3.10. Calculated detection limits for the elements observed by AAS (mg/filter)

Element	Detection Limit (ng/27 cm ² filter)	Average Concentration (ng/27 cm ² filter)
Na	$7 \cdot 10^3$	$3.0 \cdot 10^5 \pm 2.2 \cdot 10^5$
Mg	$3.24 \cdot 10^3$	$36.6 \cdot 10^3 \pm 4.7 \cdot 10^3$
Al	$2.97 \cdot 10^3$	$67.5 \cdot 10^3 \pm 37.8 \cdot 10^3$
K	$1.62 \cdot 10^3$	$47.5 \cdot 10^3 \pm 32.3 \cdot 10^3$
Ca	$18.5 \cdot 10^3$	$28 \cdot 10^4 \pm 97 \cdot 10^4$
V	50	370 ± 180
Cr	27	400 ± 185
Fe	$5.67 \cdot 10^3$	$52 \cdot 10^3 \pm 27 \cdot 10^3$
Ni	90	360 ± 175
Cu	780	19700 ± 19500
Zn	$1.2 \cdot 10^3$	$4.5 \cdot 10^3 \pm 3.0 \cdot 10^3$
Cd	60	110 ± 80
Pb	$1.5 \cdot 10^3$	$4.4 \cdot 10^3 \pm 1.4 \cdot 10^3$

are the elements either with high statistical uncertainty or observed less than 70% of the samples, therefore excluded from the data analysis. For the rest of the elements, frequency of observation and average statistical uncertainty are tabulated in Table 3.11.

Except for the elements Cl, K, Ti, Br, Eu, Tb, Dy, Yb, Lu and Hg, the average percent statistical uncertainty were less than 15%. Calculated high uncertainty for Cl is due to used standard material fly ash (SRM-1633). The Cl content of the SRM fly ash is not reliable therefore instead of SRM-1633 Cl value, by making necessary corrections orchard leaves (SRM-1572) Cl value was used for the standard and due to the corrections 50% of error for Cl were

accepted. For the rest of the elements with high uncertainties, the source of the reason is found to be mainly from step of counting statistics and the extraction of net peak areas which is due to the low concentrations of these elements.

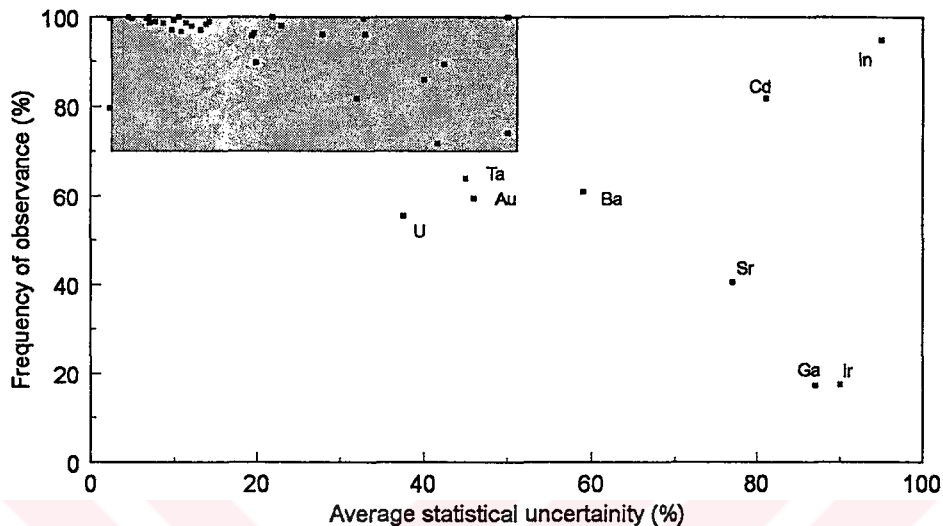


Figure 3.10. Calculated average percent statistical uncertainty and average frequency of observance of the elements measured by INAA

To calculate the propagated uncertainties in AAS results, the uncertainties arise during the following steps were considered;

1. uncertainty in absorbance reading for both samples and blanks which has been assumed to be 5% for GFAAS and 2 % for AAS,
2. uncertainty in standard preparations,
3. uncertainties in computing the slope of the calibration curve obtained by least squares method for each element,
4. uncertainty in the volume measurements,
5. uncertainty during weighing of filters.

The uncertainty associated with the AAS results in these steps were calculated for each sample by using error propagation law and average statistical uncertainties were calculated for each element and presented as a percent of the average concentration in Table 3.12 Percent frequency of observance of each element is also tabulated in the Table 3.12

Table 3.11. Elements observed by INAA, frequency of observation and Average Percent Statistical Uncertainty

Element	Frequency of observation (in 330 samples)	Statistical uncertainty (%) ^a
Na	100	9
Mg	100	5
Al	100	9
Cl	100	50
K	86	44
Sc	100	9
Ti	82	32
V	99	9
Cr	79	8
Mn	100	5
Fe	100	9
Co	100	10
Zn	99	25
As	98	13
Se	100	15
Br	100	33
Rb	96	20
Sb	100	11
Cs	97	14
La	97	11
Ce	100	9
Nd	98	15
Sm	99	12
Eu	89	20
Gd	92	12
Tb	90	42
Dy	74	50
Yb	96	33
Lu	96	28
Hf	96	20
Hg	97	24
Th	99	10

^a Statistical uncertainty includes statistical errors in γ -ray counting, uncertainties in volume determination and weighing of filters.

Table 3.12. Elements observed by AAS, frequency of observation and Average Percent Statistical Uncertainty

Element	Frequency of observation (in 309 samples)	Statistical uncertainty ^a (%)
Na	99	14
Mg	100	18
Al	97	15
K	99	14
Ca	99	15
V	100	19
Cr	100	17
Fe	99	15
Ni	94	18
Cu	100	16
Zn	97	16
Cd	60	18
Pb	86	17

^a Statistical uncertainty includes errors in absorbance reading of samples, uncertainty in standard preparations, uncertainties in computing the slope of the calibration curve, errors in the volume measurements and errors during weighing of filters.

As it is shown, for the AAS technique, the calculated percent of the propagated error were less than 10% for most of the elements. This shows that contribution of the errors during the mentioned steps to the observed concentrations were to be low to be considered as a significant contribution. Except Cd and Pb, the frequency of observance of elements in samples are higher than 90%.

3.5.4. Participation to Intercalibration Studies

Accuracy of laboratory practises can be best assessed by participating intercalibration exercises conducted by a central unit. For intercalibration of sample pre-treatment and analysis procedures of aerosol samples, a blank Whatman 41 filter, a reference aerosol sample coarse fraction and a reference aerosol sample fine fraction were prepared and distributed by WMO to various laboratories including us. These samples were analysed in the MIT Nuclear Reactor Laboratory with INAA and the results were sent to the central unit. The results obtained from different laboratories participating in this exercise were compared with true concentrations by the distributors. An example of the intercalibration results are presented in Figure 3.12 and 3.13 which show atmospheric concentrations of fine fraction As and Fe, and concentrations of coarse fraction V and Al measured independently by 19 different laboratories all over the world. An examination of these results obtained from 19 laboratories for 48 different elements shows good agreement and the precision in the case of some elements as well as an analytical bias between the results.

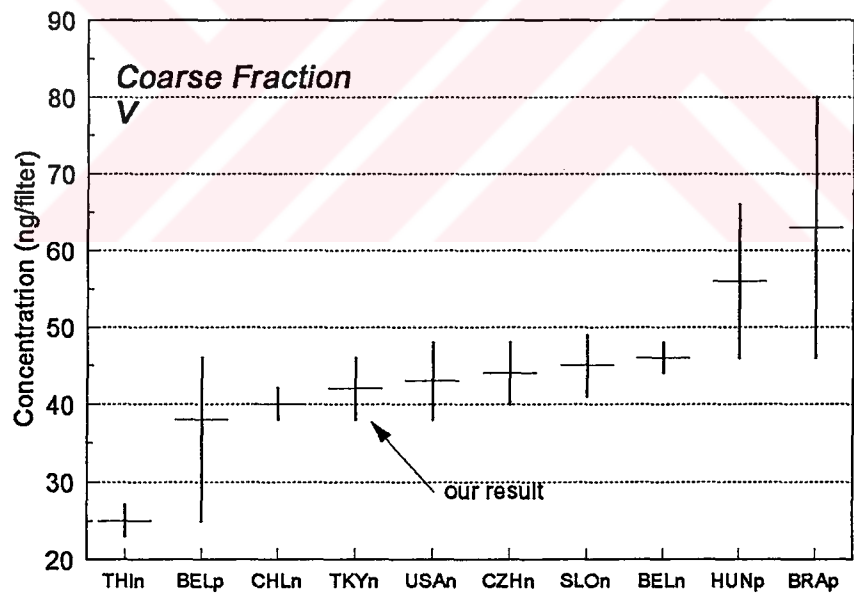
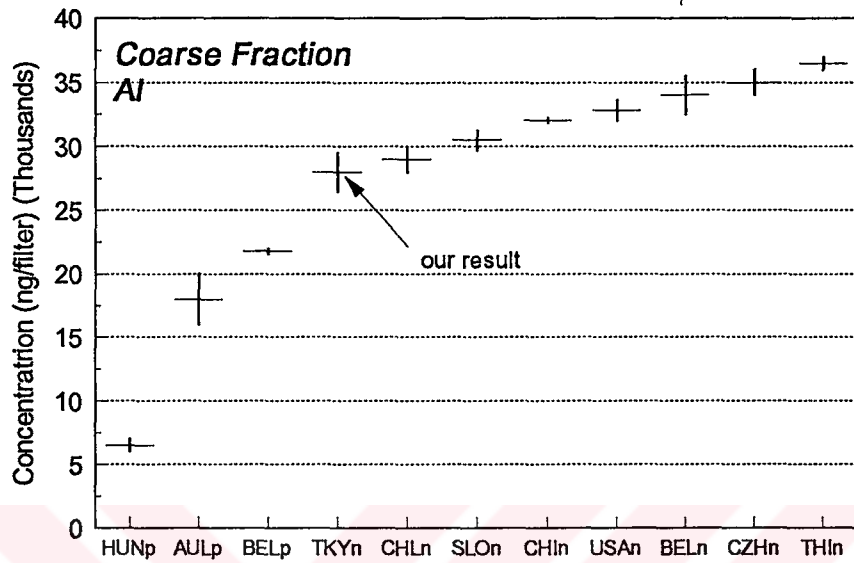


Figure 3.11. Atmospheric concentrations of coarse fraction Al and V measured by different laboratories

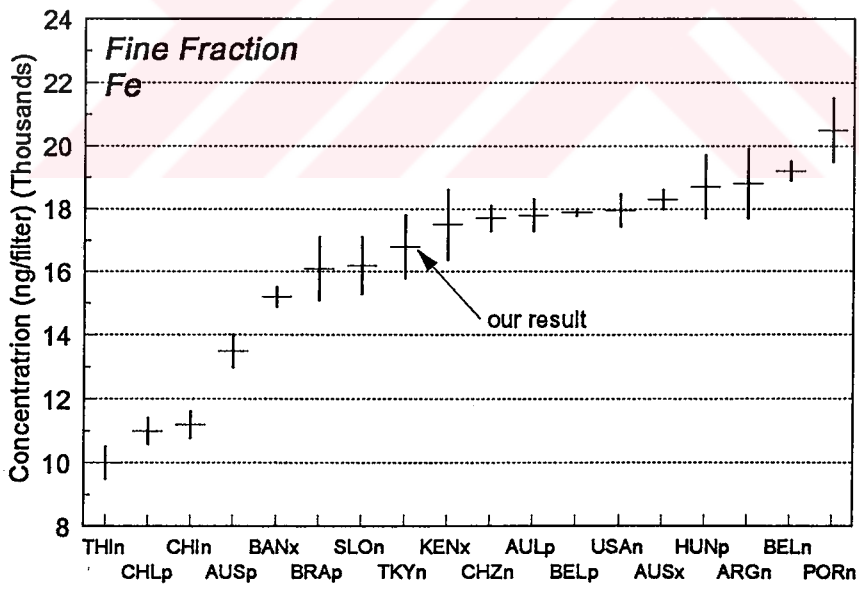
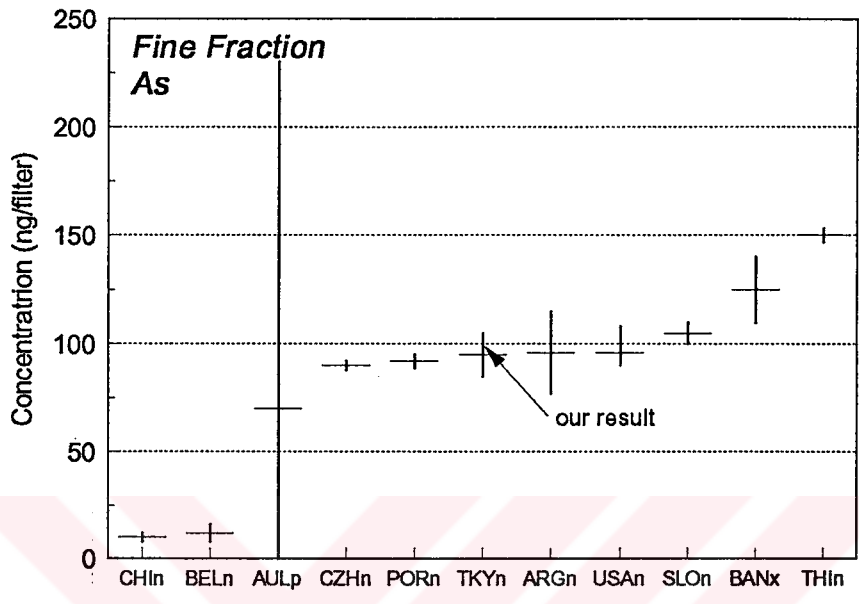


Figure 3.12. Atmospheric concentrations of coarse fraction As and Fe measured by different laboratories

3.5.5. Comparison of INAA and AAS Techniques

As it was explained previously in the earlier sections the year 1992 samples were analysed with AAS technique whereas the year 1993 samples were analysed with INAA technique. In order to compare the agreement of the two techniques, 50 samples were analysed using both methods. Common trace elements measured with the two techniques are Mg, K, Na, V, Zn, Fe, Cr, Al, and Cd. Figure 3.14 lists the average concentrations observed by AAS and INAA for elements for which reasonably reliable values from both methods, along with the ratio of averages and the square of the binary correlation coefficient for pairs of individual samples. The agreement between the two methods is within 30% for most of the elements. For Cd and Cr, a fair agreement has been found.

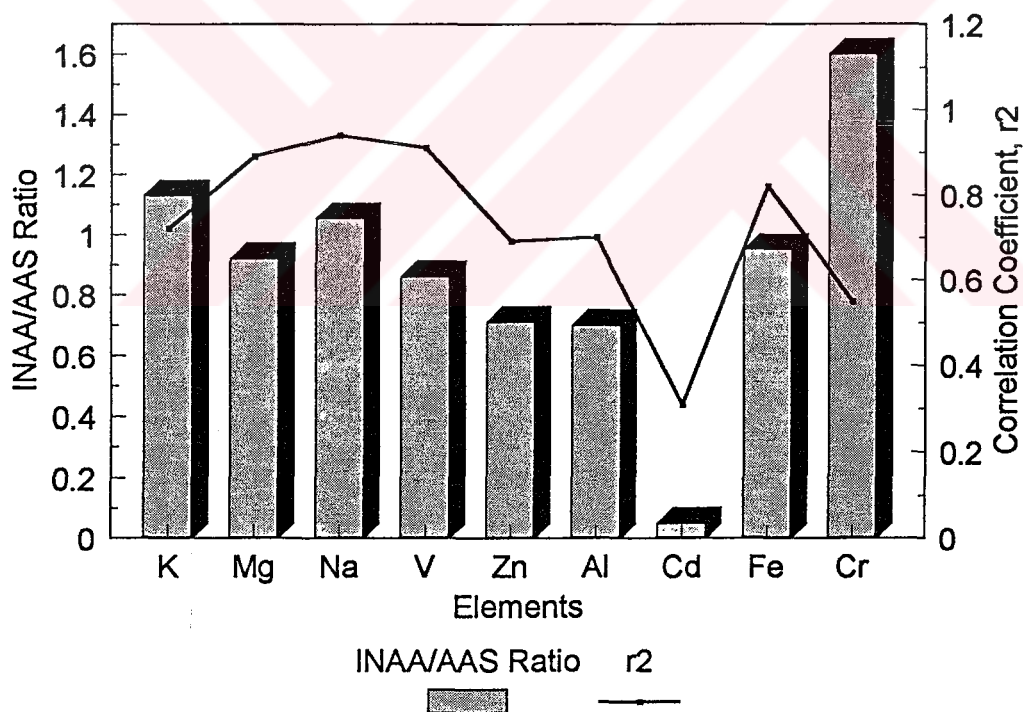


Figure 3.13. Comparison of INAA and AAS results for the elements measured with both methods

CHAPTER 4

RESULTS AND DISCUSSION

4.1. General Characteristics of Data

The concentrations of elements in aerosol samples collected in 1992 and 1993 are presented in this study. Concentrations of 13 elements (Na, K, Ca, Mg, Fe, Cu, Al, Zn, V, Cd, Cr, Pb and Ni) were determined in samples collected in 1993 using AAS. Concentrations of 40 elements were measured in all samples collected in 1993 by INAA. Major ionic species (SO_4^- , NO_3^- , Cl^- and NH_4^+) were also measured in all samples collected in 1992 and 1993.

Average concentrations and standard deviations of elements observed in the eastern Mediterranean atmosphere are presented in Table 4.1. Values shown in Table 4.1 include arithmetic, geometric means, associated standard deviations, median and mode values. Number of samples is also given in the table.

Standard deviations listed in Table 4.1 are comparable to observed concentrations for most of the elements. Such high standard deviations are not unusual for atmospheric trace element data and do not imply poor sampling or analysis. Those observed variations are due to the large variability of the atmospheric concentrations of measured species which in turn is owing to large variations in meteorological conditions, variations in

physical and chemical transformations in the atmosphere, changes in the air mass transport patterns and the variations in the source strengths.

Characteristics of atmospheric data in the literature are generally described by arithmetic mean and standard deviations that assume a symmetric Gaussian distribution. However, although the emissions from sources may be approximately constant, the successive mixing and dilution of pollutants as they are transported from source to receptor results in a log-normal frequency distribution of ambient concentrations. As can be seen in the table, there are large differences between arithmetic and geometric mean concentrations. Geometric mean and median concentrations of measured parameters on the other hand are fairly similar. This is a typical behavior observed in the log-normally distributed data set. Log-normal distributed data set can be better described by geometric mean and standard deviation.

The geometric mean is defined as:

$$\bar{x}_g = \exp \left[\frac{\sum_{i=1}^N \ln x_i}{N} \right] \quad (1)$$

where x_i is the concentration of a chemical specie.

The dimensionless geometric standard deviation (σ_g) for each chemical component represents the spread in the data around the geometric mean. The geometric standard deviations reflect the different levels of stochastic processes that influence the chemical components. The geometric standard deviation, which represents the slope of the log-probability plot, is calculated using the following definition:

$$\sigma_g = \exp \left[\frac{\sum_{i=1}^N (\ln x_i - \bar{x}_g)^2}{N-1} \right]^{1/2} \quad (2)$$

where \bar{x}_g and σ_g are geometric mean and standard deviation, respectively, and N is the number of samples. As was observed in the Table 4.1, the geometric standard deviations for reactive species (SO_4^- , NO_3^- , and NH_4^+) are consistently larger than those of the nonreactive species. This was also observed previously by Kao and Friedlander (1995). They concluded that reactivity influences the ambient concentrations and increases their variability and hence, the geometric standard deviations. The nonreactive chemical components observed in the eastern Mediterranean atmosphere have a relatively constant geometric standard deviation which changes between 2.2 for Br and 4.5 for Mo. Since geometric standard deviation is not a strong function of source type, it appears that variations in the ambient concentrations of these nonreactive elements are primarily due to meteorological influences on transport and deposition processes, and variations in source emissions do not have strong influence after the species have been transported.

4.1.1. Distribution Characteristics of the Eastern Mediterranean Aerosols

The distribution properties of aerosol composition over a long period of time are dependent on the fluctuations of meteorological and source emission variables. Concentrations of air pollutants are random variables and could be described by a probability density function or a frequency distribution. The frequency distributions of the measured air pollutants can be useful for modeling studies which are used to develop control strategies for the pollutants (Kao and Friedlander, 1995). Frequency distributions of pollutants are also useful to search for similarities and differences among the components, which may lead to insights regarding the sources and the stochastic processes that influence ambient levels.

Some advanced multivariate receptor methods that generally used for source-receptor modeling could be adversely affected by heavily skewed distributions. In order to successfully interpret the results of a receptor modeling analysis, distributional characteristics of measured chemical composition variables were determined.

For a symmetric Gaussian distribution, the values of the arithmetic mean, median and mode are identical. If the mode < median < arithmetic mean, then the upper tail of the distribution extends toward larger values (positively skewed). If the order is reversed, the distribution is negatively skewed. Arithmetic mean, median and mode values are given in Table 4.1. Mean, median and mode parameters for all of the chemical variable are in the order of mode < median < mean indicating that the distributions of all variables at the three sites are positively skewed. The skewness index (SI) can be calculated by using the below formula (Von Mises, 1964):

$$SI = \frac{n \sum_{i=1}^n (x_i - \bar{x})^3}{(n-1)(n-2)\sigma^3} \quad (3)$$

where x_i is the concentration of a chemical species, \bar{x} is the arithmetic mean of the distribution, σ is the standard deviation of the distribution and n is the number of samples.

The skewness index shown in Table 4.2 is used to determine the degree of asymmetry in a distribution around its arithmetic mean. A positive index indicates that the tail of the distribution extends out more toward the right end, while a negative index indicates that extension of the distribution is toward left. As it is shown in Table 4.2, values of the skewness are positive for all measured parameters which support the previous finding that the distributions of measured variables are positively skewed.

Table 4.1. Summary of Eastern Mediterranean Aerosol Data: Arithmetic and geometric means and standard deviations, median and mode value.

Element	Number of samples	Arithmetic mean	Geometric mean	median	mode
Na (ng m ⁻³)	594	1900±2000	1100 (2.4)	1060	1050
Mg (ng m ⁻³)	597	365±335	280 (3.2)	270	270
Al (ng m ⁻³)	587	540±700	300 (3.3)	350	340
Cl (ng m ⁻³)	313	2000±3400	990 (3.0)	860	856
K (ng m ⁻³)	551	365±425	250 (4.2)	254	254
Ca (ng m ⁻³)	282	2100±1940	1580 (2.6)	1695	1685
Sc (ng m ⁻³)	312	0.11±0.15	0.06 (3.7)	0.06	0.06
Ti (ng m ⁻³)	257	40±45	26.4 (3.6)	28.4	28.4
V (ng m ⁻³)	594	2.56±2.19	1.82 (3.2)	1.98	1.96
Cr (ng m ⁻³)	531	3.75±3.06	2.58 (4.2)	2.97	2.96
Mn (ng m ⁻³)	313	8.93±8.03	6.11 (2.5)	7.06	6.91
Fe (ng m ⁻³)	593	390±475	230 (4.1)	280	280
Co (ng m ⁻³)	310	0.24±0.35	0.14 (3.1)	0.16	0.16
Ni (ng m ⁻³)	268	2.5±2.05	1.77 (3.3)	2.12	2.12
Cu (ng m ⁻³)	283	194±231	108 (2.5)	111	107
Zn (ng m ⁻³)	586	20.8±43.3	11.3 (2.4)	11.5	11.5
As (ng m ⁻³)	307	1.6±1.4	1.2 (2.3)	1.25	1.23
Se (ng m ⁻³)	312	0.29±0.22	0.23 (3.3)	0.24	0.24
Br (ng m ⁻³)	312	18±22	14.2 (2.2)	13.6	13.5
Rb (ng m ⁻³)	301	0.92±1.00	0.62 (2.8)	0.67	0.66
Mo (ng m ⁻³)	219	0.80±1.34	0.23 (4.5)	0.22	0.22
Cd (ng m ⁻³)	416	0.31±0.70	0.09 (2.5)	0.098	0.096
Sb (ng m ⁻³)	313	0.34±0.20	0.29 (4.2)	0.31	0.31
Cs (ng m ⁻³)	305	0.094±0.075	0.069 (2.5)	0.069	0.068
La (ng m ⁻³)	305	0.35±0.38	0.20 (3.2)	0.22	0.22
Ce (ng m ⁻³)	312	0.67±0.99	0.38 (2.6)	0.42	0.40
Nd (ng m ⁻³)	308	0.59±0.97	0.31 (3.6)	0.35	0.35

Table 4.1. Cont'd.

Element	Number of samples	Arithmetic mean	Geometric mean	median	mode
Sm (pg m ⁻³)	310	51±8	2.8 (3.6)	2.9	2.9
Eu (pg m ⁻³)	279	11.3±16.3	6.2 (3.7)	7.9	7.9
Gd (pg m ⁻³)	289	51±82	21 (3.8)	31	31
Tb (pg m ⁻³)	283	6.1±9.5	3.1 (2.9)	3.7	3.6
Dy (pg m ⁻³)	232	55±68	34 (4.1)	39	39
Yb (pg m ⁻³)	301	21±30	11 (3.5)	13	13
Lu (pg m ⁻³)	302	3.5±5.2	1.9 (3.6)	2.1	1.9
Hf (pg m ⁻³)	301	30±45	15 (3.9)	16.7	16.5
Hg (pg m ⁻³)	304	96±170	41 (4.1)	35	34
Pb (ng m ⁻³)	244	21±21	13 (3.6)	15.8	15.7
Th (pg m ⁻³)	310	100±130	54 (4.1)	59	58
SO ₄ ²⁻ (µg m ⁻³)	518	5.54±4.08	4.25(11)	4.28	4.28
NO ₃ ⁻ (µg m ⁻³)	493	1.18±0.84	0.81(4.5)	1.08	1.07
NH ₄ ⁺ (µg m ⁻³)	478	1.4±1.1	0.8(5.7)	1.25	1.25

A large group of distribution functions can be used to describe the positively skewed data, such as log-normal or Weibull distributions. Many studies in the past indicated that the log-normal function fits air quality data reasonably well (i.e. Ott, 1990; Hacısalihoğlu, 1991). Ott (1990) showed that a concentration resulting from a series of independent random dilution's tends to be log-normally distributed. Therefore, while the emissions from sources may be approximately constant, the successive mixing and dilution of pollutants as they are transported from source to receptor results in a log-normal frequency distribution for the ambient concentrations measured at the receptor.

Since all of the chemical variables measured in this study were found to be positively skewed, it was assumed that the frequency distribution of elemental concentrations in the eastern Mediterranean aerosol is log-normal.

A log normal distribution has the following form:

$$f(x) = \frac{x}{\sqrt{2\pi \ln \sigma_g}} \exp \left[\frac{-(\ln x - \ln \bar{x}_g)^2}{2(\ln \sigma_g)^2} \right] \quad (4)$$

for concentration x , larger than zero, where

- x = concentration of a chemical species in ng m^{-3} ,
- \bar{x}_g = the geometric mean of the distribution
- σ_g = the geometric standard deviation of the distribution

The Kolmogorov-Smirnov (K-S DN) statistic was used to test the goodness-of-fit of the data to log-normal distribution. The K-S test involves the entire distribution of the examined variable, not just its central value, and compares the empirical cumulative distribution function to that of the hypothesized distribution. In the case of the log-normal distribution, the maximum absolute distance between the data and the hypothesized distribution is calculated to test the conformance of the two cumulative distribution functions (STATGRAPHICS Manual, 1992).

Table 4.2 Skewness, Kolmogorov-Smirnov statistic (K-S DN) for fitted variables

Element	Skewness	K-S DN	ALPHA	Distribution Type
Na (ng m ⁻³)	2.18	0.058	1.38	Log-normal
Mg (ng m ⁻³)	3.78	0.049	1.20	Log-normal
Al (ng m ⁻³)	4.16	0.069	1.31	Log-normal
Cl (ng m ⁻³)	3.94	0.078	1.36	Log-normal
K (ng m ⁻³)	5.32	0.033	0.78	Log-normal
Ca (ng m ⁻³)	4.93	0.101	1.20	Log-normal
Sc (ng m ⁻³)	5.85	0.086	1.32	Log-normal
Ti (ng m ⁻³)	4.08	0.044	0.71	Log-normal
V (ng m ⁻³)	2.72	0.043	1.05	Log-normal
Cr (ng m ⁻³)	1.91	0.115	2.66	Weibull
Mn (ng m ⁻³)	3.05	0.080	1.23	Log-normal
Fe (ng m ⁻³)	5.21	0.076	1.21	Log-normal
Co (ng m ⁻³)	6.02	0.074	1.31	Log-normal
Ni (ng m ⁻³)	2.15	0.106	1.75	Weibull
Cu (ng m ⁻³)	2.29	0.114	1.93	Weibull
Zn (ng m ⁻³)	12.6	0.031	0.75	Log-normal
As (ng m ⁻³)	2.46	0.054	0.95	Log-normal
Se (ng m ⁻³)	3.63	0.049	0.87	Log-normal
Br (ng m ⁻³)	8.23	0.065	1.16	Log-normal
Rb (ng m ⁻³)	5.05	0.066	1.15	Log-normal
Mo (ng m ⁻³)	2.61	0.048	0.72	Log-normal
Cd (ng m ⁻³)	5.57	0.052	1.07	Log-normal
Sb (ng m ⁻³)	1.52	0.058	1.03	Log-normal
Cs (ng m ⁻³)	2.62	0.095	1.07	Log-normal
La (ng m ⁻³)	2.86	0.077	1.35	Log-normal
Ce (ng m ⁻³)	6.70	0.059	1.05	Log-normal
Nd (ng m ⁻³)	5.26	0.063	1.11	Log-normal
Sm (pg m ⁻³)	6.44	0.059	1.05	Log-normal
Eu (pg m ⁻³)	6.42	0.087	1.36	Log-normal

Table 4.2. Cont'd.

Element	Skewness	K-S DN	ALPHA	Distribution Type
Gd (pg m ⁻³)	7.61	0.109	1.87	Weibull
Tb (pg m ⁻³)	7.07	0.070	1.19	Log-normal
Dy (pg m ⁻³)	5.08	0.074	1.14	Log-normal
Yb (pg m ⁻³)	5.95	0.067	1.17	Log-normal
Lu (pg m ⁻³)	6.41	0.073	1.28	Log-normal
Hf (pg m ⁻³)	5.58	0.069	1.21	Log-normal
Hg (pg m ⁻³)	5.28	0.066	1.16	Log-normal
Pb (ng m ⁻³)	2.48	0.089	1.30	Log-normal
Th (pg m ⁻³)	5.41	0.086	1.53	Weibull
SO ₄ ⁼ (μg m ⁻³)	1.51	0.047	0.72	Log-normal
NO ₃ ⁻ (μg m ⁻³)	0.85	0.126	1.14	Log-normal
NH ₄ ⁺ (μg m ⁻³)	0.88	0.165	1.16	Log-normal

The observed significance level for the Kolmogorov-Smirnov DN statistic is represented by a value of ALPHA in Table 4.2. The function that was used to calculate the significance of any non-zero values of DN can be written as the following sum (von Mises, 1964):

$$\xi(\lambda) = 2 \sum_{j=1}^{\infty} (-1)^{j-1} \exp(-2j^2 \lambda^2), \quad (5)$$

which is a monotonic function with limiting values, $\xi(0)=1$ and $\xi(\infty)=0$. In terms of Equation (3), the significance level of an observed value of DN, that is ALPHA, (as a disproof of the null hypothesis that the distribution is log-normal) is given approximately by:

$$\text{ALPHA} = \left(\sqrt{N} + 0.12 + \frac{0.11}{\sqrt{N}} \right) \cdot \text{DN} \quad (6)$$

The nature of approximation in Equation (5) is that it becomes asymptotically accurate as N becomes large. The sample size for each measured variable in this study is larger than 300 providing adequate degrees of freedom to use the DN statistic. Thus, an ALPHA greater than 1.358 as given in Table 4.2 indicates that the cumulative distribution function of a composition variable is significantly different from the log-normal function at a 95% confidence level.

As it is shown in Table 4.2, ALPHA values for the variables Na, Al, K, Ca, Sc, Cr, Mn, Fe, Ni, Cu, Cs, Eu, Gd, Tb, Pb and Th are greater than 1.358, indicating that data do not fit to the hypothesized distribution (i.e. log-normal distribution). Except Cu and Pb, all of these variables are either crustal or marine elements. Since their sources are local rather than being transported from distant regions, minimum mixing and dilution of these locally generated particles might cause less skewed distribution. There are a large family of distribution functions that are likely to fit these variables.

When the goodness of fit test was applied to these variables, Weibull distribution function has been found as the best fitted one. The frequency histograms and associated distribution curves for Ti, and V which show typical log-normal distributions are given in Figure 4.1. Typical examples of frequency histograms and associated distribution curves for the Weibull distribution for Ni and Cu are given in Figure 4.2.

4.1.2. Comparison with other data

In order to assess the extent of pollution in the study area, the observed concentrations of elements are compared with earlier observations of trace elements reported for comparable sites from other parts of the world.

The sampling site in the Antalya station is located at a coastal rural area which is far away from local sources. That's why, the literature studies were also selected to be from rural sites in the Mediterranean and other regions in the surrounding areas. Selected studies for comparison are Corsica (West Mediterranean) (Bergametti et al., 1989), Hungary (Borbely-Kiss et al., 1991), Norwegian Arctic (Maenhaut et al., 1989), Syria (Cornille et al., 1990), Erdemli (Eastern Mediterranean) (Kubilay, 1996), the Black Sea (Hacısalıhoğlu et al.; 1992), Portuguese West Coast (Pio et al., 1991).

Geometric mean concentrations of elements and ions obtained in this study were used for comparison with literature values, because, as it is explained earlier, geometric means correctly represent the concentrations obtained under normal physical conditions and bulk of the data points. Due to different purposes of experiments and different techniques used in the analysis of samples, data were not available for all elements in all studies.

Detailed description of sampling sites are given below. The sampling site,

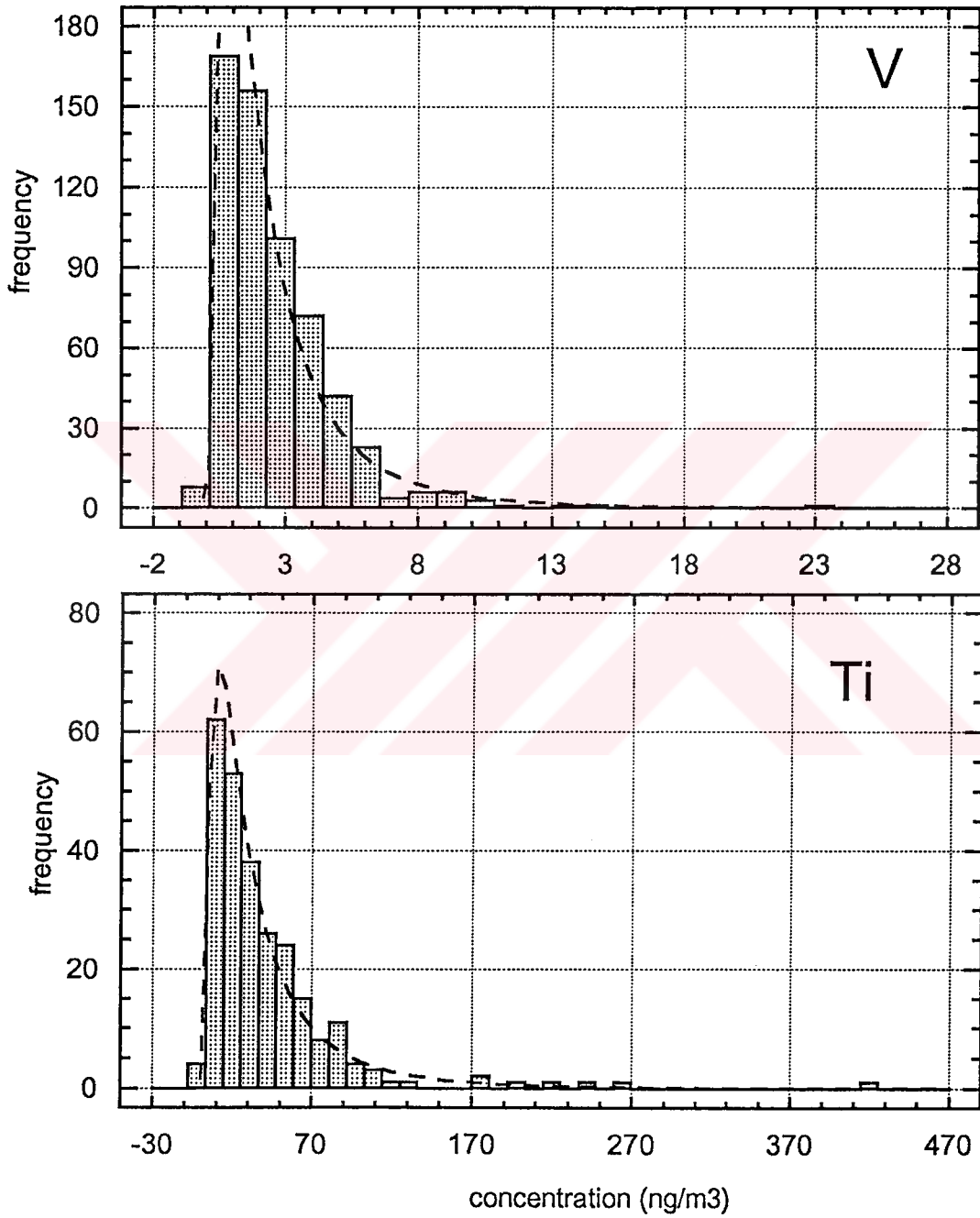


Figure 4.1. The frequency histograms and associated distribution curves for V and Ti.

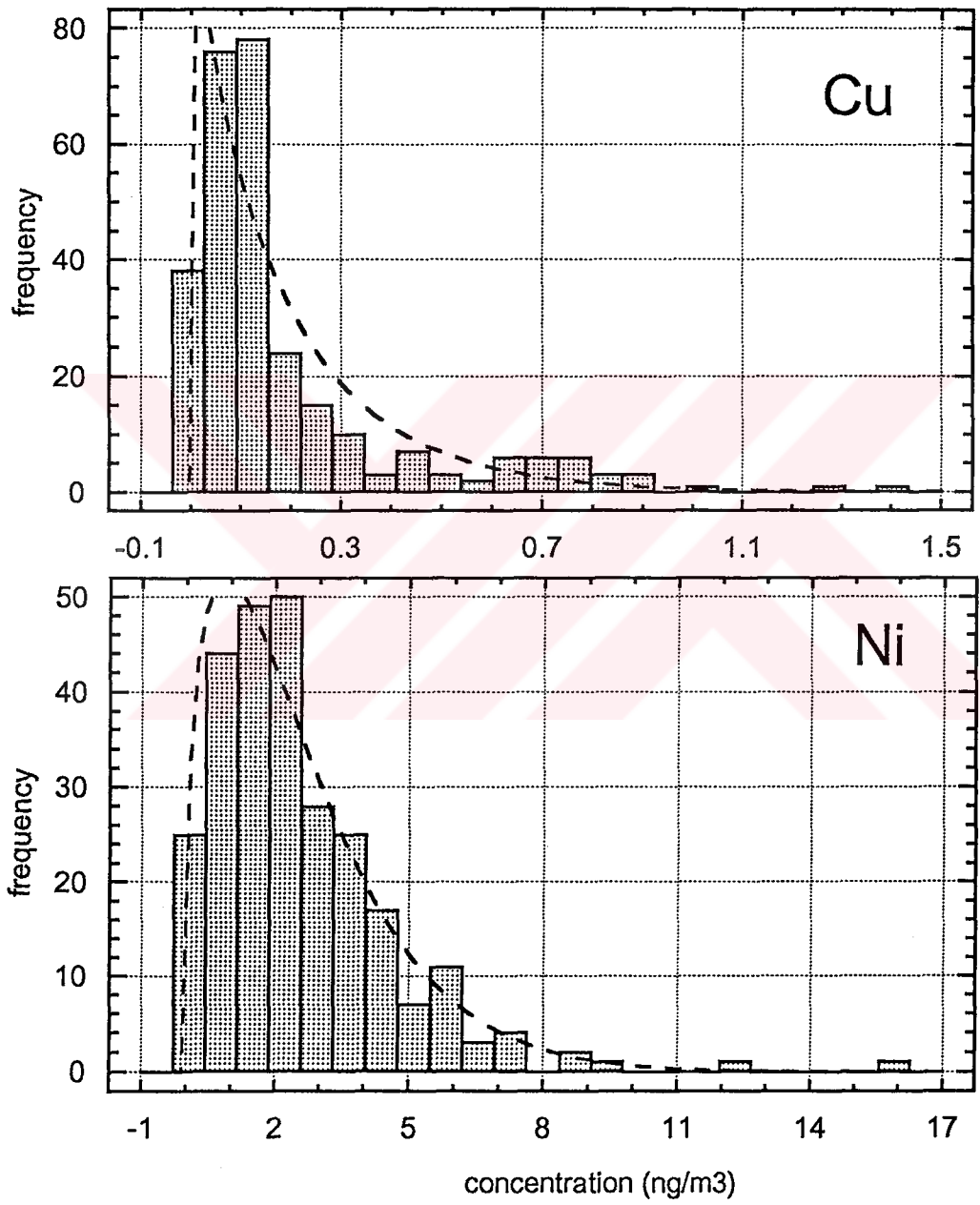


Figure 4.2. The frequency histograms and associated distribution curves for Cu and Ni

1) Corsica, Western Mediterranean (Bergametti et al., 1989)

A continuous aerosol sampling program has been undertaken at a coastal location in northwestern Corsica. Samples were analyzed by X-ray fluorescence and by flameless atomic absorption techniques. Geometric means were reported.

2) Hungary (Borbely-Kiss et al., 1991)

The results of analyses of aerosol samples collected at the Hungarian Great Plain about 70 km southeast of Budapest were given. Samples were analyzed by using PIXE method. Geometric means were reported.

3) Norwegian Arctic (Maenhout et al., 1989)

Aerosol samples were collected at two locations in the Norwegian Arctic and analyzed for up to 42 elements by a combination of INAA and PIXE techniques. Median values of atmospheric concentrations were reported.

4) Damascus, Syria (Cornille et al., 1990)

Aerosols were collected from an arid region near Damascus, Syria and analyzed for sulfate, nitrate and about 40 elements by INAA, IC and PIXE. Arithmetic means were reported.

5) Erdemli, Turkey (Kubilay, 1996)

Aerosol samples arriving at a rural site on the eastern Mediterranean were collected and analyzed by the flame and flameless AAS for 13 trace elements. Geometric means were reported.

6) The Black Sea (Hacısalıhoğlu et al., 1992)

Shipborne samples collected from the Black Sea atmosphere were analyzed by INAA, AAS and IC for about 40 elements and major ions. Geometric means were reported.

7) Portuguese West Coast (Pio et al., 1991)

Aerosol samples were collected from a coastal site near Aveiro, Portugal and analyzed for inorganic compounds and trace elements by flame and flameless AAS. Arithmetic means were reported.

Measured concentrations of elements and ions at selected sites are presented in Table 4.3. Comparison of concentrations of elements measured at the Eastern Mediterranean atmosphere with those measured in other rural sites showed that, concentrations of all elements at remote sites such as Norwegian Arctic are at least an order of magnitude less than those measured at the Eastern Mediterranean. This implies that the aerosols over the Eastern Mediterranean are under a strong influence of natural and anthropogenic emissions.

Concentrations of marine elements such as Na, Cl and Mg, Br measured in this study are higher than continental rural sites and comparable to or lower than other coastal sampling locations. The lower concentrations of marine elements in the Antalya station relative to Portuguese West coast are probably due to milder sea conditions at the Antalya site relative to Portuguese west coast which is open to the Atlantic ocean. As it is well known that sea salt concentration increases with wind speed (Tsunogai et al., 1972; Gras and Ayers, 1983). Infact, the marine elements are generated locally therefore the measured values at the Antalya station represent the sea salt concentration of aerosols in the vicinity of the station, and may not be extended to all eastern Mediterranean basin. Since the wind speed varies due to topographic differences, there might be significant differences on the marine element concentrations on two stations located adjacent to each other.

Concentration of elements associated with aluminasilicate particles which are commonly known as crustal elements (Al, Sc, Fe, etc.) are much higher than corresponding concentrations measured at pristine sites, such

Table 4.3. Concentrations of trace elements and major ions in aerosols over various regions.

Element	Corsica ¹	Hungary ²	Norwegian Arctic ³	Syria ⁴	Erdemli ⁵	Black Sea ⁶	Portuguese W. Coast ⁷	This Study ⁸
Na	1000	--	230	430	1900	1300	3600	750
Mg	--	--	48	540	1200	300	437	280
Al	168	246	40	1310	685	400	--	300
Cl	--	15	85	390	--	1200	4800	990
K	221	230	31	380	--	260	523	250
Ca	254	386	34	4300	3140	490	2000	1550
Sc	--	--	0.0043	0.26	--	0.08	--	0.06
Ti	12.4	20	1.0	97	--	58	--	26.4
V	--	2.4	0.54	3.3	7.8	2.2	15.7	1.82
Cr	--	4.6	0.4	--	8.5	5.4	6.95	2.58
Mn	5.3	10.7	0.77	16.8	13	14	34	6.11
Fe	144	272	17.8	860	685	340	1190	230
Co	--	1.6	0.0096	0.59	0.4	0.18	--	0.14
Ni	--	2.3	0.29	--	5.6	4.0	3.17	2.0
Zn	19.1	26.4	3.9	12.2	19	34	95	7.5
As	--	2.5	0.52	0.53	--	0.87	--	1.2
Se	--	1.2	0.16	--	--	0.57	--	0.23
Br	--	24	8.8	9.2	--	17	--	14.2
Sb	--	--	0.092	0.33	--	0.44	--	0.29
La	--	--	0.014	0.85	--	0.24	--	0.20
Pb	15.9	20.6	3.0	23	30	42	157	13
SO ₄ ⁼	--	--	--	--	--	6.7	7.96	3.92
NO ₃ ⁻	--	--	--	--	0.21	2.6	3.9	0.67

1) Bergametti et al., 1989 2) Borbely-Kiss et al., 1991 3) Maenhout et al., 1989 4) Cornille et al., 1990 5) Kubilay, 1996

6) Hacısalihoglu et al., 1992 7) Pio et al., 1991 8) This study

as Norwegian Arctic, lower than concentrations measured in the Syria and Erdemli and comparable to concentrations measured in the Black Sea atmosphere. The lower Al, Sc and Fe concentrations in the Eastern Mediterranean atmosphere relative to other Eastern Mediterranean site, Erdemli is due to application of a preimpactor with a cut-point of 10 μm in the hi-vol sampler in this study. The preimpactor removes particles with diameters larger than 10 μm from the air stream before they reach the filter. Consequently, measured concentrations are smaller than corresponding concentrations measured in other eastern Mediterranean sites with samplers which were not equipped with a PM-10 separator. Since Syria is more arid region than our site, high crustal element concentrations in the Syria were observed due to desert soil dispersion.

Like marine elements, crustal elements are originated from local sources. Therefore, the observed crustal elements may not represent the whole eastern Mediterranean crustal element distribution.

Concentrations of pollution derived elements, such as V, Cr, Ni, Zn, As, Se, Sb, etc. are an order-of-magnitude higher in the Antalya atmosphere than concentrations measured in remote places like Norwegian Arctic due to stronger anthropogenic influence at the eastern Mediterranean. These elements have comparable concentrations in some of the continental rural sites such as Hungary, Syria, the Black Sea and Corsica. Concentrations of these pollution derived elements are lower than other rural sites such as Portuguese West Coast and Erdemli. The low concentrations of anthropogenic elements measured at Antalya can not be explained by the preimpactor on the instrument, because these elements are associated with fine particles which were not stopped by the preimpactor. Observed higher concentrations of anthropogenic elements in the Portuguese cost and Erdemli site which is located 400 km to the east of our sampling site are probably due to local anthropogenic sources.

To be able to demonstrate the possible existence of differences in the concentrations of the concentrations of the elements in the atmosphere over the eastern and western parts of the Mediterranean and to determine the general feature of the eastern Mediterranean aerosols, data for aerosols from a number of coastal sea sites around the Mediterranean basin are compared with the concentrations measured in the present study. These sites are Corsica (Bergametti et al., 1989), Cap Ferrat (Chester et al., 1990), Tour de Valet (Guieu, 1991), Blanees (Chester et al., 1991), Syria (Cornille et al., 1990) and Erdemli (Kubilay, 1996). The locations of these sites and measured concentrations are illustrated in the Figure 4.3 and 4.4, respectively.

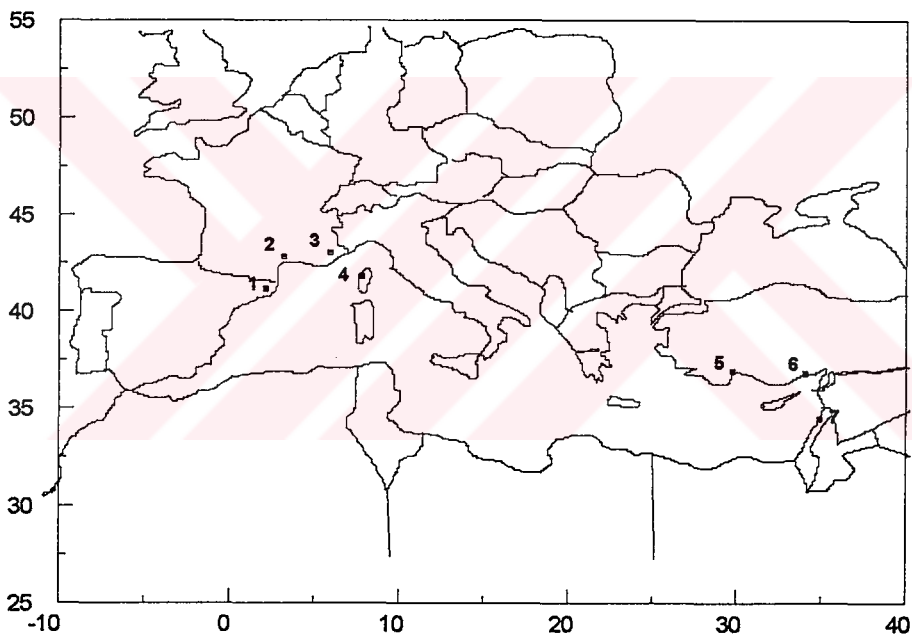


Figure 4.3. Locations of the particulate aerosol samples (1) Blanes (Chester et al., 1991), (2) Tour de Valet (Guieu, 1991) (3) Cap Ferrat (Chester et al., 1990) (4) Corsica (Bergametti et al., 1989) (5) Antalya (this study) (6) Erdemli (Kubilay, 1996) (7) Syria (Cornille et al., 1990).

Concentrations of crustal elements, like Al and Fe in the Antalya station are well within the range reported for other coastal locations in the western Mediterranean coastal sites and lower than the results reported for

the other eastern Mediterranean coastal sites, Erdemli and Syria. As it is previously stated, observed lower concentrations of crustal elements in this study relative to other eastern Mediterranean studies are probably due to the presence of preimpactor on the instrument. As it is stated by Chester et al. (1993) and according to the results of Erdemli and Syria studies, the Eastern Mediterranean atmosphere has a chemical character which is strongly influenced by crust-rich component due to the surrounding desert regions and prevailing air-mass trajectories originating at the arid lands of the Middle East and desert areas.

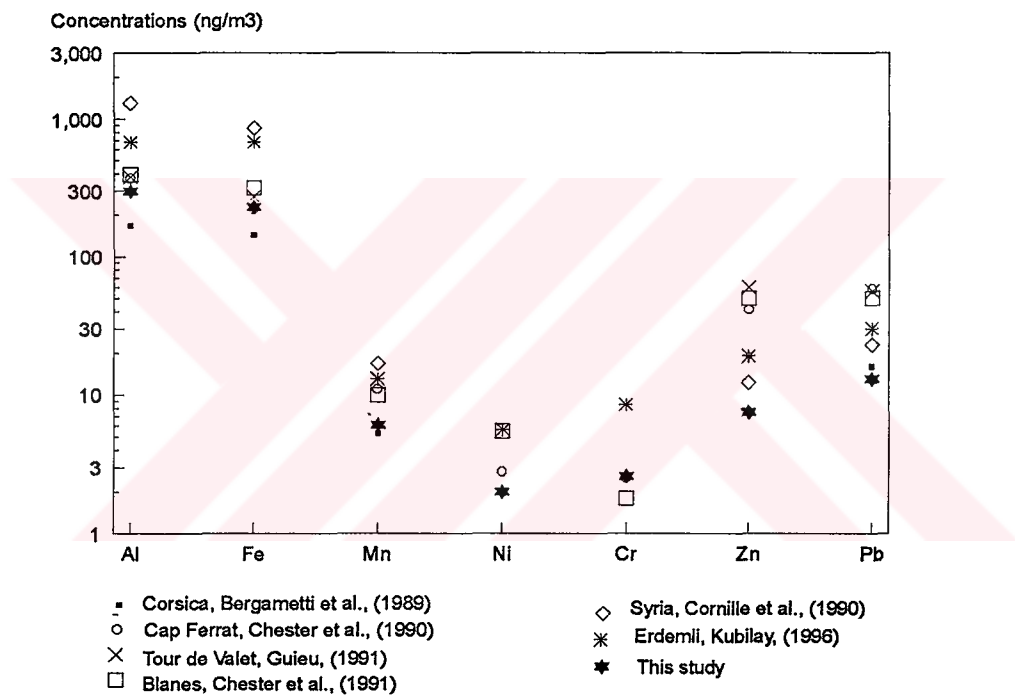


Figure 4.4. Average concentrations of some trace elements in the Mediterranean Sea Coastal Locations

Concentrations of pollution derived elements, Zn and Pb, measured in the Antalya station are generally lower than all values reported for comparable coastal sites in the Mediterranean. The main difference in the composition of atmospheric particulates observed in the eastern basin and the western basin is that particulates from the eastern basin have lower

concentrations of anthropogenic elements specifically Zn and Pb. As a general, sources on the Europe supply anthropogenic dominated particulate aerosols to the eastern and western Mediterranean atmosphere. During particle transport from source to receptor areas, particle scavenging mechanisms mainly rainout and washout, removes particles and associated elements from the atmosphere. Since European originated pollution bearing aerosols should be transported to longer distances to the eastern basin, the effect of these pollution sources on the eastern Mediterranean atmosphere is lower than western Mediterranean.

4.2. Analysis of Back Trajectories of the Eastern Mediterranean

The main conclusion of the previous studies is that the variability of the elemental concentrations in the Mediterranean atmosphere depends on the origin of the air masses arriving at a sampling site, variations in source strengths and precipitation scavenging (Chester et al., 1984; Dulac et al., 1987; Bergametti et al., 1989 and Chester et al., 1993). Back trajectories are the most widely used tool to study the effect of different source regions which describe the path of air masses before it is intercepted at a receptor site on observed variability of pollutant concentrations at a receptor.

In this study, the ARL Branching Atmospheric Trajectory (BAT) model (Heffter, 1980) was used to calculate daily 4-days back trajectories ending at Antalya station (36°08'N and 31°00'E) during 1992, 1993 and 1995. The model calculates trajectories of 4 days duration either forward or backward in time from any selected location starting every 6 hour on selected days. Trajectory segment endpoints at fixed intervals back in time from a given starting time are given in longitude and latitude of the segment endpoints. Each trajectory is calculated using transport winds averaged over a fixed or a variable vertical layer. However, for simplicity, in this study the BAT model was run using vertically averaged winds in a constant layer, 50 m - 3000 m above the surface. Trajectory calculations are based on actual upper air observations from the meteorological

stations located within the 65°N and 25°N latitudes and 10°W and 40°E longitudes. The most important difficulty to calculate trajectories on a daily basis is the need of actual upper air observations from all available rawinsonde stations in the Europe, part of the Asia and part of the north Africa. Part of the meteorological data were obtained from the Turkish General Directorate of Meteorology and part was obtained from the National Center for Atmospheric Research (NCAR).

To determine the atmospheric transport path of pollutants from source areas to the Antalya Monitoring site, 4-day back trajectories at 12 00 UT (UT: Universal Time) were calculated every day in 1992, 1993 and 1995. In order to understand annual and seasonal air mass transport patterns (frequencies) trajectories are classified using a sectoring technique shown in Figure 4.5. Frequencies of air mass transport from each of the eight wind sectors were calculated by dividing each trajectory into 3 hr segments and counting number of trajectory segments in each of the eight wind sectors for each month. In this way monthly, seasonal and three year average frequency distributions of air mass transport were calculated.

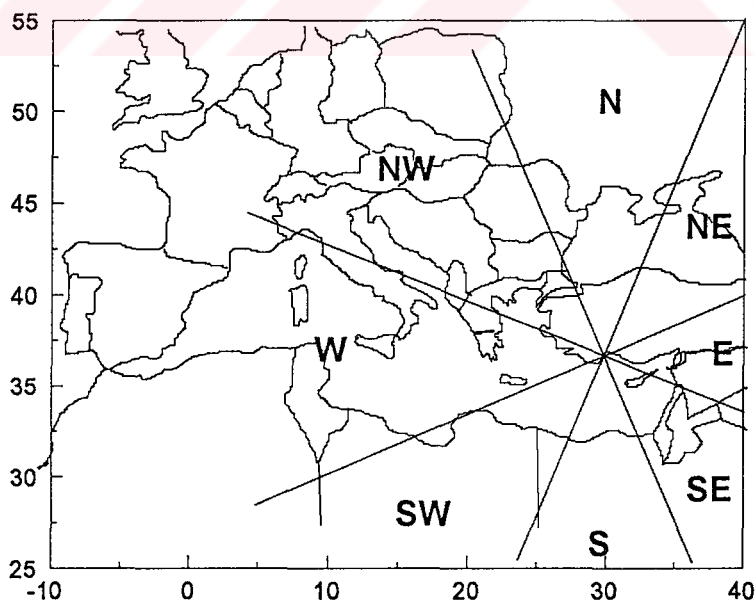


Figure 4.5. The sectoring technique to classify trajectory

Transport from different wind sectors is expected to bring different types of aerosols to our sampling site. Four main source areas were broadly identified and related to trajectory sectors.

- 1) North-Northwest Sectors: These sectors include trajectories originating from Ukraine, Central Russia, Europe and Western Anatolia. This group of trajectories are expected to bring pollutant from industrialized European countries and intense and uncontrolled industrial emissions from Ukraine and central Russia. Approximately 47% of trajectories were in these sectors.
- 2) West-Southwest Sectors: include trajectories originating and/or passing through Mediterranean Sea and northern part of Africa. Since this group of trajectories pass very close to north Mediterranean countries they can carry pollution from these areas as well as marine aerosols generated on the surface of the Mediterranean sea through bubble-bursting process. Approximately 29% of the trajectories have this origin.
- 3) South-southeast: Trajectories in this group transport Saharan dust and crustal material from the arid regions of Middle East and Arabian Peninsula to the eastern Mediterranean basin. However only 7% of the trajectories calculated in three years were in these sectors.
- 4) East-northeast: includes trajectories originating from Commonwealth of Independent States and crossing Eastern Anatolia before reaching the Antalya monitoring site. Since most of the countries which fall in these sectors are not industrialized compared to countries in North and Northwest sectors, this group of trajectories are not expected to transport pollution derived material but might be rich in crustal particles. Approximately 17% of the trajectories have an origin within these sectors.

The seasonal and three year average air flow frequencies from each sector (air flow patterns) are given in Figure 4.6 and Figure 4.7, respectively.

The frequency of air mass movements shows large variations from one wind sector to another on an annual basis. The most frequent air mass movements occur from north, northwest, west and northeast sectors. Since these wind sectors include high emission areas (Europe, former USSR countries Ukraine, Russia and western parts of Turkey), they are potential source regions of pollutants intercepted in SW Turkey and probably in the Eastern Mediterranean atmosphere.

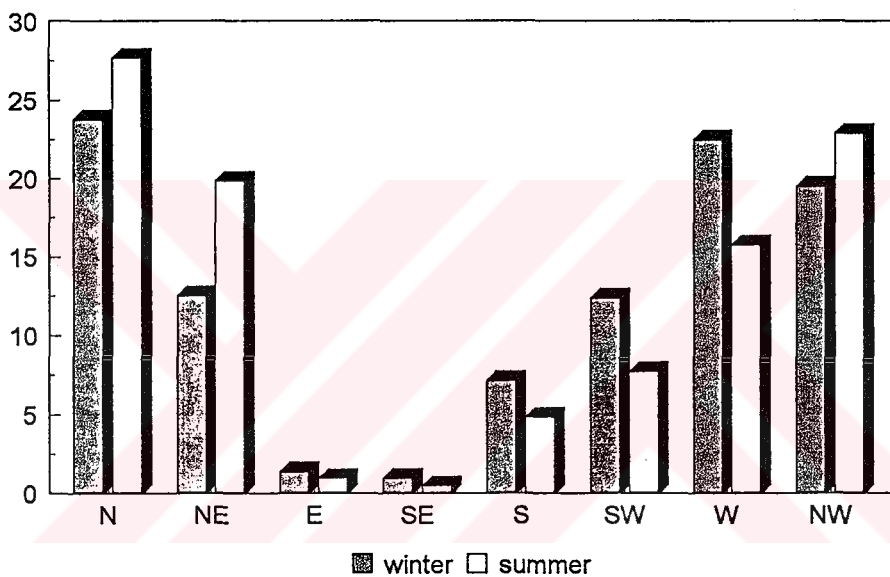


Figure 4.6 The seasonal flow patterns at Antalya station

Frequencies of air mass transport from east and south-east sectors are insignificant (2% from east and 1% from southeast). When this observation is coupled with lack of strong emission sources of pollutants in these sectors, east and southeast sectors include the least likely pollution regions for the eastern Mediterranean atmosphere. Although these sectors include Middle Eastern arid areas, contribution of crustal material from these areas is expected to be small due to the small annual air mass transport from these regions. This observation contradicts with Chester et al's (1993) suggestion that eastern Mediterranean

atmosphere should be under the influence of material brought in from the east and south-east regions.

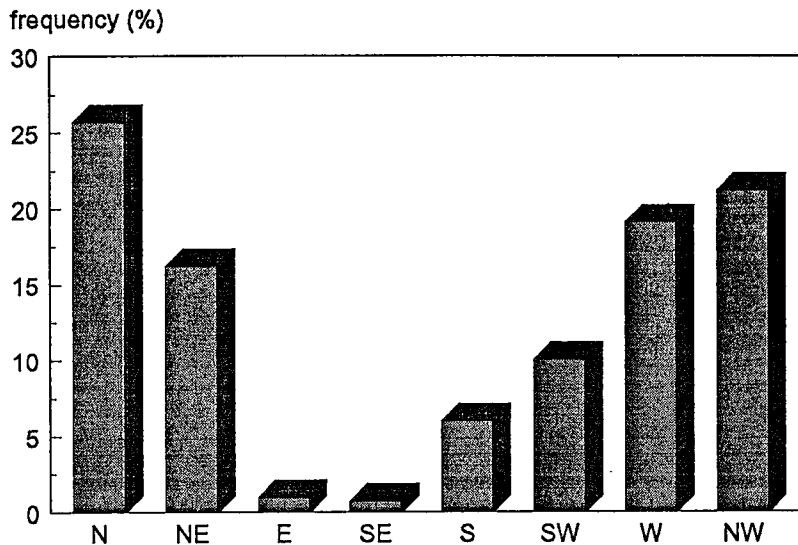


Figure 4.7 Annual frequencies of air mass transport from wind sectors

The monthly variations of percent contribution of major sectors are shown in Figure 4.8. The percent contribution of wind sectors are fluctuate significantly between months. During all months, one can see the prevailing northerly and westerly and northwesterly flow patterns. Small contribution of east, southeast and south sectors were observed during the whole year. During summer months (mainly June, July, August and September) no contribution what so ever was observed from these sectors.

At the beginning, a seasonal variation in the trajectories was expected just because of the seasonal complexity of the Mediterranean climate and from the previous studies. Seasonal variations in air flow frequencies from each sector are important as seasonal variability can explain observed seasonal variations of measured parameters. Frequencies of air mass transport, in 8 of the wind sectors during summer and winter seasons are depicted in Figure 4.6. Seasons were distinguished by assuming summer (dry) season is between May to October, and the rest of the year (October through April) is winter (wet season). There are seasonal differences in the air flow patterns. Flow from N,

NE sectors are more frequent during summer period, whereas flow from W and SW sectors are more frequent during winter. Seasonal differences were smaller at the E, SE, S and NW sectors. The seasonal differences observed in this study were more or less in the same magnitudes observed in previous studies in the western and eastern Mediterranean basin (Dayan, 1986; GESAMP, 1985). However, observed differences should be viewed from two different perspectives. Differences in observed air flow patterns in different seasons are real and significant from climatological point of view, because approximately 1100 trajectories and 35000 segments were included in the analysis which makes the results statistically sound. But, these differences between seasons which may be important in long term climatology of the region are too small to account for observed seasonal variations in the observed concentrations of elements and ions measured in this study. Consequently, statements such as "air flow patterns do not show seasonal variations" which are used in subsequent sections do not actually imply that the frequencies of air mass transport in each wind sector are identical in summer and winter seasons, but they mean that, observed differences are not large enough to explain seasonal variations in the concentrations of elements measured in this study.

During winter, 19% of trajectories have originated from south and southwest sectors, contribution of same sectors during summer months decreased down to 13%. This result is contradictory with the previous studies results that have been performed at Platanos (Crete) (GESAMP, 1985) and at Israel (Dayan, 1986). Both of those studies have been reported that, on the eastern Mediterranean basin, marked seasonal variations were observed, number of southerly trajectories is increased during summer. However, in our results, although the difference between summer to winter contribution is only around 7% which is not a significant difference to be ascertain, during winter months (especially March and April) contributions of south and southwest sectors are higher than summer months. As it is clearly seen in Figure 4.8, inclusion of rainy months, March, April and October which have high south and southwest contribution might increase winter contribution of south and southwest sectors.

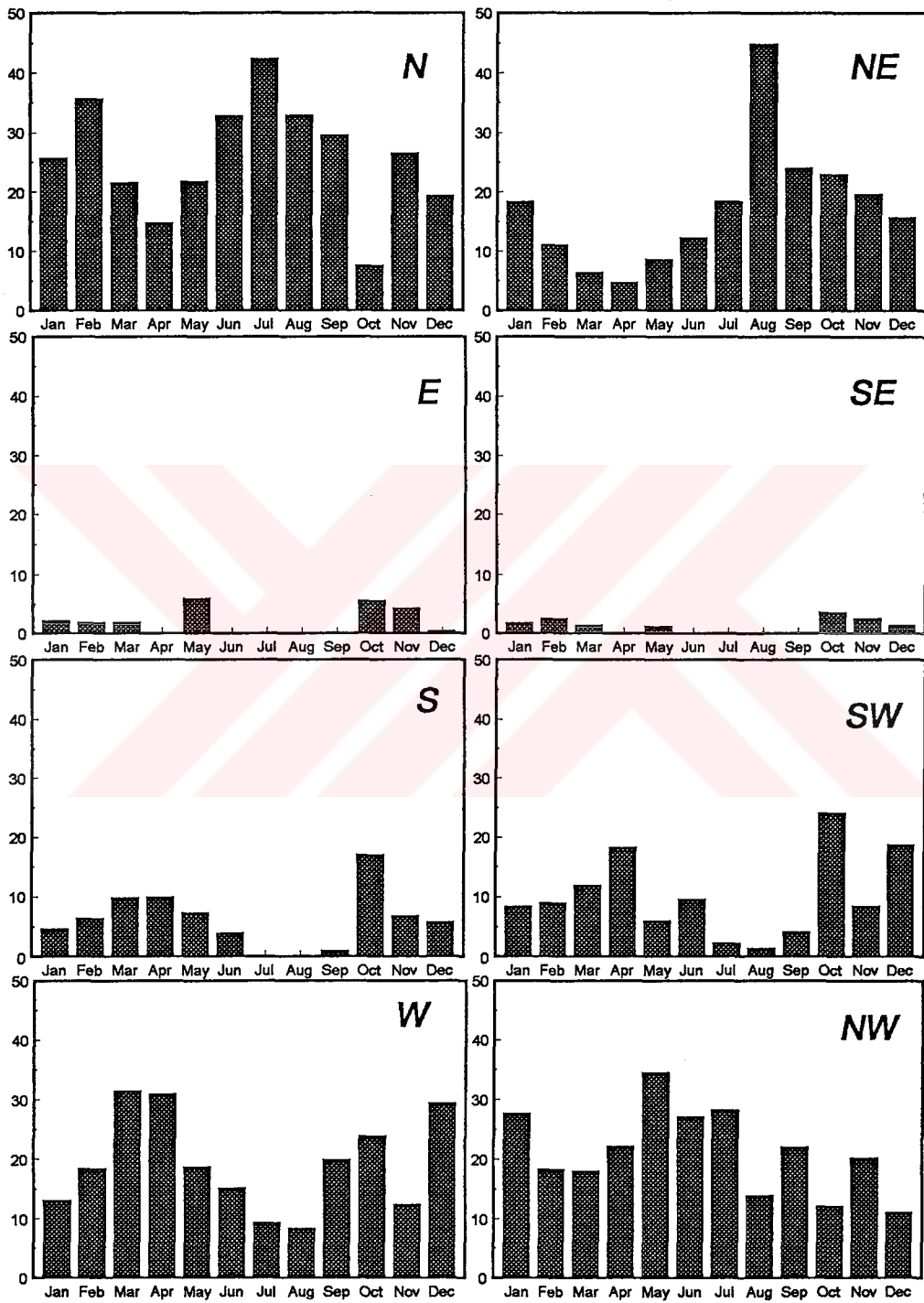


Figure 4.8. Monthly variation of percent contribution of major wind sectors

4.2.1 Comparison of Back Trajectories, Climatologies at Eastern and Western Mediterranean Basins

Results of present study have been compared with earlier studies which have been performed to determine flow climatology in the whole Mediterranean basin (GESAMP, 1985; Dayan, 1986; Kubilay, 1996) to verify the validity of the calculated back trajectories computed in this work and to establish similarities and differences in the flow climatologies of the eastern and western Mediterranean basins. Studies which were used in comparison include the computation of back trajectories at Israel for a five year period (January 1978-December 1982) by Dayan (1986), seventeen month long back trajectory calculations (August 1991-December 1992) at Erdemli, Turkey by Kubilay (1996), computation of back trajectories arriving at Platanos (Crete) (GESAMP, 1985) and nine year back trajectory computation at a point (40 °N, 6°E) in the western Mediterranean (January 1975-December 1983) (GESAMP, 1985). The mean airflow climatologies at different sites in the Mediterranean basin are depicted in Figure 4.9. Since different sector partitioning techniques were used in studies, to compare the long term climatology of the basin as a whole, the region has been divided into four major sectors, North, West, South and East, to establish a common base for comparison. Although trajectories were calculated by using different data sources and different trajectory models, most of the studies in the eastern Mediterranean showed a general agreement on the 850 hPa flow patterns. As can be seen in the figure, particularly good agreement between the present study and the study performed at Erdemli site which is 400 km to the east of the Antalya site (Kubilay, 1996) is obtained, which increased the confidence in the trajectory models used in both studies.

Although most of the results obtained from eastern Mediterranean studies showed a general agreement, there are some differences between the results obtained in this study and those obtained in the Crete and Israel works. The east component (16%) in to the study performed at Crete, is higher than the east components in the Antalya and Erdemli studies. Similarly the north

component calculated at the Israel coast (30%) is a factor of two higher than the corresponding component in other eastern Mediterranean sites.

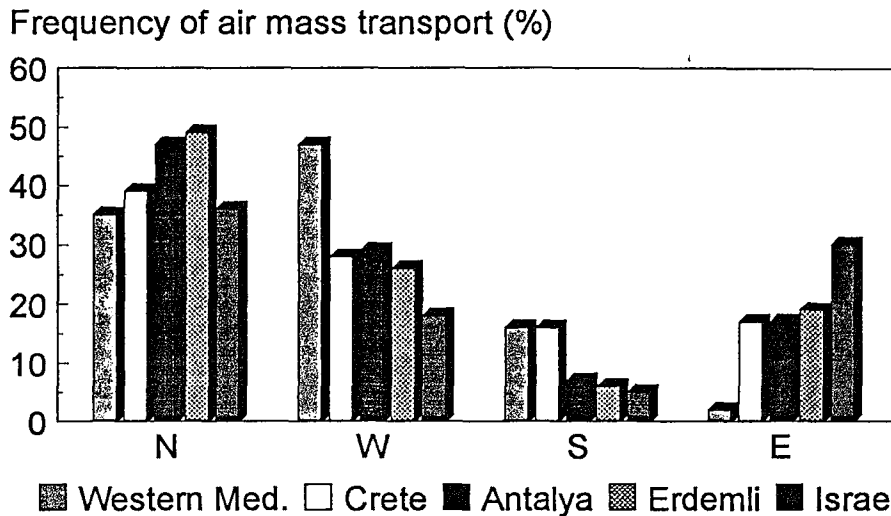


Figure 4.9. The mean frequency of air mass transport at different sites in the Mediterranean Sea

When the flow climatology compared at eastern and western Mediterranean sites, the main difference in the flow climatologies in the western and eastern Mediterranean studies is in their east and west components. Contribution of east sector on the air mass transport in the western Mediterranean is only 2% which is insignificant. However, the contribution of this sector on the air flow to eastern Mediterranean basin is around 16%. With 47%, major contribution is from the west sector in the western Mediterranean basin, whereas major contribution is from the north sector in the eastern Mediterranean basin.

Although the comparison of studies reported in the literature allowed us to understand general features of the flow climatology to the eastern and western Mediterranean basins, the studies included in the comparison were not suitable to establish fine details of the flow climatology. None of the studies used in the analysis were long enough to establish true climatology of the region. Consequently, results obtained in each of the study were true for the time period covered by that particular study, but there is no guarantee that similar result

would be exactly reproduced for another time period. But since the studies cover at least a three year period, general features of the flow should be reproducible. In addition to this, results obtained in different studies may also be slightly biased depending on the model used in calculations.

To avoid the differences in the results imposed by different time periods and different models and to produce more comparable data for the eastern and western Mediterranean basins, two sites, one in the western and one in the eastern Mediterranean regions were selected. A site from the western Black Sea was also included in the study, because transport of pollutants to the Black Sea had been extensively studied by our group and data obtained in the study have been extensively compared with the data obtained from the Black Sea region. The three sites which represent each of the basins were our Antalya station for the eastern Mediterranean, Cape Cavallo (42°31'N, 8°40'E) for the western Mediterranean and the Amasra station operated by our group (41°47'N, 32°29'E) for the Black Sea region. In each station back trajectories were calculated everyday for 3 years (1992, 1993 and 1995), segmented and evaluated as discussed in previous sections.

Calculated three year average and seasonal contributions of sectors on flow patterns are given in Figures 4.10 and 4.11, respectively. Although the general flow patterns in all three selected sites were similar with more frequent flow from N, NE, SW, W and NW sectors, there are some differences between western and eastern Mediterranean in fine structure which becomes apparent when percent contribution of flow from each sector at each site are compared with each other. The flow climatologies were found to be approximately similar at the Amasra and Antalya sites and different at the Corsica site. At the Corsica site, contributions of north and north-east sectors were found to be less and contributions of south and south east sectors were found to be higher than contributions of corresponding sector calculated for the Amasra and Antalya sites. Major contribution with 26% of the time was observed from north-west sector in Corsica whereas major contribution is observed from north, west and

north-west sectors at eastern Mediterranean sites. Contribution of east and south-east sectors were minimum at all three sites included in the study.

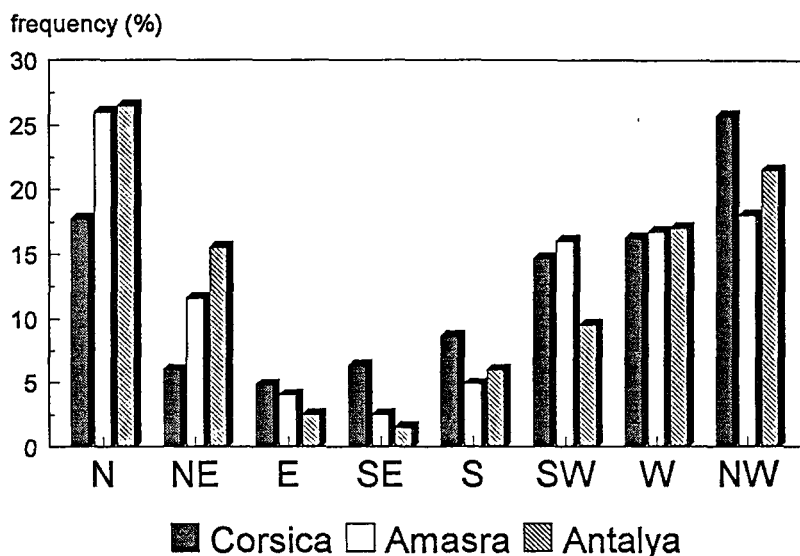


Figure 4.10 Annual frequencies of air mass transport from wind sectors at Corsica, Amasra and Antalya

The most important implication of this discussion on the flow climatologies in the eastern and western Mediterranean basins is that the source regions affecting aerosol populations in the eastern and western Mediterranean regions are different. High contribution of N sector in the Eastern Mediterranean and Black Sea regions suggests that countries like Russia and Ukraine are important source regions. These countries which lie to the NE of the Western Mediterranean region are not important source areas for Corsica site, because NE sector accounts for only 5% of the air mass transport to the western Mediterranean region.

The north western sector is also a dominant sector for the Eastern Mediterranean, former USSR countries which lie in this sector are, important source regions for the aerosol composition in the eastern Mediterranean. The NW sector is the dominant sector for the western Mediterranean on well. But the countries that lie in this sector include UK, and parts of France, Spain and Germany. The more frequent flow from SE sector to the western Mediterranean

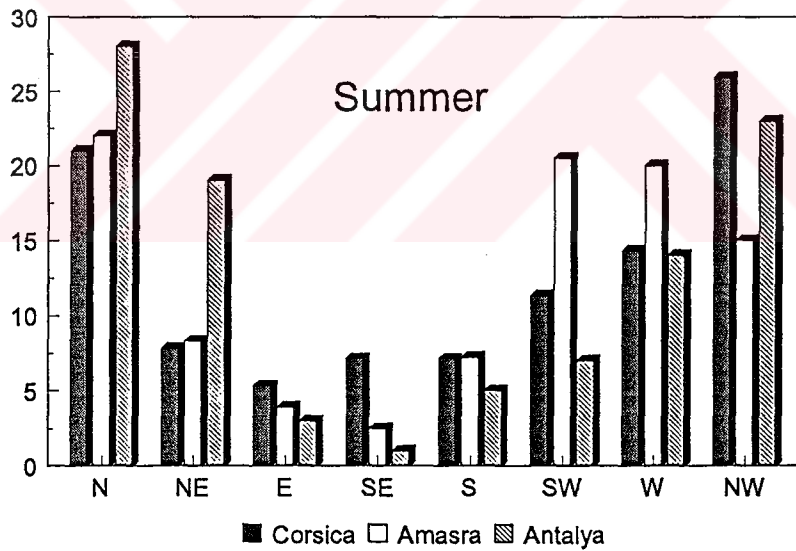
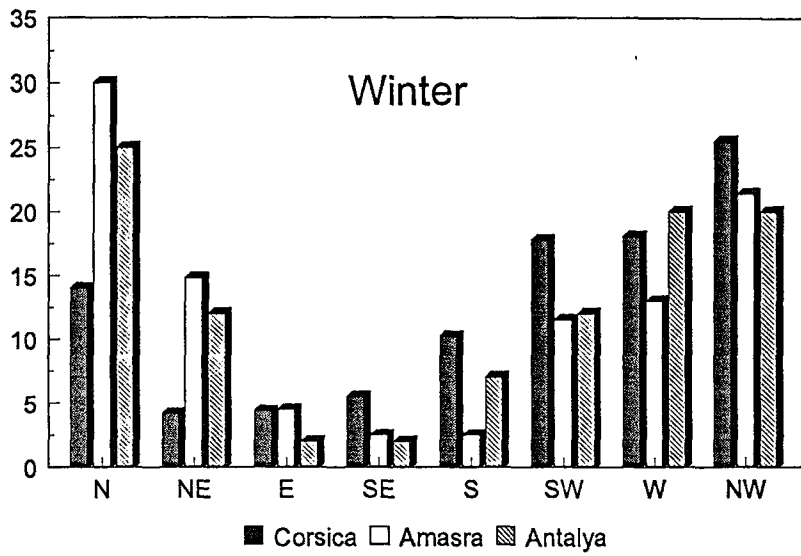


Figure 4.11 Seasonal frequencies of air mass transport from wind sectors at Corsica, Amasra and Antalya

imply that, western Mediterranean basin receives more frequent Saharan dust transport compared to eastern Mediterranean.

Based on this discussion, the aerosol populations in the eastern and western Mediterranean basins are expected to be different. Aerosols in the western Mediterranean basin are under the influence of western European countries such as Germany, France, UK, Spain and should be affected more from the desert aerosols from North Africa. Aerosols in the eastern Mediterranean region, on the other hand, are expected to be more affected from emissions in former USSR countries, and less affected from Saharan dust.

Although general climatological features of the region give indications, on the characteristics of aerosol population, one cannot predict chemical composition based only on air flow patterns, because other factors such as scavenging determines how much of the aerosol injected to an air mass arrive, to the station site in the eastern Mediterranean basin.

4.3. Temporal Variations in Aerosol Composition.

Temporal variations of concentration of aerosols depend on several factors including; the existing natural and anthropogenic sources, transport pattern and meteorological factors (e.g. wind speed, wind direction, precipitation). Since most of these parameters change in time, chemical compositions of aerosols show short and long-term variations. Short term variations generally refer to episodic changes in the concentrations which occur over a daily time scale. Long term changes in this study refer to seasonal variations.

Observed average concentrations of measured species in a region are determined by their episodic transport from various source areas. Since various receptor sites are at different distances to different source regions, reported average concentrations vary significantly from one site to another.

Consequently, average concentrations reported in the literature define characteristics of individual sampling site fairly well, but do not have too much information value in defining the characteristics of the region as a whole. The regional characteristic may be better defined by so called 'regional background concentrations of species which are average concentrations obtained after stripping all peaks in the data which correspond to episodic transport to a particular sampling site.

4.3.1. Regional Background Concentrations of the Eastern Mediterranean Atmosphere

In source attribution and apportionment studies, difficulty is encountered due to the uncertainties in the assessment of background concentrations of chemical species at a specific receptor site. The so called "natural background aerosol" does not exist anymore due to the centuries of human activities and natural processes, another concept "regional background" which represent the region was found to be more appropriate for the region. If such regional background aerosols do exist, their chemical composition should be fairly constant in time and space.

The regional background concentrations of elements were calculated by using the similar approach developed by Husain et al., (1982). The regional background concentrations are assumed to equal the most frequently occurring value. Since for two years sampling period more than 600 daily samples are available in this study, making an assumption that regional background is the most frequently observed value, is not a wrong approximation. Frequency distributions were used for computing most frequently observed values for each variable. The frequency distributions for the aerosol components are useful to search for similarities and differences among the components, which may lead to perceiving the sources and the processes that influence ambient levels. As it is shown in Figure 4.12, most frequently occurring point is the peak point of best fitted distribution.

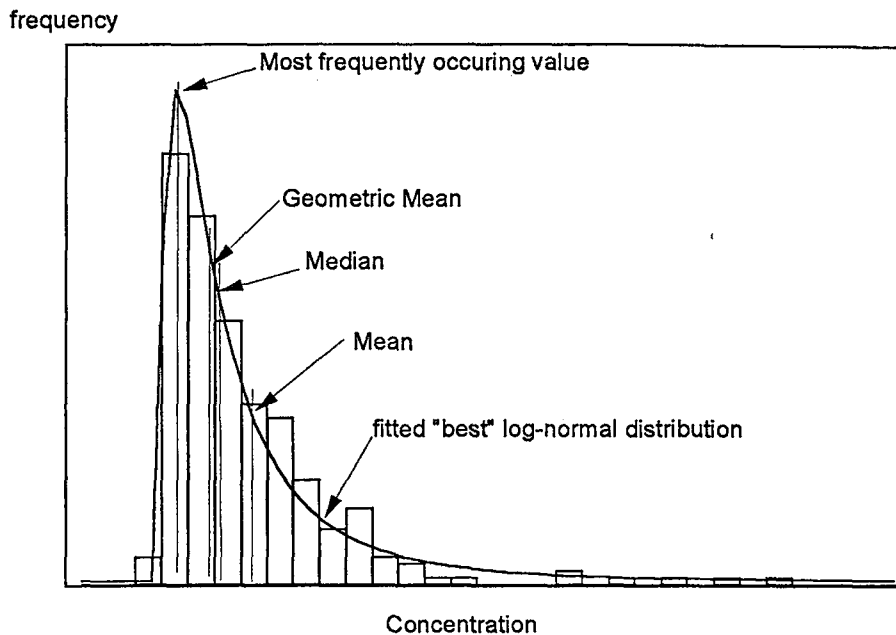


Figure 4.12. Histogram for calculation of most frequently occurring value

In order to calculate the regional background concentrations (or most frequently occurring value) first step is to find best fitted distribution. As it is given in section 4.1.1, a K-S test for each variable at the sampling site shows that the log-normal assumption. Calculated regional background concentrations of trace elements and major ions in the eastern Mediterranean atmosphere are given in Table 4.4.

Calculated regional background concentrations were compared for the year 1992 and 1993. In general, there are no significant difference of the calculated regional background concentrations. Only for the elements, Ni, SO_4^{2-} and NO_3^- , 1992 year background concentrations are higher than the year 1993.

Variation of regional background concentrations on winter and summer seasons and winter-to-summer ratios are also given in the Table 4.4. Although these regional background concentrations are expected to remain constant throughout the year, as can be seen from the table for the crustal elements there are some significant differences observed in the regional background concentrations at different seasons. Anthropogenic elements like Sb and Hg have higher winter background concentrations than summer period. Regional

background concentrations of all crustal elements are at least a factor of two higher at summer than winter season. Calculated regional background concentrations of sea salt elements, Na, Mg, Cl and Mg and anthropogenic elements like As, Se, Sb, Mo and Pb are found uniform throughout the year.

High regional background concentrations of crustal elements during summer months are attributed to resuspension of local soil. In the eastern Mediterranean, summer is the dry season. When the soil is dry, soil related elements are generated in larger quantities. As can be seen in the following sections, concentrations of crustal elements were found to be higher during summer months. This indicates that, season dependent particle generation mechanisms also affect the seasonal patterns in the observed regional background concentrations of elements.

For the secondary elements $\text{SO}_4^{=}$, NO_3^- and NH_4^+ calculated background concentrations are higher in summer season. The reason of high background concentration of NH_4^+ during summer might be increasing the use of fertilizers in this season. Whereas, for $\text{SO}_4^{=}$ and NO_3^- the higher background concentrations during summer might be attributed to the increase of photochemical oxidation.

4.3.2. Short-term (Daily) Variations of Aerosol Concentrations in the Eastern Mediterranean Atmosphere

The temporal variations in the concentrations of sea salt elements (Na, Cl), crustal elements (Al, Fe) and anthropogenic elements (Zn, nss- $\text{SO}_4^{=}$, Pb and As) between March 1992 and December 1993 are given in Figures 4.13-4.20. As can be seen in the figures, concentrations of all groups of elements are highly variable on a daily time-scale. Concentrations may change up to a factor 30 between two successive samples. Such high short term variability in the concentrations of elements was also observed on the western Mediterranean aerosols (Dulac et al., 1987; Bergametti et al., 1989).

Table 4.4. The Calculated Regional Background Concentrations of Trace Elements in the Eastern Mediterranean Atmosphere

	Geometric Mean (ng m ⁻³)		Site Background Conc. (ng m ⁻³) (number of samples)				Geo.Mean/ Backgr.		
	1992-1993 ^a		1993	1992-1993 ^b		Winter	Summer	a/b.	win/sum
	1992	1993		1992-1993 ^b					
Na	1100	330(101)	440(311)	390 (412)	340 (199)	350 (213)	2.82	0.97	
Mg	280	180(285)	210(312)	190 (597)	160 (257)	210 (340)	1.47	0.76	
Al	300	140(275)	140(312)	140 (587)	100 (248)	300 (339)	2.14	0.33	
Cl	990	610(211)	475(312)	480 (313)	440 (140)	500 (173)	2.06	0.88	
K	250	140(283)	155(268)	140 (551)	100 (225)	230 (326)	1.78	0.43	
Ca	1580	1150(283)	1160(24)	1150 (307)	770 (141)	1200 (166)	1.37	0.64	
Sc	0.06	-	0.03(311)	0.03 (312)	0.01 (140)	0.07 (172)	2.00	0.14	
Ti	26.4	-	14(256)	14 (257)	10 (94)	22 (163)	1.89	0.45	
V	1.82	1.2 (285)	0.9(309)	1 (597)	0.7 (254)	1.9 (340)	1.82	0.37	
Cr	3.75	1.75(285)	1.7(246)	1.7 (531)	0.8 (200)	2.3 (331)	2.21	0.35	
Mn	6.11	-	3.6(312)	3.6 (313)	1.7 (140)	7.1 (173)	1.70	0.24	
Fe	230	124(282)	115(311)	120 (593)	60 (254)	280 (339)	1.92	0.21	
Co	0.14	-	0.07(309)	0.07 (310)	0.04 (139)	0.16 (171)	2.00	0.25	
Ni	1.77	1.08(269)	0.51(22)	0.95 (291)	0.55 (124)	1.75 (167)	1.86	0.31	
Zn	11.3	4(40)	4(308)	4 (348)	3 (176)	7 (172)	2.83	0.43	
As	1.2	-	0.77(306)	0.77 (307)	0.78 (136)	0.75 (171)	1.30	1.04	
Se	0.23	-	0.14(311)	0.14 (312)	0.11 (140)	0.15 (172)	1.64	0.73	
Br	14.2	-	10(311)	10 (312)	9 (140)	10 (172)	1.42	0.90	
Rb	0.62	-	0.34(308)	0.34 (309)	0.25 (134)	0.64 (167)	1.82	0.39	
Mo	0.23	-	0.08(219)	0.08 (219)	0.08 (110)	0.07 (109)	2.88	1.14	
Sb	0.29	-	0.2(312)	0.2 (313)	0.2 (140)	0.2 (173)	1.45	1.00	
Cs	0.069	-	0.04(304)	0.04 (305)	0.03 (136)	0.06 (169)	1.72	0.50	
La	0.2	-	0.11(304)	0.11 (305)	0.05 (132)	0.22 (173)	1.82	0.23	

Table 4.4. Cont'd.

Geometric Mean (ng m ⁻³)	Site Background Conc. (ng m ⁻³) (number of samples)					Geo.Mean/ Backgr	win/sum	
	1992-1993 ^a	1992	1993	1992-1993 ^b	Winter			Summer
Ce	0.38	-	0.2(311)	0.2 (312)	0.1 (140)	0.4 (172)	1.90	0.25
Nd	0.31	-	0.14(307)	0.14 (308)	0.08 (136)	0.27 (172)	2.21	0.30
Sm	0.03	-	0.013(309)	0.013 (310)	0.007 (137)	0.029 (173)	2.30	0.24
Eu	0.006	-	0.003(278)	0.003 (279)	0.002 (120)	0.008 (159)	2.00	0.25
Gd	0.021	-	0.008(288)	0.008 (289)	0.003 (121)	0.02 (168)	2.62	0.15
Tb	0.003	-	0.001(282)	0.001 (283)	0.001 (114)	0.003 (169)	3.00	0.33
Dy	0.034	-	0.018(231)	0.018 (232)	0.011 (81)	0.025 (151)	1.89	0.44
Yb	0.011	-	0.005(300)	0.005 (301)	0.002 (129)	0.013 (172)	2.20	0.15
Lu	0.002	-	0.001(301)	0.001 (302)	0.0005(131)	0.002 (171)	2.00	0.25
Hf	0.015	-	0.008(300)	0.008 (301)	0.004 (132)	0.017 (169)	1.88	0.24
Hg	0.041	-	0.017(303)	0.017 (304)	0.042 (139)	0.012 (165)	2.41	3.50
Pb	13	6.9(245)	7.5(40)	7.6 (266)	6.8 (111)	7.8 (155)	1.71	0.87
Th	0.054	-	0.027(310)	0.027 (310)	0.011 (139)	0.06 (171)	2.00	0.18
SO ₄ ⁼	4250	3000(211)	2150(307)	2470 (518)	1760 (200)	3660 (318)	2.41	0.48
NO ₃ ⁻	810	700(206)	390(287)	490 (493)	200 (182)	860 (311)	1.65	0.23
NH ₄ ⁺	800	725(170)	1050(308)	960 (478)	690 (200)	1550 (278)	0.83	0.45

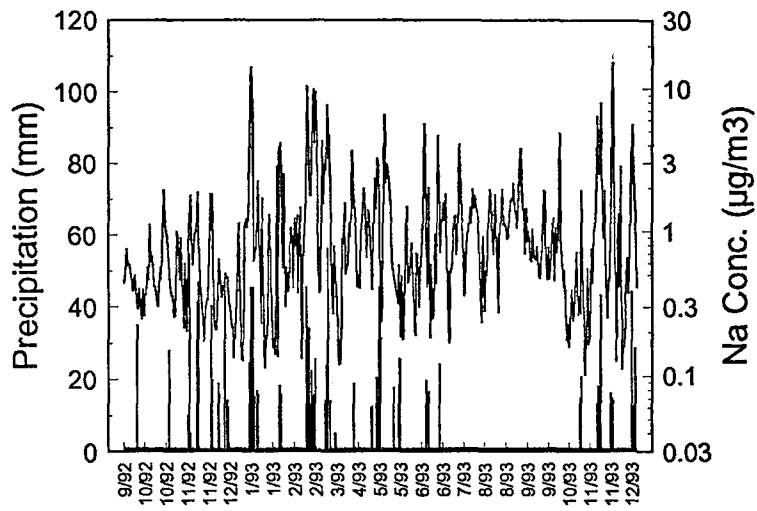


Figure 4.13. Temporal variations of Na

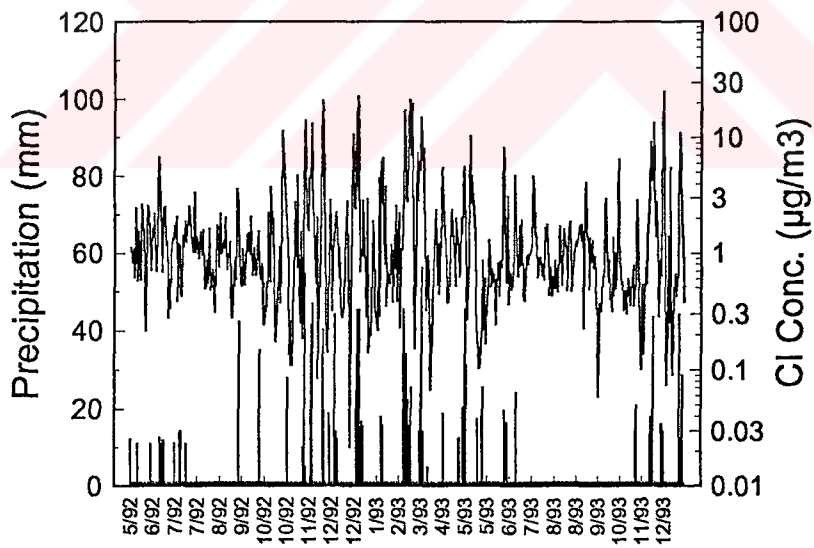


Figure 4.14. Temporal variations of Cl

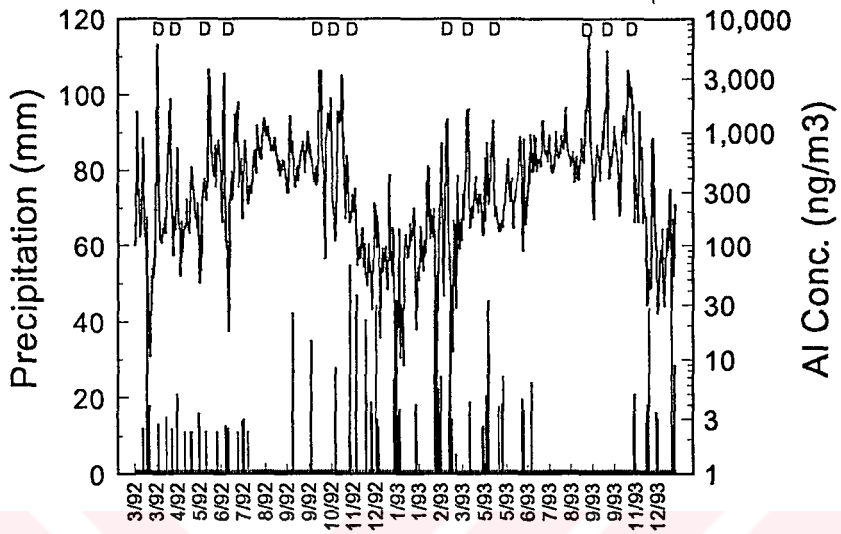


Figure 4.15. Temporal variations of Al

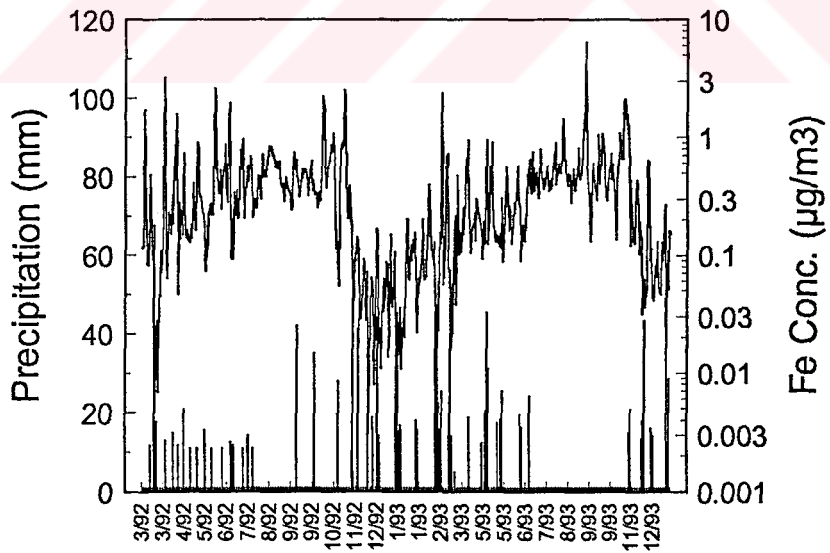


Figure 4.16. Temporal variations of Fe

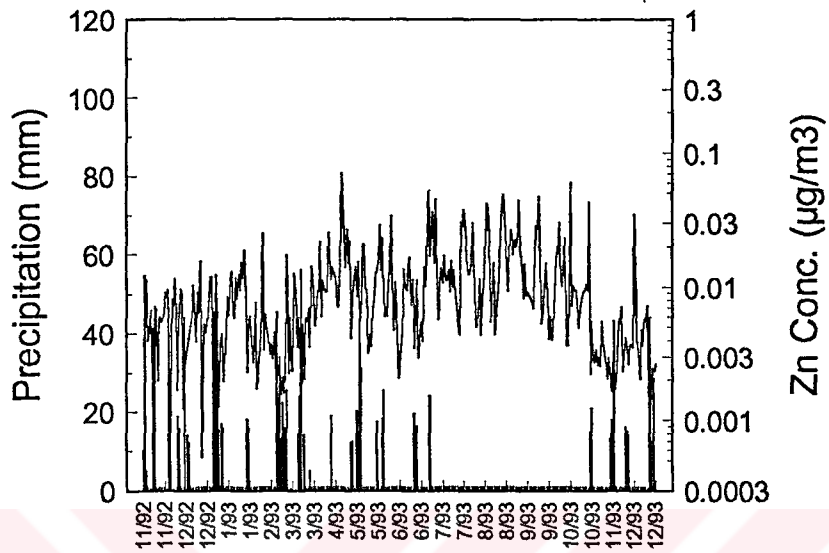


Figure 4.17. Temporal variations of Zn

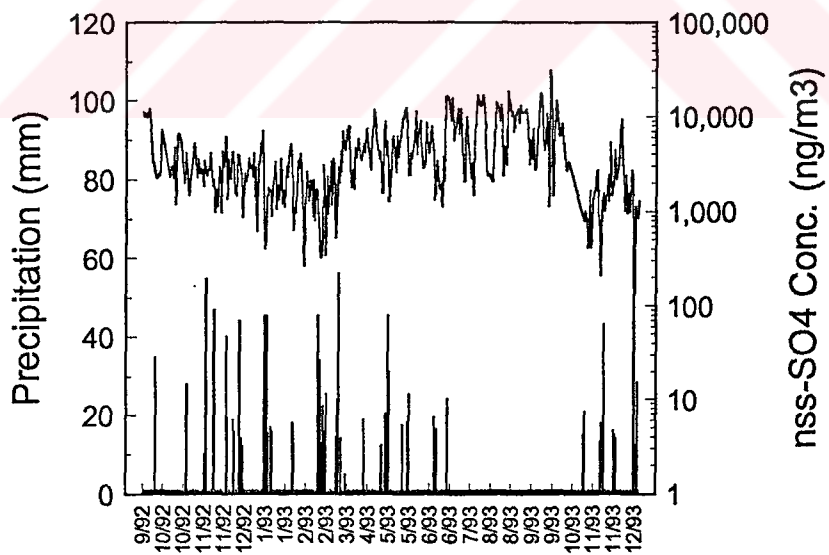


Figure 4.18. Temporal variations of nss-SO₄

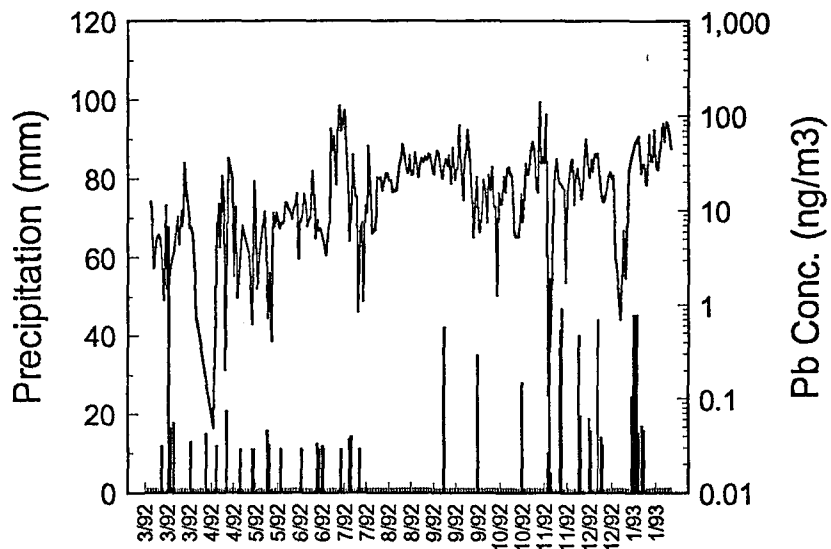


Figure 4.19. Temporal variations of Pb

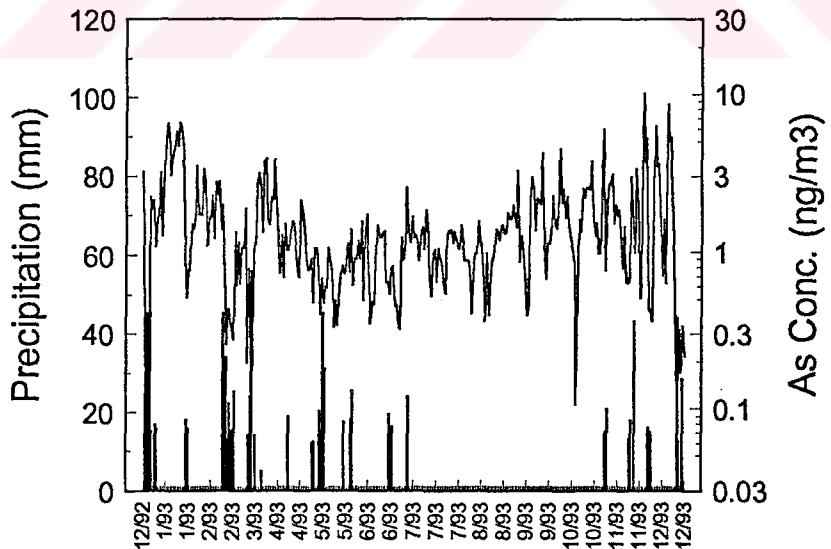


Figure 4.20. Temporal variations of As

As it is illustrated in Figure 4.13 and 4.14, sea salt elements Na and Cl have higher concentrations and strong variability particularly in winter season. Short-term variability of these elements is due to the meteorological factors. Sea salt particles and elements associated with them are generated over the sea surface through bubble-popping process (Blanchard, 1984). Generation of these particles is shown to be logarithmically related to wind speed (Tsunogai et al., 1972; Gras and Ayers, 1983). Storms which generate sea salt particles are more frequent and active during winter season, resulting in high and variable concentration of these marine elements. Since the residence of the sea salt particles in the atmosphere is short owing to their large sizes, the sea salt particles are scavenged out quickly after a storm, resulting in strong short term variability. During summer time as the winds are weak and sea surface is calm, generation of sea salt particles is at minimum and does not change significantly from one day to another.

The strong short term variations of the crustal elements like Al, Ca, K, Sc, Ti, Mn, Fe, Co, Rb, Cs, Ba, La, Sm, Ce, Yb, Lu and Th, are observed during spring and fall as can be seen in Figure 4.15 and 4.16 for Al and Fe. Low concentrations of crustal elements are frequently observed during winter when the soil on both the local and surrounding land masses is damp due to precipitation. The air-mass trajectories corresponding to unusually high dust events are frequently associated with transport from the north Africa and occasionally from Middle East.

The strong short term variability of the crustal elements is either due to transport patterns or due to the local turbulence and humidity of the local soil. The resuspension of local soil into the atmosphere is highly dependent on the local wind speed. During summer, as the soil is dry, weathering of crustal material is enhanced and atmospheric concentration of soil-derived elements increase. Once the soil is dry, air-borne concentrations of crustal elements depends only on the wind speed. Consequently daily variation in

the wind speed causes observed episodes in the concentrations of soil-related elements.

Since variability of the concentrations of both marine and crustal elements depends on the local wind speed, and their generation is enhanced by the presence of high winds, one would expect a strong correlation and similar temporal behavior of marine and crustal elements. However, such correlation does not exist and furthermore, long term variations in their concentrations are significantly different as will be discussed in the following section. The main reason of the dissimilarity of the variability of marine and crustal elements is that, generation of crustal particles in the atmosphere depends on the wind speed only if the soil is dry.

But when the soil is damp which is the case most of the time during winter, the resuspension of crustal particles is low no matter how high the wind speed is. Consequently, all the strong-wind events which generate high concentrations of marine elements over the sea do not necessarily generate high concentrations of crustal elements. Furthermore, once the soil is dry it readily responds to variations in the wind speed, because the threshold wind speed for the soil to become air borne is only 4 m s^{-1} . But, the wind speed threshold for bubble bursting to start is 10 m s^{-1} (Wang and Street, 1978; Monahan et al., 1982). Consequently, the wind speeds which are sufficient to cause soil element episodes do not necessarily generate sea-salt through bubble bursting.

Besides resuspension of local soil, the Saharan Desert and arid regions of Middle East are other important sources of crustal material observed on eastern Mediterranean and since transport from those source regions is episodic, they also cause short-term variation in the concentrations of soil related elements.

The Saharan dust transport is a well known phenomenon. A low-pressure system coming from the North African deserts when associated

with strong upper winds of the subtropical jet stream produce dust storms over north eastern Mediterranean region (Ganor, 1991). Such dust storms occur in the eastern Mediterranean basin in the rainy season anytime between September and June, but mostly from December to April (Ganor, 1991; Ganor and Mamane, 1982). The dust transport is sporadic and occurs 10-20 times a year (Loye-Pilot et al., 1986) and could last for periods of three days or more (Yaalon and Ganor, 1979). During dust incursion to the Mediterranean basin concentrations of particles and crustal elements such as Al, increase from a typical 100-200 ng m⁻³ to 1000-2000 ng m⁻³ as show in Figure 4.15. Aluminum is one of the many soil related elements measured in this study. But, it in the most widely used crustal reference element as the soil is its only source in the atmosphere and it can be measured accurately and sensitively by a variety of analytical techniques (Uemetsu et al., 1983; Prospero and Nees, 1987; Chester et al., 1991). In this study as well, Al is used as tracer for airborne soil particles.

A total of 25 dust episodes were detected in 1992 and 1993. Back trajectory calculations demonstrated that 15 of these storms were associated with air mass movements from north Africa. Examples of these back trajectories corresponding to days with high Al concentration are given in Figure 4.21. The 8 of the remaining 10 Al episodes were due to resuspension of local soil in the days corresponding to there 26 samples local wind speed was greater than 7 m s⁻¹. The wind speeds of these samples are significantly higher than average wind speed at our site which is 4 m s⁻¹. The 2 of the remaining Al episodes were due to transport from arid regions in the Middle east. The back trajectories corresponding to these days, indicated a transport from desert areas in Israel and Egypt. The Al episodes which are associated with dust transport from Sahara are indicated by "D" in Figure 4.15.

Variations in the concentrations of selected anthropogenic elements Zn, SO₄²⁻, Pb and As are given in Figure 4.17-4.20. Unlike marine and crustal

elements, anthropogenic elements measured in the immediate vicinity of the sampling site do not have local sources. Consequently, variations in emissions from their sources which are located thousands of kilometers away from the station can not have a strong impact on their concentrations. Therefore, for anthropogenic elements, variability is largely due to variations in transport patterns and different removal rates of atmospheric particles with which they are associated. In the western Mediterranean, Remoudaki et al. (1991) showed that the short term and long term variability of aerosol Pb concentrations are primarily due to the scavenging of aerosol particles by rain rather than changes in source strengths.

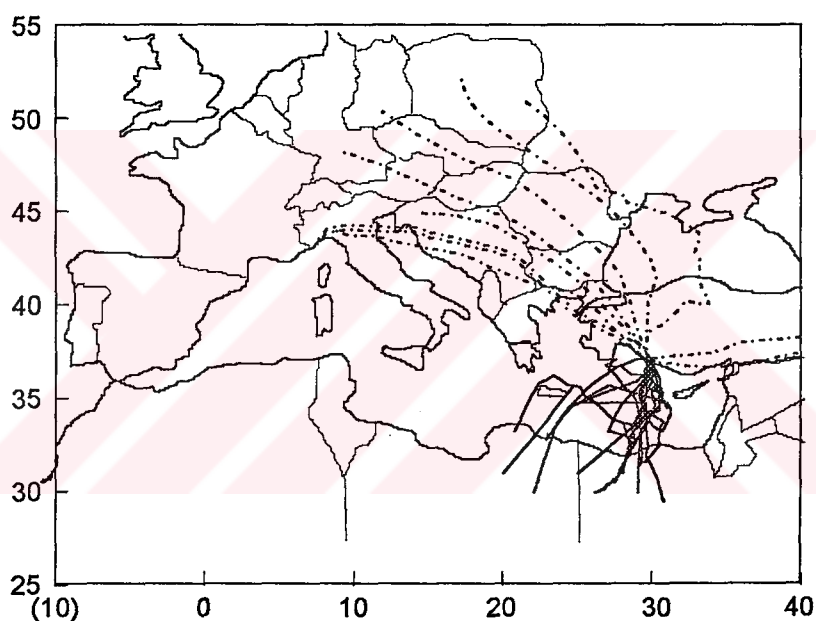


Figure 4.21. Examples of back trajectories corresponding to high Al (solid lines) and high SO₄ (broken lines) concentration days

In order to find out the reasons of variations of anthropogenic elements, high concentrations episodes were detected for the selected anthropogenic elements, nss-SO₄²⁻ and Pb. For nss-SO₄²⁻, 10 episodes were detected. Back trajectories demonstrated that 8 of these episodes were associated with air mass movements from north, north-west sectors. The back trajectories for the remaining two episodes indicate easterly flow.

During the episodes, the nss-SO_4^- concentrations increase from geometric mean $3.2 \mu\text{g m}^{-3}$ to $10.0\text{-}18.0 \mu\text{g m}^{-3}$. Precipitation occurred only within the two out of 10 episodes. The high nss-SO_4^- episode observed during 21-25 May 1993. On the 24th of May, nss-SO_4^- concentration measured as $12.25 \mu\text{g m}^{-3}$ and on the night of 25th of May, it rained and the nss-SO_4^- concentration was measured a factor of five less ($2.4 \mu\text{g m}^{-3}$) on the following day. Other than this example, there is no considerable decrease in concentrations after precipitation suggesting precipitation scavenging is not the main reason of high variability of the measured anthropogenic concentrations.

For Pb, during the study period, four high concentration episodes were identified. The back trajectories of these episodes indicate north-west and north sectors. During these episodes, the Pb concentrations reach up to 130 ng m^{-3} from an average value 13 ng m^{-3} . The largest decrease of Pb concentration (by a factor of 110) observed on 12-14 November 1992. The Pb concentration was measured 102 ng m^{-3} on the 12th of November, on 13th of November it rained and the air mass change from north-west direction to west and the Pb concentration was measured on 14th of November as 0.9 ng m^{-3} . A considerable decrease in Pb concentration after precipitation was also detected on 4-12 July 1992. Since there was no rain during the other two episodes, Pb concentration changes attributed to the changes of the transport patterns.

In general, the strongest peaks in the concentrations of chalcophilic elements were associated with back trajectories from north and north-west and significantly low concentrations were measured when the air mass originated from south and east. Consequently, short-term variations in the concentrations of pollution derived elements are determined mainly by the transport from source regions to our receptor site.

4.3.3. Long-term (Seasonal) Variations of Aerosol Concentrations in the Eastern Mediterranean Atmosphere

Concentrations of elements and ions in the Antalya station show long term (seasonal) trends depending on the seasonal variations in transport patterns, particle removal and generation mechanisms.

The monthly average concentrations of selected elements in the eastern Mediterranean atmosphere are depicted in Figure 4.22 through 4.27. Based on the variations of monthly average concentrations which indicate seasonal variations in the concentrations of elements, the measured parameters are divided in to three major categories.

Group (1): Elements which have higher concentrations in summer season.

Crustal, and anthropogenic elements V, Cr, Co, Ni, Zn, Se, nss-SO_4^{2-} and NO_3^- are in this group. Since the soil is dry during summer season, weathering of dust from surrounding regions are enhanced during summer. This results in high concentrations of soil-derived elements during summer period. Monthly variations in the concentrations of Al, Sc, Fe and La which are typical soil-derived elements are given in Figures 4.22 and 4.23.

Monthly average concentrations of anthropogenic elements Cr, Ni, nss-SO_4^{2-} and Se are depicted in Figures 4.24 and 4.25. High summer concentrations of these pollution derived elements can not be attributed to variations in airflow pattern because as discussed in previous sections, seasonal variations in the air flow patterns are not large enough to explain observed seasonal variations in concentrations. The observed seasonal differences in the concentrations of anthropogenic elements should be explained by local and distant precipitation scavenging. Since the rain is more

frequent during winter (80% of the precipitation occurred in winter season in 1992 and 1993) particles are removed more extensively during winter season. This results in lower concentrations of pollution derived elements in winter and higher concentrations in summer which is clearly seen in Figure 4.24. Although, wet removal also affects the crustal and marine particles, seasonal variations in the generation of these particles have dominating effect over the scavenging by rain events. One should note that rain has also strong effect on the generation of soil particles. It suppresses the generation of soil particles by keeping the soil damp in winter. Consequently, it has been concluded that, the atmospheric concentrations of pollution derived elements are determined mostly by the scavenging process.

Group (2) Winter -high: This group is consist of sea salt elements Na and Cl, and anthropogenic species As, Hg, Mo and NH₄. Measured high concentrations of Na and Cl during winter time are due to occurrence of strong storm activity in this season. Monthly average concentrations of Na and Cl are depicted in Figure 4.26. The classical relation between the local wind speed and Na concentrations has been previously observed by Bergametti et al. (1989) at western Mediterranean and by Hacısalıhođlu et al., (1993) at the Black Sea aerosols. The monthly variations of As and Mo are given in Figure 4.27. Contrary to other pollution derived elements, those are the ones having higher concentrations during the winter period. This pattern suggesting that they have different and probably more local sources in the aerosols.

Group (3) No trend: Sb, Pb and Br are in this group. Since those elements do not show any seasonal trend at all, their source is likely to be mostly local. The primary anthropogenic source of Pb and Br is gasoline combustion (Biggins and Harrison, 1979). Xudong et al., (1994) has been found that Sb are also emitted by motor vehicles in

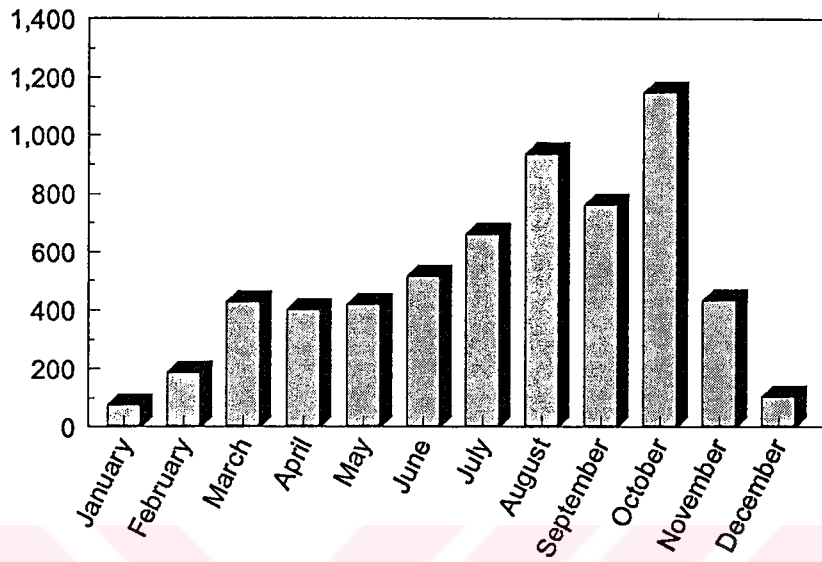
considerable amounts suggesting that Sb and Br are potential marker elements of motor vehicles.

Summer (May-October) and winter (November-April) average concentrations of elements and ions are given in Table 4.5 together with the summer to winter ratios. As can be seen on Table 4.5, the difference between summer and winter concentrations of anthropogenic elements are not as large as the differences observed in marine and crustal elements. The ratio is approximately 3 for crustal elements indicating that, summer concentrations of these elements are approximately a factor three higher than their corresponding winter concentrations. The corresponding ratio for anthropogenic elements varies between 2.7 for V and 0.8 for As.

There is a significant difference observed on seasonal concentrations of SO_4^{2-} ; summer 5840 (1.5) $\text{ng}\cdot\text{m}^{-3}$, winter 2570 (1.91) $\text{ng}\cdot\text{m}^{-3}$. Thus summer SO_4^{2-} is at least a factor of 2 higher than winter. Similar summer increases in sulfate concentrations were observed at Whiteface mountain (Husain et al., 1982) and Narragansett, RI (Rahn et al., 1982). The reasons for the observed seasonal changes can be explained due to the increased photochemical oxidation of SO_2 to SO_4^{2-} during summer to a certain degree, but it only account for part of the increase.

Like sulfate, summer average nitrate concentrations, 1210 $\text{ng}\cdot\text{m}^{-3}$ are 3.5 times higher than winter average concentrations 400 $\text{ng}\cdot\text{m}^{-3}$. Nitrate and sulfate are both formed by gas-to-particle conversion. Therefore, increase of nitrate concentrations during summer season can be attributed to oxidation of precursor gases to nitrate with increased solar flux in summer (Nodop, 1986; Galloway and Likens, 1981). Removal of sulfate and nitrate by deposition and precipitation scavenging during winter time should be another reason of observing high summer concentrations.

Average Concentrations, AI



Average Concentrations, Sc

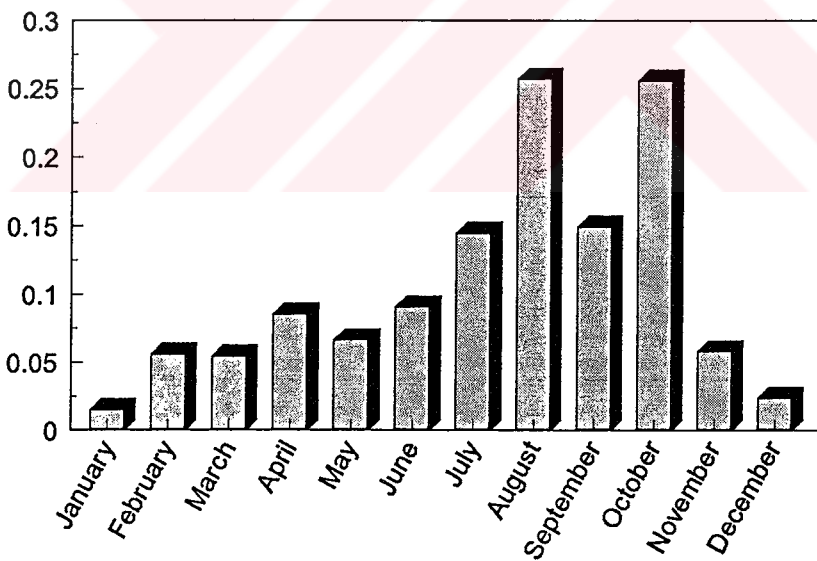
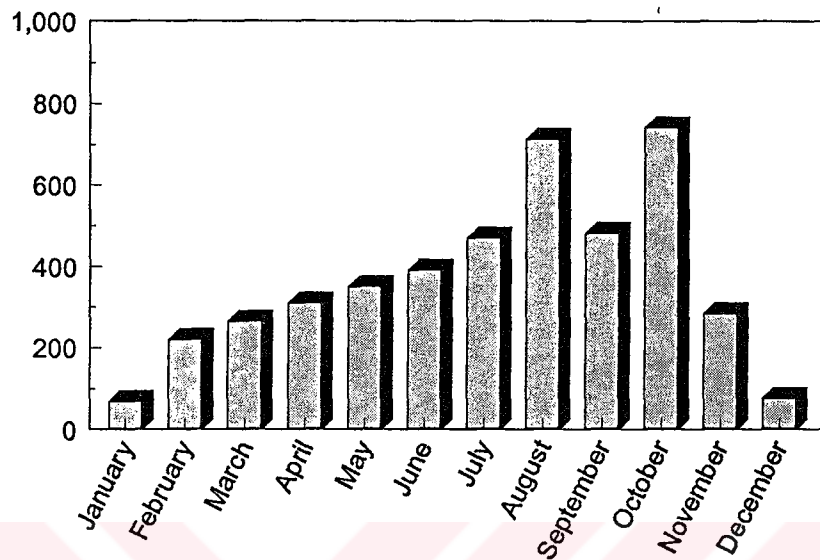


Figure 4.22 Monthly variations of AI and Sc (ng/m3)

Average Concentrations, Fe



Average Concentrations, La

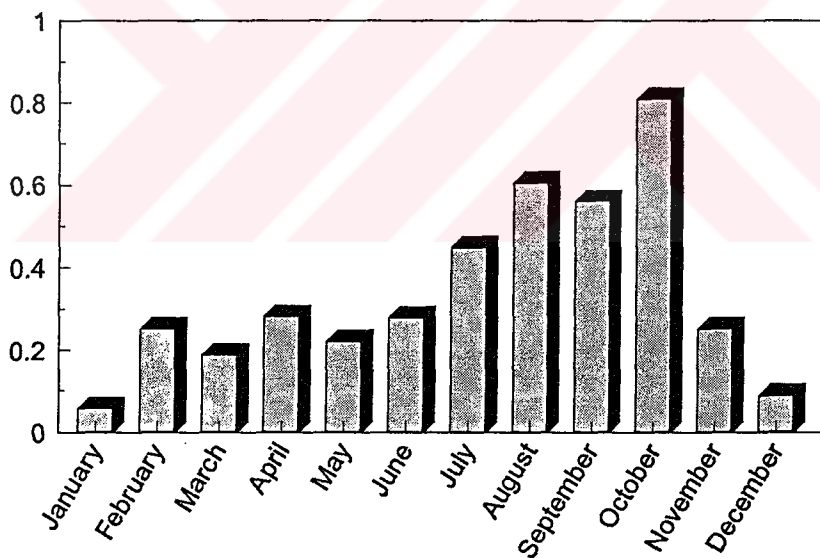
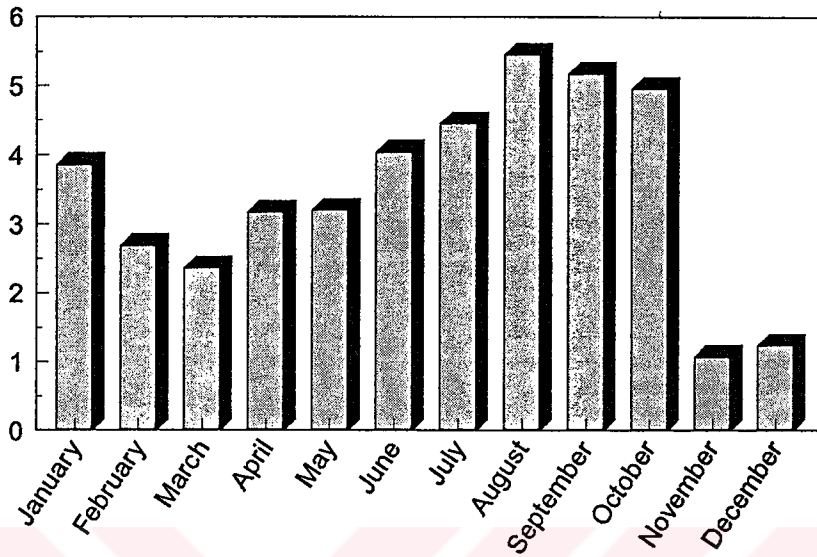


Figure 4.23 Monthly variations of Fe and La (ng/m³)

Average Concentrations, Cr



Average Concentrations, Ni

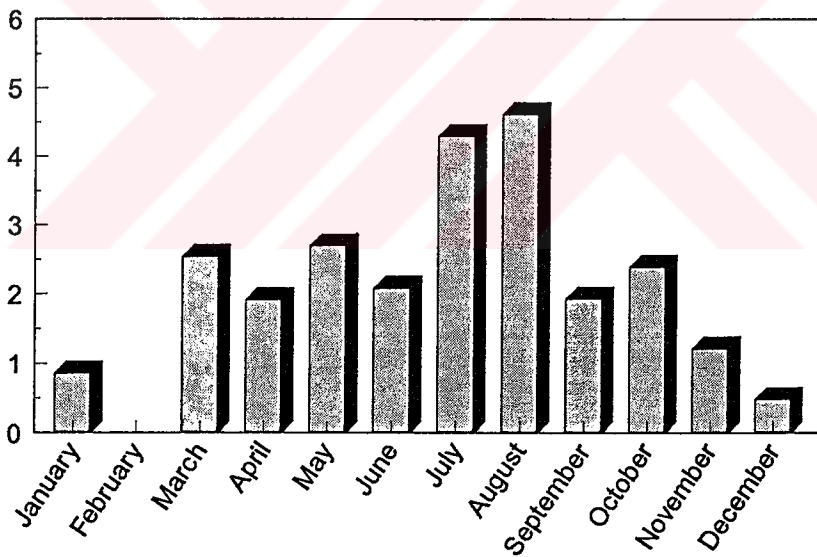
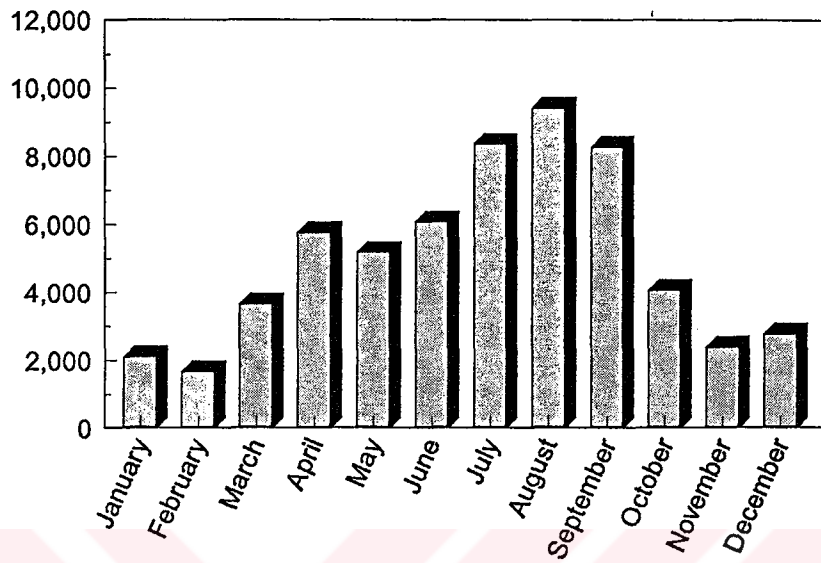


Figure 4.24 Monthly variations of Cr and Ni (ng/m³)

Average Concentrations, nss-SO₄



Average Concentrations, Se

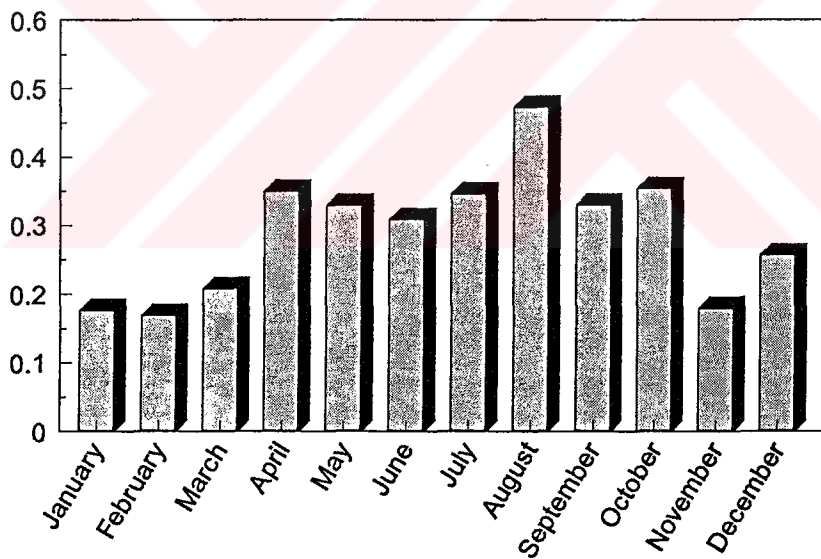
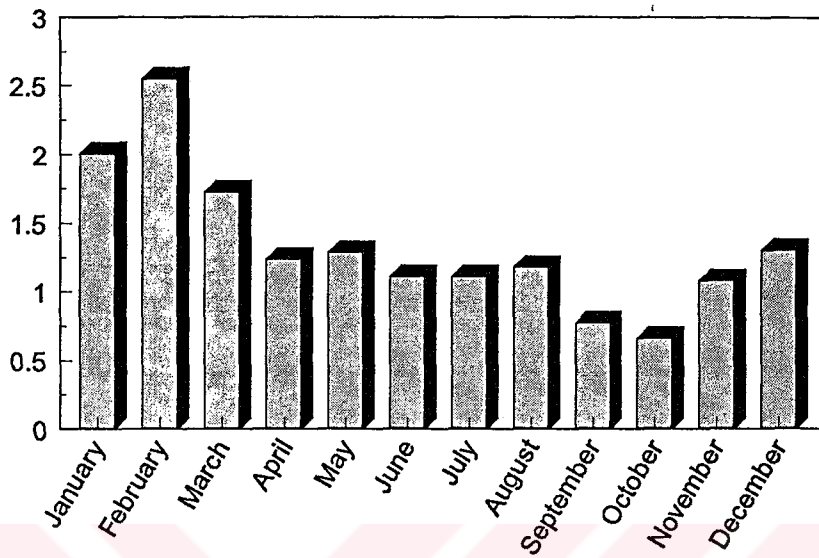


Figure 4.25 Monthly variations of nss-SO₄ and Se (ng/m³)

Average Concentrations, Na



Average Concentrations, Cl

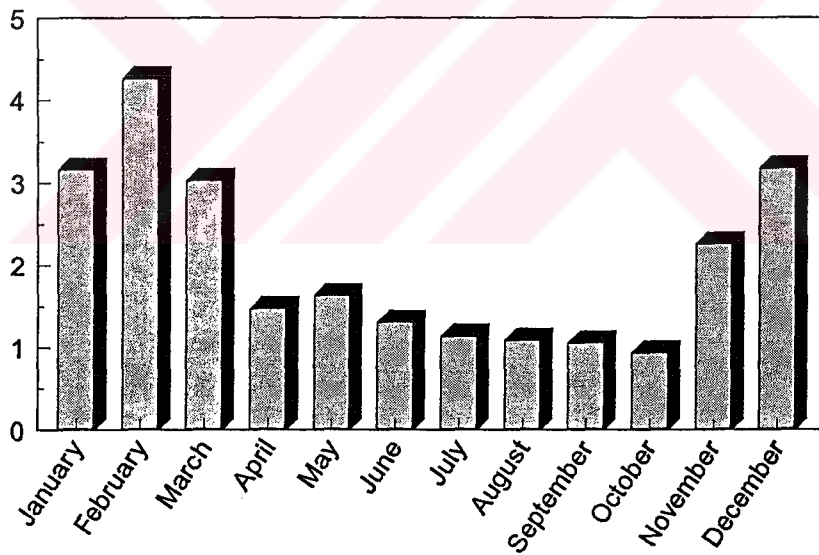
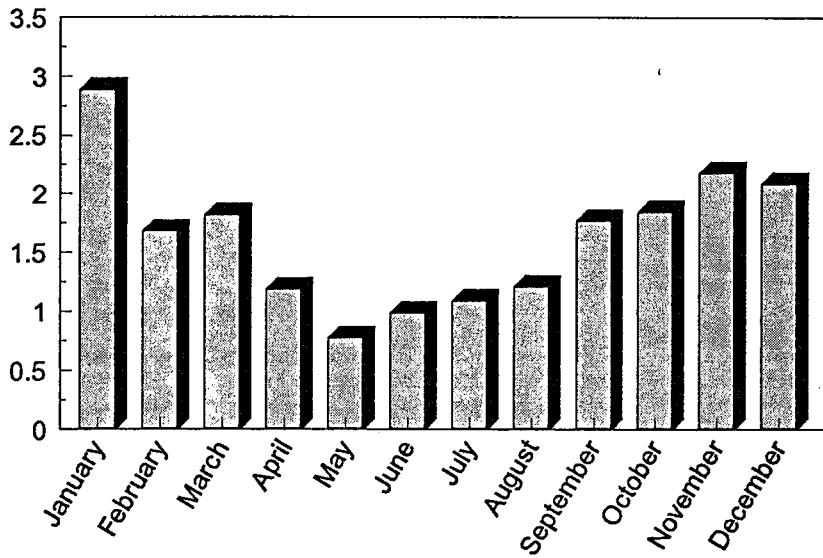


Figure 4.26 Monthly variations of Na and Cl ($\mu\text{g}/\text{m}^3$)

Average Concentrations, As



Average Concentrations, Mo

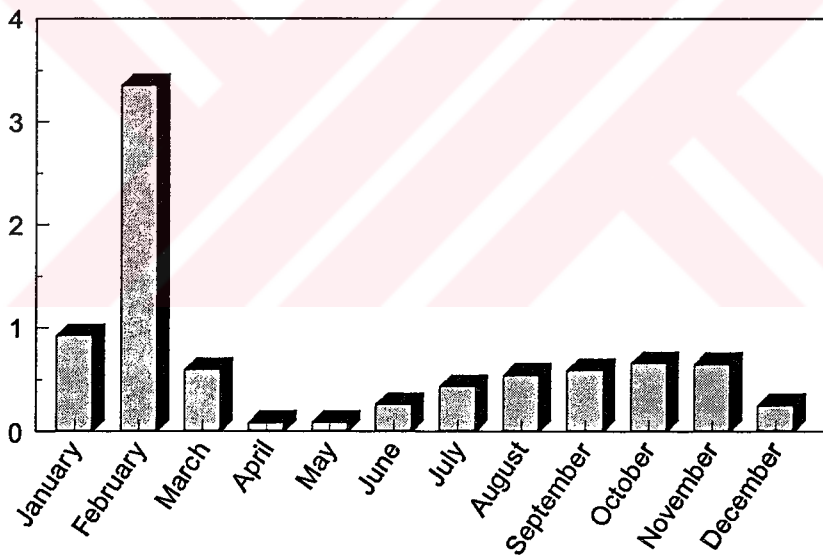


Figure 4.27 Monthly variations of As and Mo (ng/m³)

Table 4.5. Seasonal Elemental Concentrations (ng·m⁻³)

	summer (dry) Geo. mean	winter (wet) Geo. mean	Summer/Winter
NO ₃ ⁻	1210	400	3.0
SO ₄ ⁼	5840	2570	2.3
NH ₄ ⁺	680	1010	0.7
Na	640	750	0.8
Mg	310	250	1.2
Al	530	140	3.8
Cl	830	1210	0.7
K	344	155	2.2
Ca	1890	1240	1.5
Sc	0.11	0.025	4.4
Ti	37	15	2.5
V	2.8	1.03	2.7
Cr	3.6	1.5	2.4
Mn	10.3	3.2	3.2
Fe	0.41	0.11	3.7
Co	0.24	0.07	3.4
Ni	2.5	0.92	2.7
Zn	11	5	2.2
As	1.1	1.4	0.8
Se	0.3	0.17	1.8
Br	14	15	0.9
Rb	0.98	0.35	2.8
Mo	0.16	0.34	0.5
Sb	0.31	0.26	1.2
Cs	0.11	0.04	2.8
La	0.35	0.1	3.5
Ce	0.67	0.19	3.5
Nd	0.44	0.2	2.2
Sm	0.05	0.01	5.0
Eu	0.011	0.003	3.7
Gd	0.041	0.008	5.1
Tb	0.005	0.001	5.0
Dy	0.044	0.02	2.2
Yb	0.02	0.005	4.0
Lu	0.0035	0.001	3.5
Hf	0.028	0.007	4.0
Hg	0.019	0.097	0.2
Pb	15	14	1.1
Th	0.1	0.02	5.0

4.3.4. Factors Affecting Temporal Variations of Aerosols

As discussed in previous sections, concentrations of ions and elements in aerosols depend on a variety of factors, such as source strength, transport patterns, local meteorological events and scavenging efficiencies. Concentrations of measured parameters show strong short and long term variations as a result of these complex processes. In this section, the effect of the most important source of variability, namely local rain events on observed concentrations of elements will be discussed in detail.

4.3.4.1. Influence of Local Rain Events

The rain events were shown to be the main determining factor for observed variability of elemental concentrations in the western Mediterranean basin (Dulac et al., 1987; Remoundaki et al., 1991). Discussions in the previous sections have shown that, rain events is the determining factor for observed long term variations in the concentrations of marine, crustal and pollution derived elements in the eastern Mediterranean atmosphere as well.

Rain determines the extend of resuspension of soil particles and crustal elements associated with them to the atmosphere. If the soil is damp due to rain, the resuspension rate is low and when the soil is dry, particularly during summer season when the rain is scarce, resuspension of soil particles is more extensive. The effect of rain on the concentrations of sea salt related elements were also indirect. Rain in the Mediterranean region is generally associated with frontal systems which is accompanied with fairly strong winds. Storm activity associated with rain enhances the generation of sea salt particles over the sea, thus affecting the concentrations of marine elements.

Aerosols bearing elements can be removed from the atmosphere either at the vicinity of the station by local rain events or they can be

removed during their long range transport to the station site by rain events on the path of air masses that brings them to the eastern Mediterranean region. The effect of local and distant rain events can be distinguished and separately quantified as their effect on elemental concentrations may be different. In this study, the effect of local rain events on concentrations of elements was studied, and the effect of distant rain was speculated based on comparison of the results expected from local rain events and observed temporal behavior of elemental concentrations.

To understand the influence of local rain on the measured concentrations of elements and ions, days with rain events at the station site were marked on the aerosol data set. Then average concentrations of elements and ions in aerosols were computed for the rainy days and in the remainder of the data. For this, only winter data was used to avoid interference of seasonal differences on calculated averages. This was necessary, because the rain frequency is not uniform throughout the year. When winter data was used, the non-rainy period corresponds to at most 10 days after rain, because the frequency of rain events is shorter than 10 days during winter.

The ratios of the elemental concentrations in non-raining days to average concentrations in raining days are presented in Figure 4.28. In this figure, the concentrations of anthropogenic and crustal element were higher than the corresponding concentrations in rainy days by factors changing between 1.5 and 3. The differences in the ratios were due to different scavenging efficiencies of different size of particles and their solubility's in rain (Buat-Menard and Duce, 1986; Eder and Dennis, 1990). Studies in continental regions have indicated that the largest particles are scavenged more efficiently by rain (Scott, 1981). Concentrations of marine elements, on the other hand, are higher during rainy days, because rain events in the eastern Mediterranean are generally associated with frontal storms which enhances sea salt generation

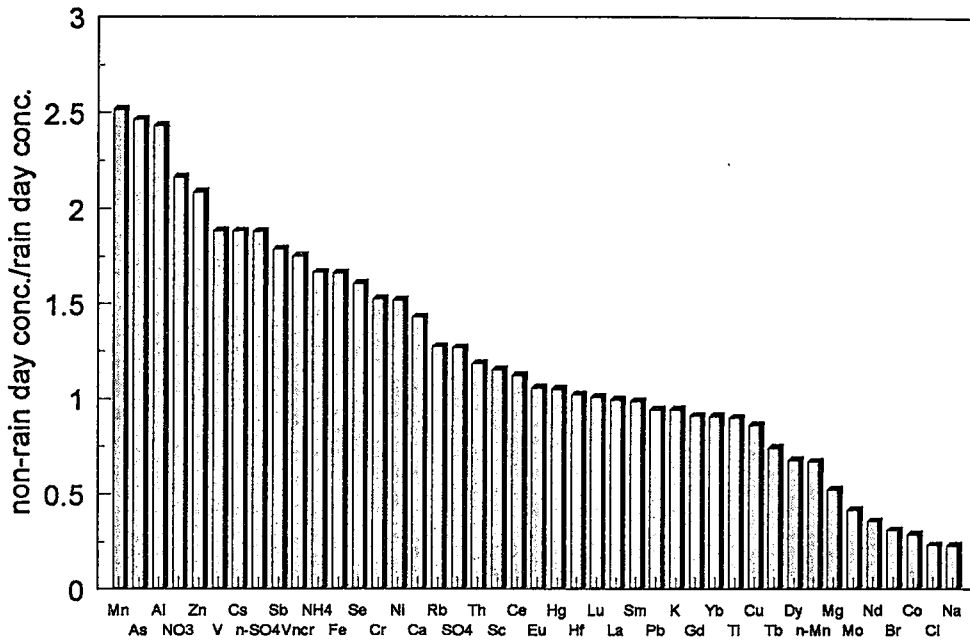


Figure 4.28. The ratio of elemental concentrations in non-raining days-to-average concentrations in raining days.

The decrease in the concentrations of crustal and anthropogenic elements due to rain shown in Figure 4.28 depends on how efficiently particles are removed from the atmosphere by the rain. Since crustal and anthropogenic elements are associated with coarse and fine particles, respectively, crustal elements are expected to washout from the atmosphere more efficiently by local rain compared to pollution-derived elements which are associated with fine particles. The concentrations of elements in aerosols in each raining day were compared with the corresponding concentration two days prior to rain to get information on the washout efficiency of each element. Results were averaged and presented in Figure 4.29. The differences in the ratios between elements from the same origin in the figure are due to different scavenging efficiencies of elements.

Four groups of elements can be identified in the Figure 4.29. The elements Na and Cl are sea salt elements and their concentrations are higher by a factor of 3 during rain day compared to the concentrations two

days before the rain event due to enhanced production of sea salt by high winds associated with frontal rain events as discussed before. Elements Br, Mg and K have mixed sources. For the mixed source elements like Br, Mg and K, as the marine component increase and crustal (anthropogenic in case of Br) component decrease during the rain day, the net effect was an increase in the concentrations during rain. But, the increase was not as large as the increase observed in purely marine elements.

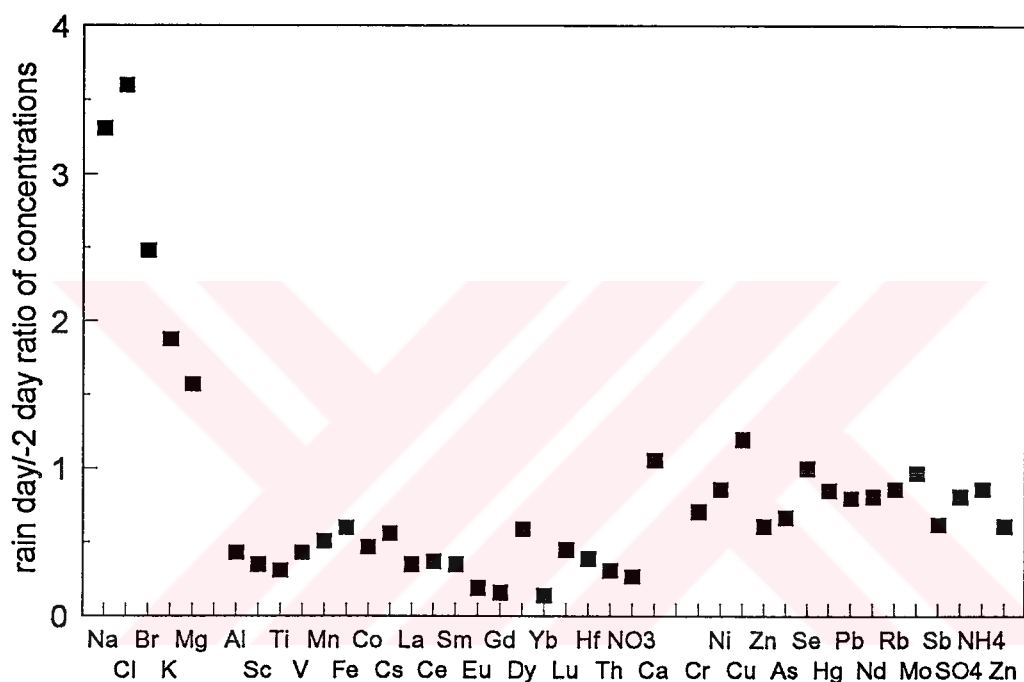


Figure 4.29. The ratio of elemental concentrations measured at the raining day to those measured two days before the rain event

Although, concentrations of both crustal and anthropogenic elements decrease in rain days, there is a well defined difference in their ratios shown in Figure 4.29. Concentrations of soil related elements decrease approximately by a factor of 3 during the rain whereas concentrations of anthropogenic elements decrease only by a factor 1.2. These ratios are consistent for each group of elements. The difference in these ratios suggest that large soil particles are scavenged approximately three times

more efficiently than fine particles bearing anthropogenic elements which is in fairly good agreement with the scavenging coefficients given in the literature for crustal and pollution derived elements (GESAMP, 1990; Galloway et al., 1993).

Investigation of the change in concentrations of different groups of elements after each rain also provides information on the reloading time of the atmosphere by pollution derived and crustal particles. Variations in the concentrations of Al and Sb, which are marker elements for crustal and pollution derived particles, as a function of time after the rain event are depicted in Figures 4.30 and Figure 4.31. Reloading time of the atmosphere is much shorter for anthropogenic elements than that of crustal elements. Investigation of Figure 4.31 and individual rainy periods have indicated that concentrations of anomalously enriched elements (AEE's) resume to their pre-rain levels within 1-3 days after rain and their atmospheric concentrations have no memory effect from the rain event after three days. On the other hand, concentrations of crustal elements increase very gradually in the first 10-15 days, then increase almost exponentially between 15-30 days and levels off after 30 days. Since the average time between two rain events is less than 10 days and it takes about 30 days for the atmospheric concentrations of soil related elements to reach their pre-rain levels. The atmosphere is never completely reloaded with crustal particles during winter.

Average concentrations of Al, Sc, Fe, La, Na, Cl, Zn, As, Sb, and nss-SO₄ starting from 3 days before the rain event until 10 days after the rain are plotted in Figure 4.32. In this figure, for example average Al concentration in -2 day (2 days before rain) is the average of all Al data measured 2 days before all rain events. Hence the Figure 4.32 provides information on the long-term averaged behavior of elemental concentrations in the course of a rain event. Different reloading behaviors of crustal and anthropogenic elements are clear in the Figure 4.32.

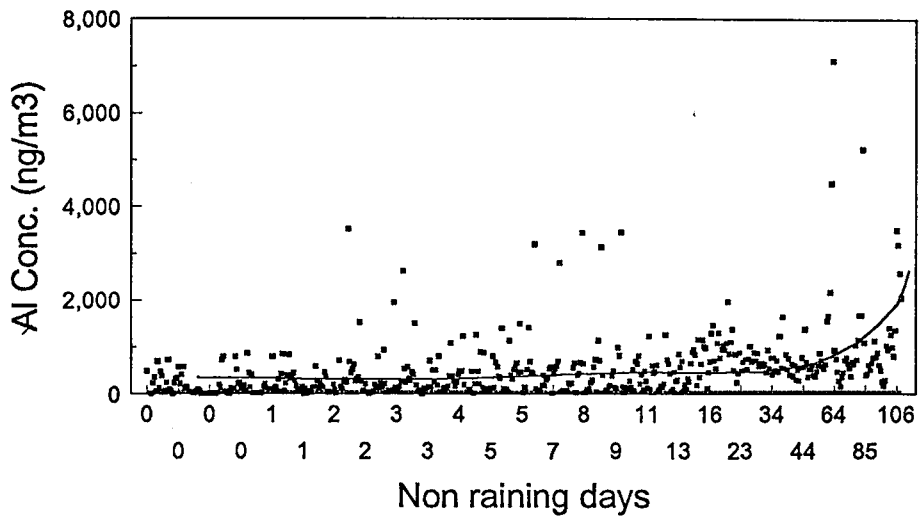


Figure 4.30 Variatiron of Al concentration as a function of number of non-raining days

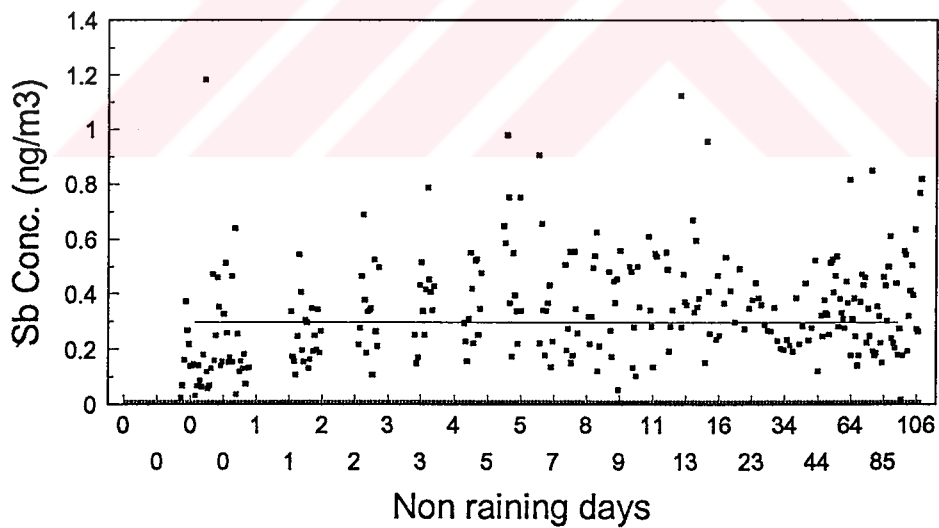


Figure 4.31 Variatiron of Sb concentration as a function of number of non-raining days

Concentration (ng/m³)

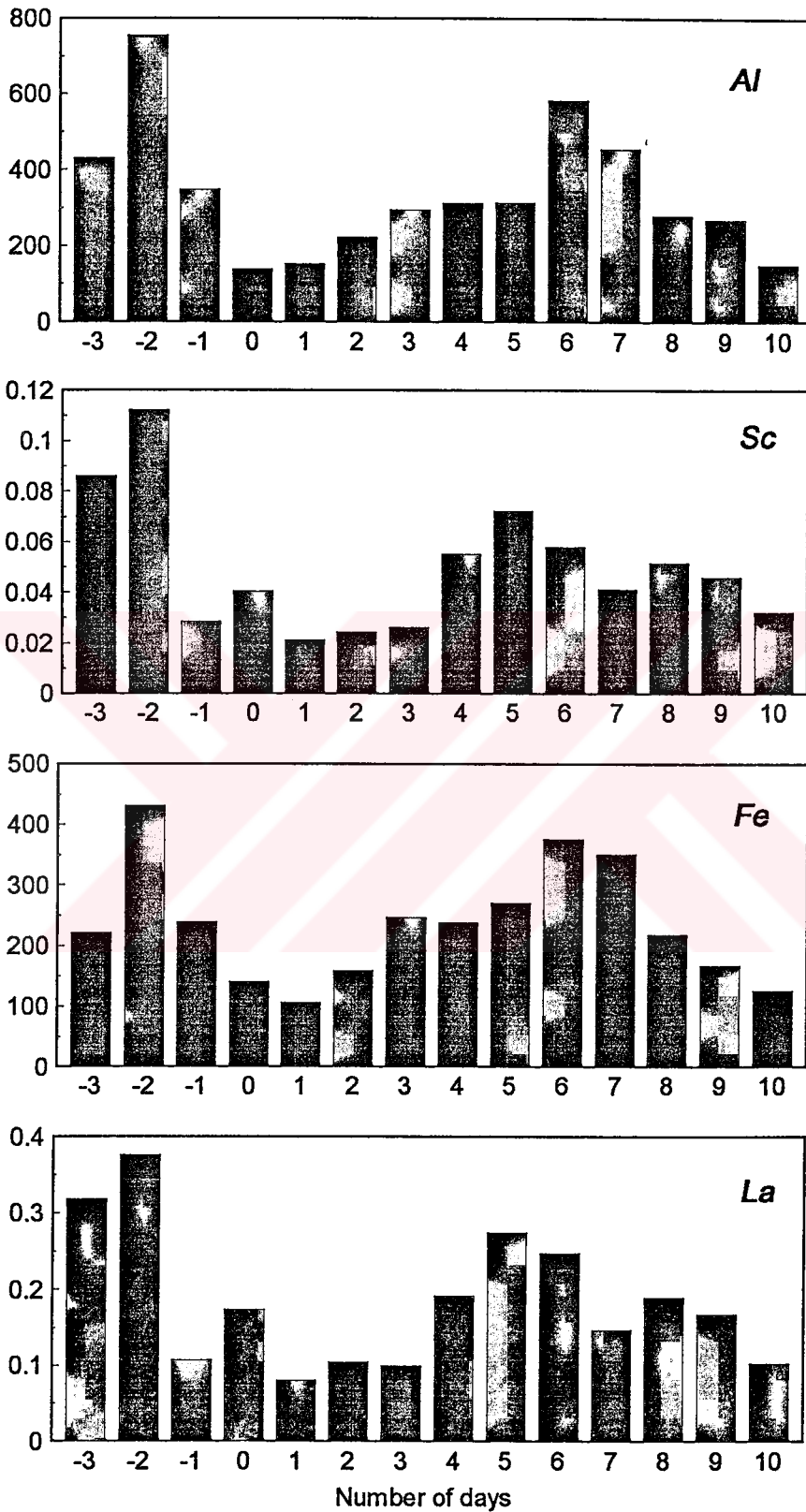


Figure 4.32 Average concentration of elements measured between 3 days before and 10 days after rain event

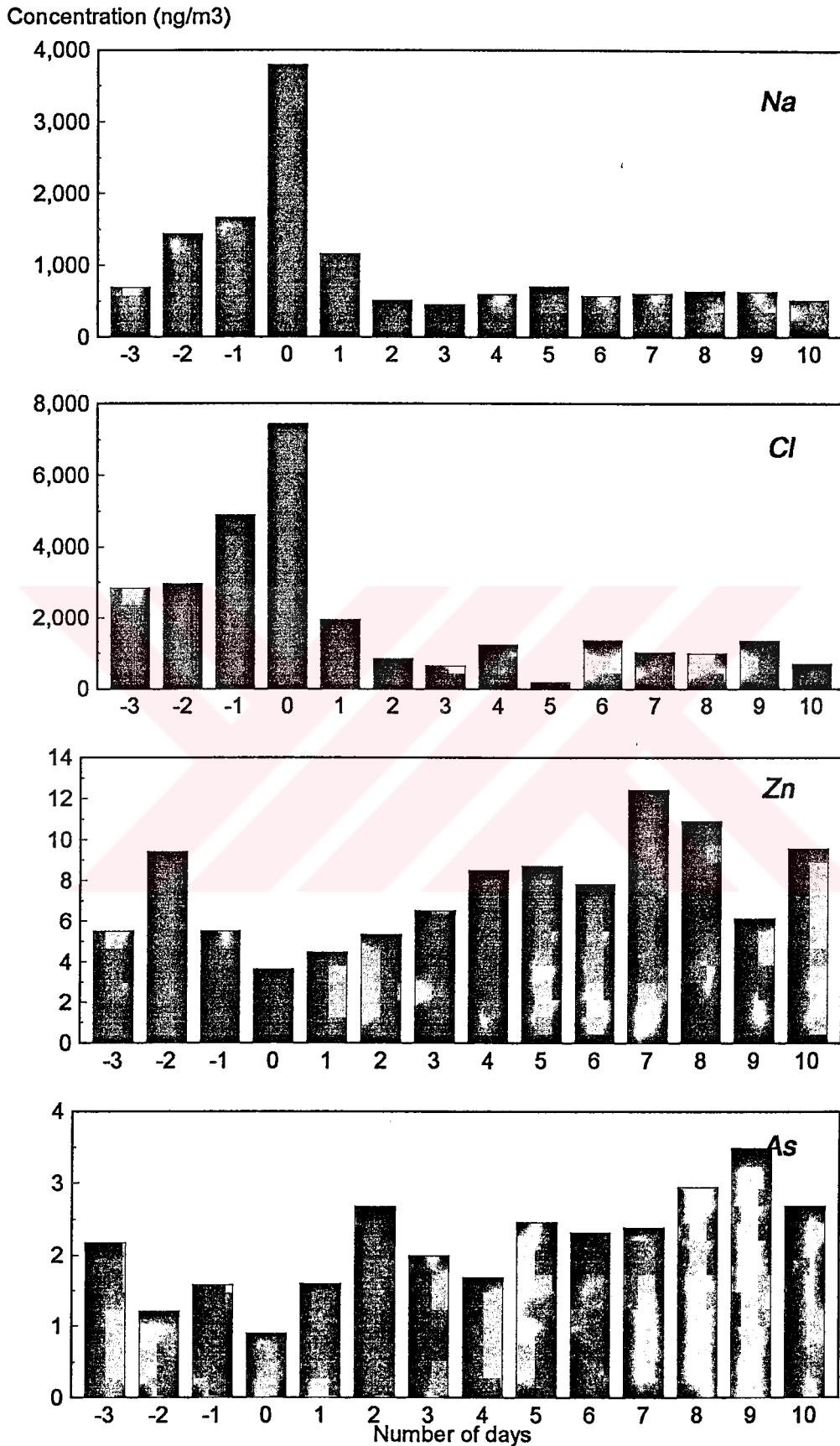


Figure 4.32 Cont'd.

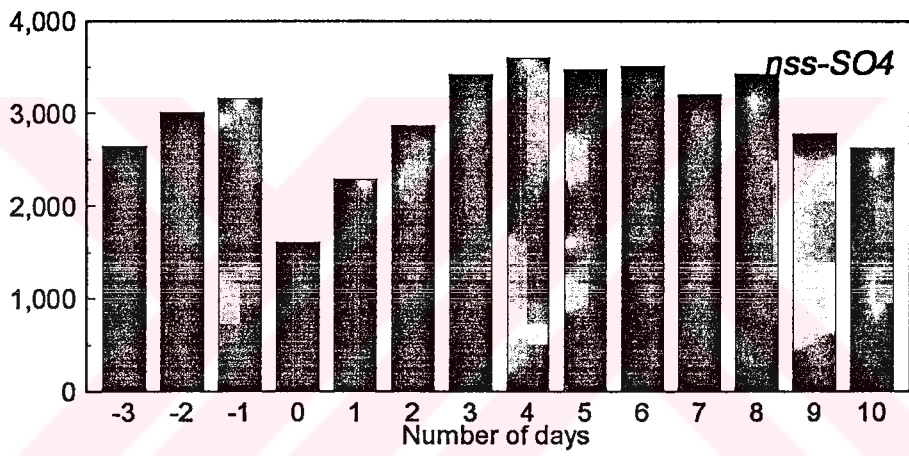
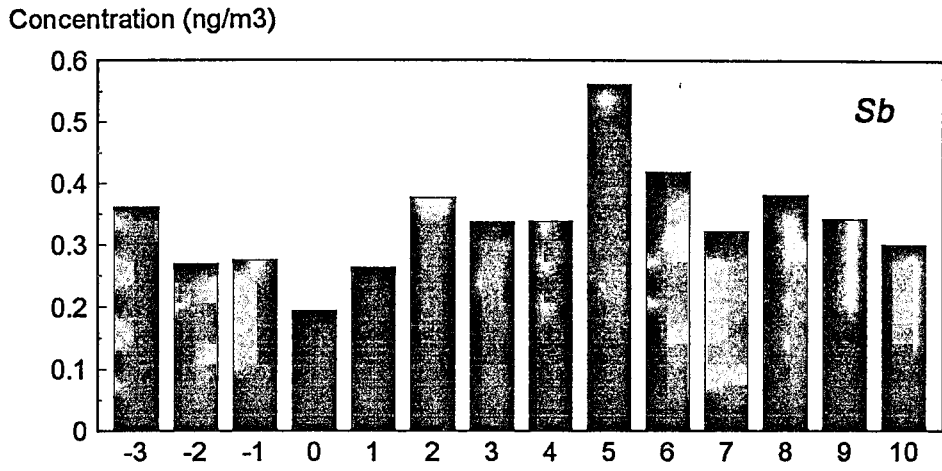


Figure 4.32 Cont'd.

The difference in the reloading behaviors of crustal and anthropogenic elements is due to their completely different sources. The anthropogenic elements are brought to the receptor site from distant sources. When precipitation occurs in an air mass, certain fraction of the fine particles which contain anthropogenic elements in the air mass is scavenged. The concentration of the anthropogenic elements in the next day depends on whether the same air mass still stays in the region or a new air mass arrives. If the atmosphere is still under the influence of the air mass in which the precipitation occurred, then low concentrations of the anthropogenic elements prevail, but if a new air mass starts to affect the region, concentrations of the anthropogenic elements starts to increase (or further decrease, depending from where the air mass originates). The same discussion can also be presented for the second, third and later days from the rain. A travel time of about 3 days corresponds to a travel distance of about 1000 km. This is approximately the distance between Antalya and north Africa region or mid-Europe from which more than 70% of the sampled air masses originates.

The crustal particles on the other hand are generated in situ and their generation rate depends on wind velocity and dryness of the soil. A rain event not only removes crustal particles from the atmosphere, but also it wets the soil and hinders the generation of dust particles. In the event of rain, certain fractions of crustal particles in the atmosphere are scavenged out. The concentrations of soil related elements in the day following rain is inevitably low, because no matter what the wind velocity is since the soil is wet, resuspension is low. As the soil gets dryer in the following days generation of dust particles starts to increase depending on the wind velocity and vertical mixing of the lower troposphere on that particular day. Average concentrations after 1-10 days of rain events (Figure 4.32) suggest that generation of airborne dust is determined completely by the drying of soil in the first five days and the effects of the wind velocity starts to affect the dust generation only after fifth day. However, even after five days of the rain

event the soil is not completely dry, consequently dust generation is still affected by the dampness of the soil. The dust generation starts to increase exponentially after 10-15 days of the rain, apparently when the surface soil becomes dry. After 30 days the soil is completely dry and dust generation is determined exclusively by wind velocity as shown in Figure 4.30.

Local rain affects the concentrations of both crustal and pollution derived elements. The atmospheric loading of the crustal dust is completely regulated by the local rain and subsequent dampness of the soil. Unlike crustal elements, concentrations of anthropogenic elements measured at the station are affected by distant rain events on their way to station as well as local rain. To understand relative contributions of local and distant rain events on annual and seasonal average concentrations of pollution derived elements, the concentrations of pollution derived elements at the rainy days and three days after each rain event were replaced with the concentrations measured three days before the rain. The seasonal averages calculated with the generic data set were compared with the seasonal averages calculated from the original data set to obtain percent contribution of local rain events on the observed seasonal variations of anthropogenic elements. The results are presented in Table 4.6. The general direction of back trajectory pairs which correspond to two days before the rain and rain days were investigated. If the two trajectories point to a totally different directions, then the data were excluded from the exercise. This was necessary because, in this analysis the differences in the elemental concentrations at -2 day and 0-day were assumed to be only due to wet scavenging of particles. However, the differences in the chemical composition of aerosols can also be due to different origins of air masses. The data was not included in the analysis if trajectories point to different source regions at -2 day and 0 day. But, since trajectories generally shift direction only gradually in time and since two days is not a long enough time for trajectories to shift from one source region to a totally different source area, only few rain events were excluded from the exercise.

Table 4.6. Contribution of rain events on the summer, winter and annual average concentrations of anthropogenic elements

	% Contribution of local rain to		
	summer average concentration	winter average concentration	annual average concentration
Cr	14.7	19.4	16.9
Zn	3.5	37.9	27.8
As	1.9	40.5	32.6
Se	1.0	29.4	33.3
Cd	14.2	5.0	22.2
Sb	1.9	6.4	35.2

Summer average concentrations of elements included in this exercise did not change significantly by the replacement of raining and post rain concentrations with pre-rain values due to small number of rain events recorded in summer. But as can be seen from the table, winter average concentrations did change significantly. The impact of local rain on winter concentrations of elements were 19% for Cr, 38% for Zn, 40% for As, 29% for Se, 5% for Cd, 6% for Sb, 39% for Au, and 4% for Hg.

Since the difference between summer and winter concentrations of elements are due to removal of particles from the atmosphere by both distant and local rain events and since the particle removal by local events can be approximated by the procedure described in the previous paragraph, then relative impact of local and distant rains on the observed summer/winter differences of elements were calculated and shown in the last column of the table. These values indicate that, the impact of local rains on seasonal behavior of elements were around 30% and the remaining 70% was due to

particle removal by rain events encountered during the transport of particles from their respective source regions to the station site.

4.3.5. Variations of the Sectorial Elemental Concentrations

As previously discussed, besides scavenging of aerosols by local rainfall and vertical mixing, the origin of air masses is another important factor causing variations of the atmospheric concentrations of elements. To get an information about the effect of the variation of the source strengths on sectorial elemental concentrations, samples were grouped with respect to emission areas by the help of back trajectories. Since the geographical area that the trajectories covered during transit is important, in determining the sectorial composition of the atmospheric particulates, the short trajectories which spent most of time in Turkey were grouped by itself. Variations of sectorial elemental concentrations for the eight sectors and short trajectory group are given in Table 4.7. Some of the representative trajectories for each group are given in Figure 4.33.

Average concentrations of marine elements Na and Cl at different wind sectors are depicted in Figure 4.34. Comparison of different sectors shows that the concentrations of sea salt elements are higher on south and west sectors. As shown in Figure 4.33, trajectories corresponding to these sectors have spent most of their time over the sea, and accumulated large quantities of sea salt during the transport. The lowest average concentrations of marine elements are in the east and north-east sectors where air masses travel over continental areas to reach our station site.

The highest average concentrations of crustal elements, Al, Sc, Ti, Fe, and rare earth's are in east, south and south-west sectors. This typical behavior of soil-related elements are depicted in Figure 4.35 for Al, Sc, Co and Dy. As previously indicated, the transport of air masses from east is a rare occasion in our sampling site. During two years of this study, only 9 out

Table 4.7. Average Contributions of elements from Different Sectors ($\text{ng}\cdot\text{m}^{-3}$)

	N			NE			E		
	avg \pm std	std	#	avg \pm std	std	#	avg \pm std	std	#
NO3	960 \pm 795		150	350 \pm 410		7	1390 \pm 870		8
nss-SO4	5200 \pm 5300		115	1640 \pm 1110		9	7280 \pm 5370		9
SO4	5490 \pm 4650		162	2380 \pm 1690		10	4140 \pm 4220		8
NH4	1400 \pm 1200		142	810 \pm 410		10	1440 \pm 800		9
Na	890 \pm 950		120	1210 \pm 1980		9	640 \pm 700		9
Mg	300 \pm 260		179	280 \pm 260		11	580 \pm 290		9
Al	460 \pm 490		175	250 \pm 330		11	1540 \pm 1230		9
Cl	1265 \pm 1630		164	1910 \pm 1830		10	800 \pm 890		9
K	330 \pm 355		164	220 \pm 160		10	585 \pm 320		9
Ca	1840 \pm 1185		90	1600 \pm 1670		5	-		
Sc	0.09 \pm 0.08		95	0.04 \pm 0.03		7	0.31 \pm 0.24		9
Ti	34.7 \pm 32.3		80	15.49 \pm 13.00		6	100.6 \pm 79.98		9
V	2.25 \pm 2.21		178	1.19 \pm 0.91		11	3.24 \pm 1.10		9
Cr	3.78 \pm 2.96		162	1.50 \pm 1.08		7	4.45 \pm 2.19		9
Mn	8.83 \pm 7.45		96	3.38 \pm 2.12		7	21.08 \pm 10.43		9
Fe	320 \pm 240		177	190 \pm 210		10	1000 \pm 730		9
Co	0.21 \pm 0.15		94	0.07 \pm 0.05		7	0.49 \pm 0.32		9
Ni	2.56 \pm 1.95		85	1.83 \pm 1.97		4	-		
Zn	11 \pm 11		105	3.6 \pm 1.9		8	18 \pm 22		9
As	1.52 \pm 0.99		95	1.92 \pm 0.83		7	1.97 \pm 0.89		9
Se	0.27 \pm 0.19		95	0.11 \pm 0.04		7	0.32 \pm 0.25		9
Br	14 \pm 7		95	10 \pm 8		7	13 \pm 3.4		9
Rb	0.852 \pm 0.621		93	0.385 \pm 0.190		7	2.271 \pm 1.554		8
Mo	0.968 \pm 1.525		60	2.338 \pm 1.995		5	0.205 \pm 0.136		6
Sb	0.343 \pm 0.192		96	0.236 \pm 0.124		7	0.471 \pm 0.169		9
Cs	0.096 \pm 0.059		94	0.041 \pm 0.019		7	0.182 \pm 0.088		8
La	0.313 \pm 0.292		94	0.215 \pm 0.170		6	1.013 \pm 0.829		9
Ce	0.568 \pm 0.521		95	0.296 \pm 0.234		7	1.930 \pm 1.482		9
Nd	0.393 \pm 0.334		94	0.187 \pm 0.125		6	1.658 \pm 2.545		9
Sm	0.039 \pm 0.034		96	0.021 \pm 0.012		6	0.148 \pm 0.123		9
Eu	0.009 \pm 0.008		86	0.004 \pm 0.003		6	0.031 \pm 0.027		8
Gd	0.044 \pm 0.043		90	0.020 \pm 0.018		7	0.118 \pm 0.096		9
Tb	0.005 \pm 0.005		86	0.003 \pm 0.001		5	0.018 \pm 0.015		8
Dy	0.041 \pm 0.042		71	0.025 \pm 0.019		4	0.144 \pm 0.088		8
Yb	0.017 \pm 0.015		91	0.006 \pm 0.007		7	0.052 \pm 0.046		9
Lu	0.003 \pm 0.003		93	0.001 \pm 0.001		6	0.009 \pm 0.007		9
Hf	0.024 \pm 0.021		93	0.011 \pm 0.008		7	0.086 \pm 0.067		8
Hg	0.051 \pm 0.072		93	0.116 \pm 0.128		7	0.091 \pm 0.102		9
Pb	23 \pm 23		80	19 \pm 12		5	-		0
Th	0.090 \pm 0.083		95	0.047 \pm 0.038		7	0.266 \pm 0.207		9

Table 4.7 Cont'd.

	S			SW			W		
	avg ± std	#		avg ± std	#		avg ± std	#	
NO3	1650 ± 1060	35		1420 ± 710	27		1330 ± 860	70	
nss-SO4	2980 ± 1730	20		5125 ± 4942	19		4550 ± 3940	56	
SO4	4370 ± 2500	38		5930 ± 4350	27		5630 ± 4075	72	
NH4	1110 ± 800	33		1590 ± 1215	26		1400 ± 1040	69	
Na	1780 ± 3050	32		1560 ± 1250	23		1900 ± 2050	60	
Mg	640 ± 690	50		495 ± 400	32		400 ± 290	80	
Al	1160 ± 1260	48		970 ± 1440	32		450 ± 440	79	
Cl	3380 ± 5080	40		2000 ± 2200	27		3150 ± 3920	72	
K	680 ± 950	47		490 ± 550	29		375 ± 310	71	
Ca	2720 ± 2540	38		1650 ± 1430	16		2260 ± 1260	35	
Sc	0.19 ± 0.19	13		0.28 ± 0.42	18		0.09 ± 0.10	47	
Ti	59.86 ± 53.16	10		90.51 ± 108.01	16		44.05 ± 31.82	30	
V	3.40 ± 2.83	49		3.34 ± 2.77	32		2.60 ± 1.96	79	
Cr	3.95 ± 2.68	49		5.88 ± 5.44	30		3.31 ± 2.64	65	
Mn	11.57 ± 10.08	13		15.57 ± 16.97	18		7.53 ± 6.35	47	
Fe	780 ± 790	49		710 ± 1180	32		310 ± 290	80	
Co	0.75 ± 1.21	13		0.38 ± 0.49	18		0.27 ± 0.31	47	
Ni	2.45 ± 2.00	37		1.92 ± 1.28	15		1.75 ± 0.91	34	
Zn	9.4 ± 6.2	18		13 ± 12	19		9.3 ± 8.5	50	
As	1.03 ± 0.77	12		1.38 ± 1.13	18		1.59 ± 1.71	46	
Se	0.27 ± 0.15	13		0.39 ± 0.26	18		0.33 ± 0.36	47	
Br	49 ± 80	13		22 ± 11	18		23 ± 20	47	
Rb	1.346 ± 1.187	12		1.982 ± 2.777	18		0.765 ± 0.664	44	
Mo	1.065 ± 2.757	8		0.907 ± 1.339	13		0.876 ± 1.448	31	
Sb	0.463 ± 0.342	13		0.352 ± 0.229	18		0.284 ± 0.205	47	
Cs	0.101 ± 0.084	13		0.154 ± 0.176	18		0.077 ± 0.056	44	
La	0.609 ± 0.660	13		0.678 ± 0.687	18		0.298 ± 0.311	45	
Ce	1.164 ± 1.253	13		1.961 ± 3.002	18		0.542 ± 0.567	47	
Nd	1.374 ± 2.321	13		1.134 ± 1.526	18		0.665 ± 0.879	47	
Sm	0.102 ± 0.100	12		0.147 ± 0.227	18		0.042 ± 0.046	47	
Eu	0.017 ± 0.016	12		0.034 ± 0.050	16		0.010 ± 0.010	40	
Gd	0.112 ± 0.115	10		0.140 ± 0.258	17		0.044 ± 0.044	40	
Tb	0.009 ± 0.009	13		0.016 ± 0.028	18		0.005 ± 0.005	40	
Dy	0.092 ± 0.068	10		0.152 ± 0.188	14		0.054 ± 0.043	35	
Yb	0.040 ± 0.034	11		0.058 ± 0.088	17		0.019 ± 0.021	44	
Lu	0.007 ± 0.006	11		0.010 ± 0.016	18		0.003 ± 0.003	43	
Hf	0.054 ± 0.054	12		0.082 ± 0.120	17		0.024 ± 0.025	42	
Hg	0.102 ± 0.083	12		0.206 ± 0.364	17		0.115 ± 0.143	46	
Pb	20 ± 14	30		16 ± 13	16		18 ± 17	30	
Th	0.161 ± 0.149	12		0.246 ± 0.370	18		0.081 ± 0.087	47	

Table 4.7 Cont'd.

	NW			SHT		
	avg ± std	#		avg ± std	#	
NO3	880 ± 730	61		1340 ± 780	136	
nss-SO4	3550 ± 2880	55		5530 ± 3530	102	
SO4	4390 ± 3200	63		6600 ± 3840	139	
NH4	1200 ± 1020	62		1560 ± 1120	128	
Na	1160 ± 1680	55		1110 ± 1760	105	
Mg	290 ± 210	79		330 ± 240	156	
Al	300 ± 300	77		490 ± 460	155	
Cl	2340 ± 3850	63		1400 ± 2480	139	
K	250 ± 240	73		330 ± 260	147	
Ca	1900 ± 1420	49		2120 ± 2600	72	
Sc	0.07 ± 0.06	35		0.09 ± 0.08	89	
Ti	28.87 ± 19.49	27		30.38 ± 23.20	80	
V	1.59 ± 1.08	79		3.01 ± 2.20	156	
Cr	3.42 ± 3.16	74		3.59 ± 2.68	134	
Mn	6.84 ± 4.44	35		8.10 ± 5.40	89	
Fe	230 ± 240	79		370 ± 330	156	
Co	0.14 ± 0.11	34		0.19 ± 0.17	89	
Ni	1.75 ± 1.84	44		3.06 ± 2.53	70	
Zn	7.9 ± 4.8	47		11.7 ± 10.3	93	
As	1.67 ± 1.43	33		1.72 ± 1.65	88	
Se	0.19 ± 0.11	35		0.33 ± 0.17	89	
Br	17 ± 18	35		16 ± 16	89	
Rb	0.678 ± 0.483	35		0.823 ± 0.634	85	
Mo	1.176 ± 1.318	26		0.365 ± 0.549	70	
Sb	0.309 ± 0.161	35		0.366 ± 0.175	89	
Cs	0.080 ± 0.055	34		0.088 ± 0.061	88	
La	0.233 ± 0.189	35		0.284 ± 0.234	86	
Ce	0.406 ± 0.318	35		0.541 ± 0.476	89	
Nd	0.389 ± 0.403	35		0.546 ± 0.756	87	
Sm	0.030 ± 0.024	35		0.041 ± 0.042	88	
Eu	0.007 ± 0.005	32		0.009 ± 0.008	80	
Gd	0.031 ± 0.033	33		0.039 ± 0.040	84	
Tb	0.004 ± 0.004	31		0.005 ± 0.006	83	
Dy	0.042 ± 0.033	24		0.040 ± 0.031	67	
Yb	0.013 ± 0.012	35		0.017 ± 0.018	88	
Lu	0.002 ± 0.002	35		0.003 ± 0.003	88	
Hf	0.018 ± 0.016	35		0.026 ± 0.042	88	
Hg	0.134 ± 0.152	34		0.095 ± 0.201	87	
Pb	20 ± 24	45		34 ± 23	60	
Th	0.069 ± 0.058	35		0.079 ± 0.073	88	

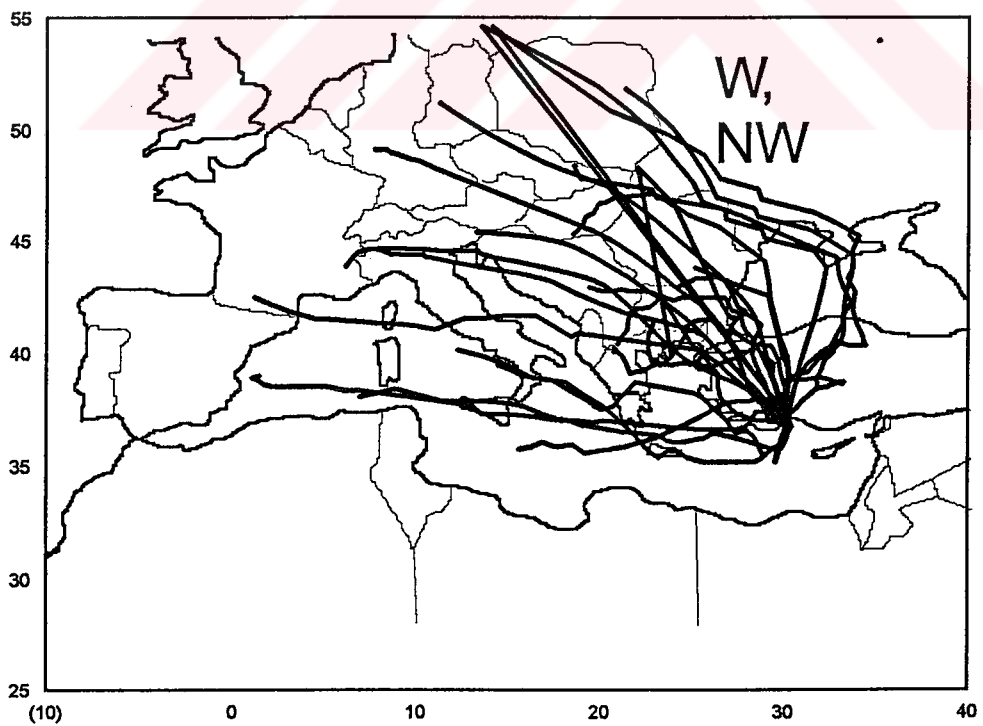
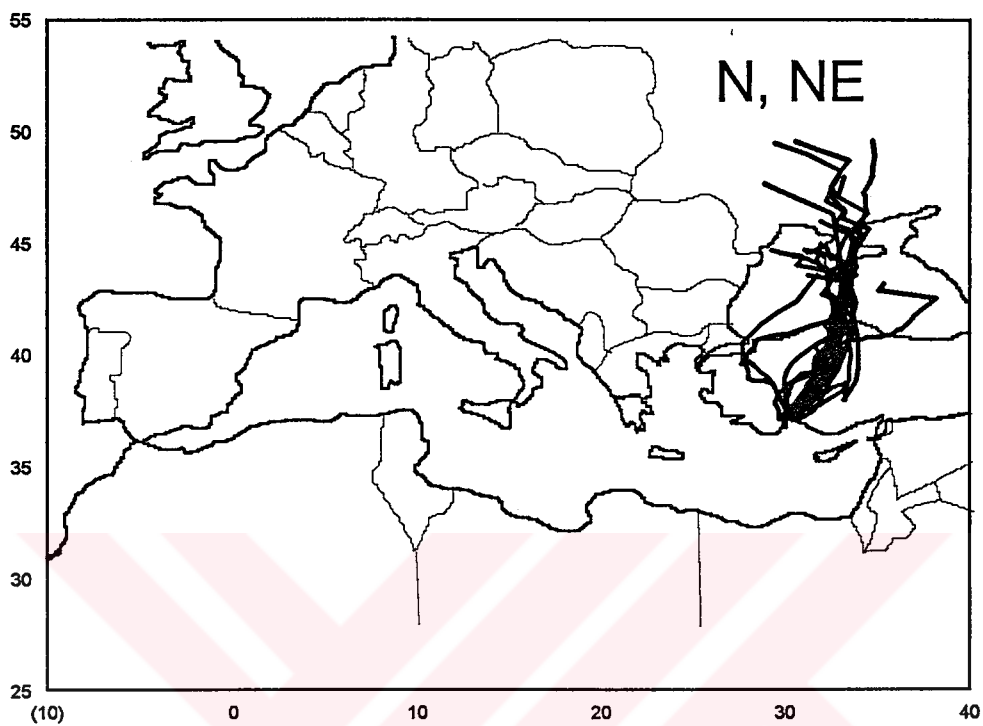


Figure 4.33 Representative trajectories for each sector

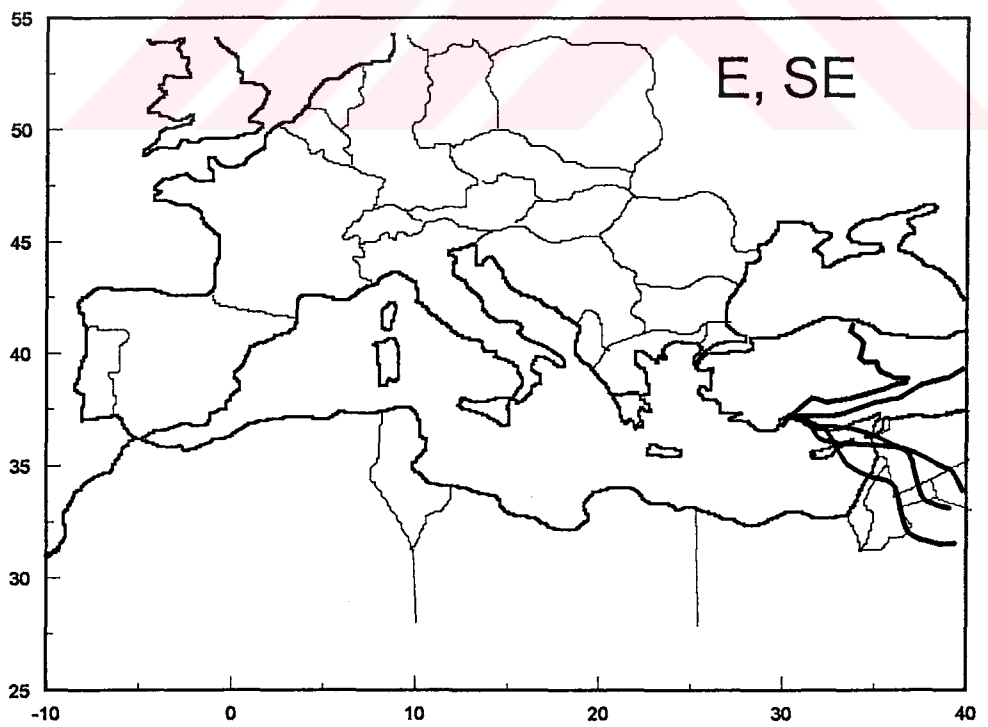
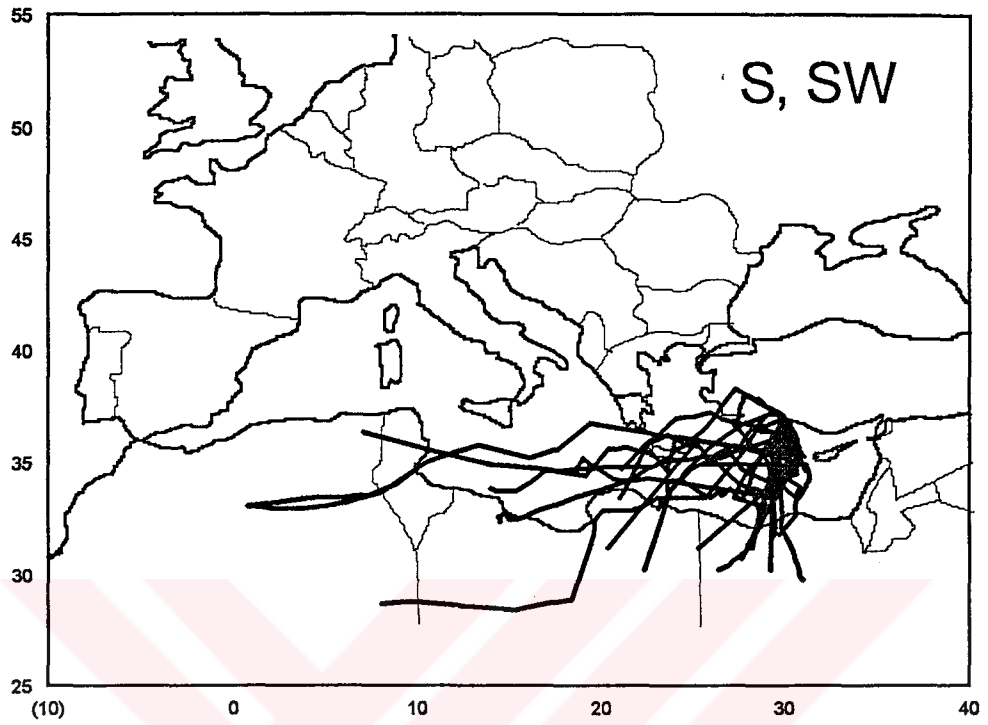


Figure 4.33 Cont'd.

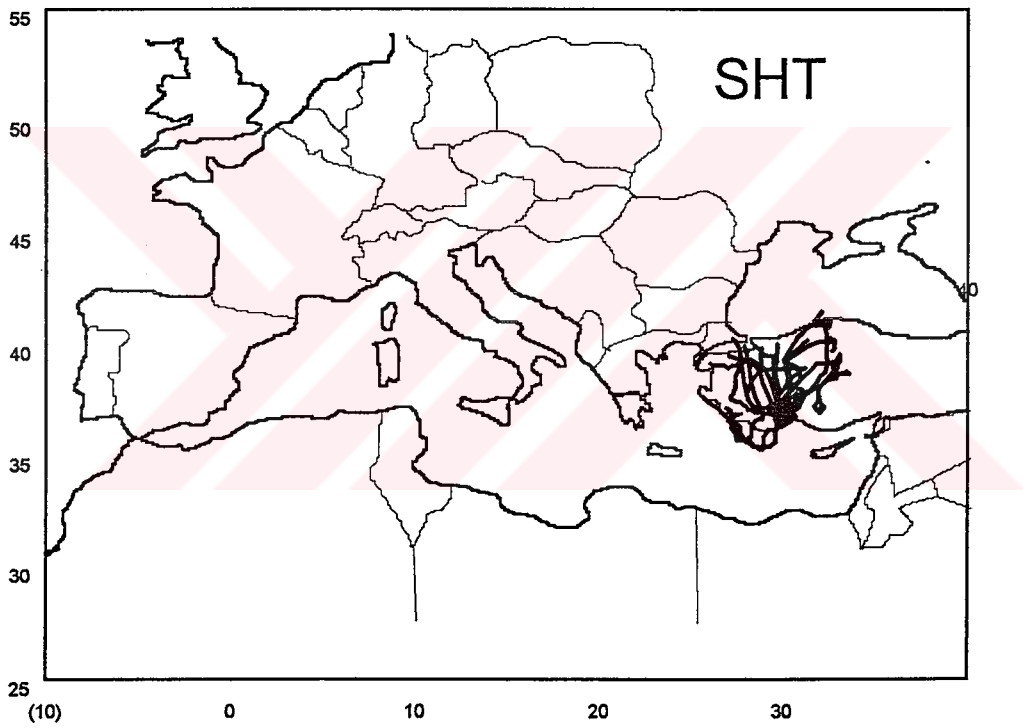


Figure 4.33 Cont'd.

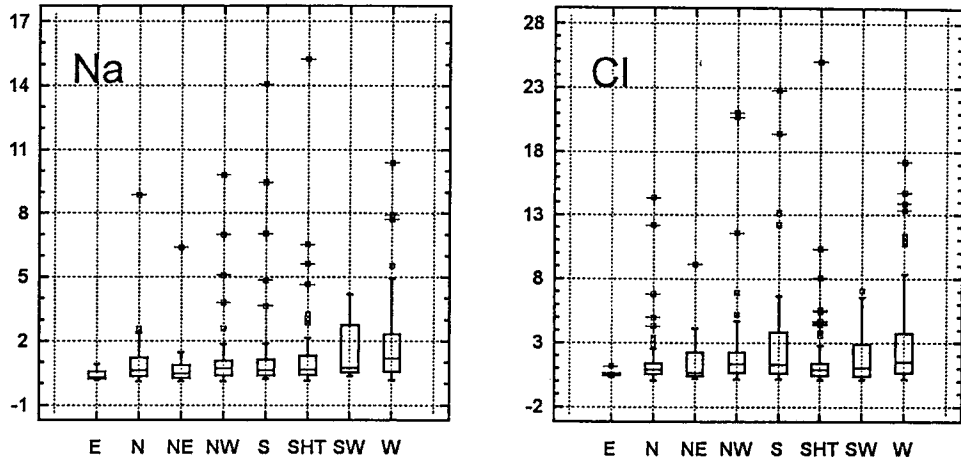


Figure 4.34 Average contribution of Na and Cl from different sector

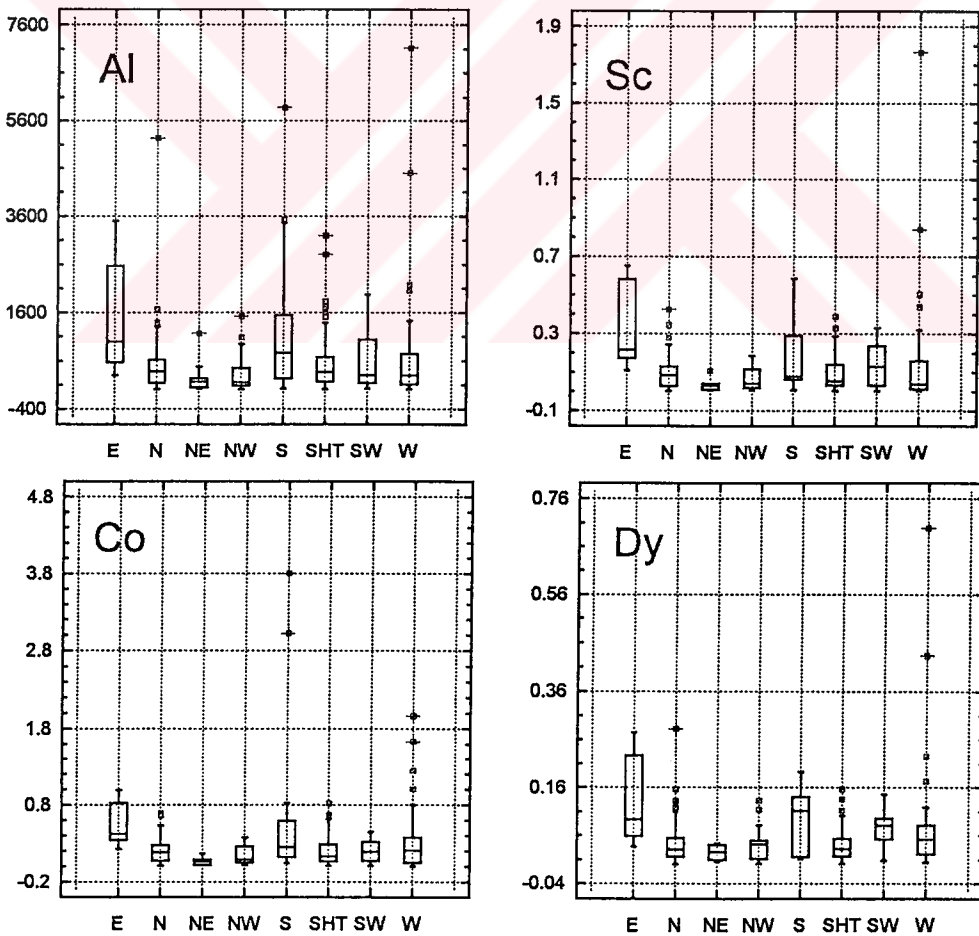


Figure 4.35 Average contribution of Al, Sc, Co and Dy from different sector

of 600 samples were associated with back trajectories from east sector. Five of these nine samples which were collected between October 16 and 20, 1993 had unusually high concentrations of crustal elements indicating a dust transport from desert areas in the Middle East. This unusual transport event increased average concentrations of crustal elements in east sector by approximately a factor of five. However, this is misleading, because dust transport depends not only on the transport path of the trajectory, but also on the meteorological conditions at the source area at that time. Consequently, every trajectory originating from east sector does not necessarily associated with high concentrations of crustal elements. Since large number of samples are associated with trajectories originating from south and south-west sectors (14% of the total), calculated high concentrations of crustal elements in south and south-west sectors are real. As will be discussed in subsequent sections, high concentrations of soil related elements in south and southwest sectors are due to transport of Saharan dust from North Africa. Whenever such transport occurs, the trajectories are in these two sectors and concentrations of crustal elements, like Al, are an order-of-magnitude higher than concentrations measured in the absence of Saharan dust at the station. In each dust episode increase in the concentrations of soil related elements are so high that, only few episodes are sufficient to effect average concentrations of crustal elements in this sector. Consequently, the high average concentrations of Al and other crustal elements in the south and southwest sectors do not imply steady transport of crustal material in these sectors but rather are due to few episodic transport of unusually high loadings of Saharan dust.

Average concentrations of selected anthropogenic elements, including Cr, Ni, Pb, nss-SO_4^- , As in each wind sector are given in Figure 4.36. Pollution derived elements have different sectorial preferences due to their different source regions relative to the station. The highest concentrations of Pb and Ni are in the SHT trajectory group which include only short trajectories that spirals around the station. Since high

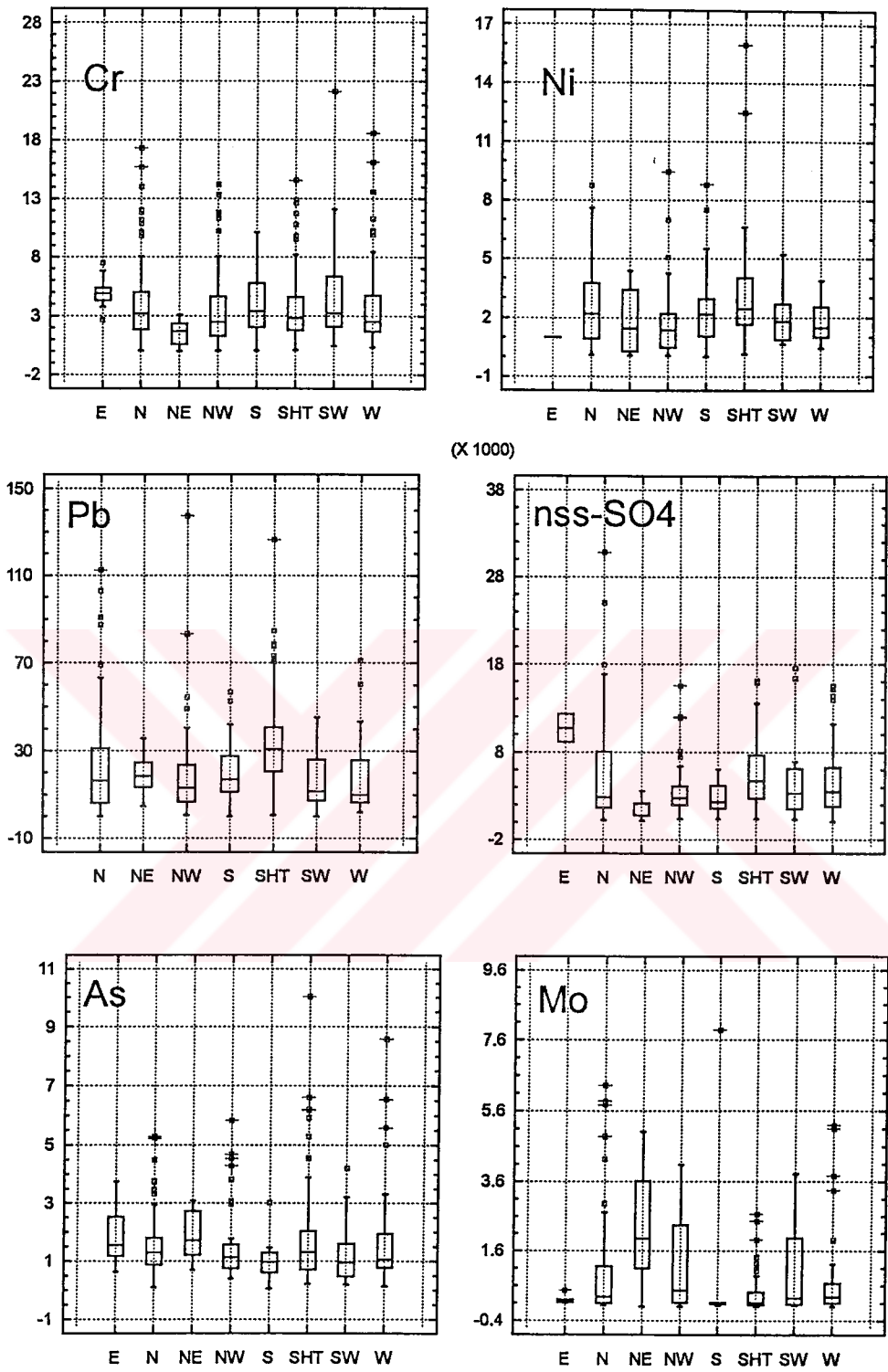


Figure 4.36 Average contribution of Cr, Ni, Pb, nss-SO₄, As and Mo from different sectors

concentrations of elements in this trajectory group imply local sources for those elements, Pb and Ni are expected to have local sources in the eastern Mediterranean atmosphere.

High Ni concentrations measured on this group is due to the presence of ophiolitic rocks which are enriched with Cr and Ni in the region (Aslaner, 1973; Tolun and Pamir, 1975). There are large Cr mines located at the Pozanti-Adana region. Guerzoni et al., (1989) and Kubilay and Saydam (1995) explained the enrichment of Cr and Ni in aerosols over the Adriatic Sea and eastern Mediterranean Sea arising from ophiolitic minerals existing in the eastern basin. Consequently, the local source of Ni which explains the high Ni concentrations consistently measured with short trajectories is mineralogy of the region. With this explanation one would expect similar high concentrations of Cr in the SHT trajectory group, as ophiolitic rocks in the region are also enriched with Cr. However, the highest average Cr concentration are in the southwest sector and concentrations in other sectors, including SHT group are fairly similar. The main difference between Ni and Cr is in their crustal contributions. Even in the absence of unusual mineralogy, crustal particles in aerosols have substantial contribution on observed Ni concentrations (rest of the measured Ni concentrations are contributed by particles emitted from oil combustion). Unlike Ni, contribution of crustal material on Cr concentrations in normal rural aerosol population is negligible. Chromium measured in aerosols is almost exclusively due to industrial emissions. Although local soil is unusually enriched in Cr, contribution of crustal material on measured Cr concentrations in the station is not very large and Cr is still dominated by anthropogenic sources. Consequently, average Cr concentrations measured in wind sectors are determined by the availability of anthropogenic sources in each sector.

High Pb concentration in the short trajectory group is expected due to existence of local sources, mainly vehicular emissions in the vicinity of the station.

The elements and ions NO_3^- , SO_4^{2-} , Zn, As, and Sb had high average concentrations in east sector. Some of the samples associated with easterly trajectories had fairly high concentrations of these elements. There are series of large coal-fired power plants located on the Israel coast and one large power plant (Afsin-Elbistan) in Turkey which lies in the east sector relative to the station. Whenever, trajectories originate from east, they had to pass industrialized regions in Israel and over some of those power plants. Consequently, the thermal power plants and industrialized regions in Israel and Adana-Mersin area are potential sources of observed high concentrations of ions and elements in the east sector. However, reliability of source apportionment in east sector is low due to limited number of trajectories in this sector.

The north-east sector has high concentrations of anthropogenic elements, As and Mo indicating their source located in that region. Contrary to expected high pollutant transport from the north-west sector which cover Europe and former Eastern Block countries have average sectorial concentration of anthropogenic elements. The higher standard deviations of the mean concentrations of most of the elements originated from this sector reveals precipitation scavenging of the atmosphere at distant locations to be most effective in generating large fluctuations in the concentrations.

Although the approach described in this section provides some limited information on the locations of sources affecting the eastern Mediterranean atmosphere, there are serious limitations associated with it. The most important limitation is the difficulty to assign trajectories in one sector. Trajectories usually do not follow simple, linear paths. They almost always cross wind sector boundaries. In this crude exercise, the trajectories were assigned the sector in which they spend most of their time. But since a trajectory which spends most of its time in one of the sectors can pick up emissions from another sector in which it spend smaller period of its time,

the reliability of source apportionment is limited. Furthermore, the source regions affecting the station site depend not only the average concentrations in each sector, but also depends on the frequency of air mass transport from that direction. For example, few trajectories in east sector had high concentrations of some of the pollution derived elements indicating that there are sources of these elements to the east of our station. But, transport from east occurred in only 9 of the 600 days of the study. Consequently, no matter how strong those sources are, they are insignificant on an annual basis. The approach described in this section is limited, because it does not take into account the frequency of air mass movement from different sectors. But, it is not totally worthless, because it does provide some information on the expected source regions of pollutants. A more sophisticated and more reliable technique to apportion source regions of pollutants will be given in subsequent sections.

4.3.5.1 Saharan Dust in the Eastern Mediterranean Atmosphere

Dust transported from arid regions of the world is important for the biogeochemistry of dust related elements and formation of oceanic sediments. Transport of dust from North African and Asian deserts over long distances have been well documented (Prospero and Carlson, 1970; Duce et al. 1980; Parrington et al., 1983). Asian dust transport which are known as "Kosta" events are known to be important in formation of sediments in the Pacific ocean (Duce et al., 1980;1983). Such dust events were intercepted at distant locations such as Hawaii (Parrington et al., 1983). Similarly dust from north African deserts, particularly from Sahara was sampled at Barbados and Florida, USA (Prospero and Nees, 1987).

Huge quantities of dust when transported over such distances over oceans, significant fraction of it deposits over the sea and contributes to the sedimentation which is a slow process in the middle of the ocean. Although the transport of Saharan dust with trade winds to North America had been documented in mid 70's, transport of dust to the Mediterranean basin

attracted attention only recently. Since the Mediterranean is close to the source region, the amount of dust reaching the Mediterranean basin is large compared to the atmospheric impact on Atlantic ocean (Chester; 1986; Quetel, 1993). Mineralogical studies have demonstrated that the material transported from the Sahara is an important source of clay minerals in the basin (Chester et al., 1977; Tomadin et al., 1984).

Impact of dust on the chemical composition of aerosol and precipitation had been extensively studied in the western part of the Mediterranean basin (Carlson and Prospero, 1972; Prospero, 1981; Morales, 1979; Loye-Pilot et al., 1986; Levin et al., 1990). Although the transport and deposition of Saharan dust across the eastern Mediterranean basin had been reported, studies on the impact of dust on both the sedimentation and chemical composition of aerosols are very limited (Chester et al., 1977, 1981; Yaalon and Ganor, 1973, 1979; Levin and Lindberg, 1979; Prodi and Fea, 1979; Levin et al., 1980; Ganor and Mamane, 1982). Since dust loading in the atmosphere increases orders of magnitude when Saharan Dust is transported to the region and since such transport occurs several times in a year, the Saharan dust should affect annual average concentrations of particularly crustal elements in aerosols and precipitation as well as their annual deposition in the eastern Mediterranean.

In order to estimate the impact of Saharan dust on the observed concentrations of elements measured in this study, samples which correspond to Saharan dust incursions at the station site were determined using Al as the marker of dust and back trajectory information. Temporal variation of Al concentrations are illustrated in Figure 4.37. There were 90 samples with back trajectories originating from north Africa, 33 out of these 90 samples have episodically high Al concentrations. These 33 samples were identified as Saharan Dust samples and formed a separate data subset. Naturally, all the southerly trajectories did not correspond to high Al

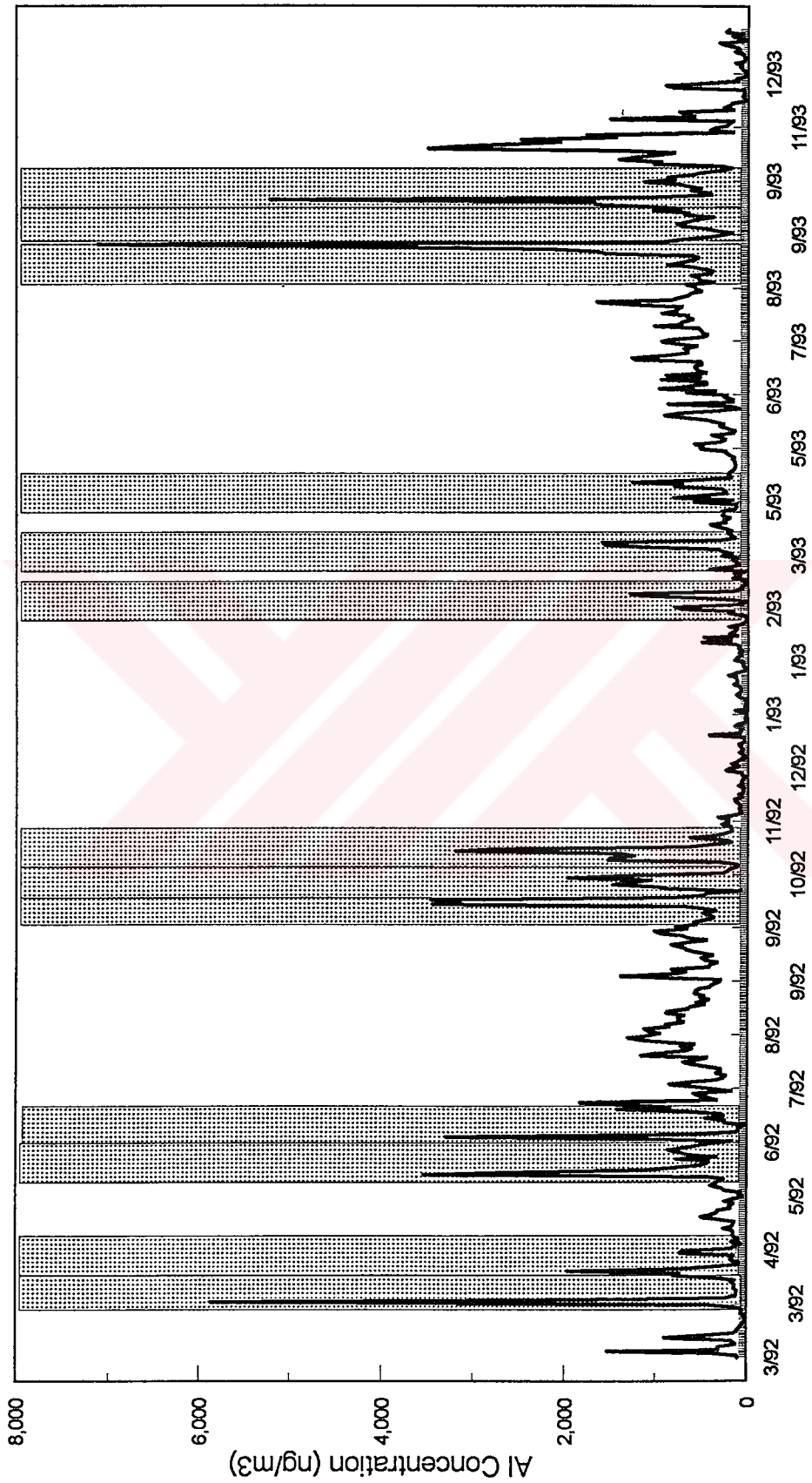


Figure 4.37 Bulk data of Al concentration together with Saharan dust episodes indicated with shaded regions

concentrations, because Saharan dust can become airborne only if a deep cyclonic system present over the source region (Alpert et al., 1990).

Among those identified as Saharan dust episodes, the one observed on 28-29 March 1992 was selected to rationalize the use of back trajectory and AI concentration data for identification of the dust episodes. The 3 days backward air mass trajectories corresponding 28 and 29 March 1992 is shown in Figure 4.38. The trajectory arriving on 28 March 1992 originated from North Africa, and the following day, 29 March 1992, sampling site was under the influence of the same air mass. During 28 and 29 March, AI concentrations was measured as $5880 \text{ ng}\cdot\text{m}^{-3}$ and $2480 \text{ ng}\cdot\text{m}^{-3}$ which are 20 to 40 times higher than winter average AI concentration which is $140 \text{ ng}\cdot\text{m}^{-3}$.

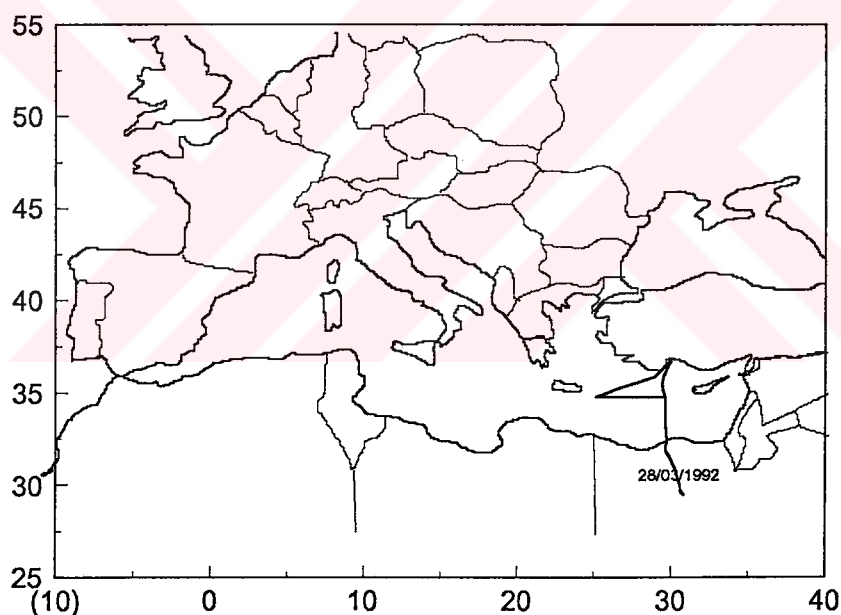


Figure 4.38 Back Trajectories of 28-29 March 1992

Meteosat images between March 25 and 31 are given in Figure 4.39 so as to provide a complete picture of the long-range transport of the atmospheric material over the eastern Mediterranean which originated from North Africa. The clear sky over the sea is in dark blue, clouds are gray or appear with color dots and dust concentrations increase from light blue to red. On 25 and 26 of March there was no dust at the eastern Mediterranean

basin, on 28 of March the red color over the Israeli coast and over a south-north flank from the coast of Libya to Turkey clearly verified that dust was being transported to the Mediterranean both from the Middle East and from the North African deserts.

The red color on 29 of March over the southern coast of Turkey clearly indicates the existence of desert dust in the atmosphere. The transit time of this dust intrusion from North Africa to the sampling site was two days. On the night of 29 of March, it rained and washed out atmosphere, thereby lowering the dust load as can be seen from the colors of the images corresponding to the 30 and 31 of March. The same dust outbreak was also observed at a land based station (Erdemli) 400 km east of Antalya (Kubilay, 1996). Thus, measured high Al concentration on aerosols during 28 and 29 March 1992, calculated southerly backward trajectories and satellite information provide direct evidence for Saharan dust incursion and deposition at the eastern Mediterranean. In the identification of the rest of the Saharan dust samples, satellite images were not always used. High Al concentration and trajectories pointing to north Africa was taken as sufficient evidence for the intrusion of Saharan dust to the sampling site.

The 33 samples which corresponds to Saharan dust episodes were grouped as a Saharan dust subset. The remaining samples which did not correspond southerly trajectories were grouped as non-Saharan data. The median concentrations of elements in each of these data subsets are presented in Table 4.8. Anthropogenic elements nss-SO_4^{2-} , NH_4^+ , Pb and As have higher concentrations in the non-Saharan samples indicating their sources are not on the pathway of the southerly trajectory air masses. The most dramatic difference were observed for crustal elements Al, Fe, Sm, La, Co, Ce, Sc, Gd, K, Lu, Hf, Yb, Eu, Br, Th, Nd, Tb, Dy and Rb for which concentrations were at least a factor of three higher than those in the non-Saharan dust subset. Therefore, the presence of the Saharan dust component could effect the short and long term variability of these elements.

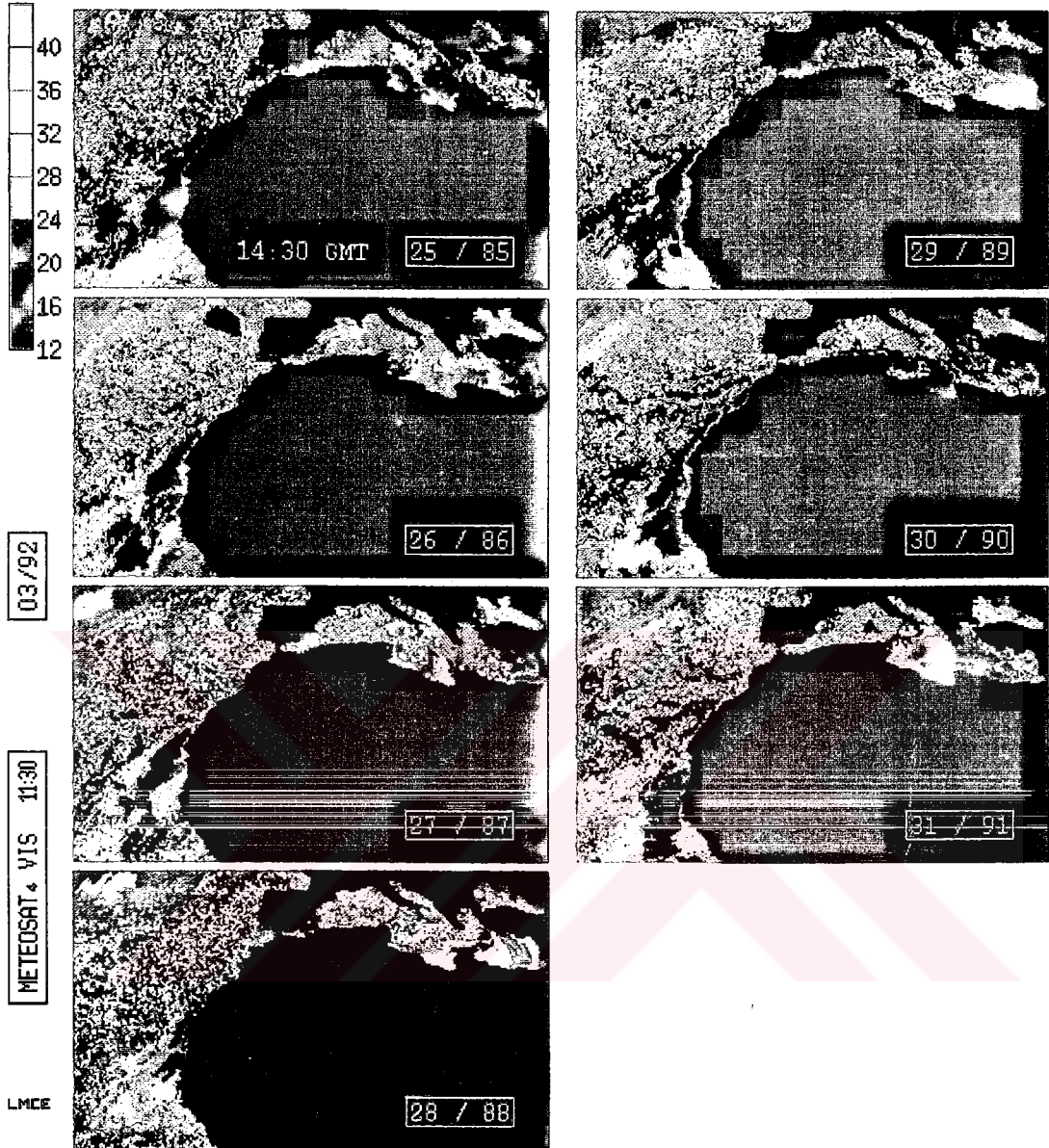


Figure 4.39. A sequence of METEOSAT vis images from 25 to 31 March 1992

Table 4.8. Concentrations of elements in Saharan dust and non-Saharan Dust data subsets (ng·m⁻³)

	SAHARAN (33)			NON-SAHARAN(565)		
	average	std	median	average	std	median
NO3	1800 ± 1040		1640	1140 ± 810		1040
nss-SO4	4820 ± 3900		3920	4770 ± 4230		3200
SO4	5110 ± 3310		4270	5570 ± 4130		4300
NH4	1470 ± 970		1230	1400 ± 1110		1250
Na	1250 ± 1800		610	1240 ± 1740		690
Mg	800 ± 690		530	330 ± 270		270
Al	2030 ± 1420		1500	440 ± 480		300
Cl	2.04 ± 3.48		820	1.88 ± 3.01		980
K	940 ± 1010		550	320 ± 300		240
Ca	3615 ± 2850		3100	1960 ± 1740		1640
Sc	0.396 ± 0.404		0.240	0.090 ± 0.094		0.058
Ti	110 ± 97		81	35 ± 33		27
V	4.78 ± 3.13		4.48	2.4 ± 2.02		1.90
Cr	6.25 ± 3.73		5.16	3.56 ± 2.93		2.78
Mn	21.9 ± 15.5		17.2	8.2 ± 6.7		6.67
Fe	1290 ± 1100		920	320 ± 300		260
Co	0.72 ± 0.92		0.32	0.21 ± 0.26		0.15
Ni	3.46 ± 1.92		2.95	2.31 ± 2.01		1.86
Zn	14 ± 10		10	10 ± 10		7
As	1.42 ± 0.77		1.13	1.61 ± 1.4		1.26
Se	0.41 ± 0.22		0.33	0.29 ± 0.22		0.24
Br	36 ± 70		19	17 ± 15		13.5
Rb	2.67 ± 2.65		1.75	0.82 ± 0.69		0.63
Mo	0.91 ± 2.32		0.9	0.79 ± 1.27		0.23
Sb	0.49 ± 0.28		0.43	0.34 ± 0.19		0.31
Cs	0.19 ± 0.16		0.14	0.09 ± 0.06		0.07
La	1.04 ± 0.66		0.81	0.30 ± 0.32		0.20
Ce	2.64 ± 2.91		1.66	0.56 ± 0.59		0.37
Nd	1.67 ± 2.20		0.80	0.53 ± 0.81		0.34
Sm	0.21 ± 0.22		0.13	0.04 ± 0.05		0.03
Eu	0.040 ± 0.046		0.027	0.009 ± 0.010		0.007
Gd	0.196 ± 0.248		0.11	0.042 ± 0.045		0.027
Tb	0.022 ± 0.027		0.012	0.005 ± 0.006		0.003
Dy	0.166 ± 0.163		0.11	0.046 ± 0.044		0.038
Yb	0.076 ± 0.082		0.045	0.017 ± 0.019		0.011
Lu	0.014 ± 0.015		0.008	0.003 ± 0.003		0.002
Hf	0.108 ± 0.114		0.06	0.025 ± 0.032		0.015
Hg	0.102 ± 0.186		0.048	0.096 ± 0.167		0.034
Pb	19 ± 10		16	24 ± 22		18
Th	0.334 ± 0.353		0.203	0.085 ± 0.089		0.053

Since the Saharan dust contributes significantly to concentrations of elements measured in Antalya station, one can have better understanding of Saharan dust contribution if chemical markers, specific to Saharan or non-Saharan dust can be identified. It is well established that there are mineralogical differences between the Saharan dust and non-Saharan soil in the Mediterranean basin (Chester et al., 1984; Ganor, 1991), but the data on similarities and differences in chemical composition is not extensive. Although, Ca is known to be enriched in the desert dust (Loye-Pilot et al., 1986; Gomes et al., 1990; Lavi et al., 1992), it is also enriched in local soil and sea salt aerosols. Consequently, Ca is not a very good marker for the Saharan dust contribution. Up to now, there is no data on the minor element composition of the Saharan dust component of aerosols. The INAA performed in this work enabled us to determine large number of crustal trace elements which were not normally measured in the Mediterranean basin. Since these trace elements associated with soil were used to identify different soil types in other studies, we have investigated their potential to be used as tracers to distinguish between the Saharan dust and local soil to obtain a better estimate of the impact of Saharan dust on the eastern and western Mediterranean aerosols.

To identify potential marker elements for the Saharan dust, the ratios of the crustal elements to Al in the Saharan dust subset were compared with the corresponding ratios in non-Saharan subset. If the concentration of an element in the Saharan and non-Saharan (local) soils are the same, then one would expect similar ratios to Al in both dust components. The elements that can be used as marker for one of the soil components are the ones with distinctly different X-to-Al ratios in the Saharan and local soil components.

The element to Al ratios of soil related elements, namely Ca, Sc, Ti, Fe, Co, Rb, Cs, La, Ce, Nd, Sm, Eu, Gd, Dy, Yb, Lu, Hf and Th in the Saharan dust and non-Saharan dust data subsets are given in Table 4.9, together with the ratio of the values obtained in two subsets and

corresponding ratios in standard soil. The ratios for marine and anthropogenic elements were not included in the table, because most of the anthropogenic elements were enriched relative to Al in non-Saharan dust subset, due to their potential source areas exist in the north of the station.

Table 4.9. Element to Al ratios in Saharan and non-Saharan dust data subsets

	X/Al Saharan		X/Al non-Saharan		ratio
Al	1	± 0	1	± 0	1.00
Ca	1.78	± 2.11	4.45	± 6.25	2.50
Sc	0.000195	± 0.000285	0.000204	± 0.000308	1.04
Ti	0.054	± 0.069	0.079	± 0.11	1.46
Mn	0.011	± 0.012	0.019	± 0.025	1.73
Fe	0.635	± 0.805	0.727	± 1.046	1.14
Co	0.000215	± 0.000378	0.000488	± 0.000794	2.27
Rb	0.001315	± 0.001714	0.001864	± 0.002571	1.42
Cs	9.56E-05	± 0.000105	0.0002	± 0.000261	2.10
La	0.000511	± 0.000627	0.000691	± 0.001047	1.35
Ce	0.001299	± 0.001981	0.001274	± 0.001931	0.98
Nd	0.00067	± 0.001346	0.001208	± 0.002257	1.80
Sm	0.000101	± 0.000155	9.47E-05	± 0.000147	0.94
Eu	1.99E-05	± 3.07E-05	2.14E-05	± 3.22E-05	1.08
Gd	9.67E-05	± 0.000161	9.43E-05	± 0.000145	0.98
Tb	1.07E-05	± 1.81E-05	1.16E-05	± 1.84E-05	1.08
Dy	8.18E-05	± 0.000113	0.000104	± 0.000152	1.28
Yb	3.72E-05	± 5.76E-05	3.96E-05	± 6.13E-05	1.06
Lu	6.66E-06	± 1.02E-05	6.61E-06	± 1.01E-05	0.99
Hf	5.32E-05	± 8.92E-05	5.64E-05	± 9.59E-05	1.06
Th	0.000165	± 0.000244	0.000194	± 0.000293	1.18

The Table 4.9 demonstrate that the X-to-Al ratios for elements Ca, Nd, Cs and Co were significantly lower in the samples that correspond to Saharan dust subset, suggesting that these are the elements with potential tracer power to distinguish between the Saharan dust and local soil. The X-to-Al ratios for the elements Sc, Fe, Ce, Sm, Eu, d, Tb, Yb, Lu and Hf were the same in two subsets, suggesting that these elements can not be used as markers to distinguish between two soil composition.

The approach described in this section provides qualitative information about potential marker elements, because in this approach the different X-to-Al ratios of elements were assumed to be due to differences in the chemical composition of the two soil components. Although this is true, contribution of non-crustal sources on the measured concentrations of the elements in the non-Saharan dust component would also result in different X-to-Al ratios. Application of multivariate statistics which includes a factor analysis and subsequent multiple linear regression on the obtained factor scores would be more appropriate to obtain quantitative information on marker elements. Such an approach which will be discussed in subsequent sections was used in this study.

4.4 Sources of Pollutants in the Eastern Mediterranean

General features of the generated data set, including levels of elements and ions in the eastern Mediterranean relative to other regions, temporal variations of measured concentrations and factors affecting temporal behaviors of elements were discussed in previous sections. One of the key questions that initiated this work was the determination of types and locations of natural and anthropogenic sources that affect chemical composition of aerosols in the eastern Mediterranean atmosphere. Understanding types and regions of sources are important because, that information dictates the direction of regulatory action. Although, general features of data which were discussed up to this point help to understand sources of elements and ions measured in the station, special statistical techniques are needed to obtain quantitative information about sources.

Following sections are about source apportionment of aerosols included in this work. First relatively simple methods, such as binary correlation's between measured parameters and crustal and marine enrichment factors are presented to obtain some limited information on the types of sources affecting collected samples. In the second step more sophisticated methods such as

receptor modeling and geographical apportionment were used to get more detailed and quantitative information of sources.

4.4.1 Correlations between species

In atmospheric studies, binary correlations between measured species are frequently used to identify types of particles in the environmental samples. In aerosol data sets, a high binary correlation coefficient between any two element indicates either similar sources for the two elements or similar generation mechanism or similar transport pattern.

The correlation coefficients (r) between the concentrations of the measured elements are given in Table 4.10. As expected, strong correlations are found among all crustal elements (Al, Sc, Fe and rare earth elements). Elements Cr and Ni are moderately correlated with crustal elements indicating at least some of the observed concentrations of these elements are associated with the local soil as suggested previously. Other than Cr and Ni, anthropogenic element Pb also show moderate correlations with crustal elements. Since Pb is mainly emitted from gasoline engines together with Br, resuspension road dust is probably the reason for this correlation. Lack of correlation between Br and crustal elements is due to the presence of another strong Br source, namely the sea salt in the close vicinity of the sampling location. The Br has several sources in rural atmosphere.

Like crustal elements, high to moderate correlations were observed among sea salt elements, Na, Cl, Mg and Br. Although the correlation between Na and Cl is strong, correlations between Na, Mg and Br are only moderate. The lack of strong correlation between Na and Mg is due to the presence of a second strong source for Mg which is crustal particles. The lack of strong correlation between Na and Br can be due to three reasons. (1) Br is a volatile element and escapes from sea salt particles during

Table 4.10. Correlation coefficients among the measured species

	NO3														
SO4	0.60	SO4													
NH4		0.65	NH4												
Na				Na											
Mg				0.72	Mg										
Al	0.33	0.31			0.57	Al									
Cl				0.87	0.58		Cl								
K	0.34	0.34			0.43	0.59		K							
Ca	0.31				0.42	0.39		0.30	Ca						
Sc	0.34	0.37			0.48	0.91		0.64		Sc					
Ti	0.27				0.67	0.96		0.62		0.90	Ti				
V	0.59	0.63			0.39	0.58		0.48	0.34	0.71	0.72	V			
Cr					0.25	0.40		0.28	0.45	0.41	0.34	0.34	Cr		
Mn	0.44	0.42	0.29		0.49	0.95		0.66	0.54	0.86	0.91	0.81	0.39	Mn	
Fe	0.35	0.37			0.52	0.92		0.59	0.45	0.99	0.88	0.58	0.45	0.84	Fe
Co				0.36	0.64	0.48	0.36	0.56		0.60	0.58	0.46		0.44	0.61
Ni	0.40	0.56			0.27	0.45		0.30	0.40	0.49	0.25	0.51	0.55	0.38	0.53
Zn	0.60	0.61	0.58		0.15	0.29		0.31	0.31	0.32	0.18	0.56	0.30	0.40	0.36
As															
Se	0.61	0.56	0.55			0.27		0.28	0.27	0.33		0.58		0.34	0.35
Br				0.75	0.66		0.79								
Rb	0.40	0.44	0.25		0.51	0.89		0.67	0.45	0.97	0.86	0.72	0.44	0.87	0.97
Mo				0.31			0.35								
Sb										0.30		0.25		0.28	0.33
Cs	0.47	0.52	0.36		0.38	0.81		0.65	0.31	0.87	0.78	0.73	0.54	0.87	0.87
La	0.32	0.30			0.51	0.77		0.56		0.78	0.75	0.61	0.31	0.75	0.74
Ce	0.31	0.30			0.48	0.89		0.62	0.29	0.99	0.88	0.68	0.40	0.82	0.99
Nd				0.35	0.53	0.40	0.35	0.35	0.05	0.51	0.43	0.33		0.36	0.52
Sm	0.30	0.29			0.50	0.89		0.60		0.98	0.88	0.67	0.39	0.81	0.98
Eu	0.30	0.32			0.52	0.90		0.63		0.99	0.90	0.68	0.41	0.83	0.98
Gd	0.27				0.55	0.85		0.60		0.95	0.84	0.64	0.37	0.79	0.96
Tb	0.28	0.30			0.51	0.83		0.59	0.41	0.93	0.82	0.64	0.34	0.77	0.93
Dy					0.64	0.92		0.56		0.91	0.93	0.66	0.38	0.85	0.90
Yb	0.33	0.34			0.53	0.87		0.62		0.97	0.86	0.69	0.40	0.82	0.97
Lu	0.33	0.37			0.53	0.90		0.63	0.25	0.99	0.89	0.70	0.42	0.84	0.99
Hf	0.30	0.29			0.52	0.82		0.58		0.92	0.81	0.65	0.41	0.77	0.92
Hg									0.45						
Pb			0.27							0.49	0.71			0.40	
Th	0.33	0.35			0.51	0.90		0.64		0.98	0.89	0.70	0.42	0.86	0.98

Table 4.10. Cont'd.

	Co													
Ni		Ni												
Zn		0.45	Zn											
As		0.47		As										
Se		0.37	0.67		Se									
Br	0.63					Br								
Rb	0.70	0.58	0.42		0.47		Rb							
Mo	0.25					0.39		Mo						
Sb		0.41	0.33	0.49	0.28		0.32		Sb					
Cs	0.53	0.50	0.53		0.54		0.92		0.42	Cs				
La	0.55	0.43					0.76		0.26	0.72	La			
Ce	0.60	0.42	0.30		0.32		0.96		0.29	0.84	0.76	Ce		
Nd	0.70				0.35	0.54	0.64			0.46	0.39	0.53	Nd	
Sm	0.60	0.39	0.29		0.32		0.94		0.29	0.81	0.77	0.98	0.53	Sm
Eu	0.68	0.38	0.28		0.36		0.96		0.25	0.84	0.74	0.99	0.69	0.97
Gd	0.74	0.34	0.25		0.28	0.25	0.93		0.29	0.82	0.68	0.97	0.62	0.96
Tb	0.61	0.59	0.29		0.39		0.93		0.26	0.80	0.63	0.93	0.69	0.92
Dy	0.61						0.88			0.77	0.68	0.90	0.44	0.91
Yb	0.70	0.27	0.32		0.40		0.97		0.25	0.86	0.73	0.97	0.58	0.95
Lu	0.68	0.68	0.32		0.39		0.97		0.27	0.86	0.75	0.98	0.53	0.97
Hf	0.71	0.52	0.27		0.35		0.91		0.25	0.80	0.73	0.93	0.64	0.89
Hg														
Pb	0.45		0.45	0.51	0.45		0.61		0.63	0.48	0.45	0.41		0.50
Th	0.69	0.52	0.32		0.34		0.97		0.28	0.88	0.80	0.98	0.56	0.96

Table 4.10. Cont'd.

	Eu											
Gd	0.95	Gd										
Tb	0.95	0.94	Tb									
Dy	0.92	0.87	0.84	Dy								
Yb	0.98	0.94	0.94	0.88	Yb							
Lu	0.99	0.95	0.92	0.92	0.99	Lu						
Hf	0.92	0.90	0.86	0.83	0.94	0.94	Hf					
Hg								Hg				
Pb	0.54	0.25	0.43		0.47	0.55	0.59			Pb		
Th	0.98	0.96	0.93	0.89	0.97	0.98	0.93			0.50		

transport of aerosols modifying Br-to-Na ratio. Since evaporation of Br from particles depends on the availability of acidic gases, such mechanism effects the correlation between Na and Br. (2) Cellulose Whatman filters are known to adsorb gas phase Br from atmosphere (Duce et al., 1973; Tuncel et al., 1989). Adsorption depends on a variety of factors and naturally totally independent of the presence or absence of sea salt particles. (3) Sea salt is not the only source of Br. It is also emitted from motor vehicles. Although the marine component of Br strongly depends on the presence or absence of sea salt particles in the atmosphere, motor vehicle component is independent of abundance of sea salt in the atmosphere. Among these, last two factors are more important than the evaporation of Br from particles, because sea salt particles are generated in the close vicinity of the station and they are collected on filters before Br had a chance to evaporate. The Cl is also known to evaporate from particles, but in our samples Cl-to-Na ratio is fairly close to the same ratio in sea water, indicating that evaporation of halogens from particles is not a significant mechanism to affect chemical composition of sea salt aerosols at our sampling site. Adsorption of gas phase Br on cellulose filters used in the study and existence of additional motor vehicle emissions both occur and results in smaller than expected correlation between Na and Br.

The correlations between anthropogenic elements and secondary pollutants were found to be weak when compared with the correlations among crustal or marine elements. Significant correlation has been found among the anthropogenic elements Pb, As and Sb (around 0.50). This may suggest certain fraction of Pb, As and Sb are from the same anthropogenic source, most probably from a Lead Smelter. These group of elements are not correlated with secondary pollutants, $\text{nss-SO}_4^{=}$, NO_3^- and NH_4^+ .

Significant correlation has been found among anthropogenic elements Se, V, Zn, Ni and gaseous pollutants, $\text{nss-SO}_4^{=}$, NO_3^- and NH_4^+ . It is interesting to note that, with the exception of Zn all of these elements are

tracers for fuel combustion (Se for coal combustion, V and Ni for oil pollution). Since these group of elements are related to fuel combustion, then they are expected to be related with nss-SO_4^{2-} which is formed by the oxidation of SO_2 emitted from combustion sources. In most of the rural studies SO_4^{2-} was found to be correlated with NO_3^- and NH_4^+ which is attributed to their similar chemistry in the atmosphere.

One has to note that interpretation of correlation coefficients in rural data sets are substantially different from interpretation of correlation coefficients in urban data sets. In urban aerosol studies, particles emitted from sources are immediately collected at the sampling site. Hence any correlations between parameters are inevitably due to similarities of their sources. But in rural studies particles are transported over long distances before they are intercepted. Similar scavenging of particles from different sources during transport, similar transport paths of particles from different sources all induce artifact correlations between elements. Consequently, in rural studies strong correlations between measured parameters do not necessarily indicate similar sources.

4.4.2. Enrichment Factors

The chemical composition of the aerosols in the atmosphere is controlled by the mixing of various natural and anthropogenic components and the extent to which the mixing occurs will vary both in space and time. Enrichment factors (EF) provide qualitative information on the natural and anthropogenic components in the aerosol (Zoller et al., 1974).

Enrichment factor (EF) of an element is the ratio of the concentrations of the test element to the reference element in the sample divided by the same ratio in reference material (e.g. rock, soil, sea water). This expression can be written as follows:

$$EF = \frac{(C_X / C_R)_{\text{sample}}}{(C_X / C_R)_{\text{reference}}}$$

where, C_X is the concentration of the element of interest in the sample and in the reference material and C_R is the concentration of the reference element in the sample and reference materials. This calculation is based on the assumption that constituents from the source are found in the sample in the same proportion as they occur in the source.

Enrichment factors are the most commonly used for identifying crustal and marine components of aerosols, because crustal material and sea salt are the components in most of the aerosol bodies and their composition are well known do not change substantially from one place to another. However, enrichment factors for other source types such as meteoritic material and volcanoes are reported in the literature (Tuncel et al., 1989; Zoller et al., 1974).

Aluminum and sodium are frequently used as reference elements for calculating crustal and sea water enrichment factors, respectively. The reference element in crustal enrichment factor calculations should be a typical non-volatile lithophile element like Al, Fe which have high abundance in crustal material. It should not have any source other than crustal material, and should be accurately measured with available analytical techniques. Although Al satisfy all of these criteria, other elements such as, Ti, Fe and Sc are also used in crustal enrichment factor calculations.

In the marine atmosphere, Na, Cl, Mg, K, Ca, Sr and Br are contributed substantially by marine sources. However with the exception of Na and Cl, all other elements have sources other than sea water and thus can not be used as marine reference element. Chloride is also not a good marine reference element, because it evaporates from particles in the presence of acidic gases (Tuncel et al., 1989). Although Na, to a certain extend, is also affected by crustal material, it can be used as a marine reference element after correcting for crustal Na, because crustal contribution on Na concentrations is generally smaller than 10%. In this study, Al was used as a reference element to calculate

crustal enrichment factors and noncrustal Na (Na_{ncr}) was used as reference element in the calculation of marine enrichment factors.

The EF values calculated in this work are based on the data given for the mean abundance's of the elements in the Earth's crust by Taylor (Taylor, 1972). For average sea water composition, composition given by Goldberg (1963) was used. If the only source of an element is crustal material (or sea water for marine enrichment factor), the EF_c for that element should be unity. However, due to natural variations in the compositions of Earth's crust and sea water, the enrichment factors should exceed 10 to indicate the influence of an additional source. Values less than unity indicate depletion with respect to crustal material or a poor choice of normalizing element.

Large enrichment factors for some trace elements imply contribution of sources other than crustal dust and sea salt. However high enrichment factors does not necessarily indicate anthropogenic sources, because natural sources such as biogenic activities (Andrea, 1985), forest fires (Andrea, 1983), volcanic eruptions (Kotra et al., 1983) were shown to cause similar enrichments of elements in the atmosphere.

4.4.2.1 Crustal Enrichment Factors

Calculated crustal enrichment factors of elements in the eastern Mediterranean aerosols are illustrated in Figure 4.40. As it is shown in the Figure 4.40 elements like Sc, Yb, Lu, Ti, Tb, Fe, Gd, Sm, Eu, Hf, Th, La, Ce, Mn, Rb, Co, Dy, K and V for which the main source in the atmosphere is the Earth's crust are not enriched in the eastern Mediterranean atmosphere. Their crustal enrichment factors are less than 10, in both summer and winter seasons. The scandium show depletion with respect to Al, which is probably due to composition difference between the sampled crustal material and Taylor's (1972) crustal abundance table. Depletion of scandium is frequently observed



Figure 4.40 Crustal Enrichment Factors

when Taylor's crustal composition is used (Cunningham and Zoller, 1981; Tuncel et al., 1989). Due to their low EF_c values, although crustal dust seems to be the main source for these elements, it does not necessarily rule out the presence of other sources. For example, V is known to be emitted from residual oil burning. However, since this element has relatively high abundance in the Earth's crust and since collected samples are not size separated, the enrichment factor for V is less than 10 as it is previously observed at the Black Sea atmosphere (Hacisalihoglu et al., 1992).

In order to distinguish the natural and anthropogenic sources of the slightly enriched elements, enrichment factor (EF) diagrams which are the log-log plots of crustal enrichment factors of elements vs. Al concentrations were prepared. The EF_c of purely crustal elements does not change with changes in the Al concentrations (since concentrations of both the crustal element and Al change similarly with increasing and decreasing loading of crustal particles in the atmosphere, EF_c remains the same) resulting in a horizontal line in the EF diagram. The EF diagrams of two purely crustal elements, Sc and La are given in Figure 4.41 as an example. Concentrations of purely non-crustal elements, on the other hand are independent of the Al concentration in the sample. Consequently, EF_c values of such elements decrease with increasing Al concentration, resulting in monotonically decreasing line in the EF diagram.

Elements with EF_c values less than 10 were grouped into three categories based on their EF diagrams. The first category included elements Hf, Gd, La, Lu, Sm, Ta, Eu, Th, Yb and Sc. Crustal enrichment factors of these elements are independent of variations in the concentration of aluminum hence generate a broad horizontal distributions typical for purely crustal elements. Any enrichments in this group was due to differences in the soil composition. The EF diagrams of Sc and La are given in Figure 4.41 as an example for this category of elements.

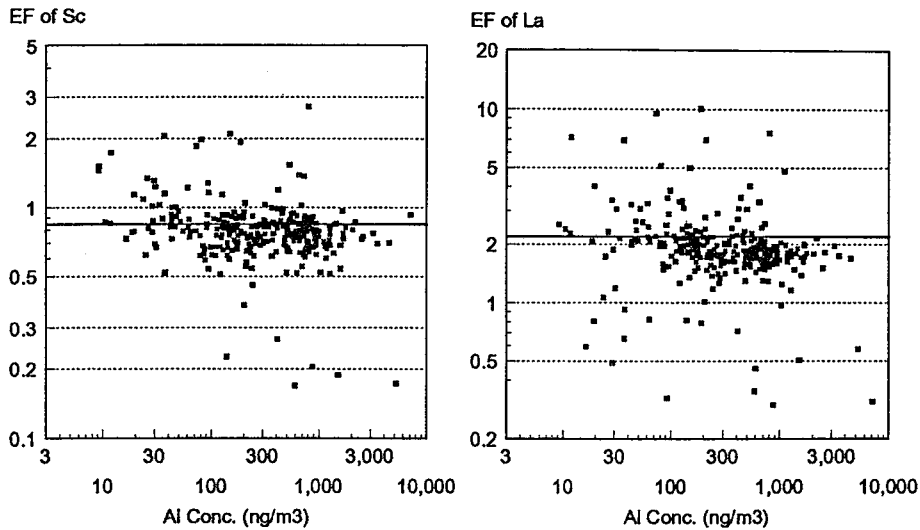


Figure 4.41 EF diagrams of Sc and La

The second group of elements include Cs, K, Mn, V, Ti and Rb. The EF diagrams of K, Mn, V and Ti are given as an example of this group in Figure 4.42. As shown in figure, crustal enrichment factors of this group of elements decrease with Al concentrations at low Al levels, but becomes independent of Al concentrations at high Al levels. Based on their EF diagrams, these elements behave like non-crustal elements at low Al concentrations, but behave like purely crustal elements at high Al concentrations. These are the elements which are known to have mixed sources. The sea salt in the marine atmosphere is known to contribute on observed concentrations of K, Cs, and Rb. The Ti and Mn concentrations are known to be high in emissions of ferro-manganese industries (Pacyna, 1984) and oil combustion is an important source of V (Kowalczyk et al., 1982; Ondov et al., 1990). The EF diagrams for these elements show that, the non-crustal sources of these elements are visible at low Al concentrations, but crustal material determines their observed concentrations at high Al loadings in the atmosphere. Consequently, slight enrichment of these elements are due to presence of non-crustal sources rather than differences in the chemical compositions of sampled soil and Taylor's compilation used in EF_c calculations.

The last category included elements Fe, Nd, Tb, Ce and Dy. These elements are known to have only crustal sources. Anthropogenic sources which effect their concentrations in aerosols are not known. The EF diagrams of Fe, Tb, Ce and Dy are given in Figure 4.43. The EF behavior of these elements shown in the figure closely resembles the behaviors of second group elements which was shown to have mixed sources in the atmosphere. Although these elements do not have known non-crustal sources in the atmosphere, they are contributed significantly by non-crustal sources at Al concentrations below $100 \mu\text{g m}^{-3}$, but dominated by crustal sources when Al concentration exceeds $100 \mu\text{g m}^{-3}$.

When horizontal lines at EF diagrams are investigated, it can be seen that for Fe and Tb the element-to-Al ratios in sampled soil is similar to the ratio of reference crustal compositions, because most of the data points lies on horizontal line with the value of 1.0. However, horizontal lines defined by the data points in the EF diagrams of Dy and Ce indicate that Ce/Al and Dy/Al ratios in the soil sampled at the station is approximately a factor of 2 to 3 higher than the corresponding ratios in the reference crustal compositions. Based on this discussion, slight enrichments observed in Fe, Tb, and Nd are due to contribution of non-crustal sources on their concentrations, whereas enrichments of Ce and Dy are due to both additional anthropogenic sources and differences in soil composition.

Elements Ni, Cr, Ca, Zn and Na, moderately, Mo, As, Sb, Cu, Pb, Hg, Se, Br and Cl are highly enriched, indicating that these elements have sources other than crustal dust. Enrichments of these elements are always seen in the data sets generated from urban, rural and remote regions and that is why this group of chalcophiles are frequently referred to as "anomalously enriched elements" (AEE's). Sources of enrichments is mostly anthropogenic in urban, rural atmosphere and natural in pristine sites. Enrichments of AEE's at the eastern Mediterranean atmosphere is due to anthropogenic sources, rather than natural ones, due to close proximity of the sampling site to strong source regions in

Europe and meteorology of the region which favors westerly and northerly air flow throughout the year.

High enrichment factors of Na, Cl and Br in the eastern Mediterranean atmosphere are due to marine contribution. In the maritime atmosphere, contribution of sea salt on Mg, Ca, K, Na and Cl appears to decrease with distance from the sea and at the coastal regions their observed concentrations are controlled mainly by marine aerosols (Boutron and Martin, 1980; Cunningham and Zoller, 1981).

In order to determine the seasonal changes in the intensities of the crustal source, average enrichment factors for summer (May-October) and winter (November-April) periods were calculated and results are given in Table 4.11. Winter to summer EF_c ratios were about unity for the crustal and rare-earth elements namely, Al, Fe, Gd, Sc, Lu, Yb, Hf, Th, La, Eu and Sm. For anthropogenic elements like $SO_4^{=}$, NO_3^- , NH_4^+ , Zn, Se, Sb, Pb, As and Hg winter enrichments were generally higher. Seasonal variations in the EF_c values of non-crustal elements are controlled by the seasonal variations in Al concentration. As discussed in previous sections, concentrations of both pollution derived elements and crustal elements are higher during summer season. However, difference between summer and winter concentrations are more dramatic for soil related elements including Al, resulting in lower crustal enrichment factors for pollution derived elements in summer.

The enrichment factor calculations have shown that chemical composition of aerosols are affected by four components including:

1. The crustal component which largely consist of airborne soil particles. The crustal component accounts for most of the observed concentrations of Al, Sc, Ti, Mn, Fe, Co, Rb, Cs, La, Ce, Sm, Eu, Gd, Tb, Dy, Yb, Lu, Hf and Th.

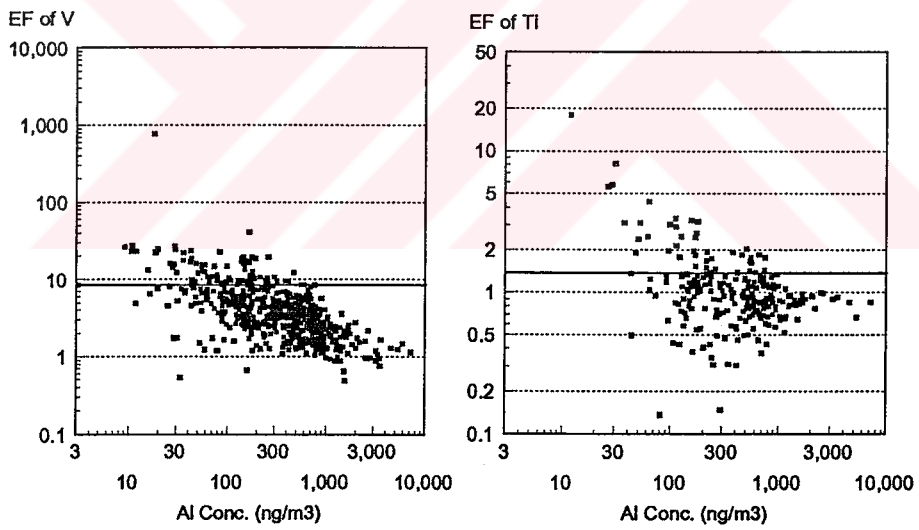
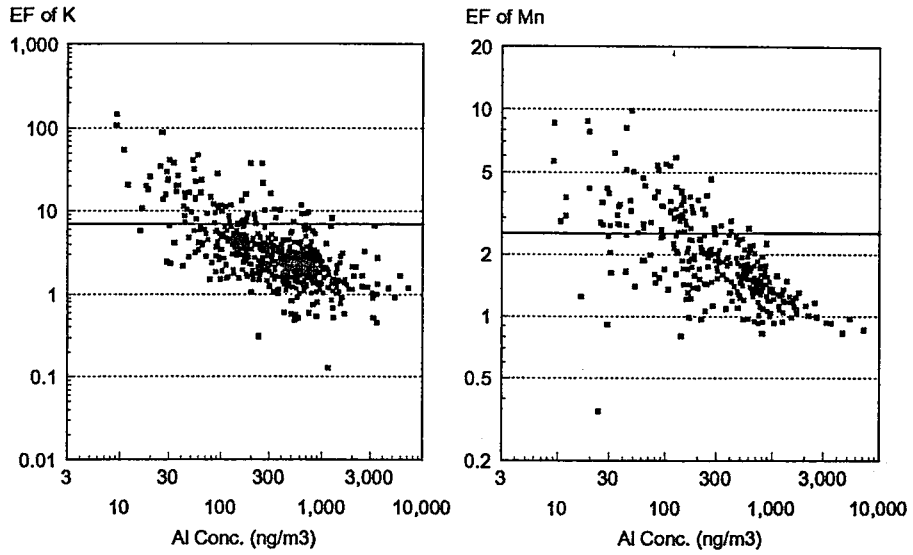


Figure 4.42 EF diagrams of K, Mn, V and Ti

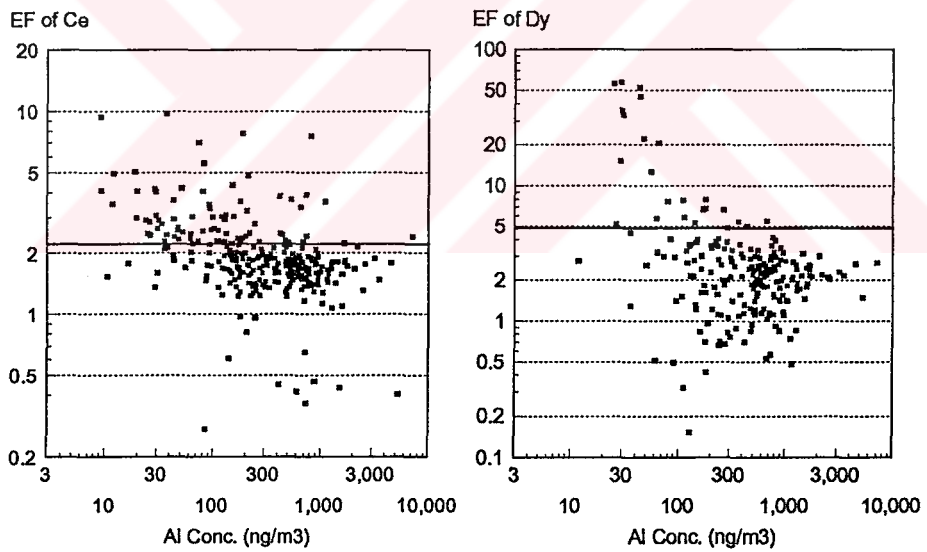
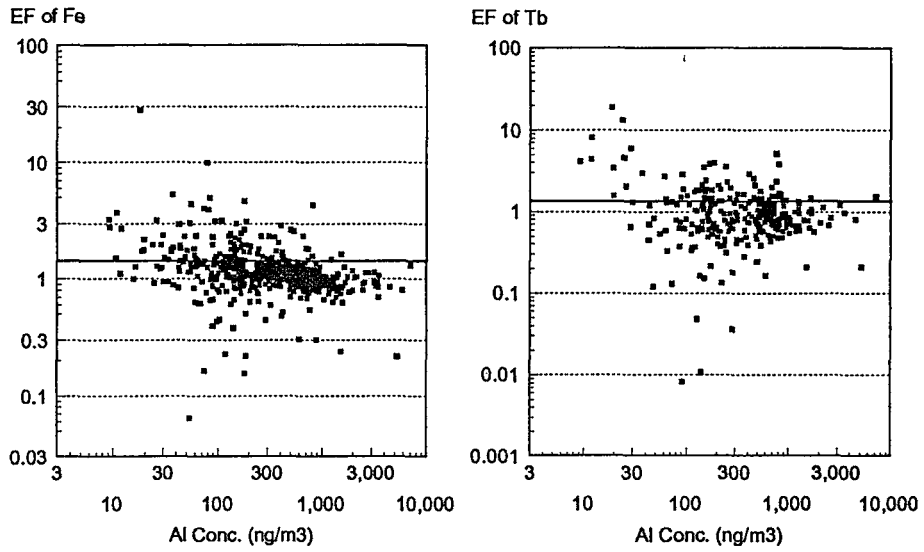


Figure 4.43 EF diagrams of Fe, Tb, Ce and Dy

Table 4.11. Seasonal mean crustal enrichment factors (EF_c) and winter to summer EF_c ratios

Element	Seasonal Mean EF _c		
	Winter	Summer	Winter/Summer
Na	100±300	8.0±7.0	12.5±39
Mg	15±50	2.8±5.9	5.4±20
Al	1.0	1.0	1.0
Cl	40700±120000	1600±1700	25±80
K	7.3±14.3	3.4±3.9	2.1±4.8
Ca	34±73	14±27	2.5±7.0
Sc	0.84±0.31	0.78±0.20	1.0±0.5
Ti	1.5±1.9	0.9±0.3	1.7±2.2
V	5.7±5.3	7.1±45	0.8±5.0
Cr	17±29	10±39	1.7±7.2
Mn	2.6±1.7	1.7±0.6	1.5±1.1
Fe	1.3±0.9	1.3±1.6	1±1.4
Co	8±40	1.6±1.3	5±25
Ni	12±24	9±20	1.3±4
Zn	79±100	38±36	2.1±3.3
As	950±1300	110±75	8.7±13.2
Se	3400±3900	1300±1100	2.6±3.7
Br	11500±28500	1120±780	10.3±26.4
Rb	3±2.6	1.8±0.6	1.7±1.5
Mo	900±2100	35±60	26±75
Sb	1310±1600	310±225	4.2±6.0
Cs	11±9	6±2.7	1.8±1.7
La	2.3±1.4	1.8±0.6	1.3±0.9
Ce	2.4±1.4	1.7±0.5	1.4±0.9
Nd	18±60	3±3.5	6±21
Sm	1.6±0.9	1.3±0.6	1.2±0.9
Eu	1.7±1.3	1.4±0.4	1.2±0.9
Gd	1.4±1.2	1.3±0.6	1.1±1.0
Tb	1.4±2.2	1.0±0.7	1.4±2.4
Dy	9±30	2.2±1.0	4±14
Yb	1.2±0.8	1.1±0.4	1.1±0.8
Lu	1.2±0.6	1.1±0.3	1.1±0.6
Hf	1.7±1.0	1.6±1.0	1.1±0.9
Hg	2150±3700	85±210	25±76
Pb	1950±4600	280±270	7±18
Th	2.0±1.1	1.7±0.5	1.2±0.7
SO ₄ ²⁻	3960±5270	1690±1620	2.34±2.41
NO ₃ ⁻	4700±5070	2900±2660	1.62±1.71
NH ₄ ⁺	41800±46000	11300±14200	3.70±4.12

2. The marine component which consist of seasalt aerosols generated over the Mediterranean sea through 'bubble-bursting' process. The marine source determines the observed concentrations of Na, Cl, Br and Mg in aerosols. It also affects the concentrations of K, Ca, Sr, Rb, Cs and SO_4^- .
3. Anthropogenic component which consists of particles emitted from various industrial activities. The anthropogenic component determine the concentrations and temporal variability of Cr, Ni, Zn, Cd, Mo, As, Sb, Hg, Se, SO_4^- , NO_3^- , NH_4^+ and affects the concentrations of Mn, V, Co, Br, Ti and Fe in aerosols.
4. There is also an unknown component in the aerosol and precipitation which appeared when the enrichment behaviors of normally crustal elements Nd, Tb, Ce and Dy were investigated. This unknown component is probably a part of the anthropogenic component most probably originates from refineries. But natural sources such as volcanic activity, biogenic emissions can not be ruled out as the source of enrichment of these normally crustal elements.

4.4.2.2. Marine Enrichment Factors

Marine enrichment factors (EF_m) are frequently used at sites where sea salt constitutes the major portion of the total particle mass (Tuncel et al., 1989; Duce et. al., 1983). Marine enrichment factors are useful to identify the sea salt contribution on observed concentrations of elements. The sea water composition given by Goldberg (1963) and Na_{ref} as the reference element were used in the calculations.

In remote marine atmosphere sea salt is the only source for Na, but previous researchers e.g. Dulac et al. (1987) and Hacısalıhoğlu et al. (1993) have shown that crustal influence on a measured sodium concentration can be significant in the Mediterranean and Black Sea atmospheres. Crustal

contribution on observed Na concentrations in the eastern Mediterranean atmosphere was calculated by using Taylor's (1972) crustal abundance pattern. As given in section 4.4.2 in detail, results showed that crustal dust can account for up to 20% of the observed Na concentration. Due to significant crustal contribution, marine enrichment factors were computed by using noncrustal Na (Na_{ncr}) as a reference.

Marine enrichment factors of elements in the eastern Mediterranean atmosphere is given in Figure 4.44. Marine enrichment factors for Cl, Br and Mg are about unity indicating sea water is the main source for these elements.

The Cl/Na_{ncr} ratio in collected samples is depicted in Figure 4.45. The average ratio is 1.57 which is less than the corresponding ratio in sea water (1.81), indicating volatilization of Cl from sea salt particles during their transport to the sampling site. Similar Cl depletion due to volatilization of was also observed in remote marine atmosphere (Duce et al. 1983; Tuncel et al., 1989; Hacısalihoğlu et al., 1993) and attributed to the reaction between aerosol NaCl and H_2SO_4 and subsequent volatilization of Cl as HCl. A negative relation between Cl/Na_{ncr} ratio and $nss-SO_4^{2-}$ concentrations our data set which is shown in Figure 4.46 suggest that similar volatilization of Cl from sea salt particles is the reason for observed small Cl/Na ratio in the eastern Mediterranean as well.

Although the marine enrichment factor of Br is around unity, probably sea salt is not the only source. The Br/Na_{ncr} ratio in samples are given in Figure 4.47. The average of Br/Na_{ncr} is calculated as 0.031 ± 0.042 which is a factor of 5 higher than corresponding sea water ratio, 0.0062. By using size separated samples collected from marine atmosphere it was shown that, Br/Na ratio in large particles is same or even sometimes less than the corresponding ratio in sea water, indicating large particle Br are of marine origin. However, high Br enrichments were observed in small particles due to anthropogenic sources, mainly due to motor vehicle emissions (Duce et al., 1983; Arimoto et al., 1987;

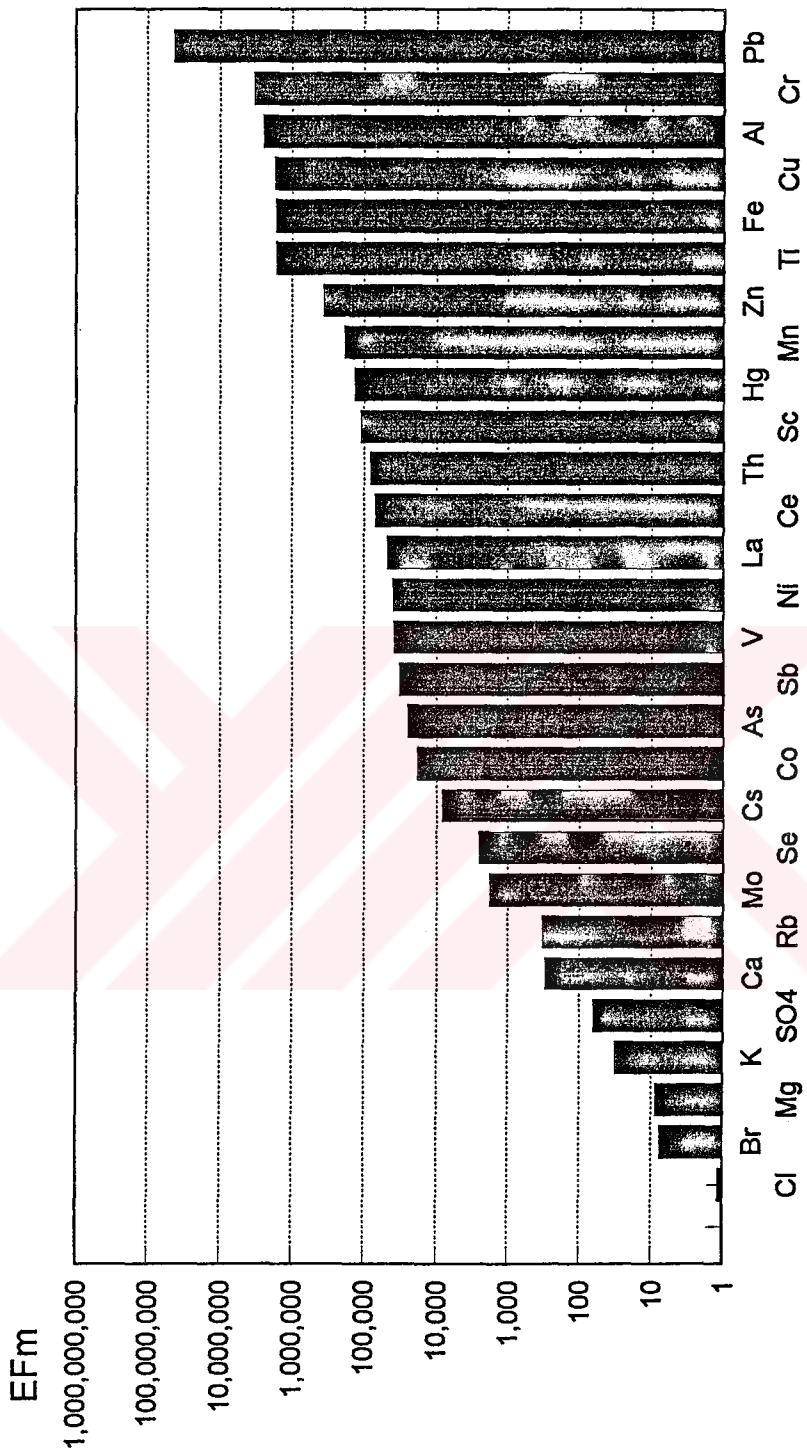


Figure 4.44 Marine Enrichment Factors

Dulac et al., 1987). Since our samples are not size separated, anthropogenic Br is masked by marine Br on large particles. However, high Pb concentration measured in some samples in which Br/Na ratio is higher than that in sea water indicate that anthropogenic Br do exist in aerosol mass.

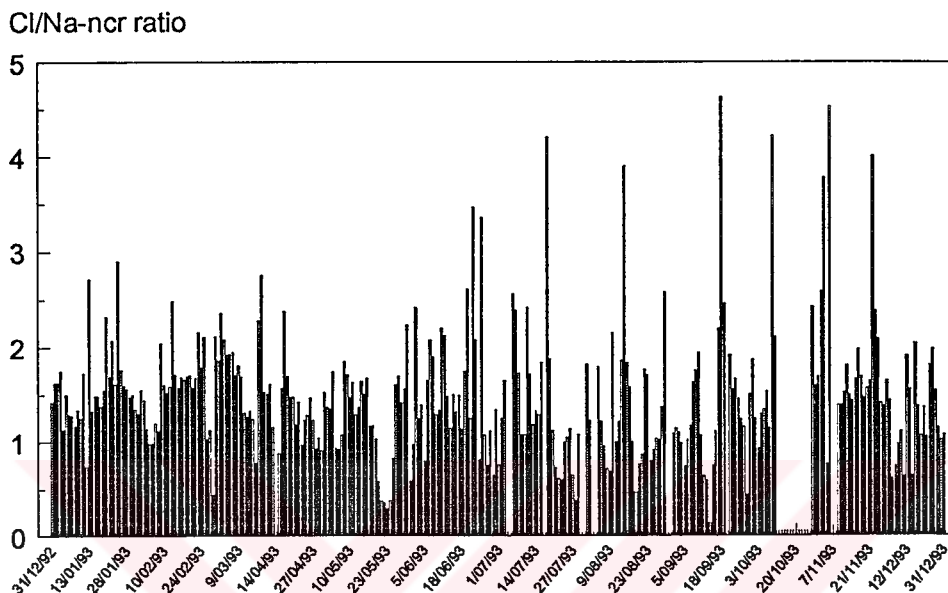


Figure 4.45 The Cl/Na-ncr ratio

The moderate enrichments of K, Ca and Rb indicate that concentrations of these elements in the eastern Mediterranean atmosphere are controlled by both sea salt and crustal dust.

The rest of the elements in the eastern Mediterranean atmosphere are highly enriched with respect to marine source. High enrichments of elements Cs, Co, La, Ce, Th, Sc, Mn, Ti, Fe and Al are due to crustal dust in the atmosphere.

In pristine marine locations, the main source of S and Se is the sea water. The S and Se is biologically released from the sea in the gas phase and subsequently condense on small particles (Parrington et al., 1983; Mosher and Duce, 1983). This gas phase release from the sea and subsequent attachment to aerosols results in high marine enrichment factors, even the source is sea.

But observed concentrations of both S and Se in the eastern Mediterranean atmosphere are much higher than corresponding concentrations measured even in the most productive regions of the world ocean, indicating that the eastern Mediterranean itself is not an important source for these elements.

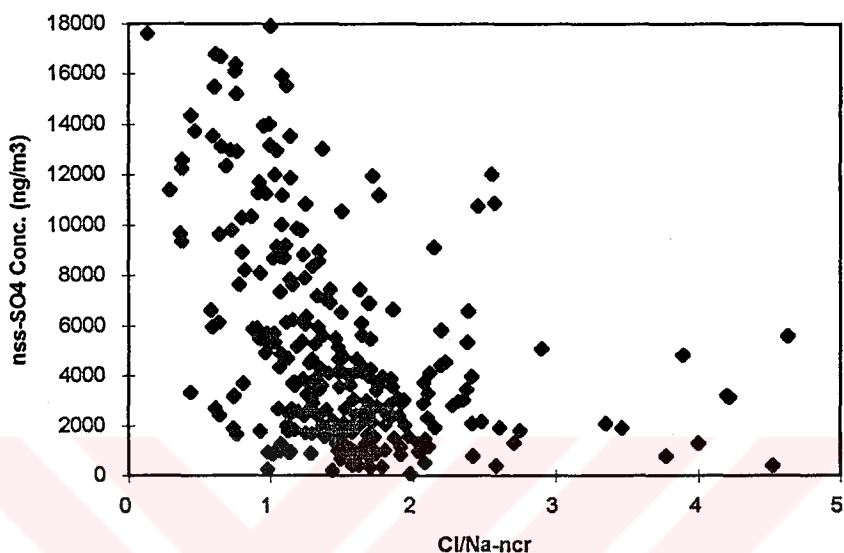


Figure 4.46 Relation between Cl/Na_{ncr} and $nss-SO_4$

Remaining elements, namely, Mo, As, Sb, V, Ni, Hg Zn, Cr and Pb are enriched relative to sea water due to anthropogenic sources. Some of these highly enriched elements are found in significant quantities at the sea surface microlayer and eventually transferred to atmosphere by bursting bubbles (Weisel et al., 1984; Wallace and Duce, 1975). As in the case of S and Se, this source may be significant in the open ocean and probably is not important in the eastern Mediterranean, because if microlayer enrichment of elements is an important source for observed concentrations of these elements at our station, one would expect at least moderate correlation between microlayer enriched elements and sea salt elements, because they are all generated by bubble bursting process over the sea. Such correlation was not observed between pollution derived elements and sea salt elements. (2) Such microlayer enrichments were proposed as the source of certain AEE's only in pristine location far from any anthropogenic source. But Mediterranean is surrounded

by strong industrial emission sources. Consequently, anthropogenic sources dominate over any small natural source of these elements at our sampling site.

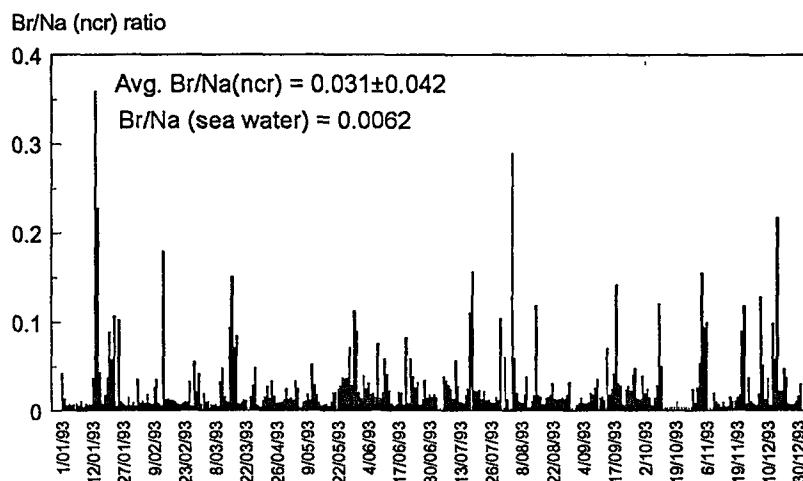


Figure 4.47 The Br/Na-ncr ratio

4.4.3 Crustal and Marine Contribution of Elements

Crustal and marine enrichment factor calculations showed that atmospheric aluminasilicate particles and sea salt can account significant fractions of large number of elements in the eastern Mediterranean atmosphere. To get a better feeling for the relative importance of marine and crustal contributions and to quantify influence of these two sources, marine and crustal contribution on the observed concentrations of elements were calculated. Results are given in Table 4.11.

The percent contribution of crustal source on the concentration of each element was calculated by assuming crustal dust is the only source of Al in samples and using element-to-aluminum ratios given for average crustal rocks in the literature (Taylor, 1972). Percent marine contributions on each element was calculated by using Goldberg's sea water composition and noncrustal Na (Na_{ncr}) as the reference element. The contribution of the crustal and marine sources on the observed elemental concentrations were calculated according to the equations given below;

$$X_{\text{crust}} = Al_{\text{air}} (X/Al)_{\text{crust}} \quad (1)$$

and

$$X_{\text{sea}} = Na_{\text{ncr}} (X/Na)_{\text{sea}} \quad (2)$$

Where X_{crust} and X_{sea} are the crustal and marine contributions on observed concentrations of elements, Al_{air} is the Al concentration in sample, $(X/Al)_{\text{crust}}$ is the element-to-Al ratio in Taylor's (1972) crustal table, Na_{ncr} is the non-crustal Na concentration in sample and $(X/Na)_{\text{sea}}$ is the element-to-Na ratio in Goldberg's (1963) sea water composition.

The Al concentrations and crustal fractions of observed Na concentration in each sample were calculated by using the above formula and results are given in Figure 4.48. The calculated crustal influence on the Na concentration of the whole sample set at Antalya is approximately 20%. The crustal influence on the measured sodium concentrations was approximately 1.8 % when the Na/Al ratio was higher than 6 and approximately 30% when the Na/Al ratio was lower than 3. During Saharan dust incursions, the loading of crustal material in the atmosphere are so high that, almost all of the Na, in those samples becomes crustal. As can be seen in Figure 4.48, calculated crustal fraction of Na is larger than measured Na concentration in some of the aerosol samples. The difference is due to composition difference between the sampled crustal material and Taylor's (1972) crustal abundance table.

As can be seen in the table, the soil particles in the atmosphere make a significant contribution on observed concentrations of Mg, Al, K, Sc, Ti, Mn, Fe, Co, Rb, La, Ce, Sm, Eu, Gd, Tb, Dy, Yb, Lu, Hf and Th whereas sea salt contributed substantially to the concentrations of Na, Mg, K, Br. Large fractions of NO_3^- , SO_4^{2-} , NH_4^+ , Ca, V, Cr, Mn, Co, Ni, Zn, As, Se, Br, Mo, Sb, Cs, Nd, Hg and Pb can not be attributed to crustal and marine sources and must be derived from anthropogenic sources.

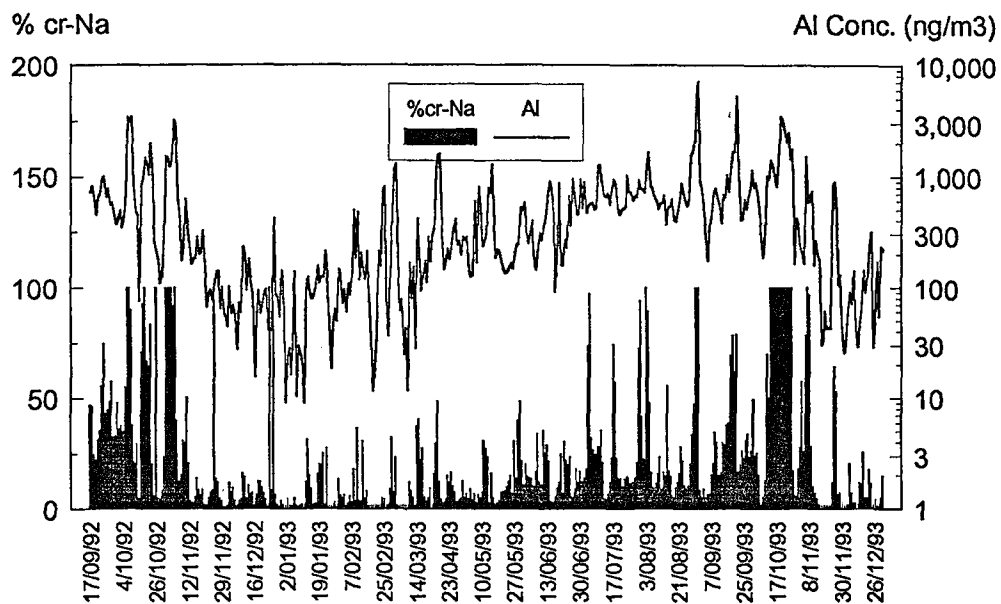


Figure 4.48 Temporal variation of % crustal Na and Al concentrations

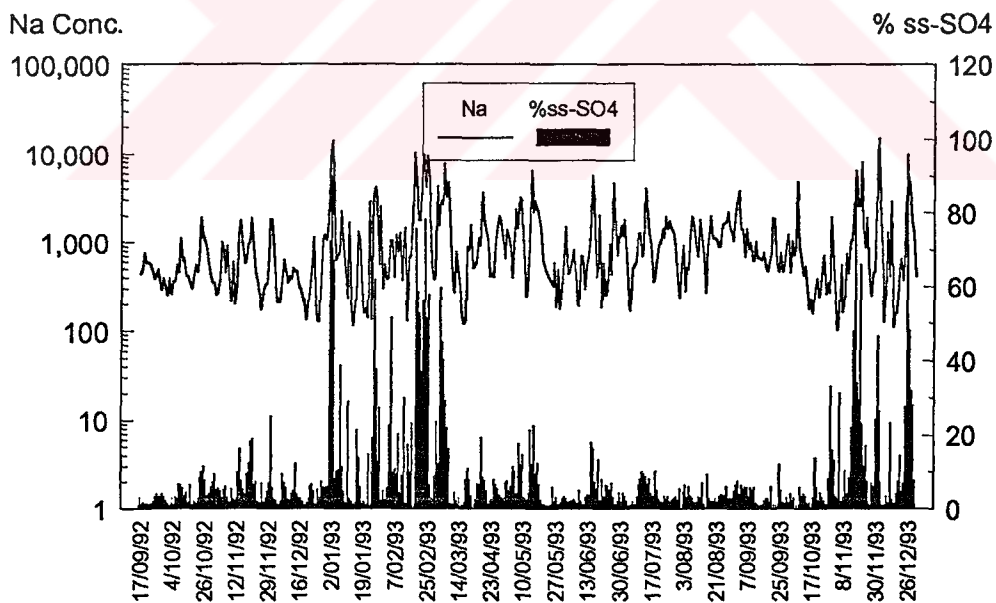


Figure 4.49 Temporal variation of % ss-SO₄ and Na concentration

The SO_4^{2-} is one of the most important parameter in regional scale studies as it represents one of the acidic components in precipitation and aerosols. Since the concentrations of S in sea water is fairly high (885 ppm), sea salt aerosols contribute to the measured concentrations of SO_4^{2-} in the atmosphere. The sea salt fractions of SO_4^{2-} concentrations in aerosol samples collected in Antalya station is given in Figure 4.49 along with the measured Na concentrations. The figure indicates that the sea salt fraction of SO_4^{2-} is approximately 5% during summer season. Only in December, January and February with strong winds, the sea salt fraction episodically increases to values larger than 30% and becomes significant fraction of measured SO_4^{2-} concentrations. Since crustal sources are insignificant source of sulfate, nss- SO_4^{2-} is assumed to be anthropogenic.



Table 4.12 Crustal and marine contribution of the observed concentrations

	%Crustal	%Marine	Other
NO3	0.1	--	99.9
SO4	0.14	9.34	90.5 2
NH4	0.1	--	99.9
Na	20	80	0
Mg	42	36.4	21.6
Al	100	0	0
Cl	0.14	93.4	6.46
K	41	18.2	40.8
Ca	14	3.11	82.89
Sc	98	0.03	1.97
Ti	87.5	0	12.5
V	34.5	0.05	65.45
Cr	24	0.001	75.999
Mn	58	0.02	41.98
Fe	84	0.002	15.998
Co	67	0.12	32.88
Ni	25	0.08	74.92
Zn	4.8	0.003	95.197
As	1.1	0.07	98.83
Se	0.13	0.4	99.47
Br	0.12	43.1	56.78
Rb	55	5.1	39.9
Mo	9	2.7	88.3
Sb	0.4	0.05	99.55
Cs	19	0.3	80.7
La	55	0.08	44.92
Ce	55.4	0.05	44.55
Nd	46.2	--	53.8
Sm	75.2	--	24.8
Eu	71.4	--	28.6
Gd	77	--	23
Tb	86	--	14
Dy	50	--	50
Yb	88	--	12
Lu	88	--	12
Hf	70	--	30
Hg	3.9	0.01	96.09
Pb	1.4	0	98.6
Th	61	0.14	38.86

4.5. Source Apportionment and Quantification

Various mathematical models had been developed in the last decade to apportion the aerosol measured at a site to its' likely sources. These models which have found widespread use in air pollution studies, include multiple regression analysis, cluster analysis, time series analysis and principal component or factor analysis (Hopke et al., 1980; Heidam, 1981; Thurston and Spengler, 1981; 1985; Morandi et al., 1991). In contrast to dispersion models, these techniques are based on analysis of ambient air samples and chemical characterization of source emissions rather than measurement of source emission rates and application of atmospheric dispersion and transport equations. To quantitatively apportion the observed airborne concentrations among the various source types, multielement analysis of large numbers of airborne particle samples are needed.

As discussed in the previous sections, four major source groups namely, crustal, marine, anthropogenic and dust outbreaks, affecting the eastern Mediterranean aerosols were identified. Among these groups, anthropogenic component is the most important one in terms of pollution transport to the eastern Mediterranean. In this thesis, one of the most widely used source apportionment technique, Factor Analysis is applied to elemental data to characterize aerosols with respect to sources and quantify the different sources and their importance for the composition of the aerosols at the monitoring site, Antalya. Application of Absolute Factor Score (AFS) technique following to the Factor Analysis enabled quantitative assessment of identified sources.

4.5.1. Principal Component Factor Analysis (FA)

Principal component factor analysis provides preliminary information about the possible sources that may influence a given receptor site. In principle, it actually distinguishes groups of elements which concentrations fluctuate together from one sample to another and separates these elements into so called 'factors' (Henry et al., 1984). Ideally, each extracted factor represents a source affecting the samples. Although there are no well-defined rules on the number of factors to be retained, usually either factors that are meaningful or factors with eigenvalues larger than one are retained. In theory, irrelevant factors have zero eigenvalues and eigenvalues less than one indicate that factor contribute less than a single variable. In this study, factors which have eigenvalues larger than unity have been retained.

4.5.1.1. Treatment of Values Below Detection Limit

In the measurement of contaminants in environmental samples, values below detection limit complicate statistical analysis. However, many of the today's air quality problems are associated with chemical levels too low to be measured precisely. When the data include many values below detection limit, the question of how to deal with these samples becomes a significant issue. Many common practices for handling values below detection limit, such as deletion of samples or substitution of the detection limit, one half of the detection limit or multiplication of detection limit with a random number between 0 and 1 (Gillion and Helsel, 1986; Gleit, 1986; Newman et al., 1989; Helsel, 1990) are known to produce biased estimates for means and variances and also lack of statistical justification. However, data that include 'below detection values' or 'not detected' values contain less information than data for which numbers are reported, even if some of those numbers are very imprecise.

The detection limits of most of the elements in neutron activation analysis vary due to Compton scattering by other elements in the sample, peak interferences due to the other elements and self shielding, etc. (Olmez 1989). Thus, using one of the above methods for substituting the missing values would produce low biased values. Therefore, the missing values for the variables for which 20% and less of the observations fell below the detection limit were filled with regional background concentrations, rather than detection limit, half of it or multiplied with a random number. The methodology used to calculate "regional background" concentrations is given in section 4.3.1.

One has to be careful in interpreting filled in values. No matter which method is used in estimation, the BDL values that are filled in are not real measurement results. These numbers are not real measurement results and they can not be used in determining features of the data set, such as averages, median mode, quartiles etc. They should only be used in statistical treatment of data which does not allow for missing values. Multiple linear regression and factor analysis are good examples of such statistical treatments. In these techniques if there is a missing value for one of the parameters included in the analysis, then that particular sample is excluded from the analysis. If in such statistical treatment BDL values are not filled in by an appropriate method, most of the samples are excluded from analysis, because they contain a BDL value for one of the 20 - 30 elements included in the exercise. Only in such cases, the filling in for BDL values can be rationalized.

Also, if too many of the values of one of the parameters are filled in values than, they effect statistical treatment of data. Consequently, BDL values can only be filled in if number of BDL values in the data is limited. Although there is no universal rule for the minimum fraction of BDL values for an element that can be safely filled in, in this work only the parameters with BDL values are not exceeding 20% of all data points for that parameter

were filled in. If BDL values of an element were larger than 20% of all data for that element, the particular element was not included in the statistical treatment. Twenty eight out of 40 elements and ions satisfies this criteria and included in the factor analysis.

4.5.1.2. Extraction of Factors

Factor Analysis has been performed using the Statgraphics Plus program package (STATGRAPHICS Manual, Ver. 6.1, 1992). The aerosol samples collected in 1993 which were analyzed with INAA were used in the analysis. The initial components were rotated using the orthogonal varimax method to obtain the final eigenvectors. Initially factor analysis was performed by using all the data points. Then the data were screened for the outliers using factor scores. In the factor analysis, the first step in the derivation of source impacts is to calculate factor scores for each sample. These factor scores are correlated with their respective pollution sources impacting the site (i.e. higher factor score implies a higher pollution impact by the pollution source) with each having a mean of zero. High factor scores indicates the samples impacted by the source more than the average, and negative factor scores indicates the samples impacted by the source less than the average. Hopke (1980) pointed out that if a sample has factor score greater than 6 at least in one of the factor, it is called outlier and should be discarded from the analysis. Totally 9 samples had been deleted from the data set. As a result total of 304 samples for 28 elements were used in the analysis.

The results of varimax-rotated factor analysis is shown in Table 4.13. Only factor loadings larger than 0.25 were included in the table, because loadings smaller than 0.25 were considered "insignificant". Four identifiable factors account for 80.3% of the total variance in the data set.

Table 4.13. Varimax rotated factor loading and corresponding probable source type

Variable	Factor 1	Factor 2	Factor 3	Factor 4	Communality
Na			0.94		0.88
Mg	0.52		0.67		0.72
Al	0.94				0.88
Cl			0.94		0.88
K	0.63	0.26			0.46
Sc	0.97				0.94
Ti	0.93				0.87
V	0.62	0.63			0.78
Cr	0.41	0.25		0.25	0.27
Mn	0.88	0.28			0.85
Fe	0.96				0.92
Co	0.76				0.58
Zn		0.80			0.64
As				0.80	0.64
Se		0.88			0.77
Br			0.93		0.87
Rb	0.92	0.26			0.91
Sb		0.26		0.78	0.65
Cs	0.80	0.41			0.81
La	0.97				0.94
Ce	0.96				0.92
Nd	0.55		0.46		0.51
Sm	0.95				0.91
Hg			0.41	0.34	0.28
Th	0.97				0.94
NO ₃ ⁻	0.26	0.79			0.69
nss-SO ₄ ⁼		0.83			0.69
NH ₄ ⁺		0.81			0.66
% variance	42.00	15.50	12.60	10.20	80.30
Probable source	Crustal	Mixed combustion	Marine	Local As Source	

The first factor was identified as crustal factor, because it included high loadings of crustal elements, such as Al, Sc, Ti, Mn, Fe, Rb, Cs, La, Ce, Sm and Th. The crustal factor accounts for a 42% of the system variance due to inclusion of large number of crustal elements in the FA and high loadings of these elements in the factor.

Factor 2 has high loadings of NO_3^- , nss-SO_4^{2-} , NH_4^+ , V, Zn, Se and weak loadings of K, Mn, Rb and Sb. This factor is identified as combustion factor owing to presence of nss-SO_4^{2-} , Se which are typical marker elements for coal combustion and V which is a marker element for oil combustion. However, the factor also includes elements which are associated with industrial emissions. As discussed previously, in rural sites where aerosol are intercepted after long range transport, compositions of factors are modified by transport as well. The plots of the factor scores are given in Figure 4.50. The peaks in the factor scores which represent the samples impacted by this particular factor coincide with north and northwesterly wind trajectories. Since the strongest fuel, particularly oil combustion sources in the region are located in the former USSR, this factor probably represents from transport of emissions from former eastern block countries.

High factor scores associated with this factor are observed during summer months. During dry summer months, air masses originating from distant locations can be transported to the eastern Mediterranean without significant loss of material with scavenging. Although, source strengths are the same in winter season, the local and distant precipitation scavenged most of the particles in the atmosphere, therefore the impact of this source is not strong. The combustion factor accounts for 15.50% of the total variance.

The third factor is highly loaded in Na, Cl and Br and moderately loaded in Mg, Nd and Hg. This factor is clearly a marine factor. Inclusion of Hg in this factor is not clear.

The fourth factor with high loadings of As and Sb is the second anthropogenic factor. Separation of As and Sb into a different factor highlights the presence of local source for these elements. As shown in factor score plot for the 4th factor (Figure 4.50) contrary to combustion factor high factor scores correspond to samples collected in winter season. This

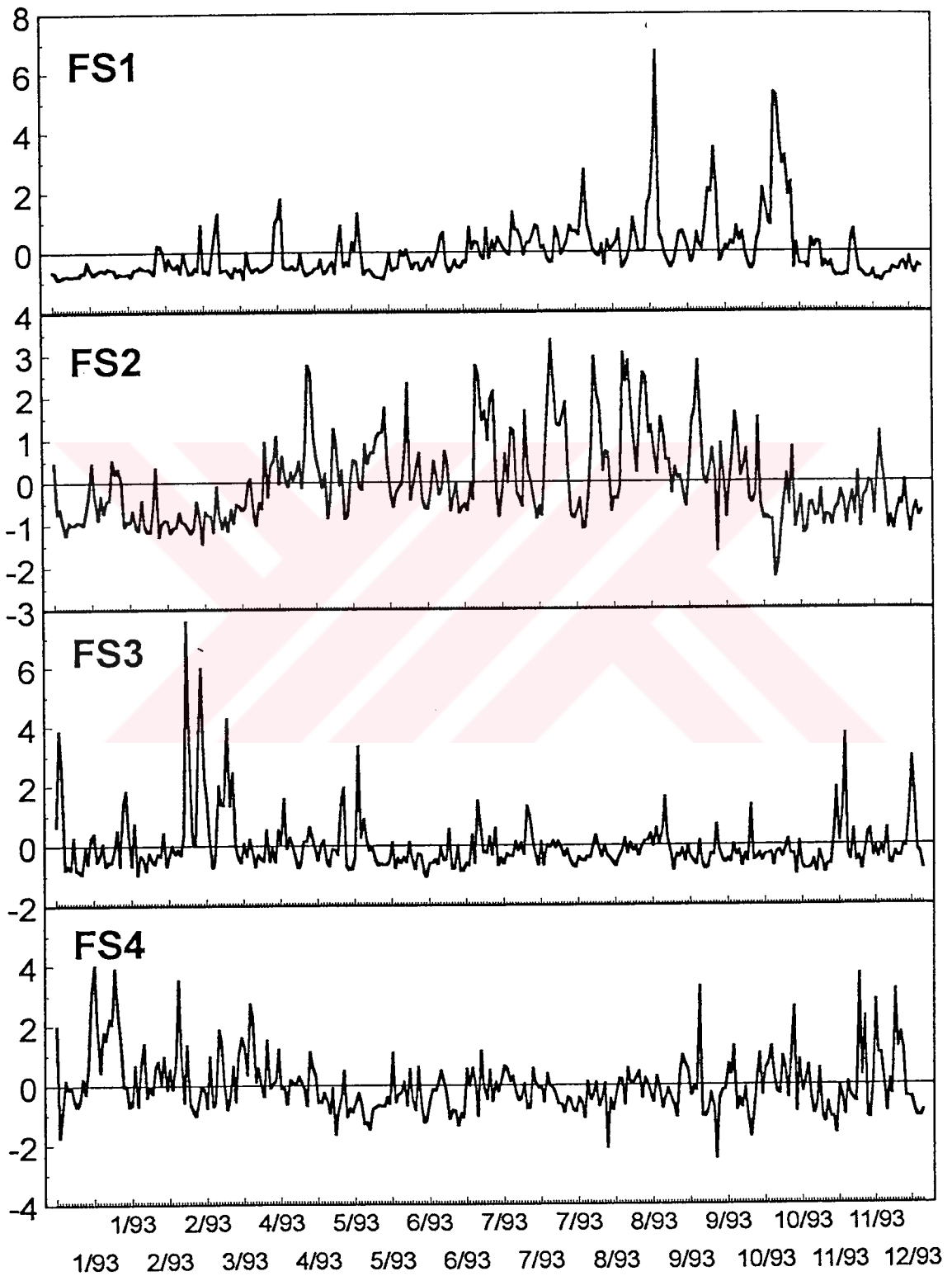


Figure 4.50 Time series plot of Factor Scores

factor is believed to represent local sources. Although Pb is not included in the factor analysis, there are significant correlation between Pb, As and Sb. Since these three elements are associated with different sources, this factor probably represent mixed local aerosol sources.

The crustal component in the eastern Mediterranean aerosols is known to be consist of two soil components corresponding to local soil and Saharan Dust. Due to the dominating influence of local soil on system variance, only one crustal component appeared in the factor analysis. A separate factor analysis was performed including only crustal elements to distinguish the two soil components and to be able to determine their chemical composition.

The results of factor analysis of crustal elements are given in Table 4.14. Two factors accounted for 75.7% of the total variance in the data set, of which 19.6% was accounted by the Saharan Dust factor. The first factor which includes high loadings of Al, Sc, Ti, Mn, Fe, Rb, Cs, La, Ce, Sm and Th and moderate loadings of K, Cr and Co represents the local soil. The second factor has high loadings of Mg, and Nd and moderate loadings of other crustal elements. High loading of Mg in this factor suggests that this factor may indicate the North African desert soil which is rich in Mg (Levin et al., 1990). High factor-2 score days which are shown in Figure 4.51 coincide with upper atmospheric flow from south. Therefore the second factor is identified as Saharan Dust factor.

4.5.2. The Use of Absolute Factor Score Method (FA-AFS)

Principal Component Factor Analysis can be used to screen a data set for potential error identification as well as source recognition, however mass contributions of individual sources cannot be obtained, because data used in the factor analysis are first normalized to have an average of 0 and standard deviation of 1. The normalization performed in the first step results

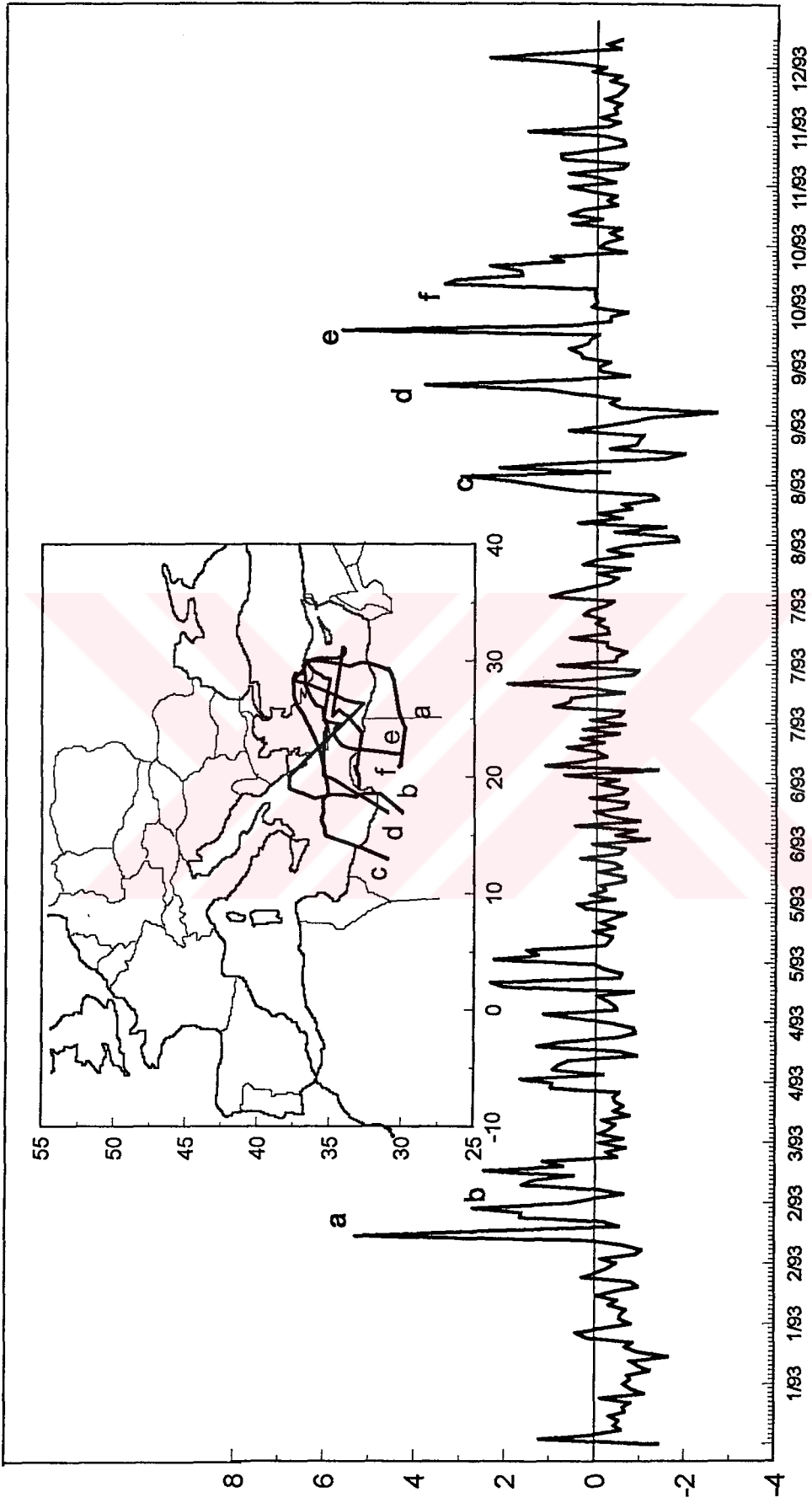


Figure 4.51 Factor score plot of Factor 2 and back trajectories corresponding to peak days

in the loss of concentration information. In order to estimate the contribution of all possible sources Factor Analysis-Absolute Factor Score Method (FA-AFS) were used (Thurston and Spengler, 1985).

Table 4.14. Varimax rotated factor analysis for crustal elements only

Variable	Factor 1	Factor 2	Communality
Mg		0.70	0.49
Al	0.81	0.49	0.90
K	0.60	0.31	0.46
Sc	0.87	0.44	0.95
Ti	0.77	0.50	0.84
V	0.69	0.27	0.55
Cr	0.64		0.41
Mn	0.83	0.40	0.85
Fe	0.89	0.41	0.96
Co	0.56	0.57	0.64
Rb	0.91	0.33	0.94
Cs	0.91		0.83
La	0.84	0.46	0.92
Ce	0.85	0.44	0.92
Nd		0.78	0.61
Sm	0.82	0.48	0.90
Th	0.87	0.43	0.94
% Variance	56.1	19.6	75.7
Probable Source	Local Soil	Saharan Dust	

The technique is based on computation of Absolute Principal Component Factor Scores (AFS) for each sample, followed by the regression of sample aerosol concentrations for each element on these AFS to derive source contribution.

After a varimax rotated factor analysis was applied to the data set, absolute factor scores were calculated for each sample and for each identified factor by scoring an extra day in which all concentrations are set equal to zero. The contributing concentration of each factor was then estimated by a multiple regression analysis using the absolute factor scores as independent variables. The resultant regression coefficients were than

employed to convert the daily absolute factor scores to estimate mean source contributions. Estimated mean source contributions for each identified factor are given in Table 4.15.

The correlation coefficients between observed elemental concentrations and absolute factor scores (r^2) are quite high. Only the elements Cr and Hg are poorly correlated with absolute factor scores. Such lack of correlation implies that significant amount of Cr and Hg were left unapportioned by the regression probably due to some unconsidered source(s). Identified sources account for 77% of the total variance in the data set. When sum of the estimated mean contributions of elements are compared, the difference between average predicted and observed concentrations are smaller than 25% for 22 out of 26 elements. Only elements As, Sb and NH_4^+ are underpredicted by larger than 25% and Sm, Sc and Cl are overpredicted by larger than 25%. The underprediction of NH_4^+ , As and Sb may indicate another source which is not identified by the factor analysis. The Cl is overpredicted probably due to evaporation of Cl from particles through reaction of NaCl with H_2SO_4 (Duce et al. 1983; Tuncel et al., 1989; Hacısalıhoğlu et al., 1993), but overprediction of Sm and Sc indicates poor apportionment of these crustal elements. Fairly good agreement between observed and predicted concentrations of the rest of the elements are encouraging for the use of this method for rural aerosols.

The second factor in the factor analysis is the most important factor, because it represent regional aerosols transported from Europe and former Eastern Block countries which is the main mode of pollution transport from north to east. Consequently, determination of the chemical composition of this component is important to compare this component with similar aerosols identified in other Mediterranean stations (although purely European aerosols are not isolated in any other station in the Mediterranean so far) and to estimate the contribution of distant sources on aerosol composition and deposition in the eastern Mediterranean.

Table 4.15. Mean source contributions ($\text{ng} \cdot \text{m}^{-3}$)

	Crustal	Mixed Comb.	Marine	Local Sour.	Σ estimated mean cont.	Observed mean conc.	(r^2)
Na		30	1460		1490±400	1320±1560	0.93
Mg	160	37	205		402±140	410±304	0.79
Al	575	72			647±190	503±614	0.91
Cl			2540		2540±680	1780±2700	0.94
K	185	77	20		282±217	310±296	0.46
Sc	0.11	0.015		0.002	0.127±0.02	0.098±0.11	0.97
Ti	33	2			35±13	34±36	0.87
V	1.03	1.05			2.08±0.76	2.19±1.68	0.80
Cr	1.37	0.77		0.79	2.93±2.87	3.74±3.35	0.27
Mn	6.40	2.03			8.43±2.68	8.74±7.23	0.86
Fe	338	63		19	420±70	340±0.35	0.96
Co	0.16	0.020	0.050	0.015	0.25±0.12	0.21±0.21	0.64
Zn	1.69	8.3		1.95	11.94±5.8	11±10	0.69
As				1.09	1.09±0.80	1.59±1.37	0.65
Se	0.025	0.16	0.004	0.024	0.21±0.08	0.28±0.18	0.81
Br	0.15	0.41	11.70	0.68	12.94±4.72	16.5±12.63	0.86
Rb	0.71	0.20		0.056	0.97±0.21	0.86±0.76	0.93
Sb	0.036	0.049		0.15	0.24±0.10	0.34±0.19	0.73
Cs	0.052	0.027		0.013	0.092±0.025	0.091±0.065	0.85
La	0.355	0.034		0.005	0.394±0.091	0.33±0.37	0.94
Ce	0.67	0.066		0.027	0.76±0.17	0.62±0.69	0.94
Nd	0.25		0.21	0.058	0.518±0.309	0.47±0.45	0.53
Sm	0.052	0.006		0.001	0.059±0.016	0.046±0.055	0.92
Hg			0.047	0.039	0.086±0.091	0.084±0.12	0.38
Th	0.096	0.012		0.003	0.111±0.022	0.092±0.099	0.95
NO ₃	200	610	18		828±430	974±771	0.69
n-SO ₄	400	3720	38		4158±2430	5270±4460	0.71
NH ₄ ⁺	117	855		33	1005±430	1830±1060	0.67

This second factor contributes 70% of the observed Zn, 76% of the observed Se, 74% of the observed NO_3^- , 89% of the observed nss-SO_4^{2-} , 85% of the observed NH_4^+ , 51% of the observed V, 26% of the observed Cr and 24% of the observed Mn concentrations in the eastern Mediterranean atmosphere. Based on this most of the non sea sulfate and other acidic ions in the eastern Mediterranean atmosphere are transported from Europe and former USSR countries. More exact locations of the sources in Europe will be discussed in subsequent sections.

Chromium, is contributed both by crustal and anthropogenic sources. But, the most important point in the distribution of Cr among sources is the high contribution of the crustal component. Approximately 46% of the observed Cr concentration in our station is due to soil particles which is due to unusual composition of local soil, as discussed in previous sections. The remaining 54% is almost equally contributed by local and European sources. Although, Ni is not included in the factor analysis exercise, high binary correlation between Ni and Cr and Ni and other crustal elements suggest that large fraction of the atmospheric Ni concentration is also due to crustal material in the atmosphere. This unusual composition of local soil provides a unique opportunity to distinguish between the contributions of local and Saharan dust components in the eastern Mediterranean atmosphere.

The local anthropogenic component accounts for most of the measured concentrations of As and Sb, approximately 10 to 20% of the measured concentrations of Se and Zn. Although, Pb is not included in the factor analysis, strong correlation of Pb with these elements as discussed in previous sections suggest that, if it was included in the factor analysis, Pb would appear in this factor. With the exception of As, Sb and Pb, contribution of local sources on aerosol composition in the eastern Mediterranean is small.

As designated in the previous section, high concentrations of sulfate and Se in the second factor represent high temperature coal combustion sources located at distant places. Since this factor represent distant mixed combustion sources located at the Europe and former USSR, determination of its chemical composition downwind of the sources is very crucial in the use of other source apportionment techniques such as Chemical Mass Balance (CMB) in the eastern Mediterranean atmosphere. One interesting feature of this local pollution component is the lack of nss-SO_4^{2-} and NO_3^- in this component. Since, the sources which emits aerosols in this component are in the close vicinity of the station, the residence time for particles in the atmosphere before they are intercepted at the station should be small. Consequently, most of the S and N should be in the form of precursor gases instead of oxidation products. Since only the oxidation products are measured in the station, this factor does not contribute significantly to the nss-SO_4^{2-} and NO_3^- concentrations measured at the station.

Same source apportionment approach was applied to the factor analysis performed only with crustal elements to distinguish the two soil components namely, local soil and Saharan dust and to determine their chemical composition. The calculated mean source contributions of local soil and Saharan dust are given in Table 4.16. The first factor namely the local soil which is identified by the presence of Cr in this factor, accounts for 60 - 70% of the observed concentrations of elements, remaining 30 - 40% accounted for by the Saharan dust. However, Saharan dust accounts for 87% of the observed Nd, 76% of the observed Mg and approximately half of the observed Co concentrations.

To determine the differences between the chemical compositions of local soil and Saharan dust, the ratios of concentrations of elements derived from factors to Al were calculated and x-to-Al ratio in local soil vs. x-to-Al ratio in Saharan dust and crustal enrichment factors of elements in two soil components are plotted in Figures 4.52 and 4.53, respectively. Although,

none of the elements in both factors are enriched relative to average crustal composition (Taylor's compilation used), there are important differences between the chemical compositions of the two soil components.

Table 4.16. Mean source contributions ($\text{ng} \cdot \text{m}^{-3}$) of Local soil and Saharan Dust

	Local Soil	Saharan Dust	Σ estimated mean cont.	(r^2)
Mg	70	220	290±210	0.54
Al	490	300	790±210	0.89
K	176	90	266±220	0.44
Sc	0.095	0.048	0.143±0.023	0.95
Ti	27.5	17.9	45.4±14.1	0.85
V	1.16	0.46	1.62±1.12	0.55
Cr	2.13		2.13±2.47	0.46
Mn	5.99	2.90	8.89±2.79	0.85
Fe	310	145	455±74	0.96
Co	0.116	0.118	0.284±0.125	0.64
Rb	0.69	0.25	0.94±0.20	0.93
Cs	0.059	0.009	0.068±0.026	0.85
La	0.31	0.17	0.48±0.10	0.92
Ce	0.59	0.31	0.90±0.19	0.92
Nd	0.06	0.41	0.47±0.33	0.61
Sm	0.045	0.026	0.071±0.017	0.90
Th	0.086	0.043	0.129±0.025	0.94

The most promising marker elements to distinguish local soil and Saharan dust are Nd, Mg, Cr and Cs, because crustal enrichment factors of these elements in two soil components are distinctly different. Although, Mg had been used as tracer for the Saharan dust before (Levin et al., 1980), the other elements are identified as marker elements for the first time in this study. Among these, Nd and Mg are more enriched in Saharan dust whereas Cr and Cs are more enriched in local soil. Among marker elements, Cr, Ni and Mg are more promising because they can be analyzed accurately by a variety of analytical techniques (including commonly used AAS), whereas analysis of Nd requires sophisticated techniques, such as

INAA. However, since Cr is also strongly contributed by anthropogenic sources as well, its presence or absence in the atmosphere does not necessarily imply the presence or absence of local soil. The same argument also applies for Mg which is contributed strongly by the marine source. In this sense, Nd appears to be the most powerful tracer for the Saharan dust.

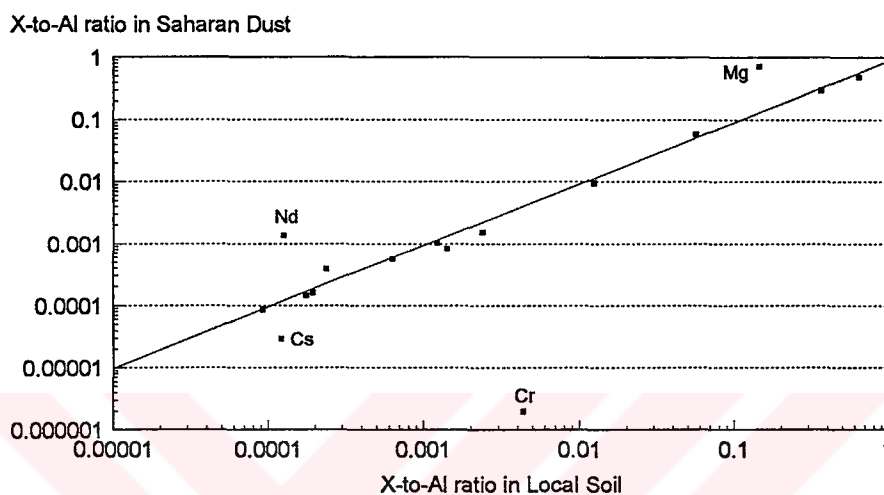


Figure 4.52 X-to-Al ratios in Local Soil and Saharan Dust

In addition to differences in their chemical composition, the marine elements can also be used to distinguish between two crustal material affecting eastern Mediterranean, because as the air mass traveling from north Africa region to Turkey, it travels over the Mediterranean sea therefore the Saharan dust particles are always enriched with sea salt elements.

4.6. Geographical Locations of Potential Source Regions

As discussed above, for the past two decades, receptor models have been used successfully in the identification of particulate sources and the determination of mass contribution of air pollutants in urban (e.g. Alpert and Hopke, 1980; 1981; Morandi et al., 1991) and rural scales (e.g. Tuncel et al., 1985; Rahn and Lowenthal, 1984; 1985; Ashbaugh et al., 1984) extensively. However, the normal receptor models can not identify geographical locations

of sources of pollutants. To address the problem, new source-receptor oriented methods which are able to identify potential source regions have been developed (Malm et al., 1986; Zeng and Hopke, 1989; Vossler et al., 1989; Cheng et al., 1991; Stohl and Wotawa, 1995).

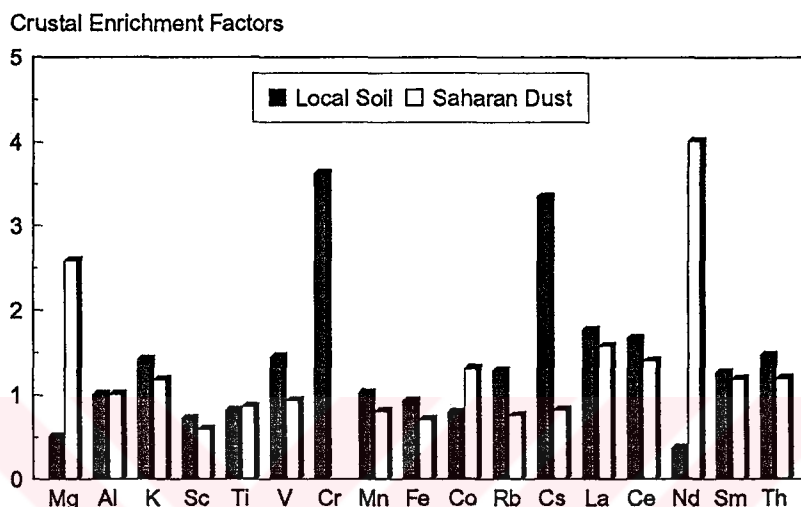


Figure 4.53. Crustal Enrichment Factors of Local soil and Saharan Dust Compositions

In these receptor oriented methods, the back trajectory information together with air quality measurements are used to identify potential source areas of air pollutants and to determine their respective contribution at receptor sites. In this work, the Potential Source Contribution Function (PSCF) technique which was first used by Malm et al., (1986) and Zeng and Hopke (1989) was used to identify source regions of pollutants in the eastern Mediterranean aerosol.

4.6.1. Potential Source Contribution Function (PSCF)

The 4-day back-trajectories calculated as discussed in previous sections were segmented 3 h time intervals and the coordinates of each trajectory segment endpoints were determined.

Twenty-seven subregions were selected within the distance covered by 4-day trajectories. Boundaries of the selected subregions were matched with the EMEP grid system. The EMEP network consists of 150 km x 150 km grids which covers whole Europe but not important potential source regions for the eastern Mediterranean, such as Turkey, Middle East and North Africa. To be able to include these subregions and match them to EMEP grid system, the EMEP grid system was extended to cover these areas. The EMEP grids in each country in the study region were combined to form a subregion. In this way, each of the countries in Europe, Middle East and North Africa are selected to be individual subregions. However, since several countries in Europe are too small to be individual subregions, countries such as Belgium, Holland etc. were combined to make one subregion. The subregions used in the study are given in Figure 4.54. Since each of the countries in the study area is defined as one subregion, the use of EMEP grid system was not necessary. However, it was convenient to use the EMEP grid system, because it is easy to determine the coordinates of the corners of EMEP grids, thus it was easy to define the coordinates of each subregion when they are formed by combining several grids with known coordinates.

To calculate the potential source contribution function, PSCF, first the residence time of air masses in each of the subregions, $P(A_j)$ was calculated by dividing the number of trajectory segments in each of the defined subregions (n_j) to the total number of trajectory segments, N . Then, the trajectories which correspond to high concentrations of a specific parameter were selected and number of segments of only these polluted trajectories in each of the subregions (m_j) were counted. Once n_j and m_j were determined the PSCF were calculated by simply dividing m_j to n_j . Since n_j is the residence time of air parcels in subregion j and m_j is the residence time of polluted air parcels in the same subregion j , the ratio of the two is a measure of the fraction of trajectory segments in the subregion which results in high concentration of pollutants in the station. Hence, PSCF can be used to

identify source regions that have a potential to contribute on observed concentrations of measured parameters in the eastern Mediterranean atmosphere.

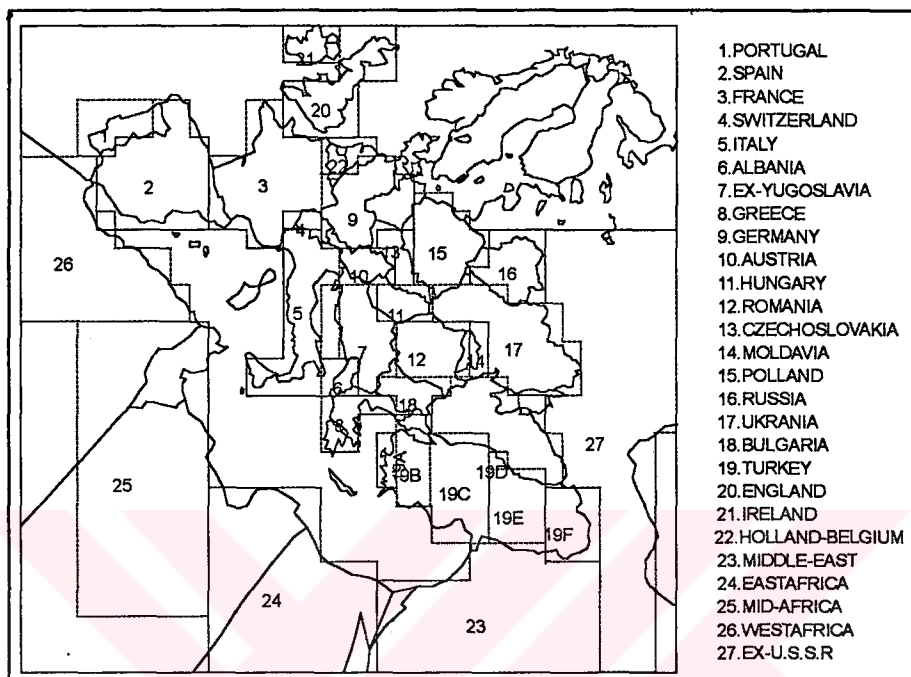


Figure 4.54. The subregions used in the source apportionment of aerosol data

Although this is a powerful technique to determine potential source regions, one has to be aware of its weaknesses as well. The reliability of estimates in this technique depends on the number of trajectory segments in each subregion. In general since approximately 600 samples (and hence trajectories) were included in this study, statistics was not a drawback for most of the subregions. But, since the frequency of air mass transport is scarce from east sector, reliability of contribution estimates in eastern subregions was not as high as the estimates for subregions in other wind sectors. This limitation of small number of trajectory segments in a given subregion was minimized by a weighting suggested by Zeng and Hopke (1989). In the suggested procedure, a weighting factor of 0.5 was used if there is only one segment in a given subregion, calculated PSCF was

multiplied by 0.68 and 0.85 if there are two and three trajectory segments, respectively. If the number of segments is larger than four, then PSCF was multiplied by 1.0.

In this study, PSCF's were calculated on a monthly basis for the two years of this study for the defined subregions for 27 species which are detected in sufficient number of samples. Polluted trajectories were tentatively defined as the trajectories corresponding to elemental concentrations one standard deviation higher than annual average concentrations of elements. Calculated PSCF values of crustal elements Al, Fe, Nd, Ca, and anthropogenic elements As, Se, Sb, Pb, NO_3^- and nss-SO_4^{2-} are given in Figures 4.55 - 4.57.

As depicted in Figure 4.55 for Al, Fe and Ca, PSCF's of crustal elements are higher in the central and eastern parts of the North Africa and eastern parts of Turkey. Obviously arid regions in North Africa and eastern Turkey are the main sources of dust in the Antalya area. The results of factor analysis exercise had pointed out the presence of two separate soil components which can be distinguished by elements such as Cr, Mg, Cs and Nd. The PSCF for Nd is larger than 0.6 in the central and eastern parts of the north Africa and substantially smaller in every other subregion. This confirms that the Nd is a good tracer for the Saharan dust and demonstrate the reliability of PSCF approach in identifying source regions.

Contributions of subregions in the western parts of the north Africa on crustal elements in the Antalya station are low compared to contribution subregions in the central and eastern parts of the north Africa. This suggest a distinctly different source regions for the Saharan Dust in the eastern and western parts of the Mediterranean. Previous research on the impact of the Saharan dust on the Mediterranean basin have shown that western Mediterranean basin are effected by the dust originating in central and western parts of the north Africa, such as Algeria and composition of dust in

different parts of the north Africa may be different (Bergametti et al., 1989; Loye-Pilot and Morelli, 1988). Since the backtrajectories were not extended till to the western part of the Sahara, the PSCF exercise performed in this study showed that, the eastern Mediterranean basin is not affected by the dust originating from western parts of the Sahara, but rather affected by the dust originating from eastern parts of the north Africa. If the chemical composition of dust from different parts of the north Africa are different, then chemical composition of the Saharan dust intercepted at the western and the eastern parts of the Mediterranean may be different. Unfortunately, studies on the chemical composition of Saharan dust are scarce and this question can be addressed only when such data become available.

Since the source regions of crustal and marine elements are more or less known already, identification of source regions of pollution derived elements by the help of PSCF analysis are much more important. As shown in the Figure 4.56, anthropogenic elements As, Se, Sb and Pb usually originates from the surrounding countries and Balkan countries which are fairly close to the region. This general conclusion is in good agreement with the results of modeling work performed by the EMEP East Synthesizing center for the transport of sulfur, nitrogen species and trace elements to the Mediterranean region (UNEP, 1994). In EMEP study, it was concluded that 75% of the pollutants deposited in the Mediterranean basin originate from countries surrounding the basin. Although the approach used in this work did not reveal percentage contribution it clearly demonstrated that countries close to the eastern Mediterranean are main sources of pollutants observed in SW Turkey.

The PSCF values of As is plotted in Figure 4.56. Among the all pollutant derived elements only As (and to a certain degree for Se) high PSCF values (>0.61) were calculated in the former USSR (include Kazakhstan, Uzbekistan, Russia), Yugoslavia and in the eastern Turkey besides the European sources. This result is in good agreement with the

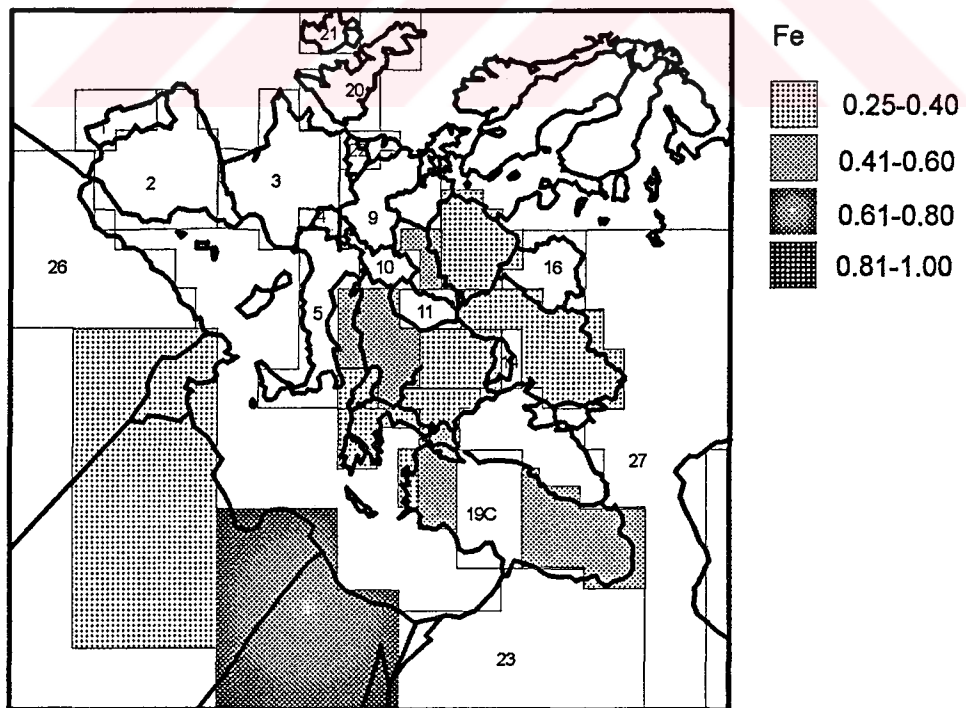
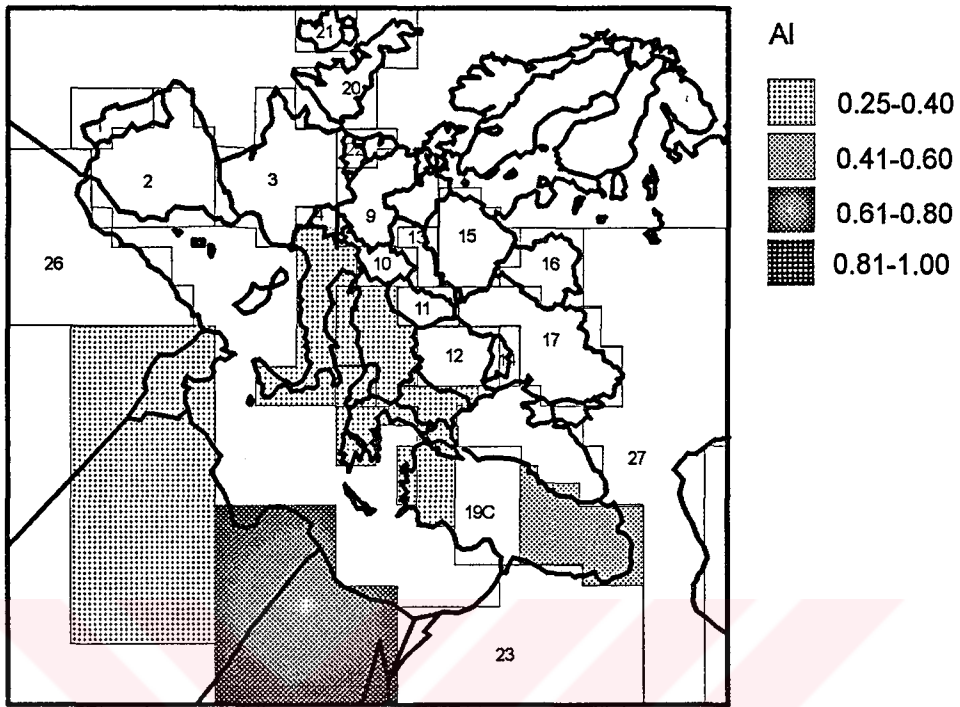


Figure 4.55 The Potential Source Contribution Function of Al, Fe, Nd and Ca

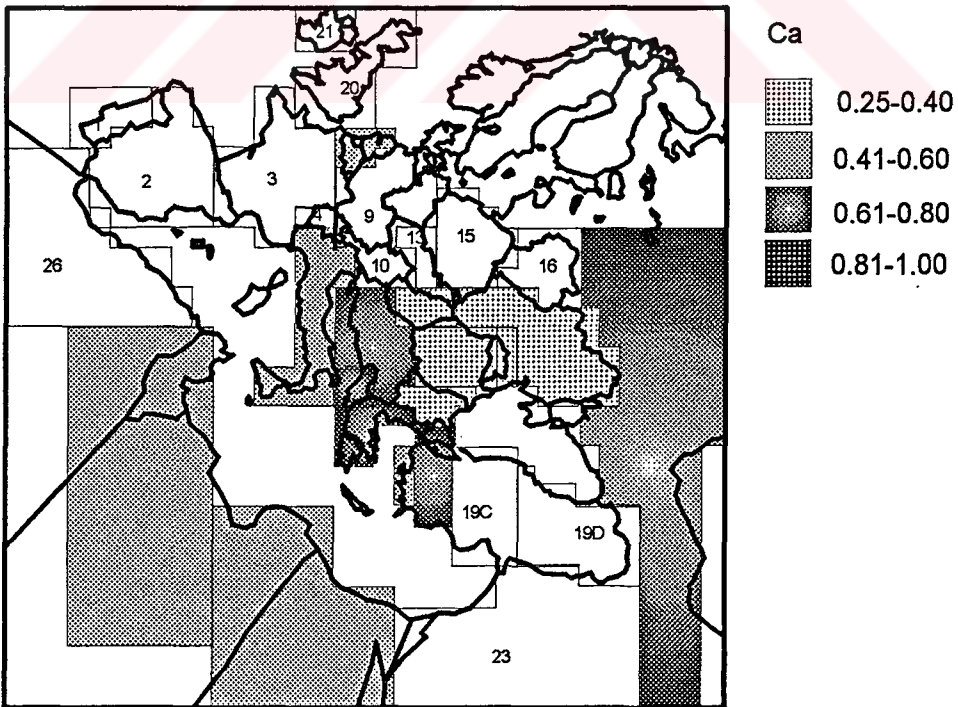
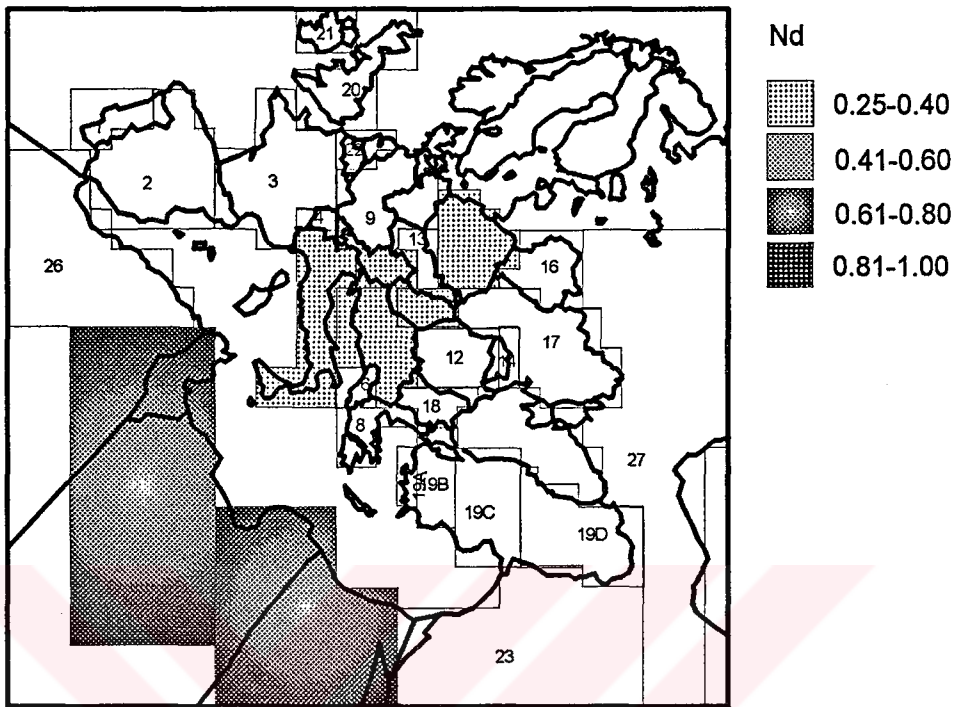


Figure 4.55 Cont 'd

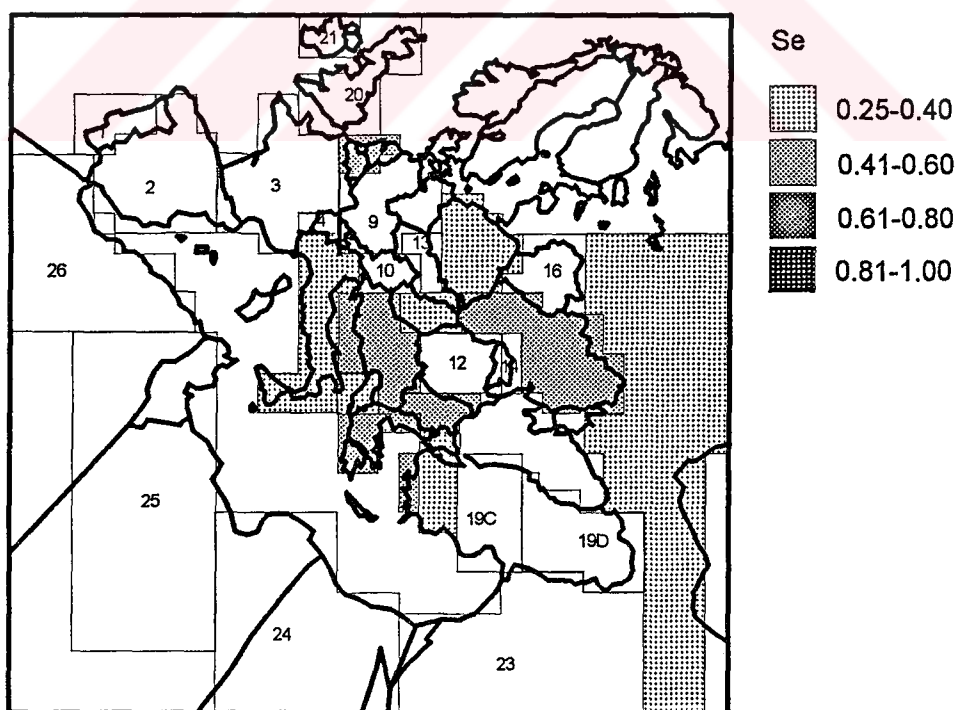
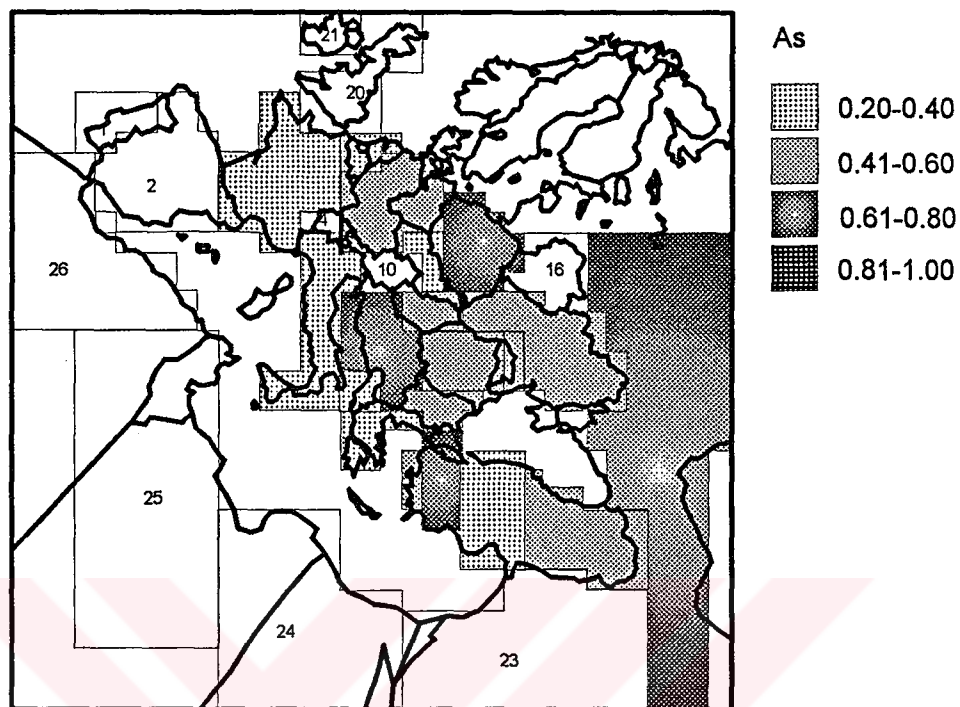


Figure 4.56 The Potential Source Contribution Function of As, Se, Sb and Pb

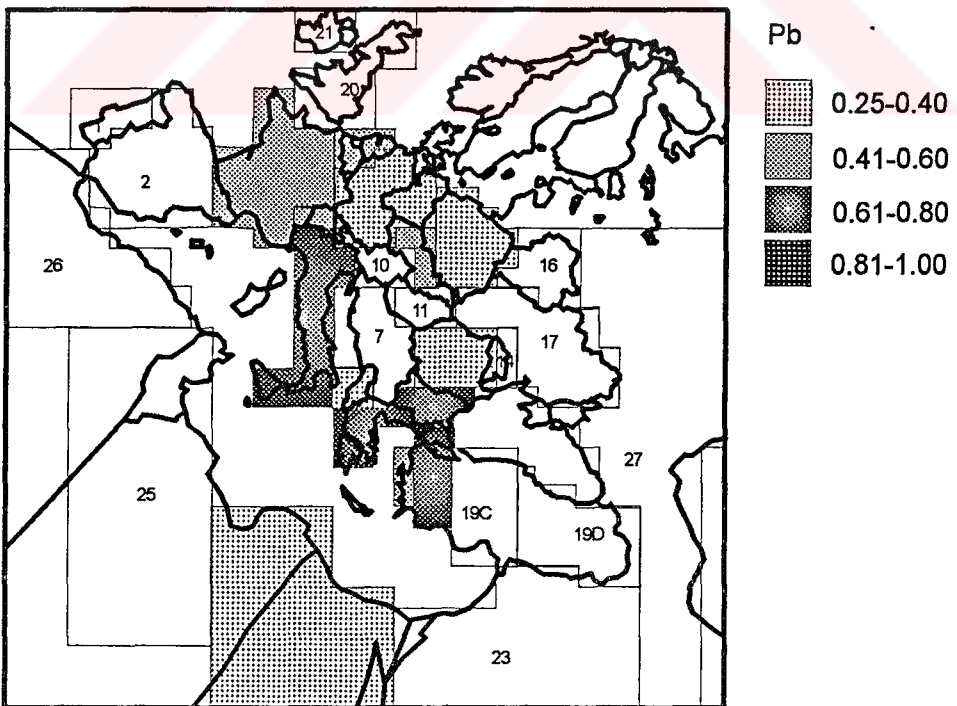
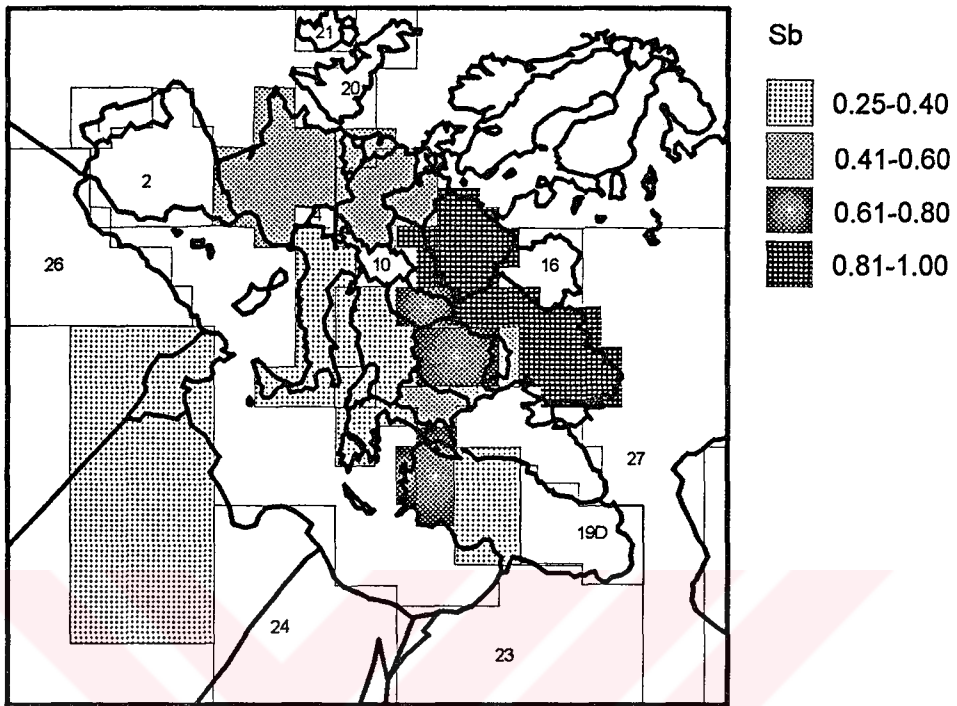


Figure 4.56 Cont 'd

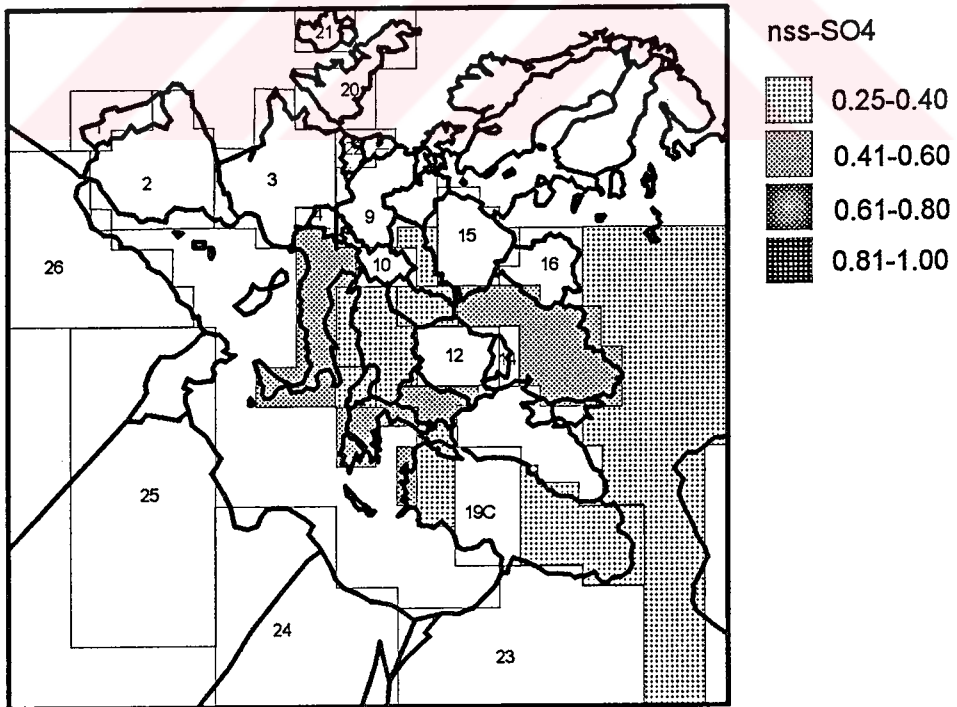
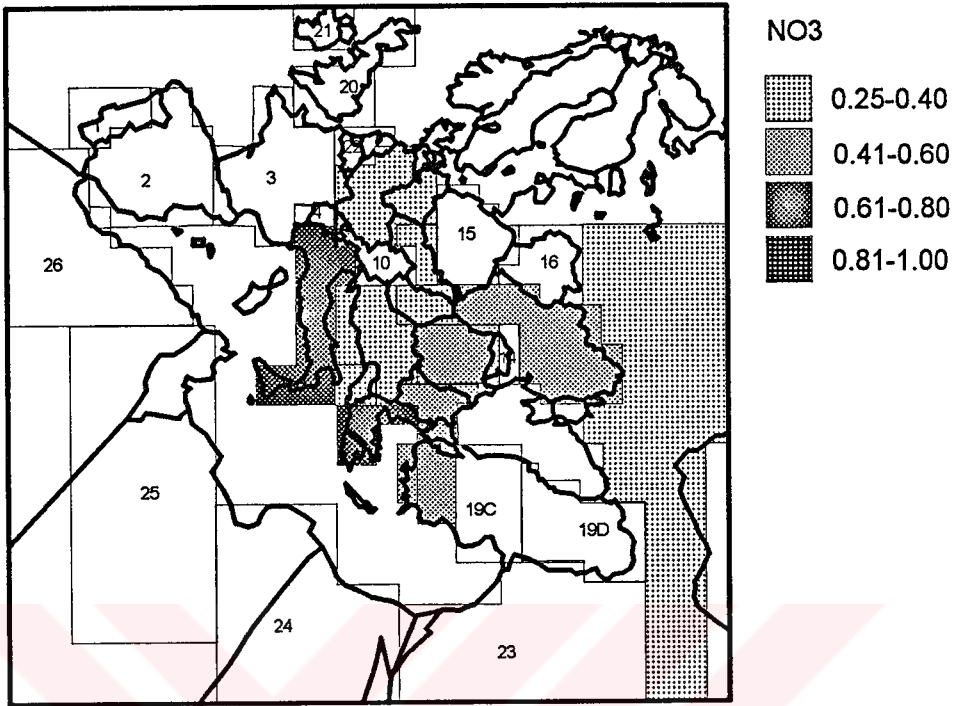


Figure 4.57 The Potential Source Contribution Function of NO₃ and nss-SO₄

EMEP study (UNEP, 1994). In the EMEP study, Yugoslavia has been stated the biggest As emitter among the Mediterranean countries and proposed that As pollution from Yugoslavia together with Bulgaria and Turkey spreads over central and eastern Mediterranean. In our calculations, high potential contribution probability for As were found at the former USSR countries, the uncontrolled emissions in these countries indicate these regions as a high probable source areas. An examples of backtrajectories corresponding to high As concentration days are depicted in Figure 4.58. However, although the former USSR region seems potential source region of As from the PSCF analysis, as the frequency of air mass transport from east to west is minimal in general, the effect of As emissions from the former USSR countries to the total burden of As in the atmosphere can be negligible.

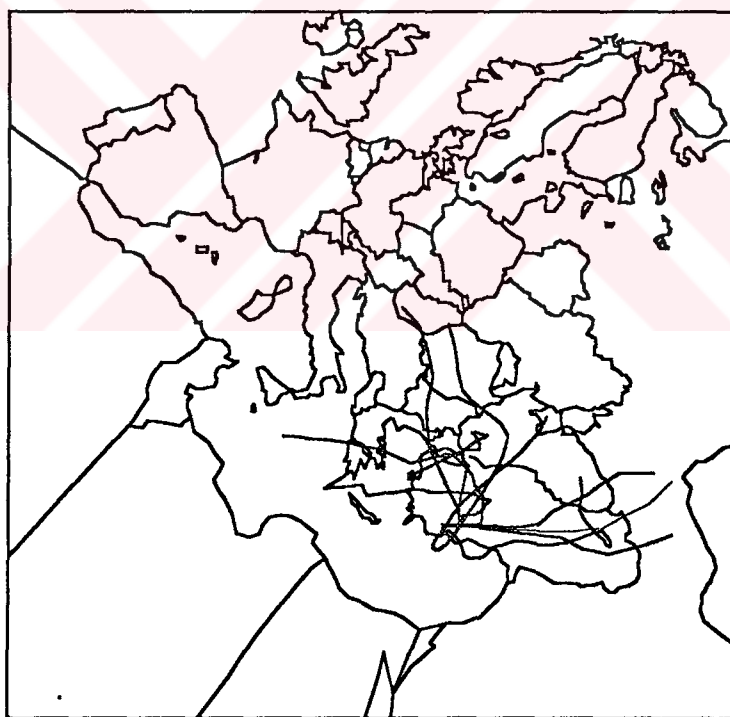


Figure 4.58. Examples of backtrajectories corresponding to high As concentration days

The PSCF of nss-SO_4 and NO_3 are given in Figure 4.57. The figures reflect that the potential contribution areas of these acid precursors are basically industrialized western Europe and the former USSR countries on the north, and east. These results are consistent with the distribution of emissions of SO_2 and NO_x (UNEP, 1994). The Ukraine, Italy, Greece and Bulgaria has the highest PSCF values for nss-SO_4 , and NO_3 . The former USSR countries has high potential source probability value.

As a conclusion the PSCF analysis show that there two principal components in the eastern Mediterranean. The main source regions of crustal elements is western Turkey and middle and eastern part of the north Africa whereas the anthropogenic components usually originates from the western Europe and former USSR.

The PSCF exercise described in this section have demonstrated at least two important points about the source regions of aerosols affecting eastern Mediterranean atmosphere. (1) The source regions and chemical compositions of soil derived elements in the north Africa affecting eastern and western Mediterranean basins are different. (2) Countries which surround the Mediterranean basin and Balkan countries are the most important source areas for the pollution derived aerosols in the eastern Mediterranean. Both of these conclusions imply that, distance rather than source strength is the determining factor for the impact of source regions on the chemical composition of aerosols in the eastern Mediterranean atmosphere. Based on this it can be concluded that, the anthropogenic aerosols in the eastern and western Mediterranean basins have different source regions. Aerosols in the western Mediterranean originate primarily from western European countries, whereas anthropogenic aerosols in the eastern Mediterranean atmosphere originate from eastern European countries, Balkan countries, Turkey and former USSR countries lying to the north of the region.

4.7. The Temporal Variability of Scavenging Ratios over the Eastern Mediterranean Basin

Scavenging ratio (SR) is defined as the ratio of the average concentration of a species in precipitation to the average concentration in air. Scavenging ratio's have been frequently used to estimate wet deposition fluxes on marine locations when actual wet deposition data are absent (Duce et al., 1983; 1991; Arimoto et al., 1985; Uematsu et al., 1985). This aspect is particularly important, since aerosol studies are more abundant and more complete than studies on wet deposition.

There are many factors including particle size distribution and solubilities of elements (Buat-Menard and Duce, 1986; Jaarezo and Colin, 1988; Eder and Dennis, 1990), precipitation rates and amounts (Scott, 1981; Savoie et al., 1987), air mass trajectories (Jaffrezo et al., 1990) and interactions of gas-phase pollutants between particles (Harrison and Pio, 1983; Wolff et al., 1987) that influence the magnitude and variability of SR's. However, it is important to bear in mind the limitations of precipitation scavenging approach for calculation of flux. Scavenging ratio implies that the ambient air concentrations measured on the ground level are the same as cloud level. This may be a reasonable assumption in a well mixed air mass, but not under all meteorological conditions. Since average SR may vary significantly from one geographical region to another, it is crucial to determine the SRs calculated from a multi-year data set on aerosol and precipitation composition to explore the temporal variability of SRs over the eastern Mediterranean.

As part of the ongoing MEDPOL program, we have also collected precipitation samples at the same time interval with aerosol sampling at the same station. Precipitation was collected in two types of samplers. The wet only collector used to collect precipitation for metal analysis is manufactured by the Karlbe Co. The second sampler, ANDERSEN 'Acid Precipitation

sampler' was used for ion determination. The ions Cl^- , SO_4^{2-} , and NO_3^- determined by IC and NH_4^+ by colorimetry. The trace metals and major cations determined with Atomic Absorption Spectrometry. The details of the precipitation sampling program has already been presented elsewhere (Al-Momani, 1995). As the first time, the simultaneous measurements of aerosol and precipitation for almost 2-year period enabled us to determine the temporal variability of SRs at the eastern Mediterranean. During the sampling period 2/3/1992 to 31/12/1993, a total of 82 matched aerosol and precipitation samples were collected.

The following formula was used to calculate scavenging ratios of elements (SR):

$$SR = \left(\frac{C_p}{C_a} \right) \rho_{air}$$

where C_p is the concentration of the species in precipitation (ppb), C_a is the concentration of the species in the aerosol ($\mu\text{g} \cdot \text{m}^{-3}$) and ρ_{air} is the density of air ($1.170 \text{ kg} \cdot \text{m}^{-3}$).

Annual SRs were calculated from the volume-weighted mean concentration calculated from all precipitation samples collected during a given period and the average concentration from all aerosol samples collected during the same period (2/3/1992 to 31/12/1993). The use of almost 2 years of data eliminated the differential weighting of the annual SRs by seasonal variability.

The annual average SRs are summarized in Table 4.17 together with the average concentrations in aerosols and the volume-weighted mean concentrations in precipitation.

The results of annual SRs indicate significant variations from one constituent to another. Although there are some variations within the groups, in general the order of SRs is seasalt elements > crustal elements >

Table 4.17. Summary of annual average aerosol concentrations and precipitation composition and scavenging ratios

Variable	Aerosol mean \pm Std.dev (ng·m ⁻³)	Rainwater vol.weig.mean ^c (μ g·L)	Scavenging Ratio
Crustal Elements			
Al	542 \pm 703	513	1110
Ca	2083 \pm 1894	2492	1400
Sc	0.11 \pm 0.15	0.0215	229
V	2.56 \pm 2.19	0.6177	282
Fe	387 \pm 475	431	1300
Co	0.24 \pm 0.35	0.414	2020
Cs	0.094 \pm 0.075	0.0181	225
La	0.35 \pm 0.38	0.1494	500
Ce	0.67 \pm 0.99	0.287	500
Seasalt Elements			
Na	1240 \pm 1742	12851	12125
Cl	2000 \pm 3377	20762	12145
Br	18.23 \pm 22.16	10.98	705
Mg	365 \pm 335	1862	5970
K	365 \pm 425	988	3167
Anthropogenic Elements			
Cr	3.75 \pm 3.07	6.48	2020
Zn	11 \pm 10	24.04	2552
Se	0.29 \pm 0.22	0.198	802
Sb	0.34 \pm 0.20	0.189	650
Pb	23.9 \pm 21.8	8.69	434
Secondary Pollutants			
NO ₃ ⁻	1180 \pm 840	5472	5425
nss-SO ₄ ⁼	4770 \pm 3850	4908	1200
NH ₄ ⁺	1400 \pm 1100	1125	940

anthropogenic elements. For seasalt elements, Na and Cl very high SRs have been calculated. Calculated SRs for Na and Cl is around 12000 which is much higher than the values (range from 500 to 2000) calculated over the open ocean (Arimoto et al., 1985; Basrrie, 1985; Savoie et al., 1987; Galloway et al., 1993). Because of the non linear temporal variability between deposition fluxes and atmospheric aerosols due to the low precipitation frequency and different cloud properties results high scavenging ratios in the eastern Mediterranean basin. As was indicated in GESAMP (1990) similar high scavenging ratios (range from 3000 to 5000) were previously observed in western Mediterranean basin by Bergametti (1987). For Mg and K the calculated SRs are 5970 and 3167, respectively. Since crustal material contribute significant amount of Mg and K in addition to seasalt, calculated SRs are less than major seasalt elements Na and Cl. Among the marine elements, Br is the one with the lowest SR which is 705. Calculated low SR for Br indicates the presence of anthropogenic local sources most probably vehicular emissions. The presence of such sources would result in higher concentration on the surface than at cloud level. Consequently, the lower SR for Br are probably due to the presence of local Br sources.

Based on the calculated SRs values, crustal elements can be divided into Al, Ca, Fe group and Sc, V, Cs, La and Ce group. The SR values for the Al, Ca, Fe group range from 1100 to 1400 with a mean of 1270 ± 147 , while the other group's ratios vary from 225 to 500 with a mean of 347 ± 141 . The low ratios for Sc, V, Cs, La and Ce may be due to presence of local sources. From the previous analysis, correlation and factor analysis, the Sc, V, Cs, La and Ce was primarily of crustal origin and strongly associated with other crustal elements. Thus, the scavenging ratios for these and other crustal elements would be expected to be similar. However, the ratios for Al, Ca and Fe appear to be much higher than for Sc, V, Cs, La and Ce. There are two potential explanations for this discrepancy. The first is that, the differences reflect the uncertainty in the SR for the crustal constituents. The

second is that these elements measured in precipitation only in the soluble phase while Al, Ca and Fe are measured in soluble and insoluble phases. Ignoring insoluble fraction might artificially reduce the concentrations in the precipitation hence low SRs calculated.

According to the calculated SRs for anthropogenic elements, there are two groups, Cr-Zn group and Se-Sb-Pb group. While the SRs of the Se-Sb-Pb group vary from 434 to 802 with a mean of 628 ± 184 , the SRs for Cr and Zn are calculated a factor of 4 higher, 2020 and 2552, respectively. The ratios of Cr and Zn are considerable high when compared with other studies performed both at urban (Jaffrezo et al., 1990) and regional regions (Wolff et al., 1987; GESAMP 1990). If all those anthropogenic elements are originated at distant locations, during long transit times, particles in the air mass would be an aged, internally mixed aerosol. Consequently, the particle size distributions and scavenging efficiencies of these species should be similar. If this is the case, then higher Cr and Zn scavenging ratios would likely be due to different vertical concentration profiles, scavenging mechanisms or scavenging efficiencies.

The SRs of secondary pollutants ranges from 940 for NH_4^+ to 5425 for NO_3^- . The SR for nss-SO_4^{2-} is calculated as 1200. As proposed by Wolff (1987) previously, significantly larger scavenging ratio of NO_3^- compared with pollutant elements and sulfate is most probably due to the incorporation of gaseous HNO_3 and coarse particulate NO_3^- which were three times more abundant than fine NO_3^- into the droplets. It has been known after Savoie and Prospero (1982) that the reactions between HNO_3 and sea salt formed coarse NO_3^- . And also it should be kept in mind that the concentration of seasalt aerosol decreases rapidly with altitude. For species like NO_3^- , which are associated primarily with seasalt aerosol in the near surface, the decrease in seasalt with increasing altitude can alter the partitioning between the vapor and particulate phases (Hastie et al., 1990). In this respect, using

ground level nitrate concentrations together with nitrate amount in the precipitation might have significant influence on SRs.

The SR for nss-SO_4^- is 1200 which is considerably higher than the ratios for the trace elements. As explained in the section 4.5.1, factor analysis indicated that nss-SO_4^- was strongly associated with Se and both of them originated from high temperature combustion processes at distant places. Therefore the higher SR of nss-SO_4^- might probably due to in-cloud SO_2 oxidation. This suggestion is also supported by the observation that the $\text{NH}_4^+/\text{SO}_4^-$ ratio (0.21) is lower in precipitation than in the particulate phase (0.30).

In order to illustrate the effects of variations of precipitation and aerosol composition on the SR, monthly average SR were calculated and results are plotted along with the monthly average concentrations in aerosols and precipitation for the species Al, Ca, Fe, Mg, Cl, Na, Pb, Sb, Zn, nss-SO_4^- , NH_4^+ and NO_3^- in Figure 4.59-4.62.

As shown in the figures the aerosol data show more pronounced seasonal signals relative to precipitation hence SRs vary significantly from month to month. There are so many reasons of this temporal variation discrepancy among the aerosols and precipitation like vertical concentration differences, additional surface sources, influences of precipitation amount on concentration, etc.

Monthly SRs for sea salt elements Na and Cl change by a factor of 4. Due to the vertical turbulence in the lower troposphere during strong storm activities especially on winter season cause increase in sea salt concentrations in the precipitation relative to aerosols, therefore the winter SRs for seasalt elements is higher than summer months.

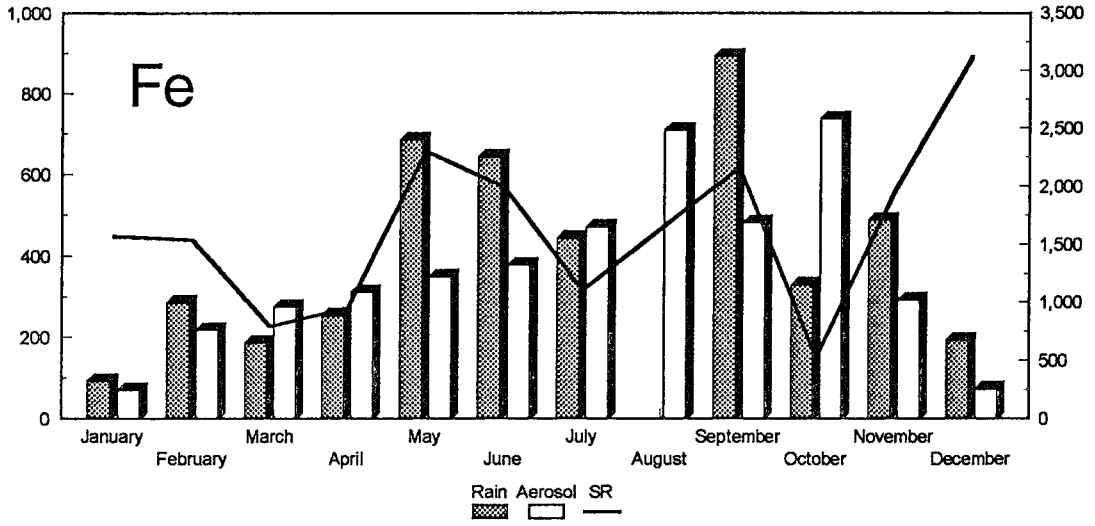
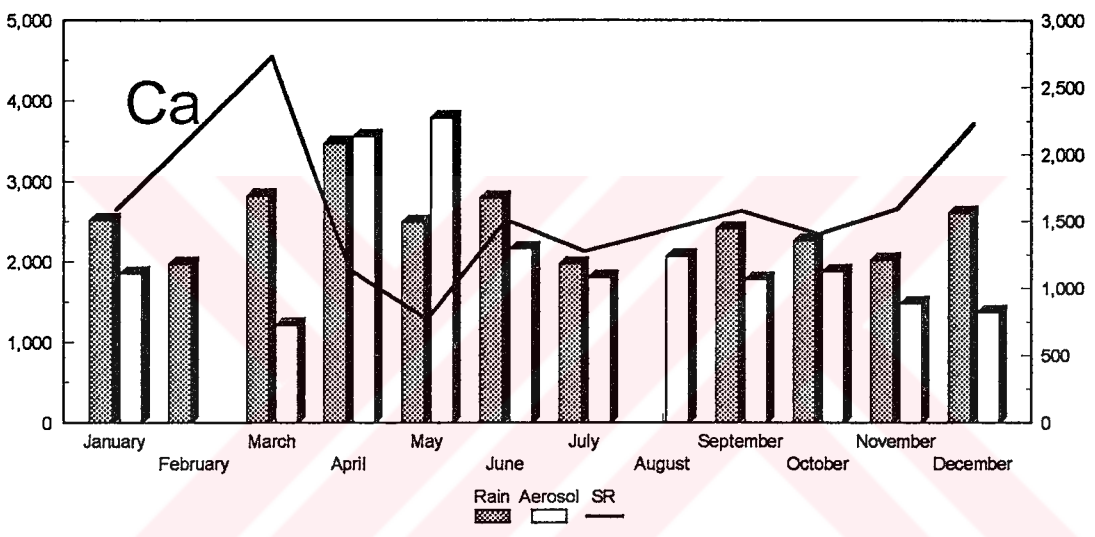
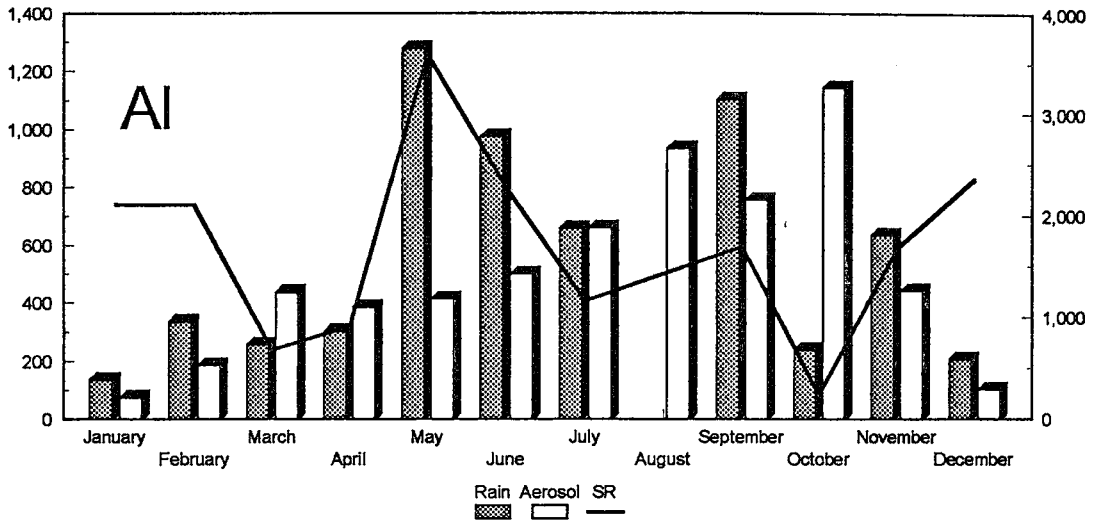


Figure 4.59. The monthly SRs for Al, Ca and Fe and the arithmetic mean of aerosol composition and volume weighted mean precipitation composition at Antalya Station

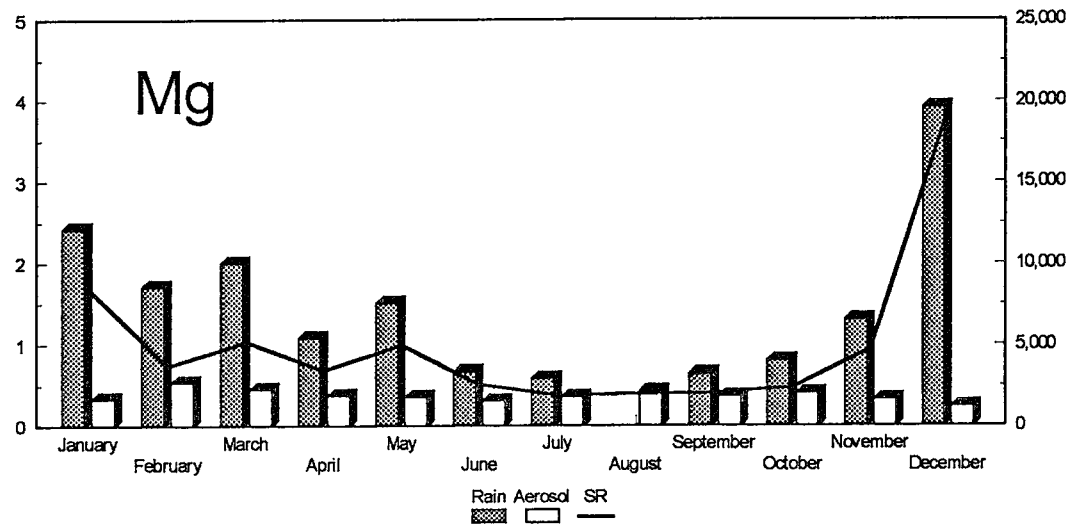
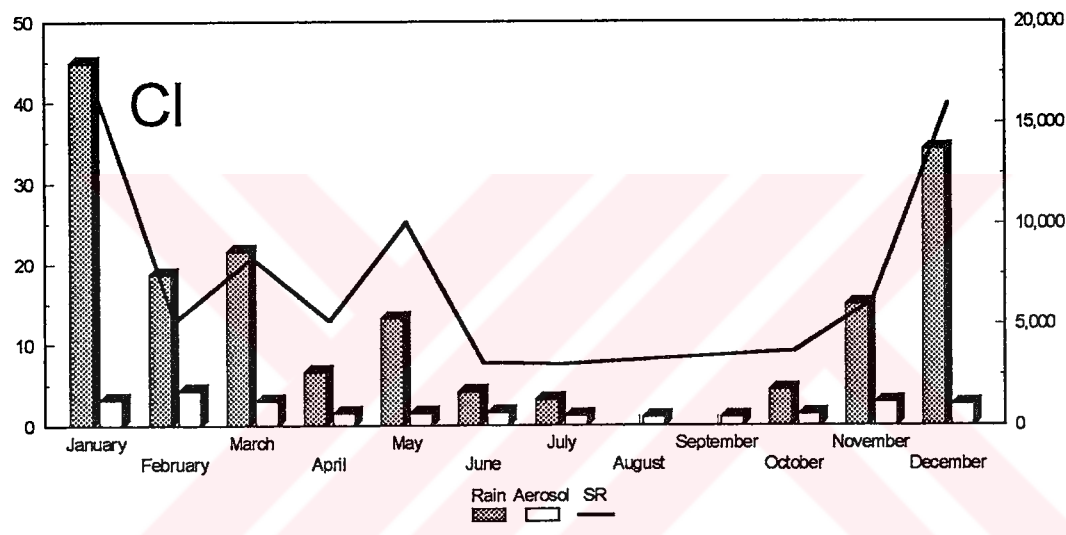
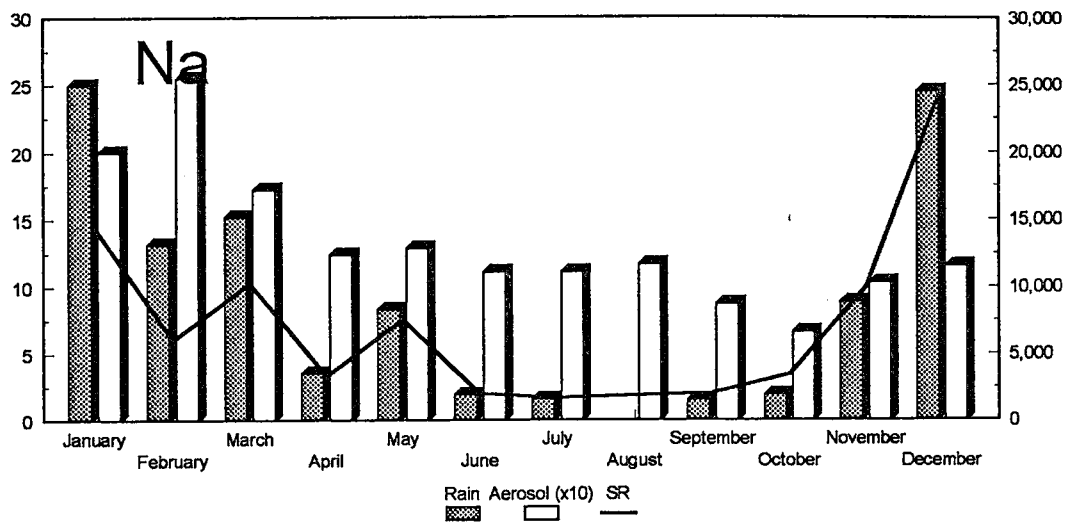


Figure 4.60. The monthly SRs for Na, Cl and Mg and the arithmetic mean of aerosol composition and volume weighted mean precipitation composition at Antalya Station

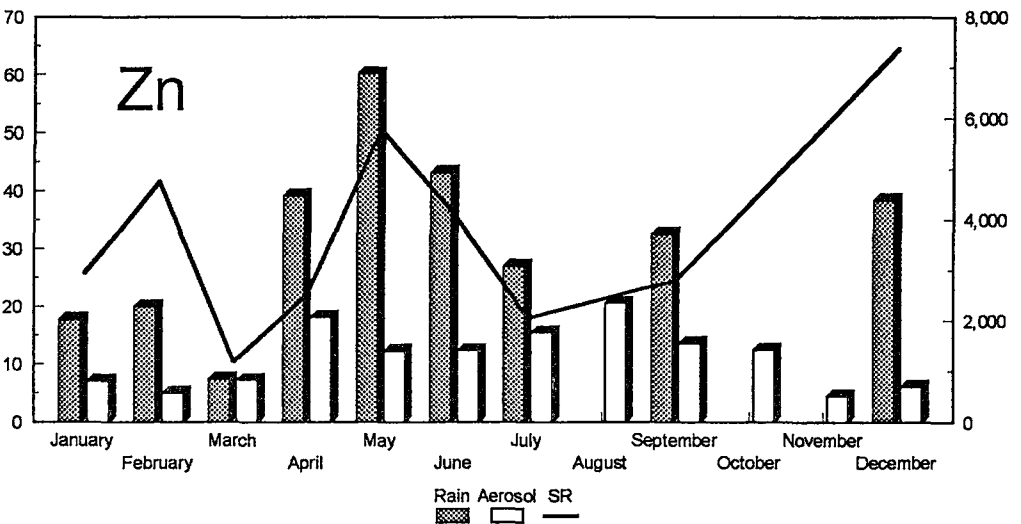
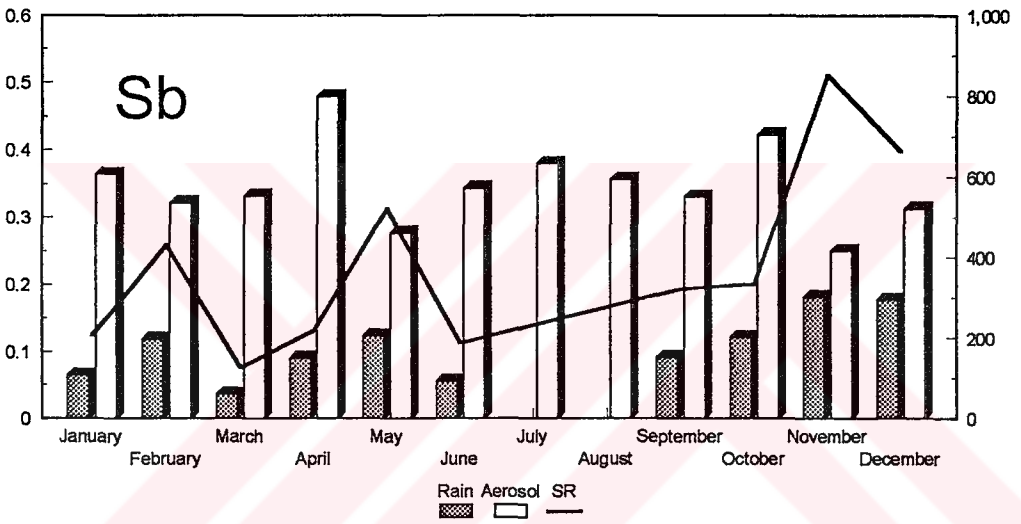
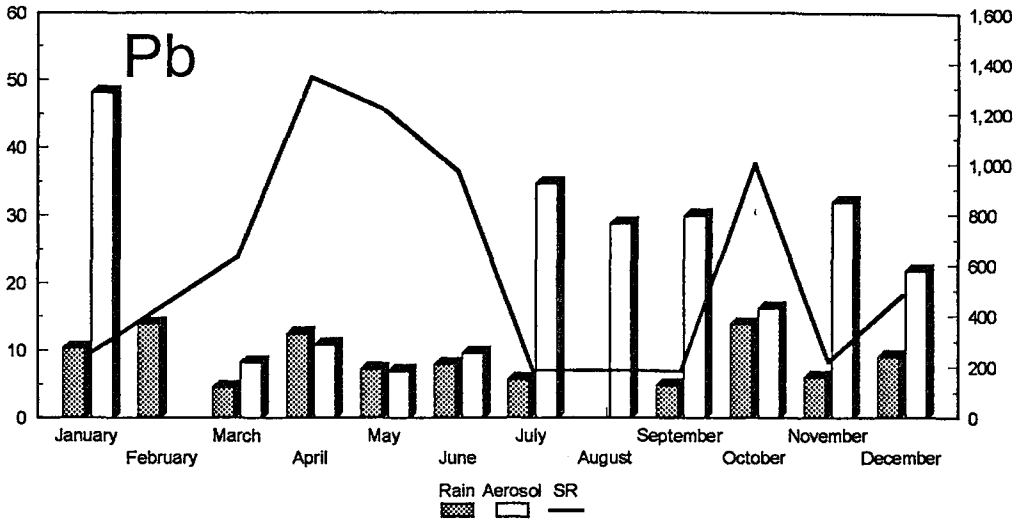


Figure 4.61. The monthly SRs for Pb, Sb and Zn and the arithmetic mean of aerosol composition and volume weighted mean precipitation composition at Antalya Station

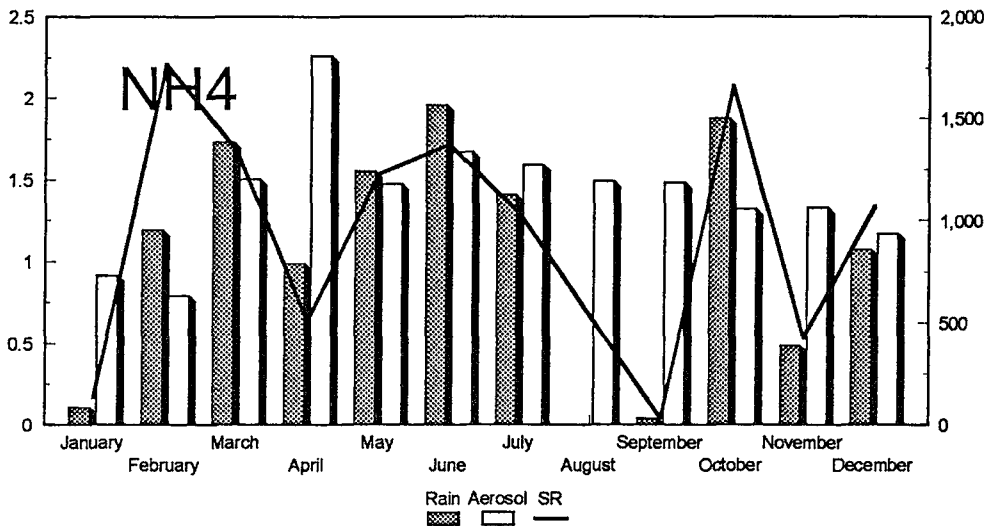
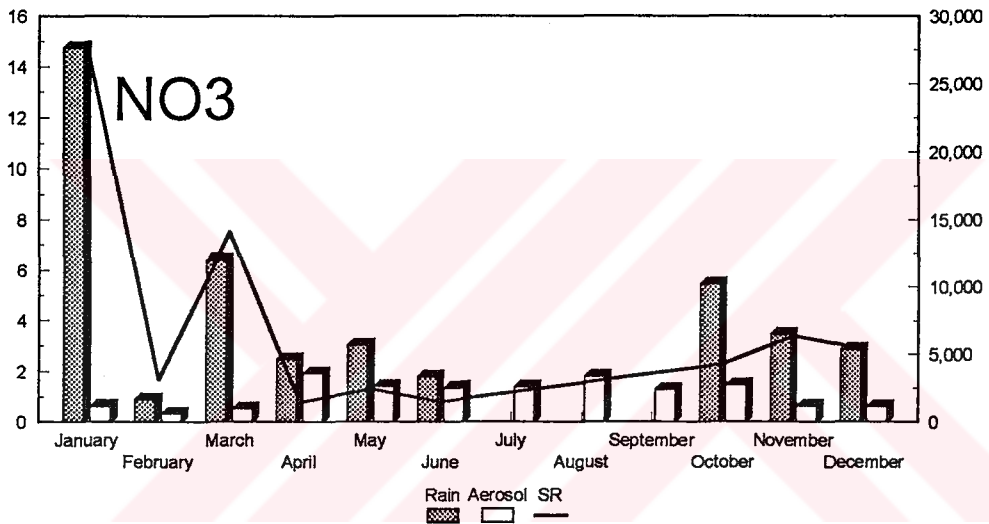
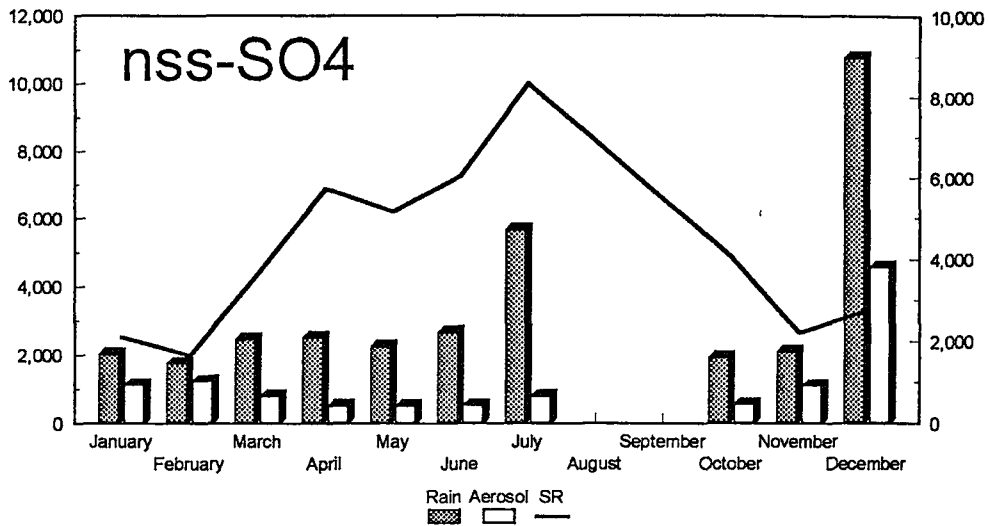


Figure 4.62. The monthly SRs for nss-SO₄, NO₃ and NH₄ and the arithmetic mean of aerosol composition and volume weighted mean precipitation composition at Antalya Station

More than a factor of 7 difference were observed on monthly SRs of crustal elements namely Al and Fe. The crustal element concentrations increase during summer months due to resuspension of local soil since the summer is the season of minimum precipitation frequency. Therefore, there is a substantial variability in the SRs of the crustal elements.

In the case of anthropogenic elements Pb, Sb and Zn, there is significant variability in the SRs. Since the monthly trend of pollution derived aerosol concentrations are not matched by seasonal trends in corresponding precipitation composition as clearly shown in the Figure 4.61, high variable SRs were calculated for these species.

For NO_3^- and nss-SO_4^{2-} , except one extreme storm, there is not obvious seasonal behavior of the SRs. The nitrate and sulfate concentrations in the aerosol and precipitation are varying in a similar manner, therefore the value of SR is relatively constant for these species.

As a result it has been concluded that, as the averaging time and hence the amount of data being averaged are reduced, the variability of the SR increases. Since almost two years precipitation and aerosol results used in this study, the calculated scavenging ratios by using the volume weighted mean precipitation and average aerosol contributions will be quite representative for the eastern Mediterranean basin.

CHAPTER 5

CONCLUSION

Elemental concentrations of major ions and trace elements detected by INAA, AAS and IC in the Eastern Mediterranean atmosphere for the years 1992 and 1993 were discussed in this study.

To be able to demonstrate the possible existence of differences in the concentrations of the elements in the atmosphere over the eastern and western parts of the Mediterranean and to determine the general feature of the eastern Mediterranean aerosols, data for aerosols from a number of coastal sea sites are compared with the results of the present study. Concentrations of crustal elements and pollution derived elements, measured in the Antalya station were found to be lower than all values reported for comparable coastal sites in the Mediterranean. Since the observed lower concentrations of crustal elements in this study relative to other eastern Mediterranean studies is explained by the presence of preimpactor on the instrument, the main difference in the composition of atmospheric particulates observed in the eastern basin and the western basin is that particulates from the eastern basin have lower concentrations of anthropogenic elements specifically Zn and Pb.

Concentrations of elements were found to be vary greatly on time scales ranging from days to seasons. In the past studies, the variability of the elemental concentrations in the Mediterranean atmosphere mainly explained by

the seasonal transport patterns, precipitation scavenging and source strengths. In order to understand air mass transport patterns and to explain observed seasonal variations of the measured concentrations, 4-day back trajectories ending at the Antalya station were calculated daily for the years 1992, 1993 and 1995. The classification of trajectories indicates that most frequent air mass movements occur from north, northwest, west and northeast sectors. Although the contribution of south and southwest sectors are small on annual basis, their contribution on the atmospheric concentrations of crustal elements at the eastern Mediterranean are very important. Contrary to expectations, no obvious change of percent contribution of wind sectors from season to season were found. Therefore, it has been concluded that such strong short and long term variability in the concentrations of elements can not be due to the transport patterns.

For the long term variations of the concentrations of marine, crustal and pollution derived elements, it has been found that, the local rain event is the determining factor over the eastern Mediterranean atmosphere. Concentrations of both crustal and marine elements decrease during rain events due to scavenging of particles bearing these elements. It has been calculated that the impact of local rains on seasonal behavior of pollution derived elements were around 30% and the remaining 70% was due to particle removal by rain events encountered during the transport of particles from their respective source regions to the station site.

To get an information about the effect of the variation of the source strengths on sectorial elemental concentrations, samples were grouped with respect to emission areas by the help of back trajectories. With 30% frequency, the north sector has been found the major sector, 26.7% of the time samples originate from west sector and northwest. Only 3.3% of the air mass trajectories originated from east and north-east sectors. The contribution of south and southwest sectors is around 14%. The 26% of the samples have short trajectories and grouped by itself. Comparison of

compositions of different sectors shows that the sea salt elements were significantly higher on south and west sectors. The maximum sectorial concentrations of crustal elements, Al, Sc, Ti, Fe, and rare earth's were observed on east, south and south-west sectors. Since, large amount of desert particles were carried episodically from south and south-west sectors, these sectors were found to be the most important source regions effecting the atmospheric concentrations of the crustal elements at the Antalya site.

Studies performed to identify sources were performed in two levels. First, general source categories were identified by enrichment factors and correlation analysis. Calculation of enrichment factors have revealed four general source groups, namely a crustal source, a marine source, an anthropogenic source and an unknown source which has small but observable contribution on the concentrations of some ultra trace elements. Then, one of the most widely used source apportionment technique, Factor Analysis is applied to elemental data to characterize aerosols with respect to sources and quantify the different sources and their importance for the composition of the aerosols at the monitoring site, Antalya. Principal component factor analysis identifies two crustal components, one marine component, one local pollution component and one distant pollution component. Following to the Factor Analysis, quantitative assessment of identified sources were accomplished by application of Absolute Factor Score (AFS) technique. According to the quantitative analysis of two soil components the most promising marker elements to distinguish Saharan Dust from local soil were found to be Cr, Nd, Mg and Cs as they have significantly different compositions in the local soil and Saharan Dust.

To identify source regions of pollutants in the eastern Mediterranean atmosphere, the Potential Source Contribution Function (PSCF) technique was used. The PSCF analysis show that there two principal components in the eastern Mediterranean. The main source regions of crustal elements is western Turkey and middle and eastern part of the north Africa whereas the

anthropogenic components usually originate from the countries surrounding the basin and former USSR countries which lie to the north of the station..

Annual SRs were calculated for the eastern Mediterranean by using volume-weighted mean concentration of precipitation samples collected during a given period and the average concentration of all aerosol samples collected during the same period. Because of the non linear temporal variability between deposition fluxes and atmospheric aerosols due to the low precipitation frequency and different cloud properties, high scavenging ratios in the eastern Mediterranean basin were found. Although there are some variations for some species within the groups, in general the order of SRs is determined as sea salt elements > crustal elements > anthropogenic elements.

In order to illustrate the effects of variations of precipitation and aerosol composition on the SR, monthly average SR were calculated. Due to the large amount of data set, it has been decided that, the calculated scavenging ratios by using the volume weighted mean precipitation and average aerosol contributions will be quite representative for the eastern Mediterranean basin.

The conclusions of this study concerning the major sources of aerosol material are similar to those reported in many other studies, though the relative importance of the sources change from place to place. Very large data set does allow us to identify the sources and also to attempt to characterize the compositions of the sources by the help of meteorological information. The interactions of meteorological factors with emission source distributions and strengths make the eastern Mediterranean aerosol as a unique character. In this study, most of the effort has been spent to the understanding of these interactions which is very critical for the accurate prediction of atmospheric inputs.

Within the numerous environmental problems, the impact of human-induced chemical perturbations on the atmosphere has received the majority of attention during the last two decades. Over the next 10-20 years, many difficult decisions will have to be made by policy-makers world-wide to deal with atmospheric pollution problems such as acid deposition, increasing greenhouse gas concentrations, stratospheric ozone depletion, increasing tropospheric ozone, direct and indirect climatic response of tropospheric aerosols and anthropogenic sulfate aerosol in particular. In order to give proper policy decisions, the atmospheric science must continue, and strive to increase.



CHAPTER 6

RECOMMENDATIONS FOR FUTURE RESEARCH

The work presented here is the most extensive study of aerosols in terms of both sampling duration and analytical protocol at both eastern and western Mediterranean basins. The aerosol samples were analyzed for a wide range of inorganic species including major ions and approximately 40 elements in order to determine the state of pollution and source regions affecting concentrations of these species in the eastern Mediterranean Basin. On the same sampling site, besides aerosols, dry and wet deposition samples were collected. Therefore it is recommended that, for studying the long range transport of pollutants and their fluxes to the Eastern Mediterranean Basin with all aspects, aerosol data should be coupled with dry and wet deposition data. And to understand interannual variability in the long range transport , the monitoring program should be continued for several years.

In 1994, in addition to dry, wet deposition and aerosol sampling, gas phase analyzers were installed in the station to determine the levels of NO_x , SO_2 , O_3 and gaseous Hg at the sampling site. Gas phase analyzers together with aerosol data will provide valuable information about gas-to-particle conversion process in the eastern Mediterranean basin.

The multi element data set generated in this study enabled us to apply various statistical methods to determine the sources and source

regions of atmospheric particles. To investigate the location of the sources, the trajectory information as well as multi-element data set were used. Therefore, the uncertainty of the used trajectory model is very important for identification of source regions. Instead of using single layer isobaric back trajectories, 3D trajectories will be particularly useful for the identification of the meteorology associated with pollution transport.

Installing size separated samplers like dichotomous sampler or cascade impactors will improve better resolution in the identification of source for the pollution derived elements. In addition to this, concentration data for different size ranges can also be used in the models to estimate dry deposition fluxes of elements to the sea surface.



REFERENCES

_____. (1989). *Standard Methods for the Examination of Water and Wastewater*. (ed. by Clesceri, L.S., Greenberg, A.E., Trussell, R.R.), 17th edition, American Public Health Association, Washington, DC.

Ackerman, S.A. and H. Chung (1992). Radiative Effects of Airborne Dust on Regional Energy Budgets at the Top of the Atmosphere. *Journal of Applied Meteorology*, **31**, 223-233.

Adams, F., Dams, R., Guzman, L., and J.W. Winchester (1977). Background aerosol composition on Chocaltaga Mountain, Bolivia. *Atm. Environ.*, **11**, 629-634.

Adams, F., Espen, P.V., Maenhout, W. (1983). Aerosol Composition at Chacaltaya, Bolivia, as Determined by Size Fractionated Sampling. *Atm. Environ.*, **17**, 1521-1526.

Adams, F.C., Van Crean, M.J., P.J. Van Espen (1980). Enrichment of trace elements in remote aerosols. *Environ. Sci. Technol.*, **14**, 1002-1005.

Al-Momani, I.F. (1995). Long-Range Atmospheric Transport of Pollutants to the Eastern-Mediterranean Basin. Ph.D. Dissertation. METU Department of Environmental Engineering, Ankara, 223.

Al-Momani, I.F., Tuncel, S., Eler, Ü, Örtel, E., Sirin, G., Tuncel, G. (1995). Major ion composition of wet and dry deposition in the eastern Mediterranean basin, *The Science of the Total Environment*, **164**, 75-85.

Alpert, D.J. and P.K. Hopke (1980). A quantitative determination of sources in the Boston urban aerosol. *Atm. Environ.*, **14**, 1137-1146.

Alpert, D.J. and P.K. Hopke (1981). A determination of the sources of airborne particles collected during Regional Air Pollution Study. *Atm. Environ.*, **15**, 675-687.

Alpert, P., U. Neeman and Y. Shay-El (1990). Climatological Analysis of Mediterranean Cyclones Using ECMWF Data. *Tellus*, **42A**, 65-77.

Andrea, M.O. (1983). Soot carbon and excess fine potassium: Long-range transport of combustion derived aerosols. *Science*, **220**, 1148-1151.

Andrea, M.O. (1985). The emission of sulfur to the remote atmosphere in the biogeochemical cycling of sulfur and nitrogen in the remote atmosphere. (Ed. by J.N. Galloway, R.J. Charlson, M.O. Andreas and H. Rodhe) Hingham, MA.

Andrea, M.O., Berrosheim, H., Andreae, T.W., Kritz, M.A., Bates, T.S. and J.T. Merrill (1988). Vertical distribution of dimethyl sulfide, sulfur dioxide, formic acid, aerosol ions and radon over the north-east Pacific Ocean. *Atm. Chem.*, **6**, 149-173.

Arimato, A., R.A. Duce, B.J. Ray, A.D. Hewitt and J. Williams (1987). Trace Elements in the Atmosphere of American Samoa: Concentrations and Deposition to the Tropical South Pacific. *J. Geophys. Res.*, **92**, 8465-8479.

- Arimoto, R., Duce, R.A., Ray, B.J. and C.K. Unni (1985). Atmospheric trace elements at Enewetak Atoll: 2. Transport to the ocean by wet and dry depositions. *J. Geophys. Res.*, **90**, 2391-2408.
- Arnold, M., Seghair, A., Martin, D., Buat-Menard, P., and Chesselet, R. (1982). Géochimie de l'aérosol marin au-dessus de la Méditerranée occidentale. in: Proceedings of Vth Journées d'Etudes sur les Pollutions marines en Méditerranée, Cannes, France, 27-37.
- Ashbaugh, L.L., Myrup, L.O. and R.G. Flacehini (1984). A principal component analysis of sulfur concentrations in the western United States. *Atm. Environ.*, **18.4**, 783-791.
- Aslaner, M. (1973). Geology and Petrography of the Ophiolites in the Iskenderun-Kirikhan Region. Publ. Min. Res. and Explor. Inst. Publ., Ankara, No.50, 71p. & appendices.
- Barrie, L.A. (1985). Scavenging ratios, wet deposition and incloud oxidation: An application to the oxides of sulfur and nitrogen. *J. Geophys. Res.*, **90**, 5789-5799.
- Barrie, L.A. (1989). Arctic air pollution: A case study of continent-to-ocean-to-continent transport. In the long range atmospheric transport of natural and contaminant substances. (Ed. by A.H. Knap, M.S. Kaiser) NATO ASI series, Vol. 297.
- Bassett, M.E. and J.H. Seinfeld. (1983). Atmospheric Equilibrium Model of Sulfate and Nitrate Aerosols- II. Particle Size Analysis. *Atm. Environ.*, **18**, 1163-1170.
- Bergametti, G. (1987). Apports de matière par voie atmosphérique à la Méditerranée occidentale: Aspects géochimiques. Ph.D. Dissertation. Univ. of Paris, 296.
- Bergametti, G., Dutot, A.L., Buat-Menard, P., Losno, R., and Remoudaki, E. (1989). Seasonal variability of the elemental composition of atmospheric aerosol particles over the Northwestern Mediterranean, *Tellus*, **41B**, 353-361.
- Bertrand, J., Baudet, J., and Drochon, A.. (1974). Importance des aérosols naturels en Afrique de l'Ouest, *J. Rech. Atmos.*, **8**, 845-860. As cited in: Coude Gaussen et al., 1987.
- Bewers, M., Duce, R., Jickells, T., Liss, P., Miller, J., Windom, H. and R. Wallast (1988). Land to sea transport of contaminants: Comparison of riverine and atmospheric fluxes. GESAMP Rept. UNEP.
- Biggins, P.D.E. and R.M. Harrison (1979). Atmospheric Chemistry of Automotive Lead. *Environ. Sci. Technol.*, **13**, 558-565.
- Blifford, I.H. and G.O. Meeker (1967). A factor analysis model of large scale pollution. *Atm. Environ.*, **1**, 147-157.
- Borbély-Kiss, I., Bozo, L., Koltay, E., Meszónos, E., Molnar, A., G. Szabo (1991). Elemental composition of aerosol particles under background conditions in Hungary. *Atm., Environ.*, **25A**, 661-668.
- Boutron, C. and C. Lorius (1979). Trace metals in Antarctic snow since 1914. *Nature*, **277**, 1-15.
- Boutron, C. and S. Martin, (1980). Sources of 12 trace metals in Antarctic snow determined by principal component analysis. *J. Geophys. Res.*, **81**, 5631.
- Buat-Menard, P. and M. Arnold (1978). The heavy metal chemistry of atmospheric particulate matter emitted by Mount Etna Volcano. *Geophys. Res. Letts.*, **5**, 245-248.
- Buat-Menard, P. and Duce, R.A. (1986). Precipitation Scavenging of Aerosol Particles Over Remote Marine regions. *Nature*, **321**, 508-509.

Cawse, P.A.. (1987). Trace and major elements in the atmosphere at rural locations in Great Britain, 1972-81, Pollutant Transport and Fate in Ecosystems, Special Publication Number, 6, Blackwell Scientific Publications, Boston, 89-112.

Charlson, R. J., Schwartz, S.E., Hales, J.M., Cess, R.D. Coakley, J.A., Hansen, J.E., and Hofmann, D.J. (1992). Climate Forcing by Anthropogenic Aerosols, *Science*, **255**, 423-430.

Cheng, M.D., Hopke, P.K., Landsberger, S. and L.A. Barrie (1991). Distribution characteristics of trace elements and ionic species of aerosol collected at Canadian High Arctic. *25A*, **12**, 2903-2909.

Chester, R. (1986). The Marine Aerosol. In: The Role of Air-Sea Exchange In Geochemical Cycling, P.Buat-Menard (ed). NATO ASI Series, 185, 443-476. D. Reidel Publishing Company.

Chester, R., M. Nimmo, K.J.T. Murphy and E. Nicolas (1990). Atmospheric Trace Metals Transported to the Western Mediterranean: Data From a Station on Cap Ferrat. In: Water Pollution Research Reports, 20, J.M. Martin and H. Barth (eds.), 597-612. EROS 2000, Second Workshop on the North-West Mediterranean Sea. Commission of the European Communities, Brussels.

Chester, R., M. Nimmo, M. Alarcon, C. Saydam, K.J.T. Murphy, G.S. Sanders and P. Corcoran (1993). Defining the Chemical Character of Aerosols from the Atmosphere of the Mediterranean Sea and Surrounding Region. *Oceanologica Acta*, **16**, 231-246.

Chester, R., Baxter, G.G., Behairy, A.K.A., Connor, K., Cross, D., Elderfield, H., Padgham, R.C. (1977). Soil-sized eolian dusts from the lower troposphere of the Eastern Mediterranean Sea, *Mar. Geol.*, **24**, 201-217.

Chester, R., Griffiths, A.G., and Hirst, J.M. (1979). The Influence of Soil-sized atmospheric Particulates on the Elemental Chemistry of the Deep-sea Sediments of the northeastern Atlantic. *Mar. Geol.*, **32**, 141-154.

Chester, R., Saydam, A.C., and Sharples, E.J. (1981). An approach to the assessment of local trace metal pollution in the Mediterranean marine atmosphere, *Mar. Pollut. Bull.*, **12**, 426-431.

Chester, R., Sharples, E.J., Sanders, G.S. (1984). Saharan dust incursion over the Tyrrhenian Sea, *Atmos. Environ.*, **18**, 929-935.

Chivers, D.C. and Peterson, P.J. (1987). Global cycling of arsenic. In Lead, Mercury, Cadmium and Arsenic in the Environment (T.C. Hutchinson and K.M. Meema, Eds.), Wiley, New York, 279-301.

Cooper, J.A. and J.G. Watson (1980). Receptor oriented methods of air particulate source apportionment. *J. Air Pollut. Control Ass.*, **30**, 1116-1124.

Cornille, P., Maenhaut, W., J.M. Pacyna (1990). Sources and characteristics of the atmospheric aerosol near Damascus, Syria. *Atm., Environ.*, **24A**, **5**, 1083-1093.

Coude-Gaussens, G., Rognon P., Bergametti G., Gomes, L., Strauss, J., Gros, M., and Le Coustumer, M.N. (1987). Saharan dust on Fuerteventura Island (Canaries): Chemical and Mineralogical Characteristics, Air Mass Trajectories, and Probable Sources, *J. Geophys. Res.*, **92**, 9753-9771.

Cunningham, W.C., and Zoller, W.H. (1981). The Chemical Composition of Remote Area Aerosols, *J. Aerosol Sci.*, **12**, No. 4, 367-384.

- Darwin, C. (1846). An account of the fine dust which often falls on vessels in the Atlantic Ocean. *Geol. Soc. London, Q.j.* **2**, 26-30.
- Dams, R., Rahn, K.A., Winchester, J.W. (1972). Evaluation of Filter Materials and Impaction Surfaces for Nondestructive Neutron Activation Analysis of Aerosols, *Anal. Chem.*, **6**, 441-448.
- Dayan, U. (1986). Climatology of Back Trajectories from Israel Based on Synoptic Analysis, *J. Clim. Appl. Meteorol.*, **25**, 591-595.
- Dayan, U., and Miller, J.M. (1989). Meteorological and Climatological Data from Surface and Upper Air Measurements for the Assessment of Atmospheric Transport and Deposition of Pollutants in the Mediterranean Basin: A Review, MAP Technical Report Series No: 30. UNEP, Athens.
- Domergue, J.L.. (1980). Contribution à l'étude de l'aérosol atmosphérique en région intertropicale, doctoral thesis, Univ. of Toulouse, France. As cited in: Coude Gausson et al., 1987.
- Duce, R.A., Hoffman, G.L., Fasching, J.L. and J.L. Mayers (1973). The collection and analysis of trace elements in atmospheric particulate matter over the North Atlantic Ocean. Paper presented at technical conference on the observation and measurement of atmospheric pollution, Helsinki, 30 July-4 August 1973, pp 3650-3656.
- Duce, R.A., R. Arimoto, B.J. Ray, C.K. Unni and P.J. Harder (1983). Atmospheric Trace Elements at Enewatak Atoll: 1, Concentrations, Sources, and Temporal Variability. *Journal of Geophysical Research*, **88**, 5321-5342.
- Duce, R.A. and N.W. Tindale (1991). Atmospheric Transport of Iron and its Deposition in the Ocean, *Limnology and Oceanography*, **36(8)**, 1715-1726.
- Duce, R.A., Unni, C.K., Ray, B.J., Prospero, J.M., and Merrill, J.T. (1980) Long-range transport of soil dust from Asia to the tropical north Pacific: temporal variability, *Science*, **209**, 1522-1524.
- Dulac, F., Buat-Menard, P., Arnold, M., Ezat, U., and Martin, D. (1987). Atmospheric Input of Trace Metals to the Western Mediterranean Sea: 1. Factors Controlling the Variability of Atmospheric Concentrations, *J. Geophys. Res.*, **92**, 8437-8453.
- Dzubay, T.G. and R.K. Stevens (1984). *Environ. Sci. Technol.*, **9**, 663.
- Eder, B.K. and R.L. Dennis. (1990). On the use of scavenging ratios for the influence of surface-level concentrations and subsequent dry deposition of Ca, Mg, Na and K. *Wat. Air Soil Pollut.*, **52**, 197-216.
- Ediger, R.D., Peterson, G.E. and Kerber, J.D. (1974). *At. Absorpt. Newsl.*, **13**, 61-80.
- Eliassen, A. (1984). Aspects of Lagrangian Air Pollution Modelling. In: Air Pollution Modeling and its Application, III, edited by C. De Wispelaere, Plenum, New York. Fisher, 1983.
- Fisher, B.E.A.. (1983). A Review of the Processes and Models of Long-Range Transport of Air Pollutants, *Atmos. Environ.*, **10**, 1865-1880.
- Fitzgerald, W.F. (1986). Cycling of mercury between the atmosphere and oceans. In *The Role of Air-Sea Exchange in Geochemical Cycling* (P. Buat-Menard, Ed.), D. Reidel.
- Friedlander, S.K.. (1973). Chemical Element Balances and Identification of Air Pollution Sources. *Environ. Sci. Technol.*, **7(3)**, 235-340.

Galloway, J.N. and Likens G.E. (1981). Acid Precipitation: The Importance of Nitric Acid. *Atmospheric Environment*, **15**, 1081-1085.

Galloway, J.N., Savoie, P.L., Keene, W.C., Prospero, J.M. (1993). The Temporal and Spatial Variability of Scavenging Ratios for Sulfate, Nitrate, Methanesulfonate and Sodium in the Atmosphere over the North Atlantic Ocean. *Atmospheric Environment*, **27A**, 2, 235-250.

Ganor, E., H.A., Foner, S., Brenner, E., Neeman and N. Lavi (1991). The Chemical Composition of Aerosols Settling in Israel Following Dust Storms. *Atmospheric Environment*, **25A**, 2665-2670.

Ganor, E. (1991). The Composition of Clay Minerals Transported to Israel as Indicators of Saharan Dust Emission, *Atmospheric Environment*, **25A**, No:12, 2657,2664.

Ganor, E., and Mamane, Y. (1982). Transport of Saharan Dust Across the Eastern Mediterranean, *Atmos. Environ.*, **15**, 57-64.

GESAMP (1990). The Atmospheric Input of Trace Species to the World Ocean. *GESAMP Report and Studies*, No. 38, WMO, Geneva.

GESAMP (Joint Group of Experts on the Scientific Aspects of Marine Pollution) (1985). Atmospheric Transport of Contaminants into Mediterranean Region. *Reports and Studies*, No.26, 53.

Gillion, R.J. and Helsel, D.R. (1986). *Water Resour. Res.*, **22**, 135-155.

Glaccum, R.A. and Prospero, J.M. (1980). Saharan Aerosols over the Tropical North Atlantic Mineralogy, *Mar.Geol.*, **37**, 295-321.

Glavas, S. (1988). A Wet-only Precipitation Study in a Mediterranean Site, Patras, Greece. *Atmospheric Environment*, **22**, 7,1505-1507.

Gleit, A. (1986). *Environ. Sci. Technol.*, **19**, 1201-1206.

Goldberg, E.D. (1963). The Ocean as a Chemical System, in the Sea, Edited by M.N. Hill, Vol. 2, Ch.1, Interscience: New York.

Gomes, L. and Bergametti, G. (1990). Submicron Desert Dusts: A Sandblasting Process. *J. of Geophys. Res.* **95(D9)**, 13927-13935.

Gordon, G.E. (1980). Receptor Models. *Environ. Sci. Technol.* **14**, 972.

Guerzoni, S., Correggiari, A., Misomicchi, S. (1989). Wind-blown Particles from Ships and Land-based Stations in the Mediterranean Sea: A Review of Trace Metal Studies. In: *Water Pollution Reports*, **13**, Martin, J.M. and Barth, H., ed. Commission of the European Communities, 377-384.

Guieu, C., Thomas, A.J., Martin, J.M., Brun-Cotton, J.C. (1991). Multielemental Characterization of the Atmospheric Input to the Gulf of Lions.

Hacısalihoğlu, G., Eliyakut, F., Olmez, I., Balkas, T.I. and Tuncel, G. (1993). Chemical Composition of Particles in the Black Sea Atmosphere. *Atmospheric Environment*, **26A(17)**, 3207-3218.

Hacısalihoğlu, G. (1989). M.Sc. Thesis, Middle East Technical University, Env. Eng. Dept., Ankara, Turkey.

- Harrison, R.M. and Pio, C.A. (1983). An Investigation of the Atmospheric $\text{HNO}_3\text{-NH}_3\text{-NH}_4\text{-NO}_3$ Equilibrium Relationship in a Cool Humid Climate. *Tellus*, **35B**, 155-159.
- Hastie, D.R., Schiff, H.L., Whelpdale, D.M., Peterson, R.E., Zoller, W.H., Anderson, D.L. (1988). Nitrogen and Sulfur over the Western Atlantic Ocean. *Atmos. Environ.*, **22**, 2381-2391.
- Heffter, J.L. (1983) Branching Atmospheric Trajectory (BAT) Model, NOAA Technical Memorandum NRL ARL-121.
- Heidam, N.Z. (1981). On the origin of the Arctic aerosol-a statistical approach. *Atmos. Environ.*, **15**, 1421-1427.
- Heidam, N.Z. (1985). Crustal enrichments in the Arctic aerosol. *Atmos. Environ.*, **19**, 2083-2097.
- Heintzenberg, J., Strom, J., Ogren, J.A. (1991). Vertical Profiles of Aerosol Properties in the Summer Troposphere of Central Europe, Scandinavia and Svalbard Region, *Atmos. Environ.*, **25A**, No.3/4, 621-627.
- Helsel, D.R. (1990). Less than obvious. *Environ. Sci. Technol.* **24**, 1766-1774.
- Henry, R.C., Lewis, C.W., Hopke, P.K. and Williamson, H.J. (1984) Review of receptor model fundamentals. *Atmos. Environ.*, **18**, 1507-1515.
- Hopke, P.K., Gladney, E.S., Gordon, G.E., Zoller, W.H. and Jones, A.G. (1976). The Use of Multivariate Analysis to Identify Sources of Selected Elements in the Boston Urban Aerosol. *Atmospheric Environment*, **10**, 1015-1025.
- Hopke, P.K., Lamb, R.E. and Natusch, D.F.S. (1980) Multielemental characterization of urban roadway dust. *Environ. Sci. Technol.*, **14**, 164-172.
- Hopke, P.K. (1985). Receptor Modelling in Environmental Chemistry, 155-197, John Wiley, New York.
- Husain, L., P.P, Parekh, J.A, Halstead, V.A. Dutkiewicz (1982) Sources of aerosol sulfate and trace elements of Whiteface Mountain, New York. presented at the 75 th Annual Meeting of the Air Pollution Control Association, New Orleans, LA.
- Jaarezo, J.L. and Colin, J.L. (1988). Rain-Aerosol Coupling in Urban Area: Scavenging Ratio Measurement and Identification of Some Transfer Processes. *Atmos. Environ.*, **22**, 929-935.
- Jaffrezo, J.L., Colin, J.L., Gros, J.M. (1990). Some Physical Factors Influencing Scavenging Ratios. *Atmos. Environ.*, **24A**, 3073-3083.
- Joseph, J.H., and Manes, A. (1971) Secular and Seasonal Variation of Atmospheric Turbidity over Jerusalem, *J. appl. Met.*, **10**, 453-462.
- Junge, C.E. (1963). Air Chemistry and Radioactivity, Academic Press, New York.
- Kao, A.S. and Friedlander, S.K. (1995). Frequency Distributions of PM_{10} Chemical Components and Their Sources. *Environ. Sci. Technol.*, **29**, 19-28.
- Katsoulis, B.D., and Whelpdale, D.M. (1990). Atmospheric Sulfur and Nitrogen Budgets for Southeast Europe. *Atmos. Environ.*, **24A**, No. 12, 2959-2970.
- KotraP.J., Finnegan, D.L., Zoller, W.H. (1983). El Chichon: Composition of Plume Gases and Particles. *Science, Wash.*, **222**, 1018-1021.

Kowalczyk, G.ssS., Gordon, G.E., Rheingrover, S.W. (1982). Identification of Atmospheric Particulate Sources in Washington D.C. Using Chemical Element Balances. *Environ. Sci. Technol.*, **16**, 79.

Kubilay, N. and A.C. Saydam (1995). Trace Elements in Atmospheric Particulates over the Eastern Mediterranean; Concentrations, Sources, and Temporal Variability. *Atmospheric Environment*, **29**, 2289-2300.

Kubilay, N. The Composition of Atmospheric Aerosol over the Eastern Mediterranean: The coupling of Geochemical and Meteorological Parameters, Ph.D. Dissertation, METU Institute of Marine Sciences, Erdemli, 1996.

Lavi, N., Ganor, E., Neeman, E., Bremer, S. (1992). Determination of Elemental Composition of Settling Particles in Israel Following Saharan Dust Storms by Neutron Activation Analysis. *J. Radio & Nuclear Chemistry*, **163**, 313-323.

Levin, Z and Lindberg, J.N. (1979). Size Distribution, Chemical Composition, and Optical Properties of Urban Aerosols in Israel. *J. Geophys. Res.*, **84**, 6941-6950.

Levin, Z., Joseph, J.H., Mekler, Y. (1980). Properties of Saharan (Khamsin) Dust Composition of Optical and Direct Sampling Data. *J. Atmos. Sci.*, **37**, 882-891.

Levin, Z., Price, C., Ganor, E. (1990). The Contribution of Sulphate and Desert Aerosol to the Acidification of Cloud and Rain in Israel. *Atmos. Environ.*, **24A**, 1143-1151.

Lindahl, P.C., Voight, K.C., Bishop, A.M., Lafon, G.M. and Huang, W.L. (1984). Determination of Aluminum in Hydrothermal Reaction Fluids by Graphite Furnace Atomic Absorption Spectrometry. *Atomic Spectroscopy*, **5(4)**, 137-141.

Losno, R., G. Bergametti, P. Carlier and G. Mouvier (1991). Major Ions in Marine Rainwater with Attention to Sources of Alkaline and Acidic Species. *Atmospheric Environment*, **25A**, 763-770.

Lowenthal, D.H., Rahn, K.A. (1987). Comments on use of Whatman 41 Filter Papers in Particle Sampling, *Atmos. Environ.*, **21**, 2732-2734.

Loye-Pilot, M.D. and J. Morelli (1988). Fluctuations of Ionic Compositions of Precipitations Collected in Corsica Related to Changes in the Origins of Incoming Aerosols. *J. Aerosol Sci.*, **19**, 577-585.

Loye-Pilot, M.D., Cauwet, G., Spitzky, A., and Martin, J.M. (1991). Preliminary Results on Atmospheric Wet Deposition of Organic Carbon and Nitrogen in Corsica, in: *Water Pollution Reports*, **28.**, J.M. Martin and H. Barth, editors, 519-532.

Loye-Pilot, M.D., Martin, J.M., Morelli, J. (1986). Influence of Saharan Dust on the Rain Acidity and Atmospheric input to the Mediterranean, *Nature*, **321**, 427-428.

Maenhaut, W., Cornilla, P., Pacyna, J.M., Vitols, V. (1989). Trace Element Composition and Origins of the Atmospheric Aerosols in the Norwegian Arctic. *Atmos. Environ.*, **23**, 2551-2569.

Maenhaut, W., Zoller, W.H., Duce, R.A., Hoffman, G.L. (1979). *J. Geophys. Res.*, **84**, 2421-2431.

Malm, W.C., Johnson, C.E. and Bresch J.F. (1986). Application of Principal Component Analysis for Purposes of Identifying Source-Receptor Relationships. In Receptor Methods for Source Apportionment (Edited by T.G. Pace), Publication TR-5. Air Pollution Control Association, Pittsburgh, PA.

- Mamane, Y., U. Dayan and J.M. Miller (1987). Contribution of Alkaline and Acidic Sources to Precipitation in Israel. *The Science of the Total Environment*, **61**, 15-22.
- Mamane, Y., Ganor, E., and Donagi, A.E. (1980) Aerosol composition of urban and desert origin in the Eastern Mediterranean. I: Individual particle analysis, *Wat. Air Soil Pollut.* **14**, 29-43.
- Martin, J.L., Elbaz-Poulichet, F., Guieu, C., Loye-Pilot, M.D., and Han, G. (1989). River Versus Atmospheric Input of Material to the Mediterranean Sea: an overview, *Mar. Chem.*, **28**, 159-182.
- Migon, C. and Caccia, J.L. (1990). Separation of Anthropogenic And Natural Emissions of Particulate Heavy Metals in the Western Mediterranean Atmosphere. *Atmos. Environ.*, **24A**, 399-405.
- Migon, C. and Caccia, J.L. (1993). Separation of Anthropogenic And Natural Heavy Metals in the North Western Mediterranean Rainwater and Total Atmospheric Deposition. *Chemosphere*, **27,12**, 2389-2396.
- Migon, C., Alleman, L., Leblond, L., Nicolas, E. (1993). Evolution of Atmospheric Lead over the Northwestern Mediterranean between 1986 and 1992. *Atm. Env.*, **27**, 2161-2167.
- Migon, C., Copin-Montégut, G., Elégant, L., and Morelli, J. (1989). Etude de l'apport atmosphérique en sels nutritifs au milieu cotier méditerranéen at implications biogéochimiques, *Oceanologica Acta*, **12**, 187-191.
- Miller, M.S., Friedlander, S.K., Hidy, G.M. (1972). A Chemical Element Balance for the Pasadena Aerosol. *J. Colloid Interface Sci.*, **39**, 165-176.
- Miller, J.M. (1981a). A Five-Year Climatology of Five-Day Back Trajectories from Barrow, Alaska, *Atmos. Environ.*, **15**, 1401-1405.
- Miller, J.M. (1981b). A Five-Year Climatology of Five-Day Back Trajectories from Mauna Loa Observatory, Hawaii, *Atmos. Environ.*, **15**, 1553-1558.
- Miller, J.M., and Harris, J. (1985). The Flow Climatology to Bermuda and its Implications for Long-Range Transport, *Atmos. Environ.*, **19**, 409-414.
- Miller, J.M., Martin, D., and Strauss, B. (1987). A Comparison of Results from Two Trajectory Models Used to Produce Flow Climatologies to the Western Mediterranean, NOAA Tech. Memo. ERL ARL-151, Air Resources Laboratory, Silver Spring, MD, 11 pp.
- Morales, C., (Ed.) (1979). Saharan Dust: Mobilization, Transport, Deposition (SCOPE 14) 297 pp., John Wiley, New York.
- Morandi, M.T., Liou, P.J., Daisey, J.M. (1991). Comparison of two multivariate modeling approaches for the source apportionment of inhalable particulate matter in Newark, NJ, *Atmos. Environ.*, **25A**, 927-937.
- Mosher, B.W., and Duce, R.A. (1983). *J. Geophys. Res.*, **88**, 6761-6766.
- Mosher, B.W. and Duce, R.A.. (1988). Global Atmospheric Selenium Budget, *J. Geophys. Res.*, **92**, 13289-13298.
- Migon, C., Morelli, J., Nicolas, E. and Copin-Montegut, G. (1991). Evaluation of Total Atmospheric Deposition of Pb, Cd, Cu and Zn to the Ligurian Sea. *Sci. Total Envir.*, **105**, 135-148.

- Neustadler, H.E., Sidek, S.M., King, R.B., Fordyce, J.S., Barr, J.C. (1975). The Use of Whatman-41 Filters for High Volume Air Sampling, *Atmos. Environ.*, **9**, 101-109.
- Newman, M.C., Dixon, P.M., Looney, B.B., Pinder J.E. (1989). *Water Resour. Bull.*, **25**, 905-915.
- Nodop, K. (1986). Nitrate and Sulphate Wet Deposition in Europe, in G. Angeletti and G. Restelli (Eds), *Physico-Chemical Behavior of Atmospheric Pollutants*, Reidel D., Dordrecht, 520-528.
- Nriagu J.O. and Pacyna J.M. (1988). Quantative assesement of worldwide contamination of air, water a soils by trace metals, *Nature*, **333**, 134-139.
- Nriagu, J.O. (1989). A Global Assessment of Natural Sources of Atmospheric Trace Metals, *Nature*, **338**, 47-49.
- Olmez I. and Gordon G.E. (1985). Rare earths: atmospheric signatures for oil fired power plants and refineries, *Science*, **229**, 966-968.
- Olmez I. (1989) Instrumental neutron activation analysis of atmospheric particulate matter in *Methods of Air Sampling and Analysis* (Edited by Lodge J.P.Jr.) 3rd Ed, 143-150.
- Ondov, J.M., Dodd, J.A.. and Tuncel, G. (1990). Nuclear Analysis of Trace Elements in Size-Classified Submicrometer Aerosol Particles from a Rural Airshed. *Aerosol Science and Technology*, **13**, 249-263.
- Ondov, J.M. and W.R. Kelly (1991). Tracing Aerosol Pollutants with Rare Earth Isotopes. *Analytical Chemistry*, **63**, **13**, 691-697.
- Ott, W.R. (1990). A Physical Explanation of the Lognormality of Pollutant Concentrations, *J. Air Waste Manage. Assoc.*, **40**, 1378-1383.
- Pacyna, J.M.(1986). Emission factors of atmospheric elements, in *Toxic Metals in the Atmosphere* (ed. by Nriagu, J.O. and Davidson, C.I.), pp. 1-32, Wiley, New York.
- Pacyna, J.M., Semb, A., and Hanssen, J.E. (1984). Emissions and Long-Range Transport of Trace Elements in Europe. *Tellus*, **36B**, 163-178.
- Parekh,P.P. and Husain L. (1988). Selective leaching of atmospheric aerosols: resolution of limestone and cement, *Atmosp. Environ.*, **22**, 1267-1274.
- Parrington,J.R.,Zoller,W.H.,Aras,N.K. (1983). Asian Dust: Seasonal transport to Hawaian Islands, *Science*, **220**, 195-197.
- Pio, C.A., Salgueiro, M.L.. and Nunes, T. (1991). Seasonal and Air-Aass Trajectory Effects on Rainwater Quality at the South-Western European Border. *Atmospheric Environment*, **25A(10)**, 2259-2266.
- Prodi,F. and Fea,G. (1979). A case of transport and deposition of Saharan dust over the Italian Peninsula and Southern Europe, *J. Geophys. Res.*, **84C**, 6951-6960.
- Prospero,J. and R.B. Nees (1987). Deposition Rate of Particulate and Dissolved Aluminum Derived from Saharan Dust in Precipitation at Miami, Florida. *Journal of Geophysical Research*, **92(D12)**, 14723-14731.
- Prospero, J.M. (1981). Eolian Transport to the World Ocean. In: *The Oceanic Lithosphere*, **7**, The Sea, edited by C. Emiliani, 801-874, John Wiley, New York.

- Prospero, J.M. and Carlson, T.N. (1970) Radon-222 in the North Atlantic Trade Winds: Its Relationship to Dust Transport from Africa, *Science*, **167**, 974-977.
- Prospero, J.M., Charlson, R.J., Mohnen, V., Jaenicke, R., Delany, A.C., Moyers, J., Zoller, W., and Rahn, K. (1983) The Atmospheric Aerosol System: An overview, *Rev. Geophys.* **21**, 1607-1629.
- Quetel, C.R., Remoudaki, E., Davies, J.E., Miquel, J.C., Fowler, S.W., Lambert, C.E., Bergametti, G., Buat-Menard, P. (1993). Impact of Atmospheric Deposition on Particulate Iron Flux and Distribution in Northwestern Mediterranean waters, *Deep-Sea Research*, **40**, 989-1002.
- Radlein, N. and Heumann, K.G. (1992). Trace analysis of heavy metals in aerosols over the Atlantic Ocean from Antarctica to Europe, *Intern. J. Environ. Anal. Chem.*, **46**, 127-150.
- Rahn, K.A. and Lowenthal, D.H. (1984). Elemental Tracers of Distant Regional Pollution Aerosols. *Science*, **223**, 132-139.
- Rahn, K.A. and Lowenthal, D.H. (1985). Pollution aerosols in the Northeast: northeastern and midwestern contributions, *Science*, **228**, 275-284.
- Rahn, K.A., and McCaffrey, R.J. (1979). Proc. WMO symp. on the long range transport of pollutants, Sofia, Bulgaria.
- Rahn, K.A., Lowenthal, D.H., Lewis, N.F. (1982). Elemental tracers and source areas of pollution aerosols in Narragansett, R.I. technical Report, University of Rhode Island, Narragansett, R.I.
- Rahn, K.A., Borys, R.D., Shaw, G.E., Schütz, L. and Jaenicke R. (1979) Long Range Impact of Desert Aerosol on Atmospheric Chemistry: Two Examples. In: Saharan Dust: Mobilization, Transport, Deposition Scope 14. C. Morales, Ed.: 243-266. Wiley and Sons, Chichester, UK.
- Rahn, K.A., Lewis, N.F., Lowenthal, D.H., Smith, D.L. (1983). Noril'sk, only a minor contributor to Arctic haze, *Nature*, **306**, 459-461.
- Remoudaki, E., Bergametti, G., and Losno, R. (1991). On the Dynamic of the Atmospheric Input of Copper and Manganese into the Western Mediterranean Sea, *Atmos. Environ.*, **25A**, 733-744.
- Robinson, E., Bodhaine, B.A., Komhyr, W.D., Oltmans, S.J., Steele, L.P., Tons, P., Thompson, T.M. (1988). Long term air quality monitoring at the South Pole by the NOAA Program Geophysical Monitoring for Climatic Change, *Rev. Geophys.*, **26**, 63-80.
- Ross, H.B. (1985). An Atmospheric Selenium Budget for the Region 30°N to 90°N. *Tellus*, **37B**, 78-90.
- Savoie, D.L. and Prospero, J.M. (1982). Particle size distribution of nitrate and sulphate in the marine atmosphere, *Geophys. Res. Lett.*, **9**, 1207-1210.
- Savoie, D.L., Prospero, J.M., Nees, R.T. (1987). Washout ratios of nitrate, non-sea-salt sulfate and seasalt on Virginia Key, Florida and on American Samoa, *Atm. Environ.*, **21**, 103-112.
- Savoie, D.L. and Prospero, J.M. (1977) Aerosol Concentration Statistics for the Northern Tropical Atlantic. *J. Geophys. Res.*, **82**, 5954-5964.
- Savoie, D.L., Prospero, J.M. (1980). Water Soluble Potassium, Calcium, and Magnesium in the Aerosols Over the Tropical North Atlantic. *J. Geophys. Res.*, **85**, 385-392.

Schutz, L.W., P. Buat-Menard, R. A.C. Carvalho, A. Cruzado, J.M. Prospero, R. Harris, N.Z. Heidam, R. Jaenicke (1990). The Long-Range Transport of Mineral Aerosols: Group Report. In: The Long-Range Atmospheric Transport of Natural and Contaminant Substances, A.H. Knap (ed.), Kluwer Academic Publishers, Netherlands, 197-229.

Scott, B.C. (1981). Sulfate washout ratios in winter storms, *J. Appl. Met.*, **20**, 619-625.

Shaw, G.E. (1980). Transplant of Asian desert aerosol to the Hawaiian Islands, *J. Appl. Met.*, **19**, 1254-1259.

Simo, R., Colom-Altes, M., Grimalt, J.O., and Albaiges, J. (1991). Background Levels of Atmospheric Hydrocarbons, Sulfate and Nitrate Over the Western Mediterranean. *Atmos. Environ.*, **25A**, 1463-1471.

Small, H., Stevens, T.S., Bowman, W.C. (1975). Novel ion exchange chromatographic method using conductimetric detection. *Analytical Chemistry*, **47**, 1801-1809.

Statgraphics Manual, 1992

Sterns, C.R. and Wendler, G. (1988). Research results from Antarctic Automatic Weather Station, *Rev. Geophys.*, **26**, 45-61.

Stohl, A. and Wotawa, G. (1995). A method for computing single trajectories representing boundary layer transport. Submitted to *Atmos. Environ.*

Sturgeon, R.E., Berman, S.S., Desaulniers, A. and Russell, D.S. (1979). *Anal. Chem.*, **51**, 2364.

Talbot R.W., Harriss, R.C., Browell, E.V., Gregory, G.L., Sebacher, D.I., and Beck, S.M. (1986). Distribution and Geochemistry of Aerosols in the Tropical North Atlantic Troposphere: Relationship to Saharan Dust. *J. Geophys. Res.*, **91**, 5173-5182.

Taylor, R. (1972) Abundance of Chemical Elements in the Continental Crust: A New Table *Geochim. Cosmochim. Acta*, **28**, 1273.

Thurston, G.D. and Spengler, J.D. (1981). An assessment of fine particulate sources and their interaction with meteorological influences via factor analysis. Presented at the 74th Annual Meeting of the Air Pollution Control Association, San Francisco, CA.

Thurston, G.D. and Spengler, J.D. (1985). A quantitative assessment of source contributions to inhalable particulate matter pollution in Metropolitan Boston. *Atm. Env.*, **19**, 1, 9-25.

Tolun, N. and A.N. Pamir (1975). Explanatory Text of the Geological Map of Turkey, Hatay sheet. Publ. Min. Res. and Explor. Inst. Publ., Ankara, 99 p. & appendices.

Tomadin, L., Lenaz, R., Landuzzi, V., Mazzucotelli, A., and Vannucci, R. (1984). Wind-Blown Dusts Over the Central Mediterranean. *Oceanologica Acta*, **7**, 13-23.

Tschiersch, J., Hietel, B., Schramel, P., Trautner, F. (1990). Saharan dust at Jungfraujoch. *J. Aerosol. Sci.*, **21**, 357-360.

Tsunogai, S. and Kondo, T. (1972). Sporadic transport and deposition of continental aerosols to the Pacific Ocean. *J. Geophys. Res.*, **77**, 8870-8874.

Tuncel, S.G., Olmez, I., Parrington, J.R., Gordon, G.E. and Stevens, R.K. (1985). Composition of Fine Particle Regional Sulfate Component in Shenandoah Valley. *Envir. Sci. Technol.*, **19**, 529-537.

Tuncel, G., Aras, N.K. and Zoller, W.H. (1989). Temporal Variations and Sources of Elements in the South Pole Atmosphere: 1. Nonenriched and Moderately Enriched Elements. *J. of Geophysical Res.*, **94(D10)**, 13025-13038.

Turner, S.M., Malin, G., Liss, P.S., Harbour, D.S., Holligan, T.M. (1985). The seasonal variation of dimethylsulfide and dimethylsulfoniopropionate concentrations in nearshore waters. *Limnol. Oceanogr.*, **32**, 364-375.

Uematsu, M., Duce, R.A., Prospero, J.M. (1985). Deposition of atmospheric mineral particles in the North Pacific Ocean. *J. Atmos. Chem.*, **3**, 123-128.

Uematsu, M., Duce, R.A., Prospero, J.M., Chen L., Merrill, J.T. and McDonald, R.L. (1983) Transport of Mineral Aerosol from Asia over the North Pacific Ocean, *J. Geophys. Res.* **88**, 5343-5352.

United Nations Environment Program, World Meteorological Organization (UNEP,WMO) (1989). Meteorological and Climatological Data From Surface and Upper Air Measurements for the Assessment of Atmospheric Transport and Deposition of Pollutants in the Mediterranean Basin: A review. *MAP Technical Reports Series No.30*, Athens, UNEP, 137.

United Nations Environment Program, World Meteorological Organization (UNEP,WMO) (1994). Assessment of Airborne Pollution of the Mediterranean Sea by Sulphur and Nitrogen Compounds and Heavy Metals in 1991. *MAP Technical Reports Series No.85*, Athens, UNEP, 304.

von Mises, R. (1964). Mathematical Theory of Probability and Statistics, Chapter 1(C) and 1(E). Academic Press, New York.

Vossler, T.L., Lewis, C.W., Stevens, R.K., Gordon, G.E., Tuncel, S.G., Russwurm, G.W. and Kleber, G.J. (1989). Composition and Origin of Summertime Air Pollutions at Deep Creek Lake, Maryland. *Atmospheric Environment*, **23**, 1535-1547.

Wall, S.M., W. John, and J.L. Ondo (1988). Measurement of Aerosol Size Distributions for Nitrate and Major Ionic Species. *Atmospheric Environment*, **22**, 8, 1649-1656.

Wallace, G.T. and Duce, R.A. (1975). Concentration of particulate trace matters and particulate organic carbon in marine surface waters by a bubble floatation mechanism. *Mar. Chem.*, **3**, 157-181.

Wang, C., Bunday, S.D., Tartar, J.G. (1983). Ion chromatographic determination of fluoride, chlorine, bromine and iodide with sequential electrochemical and conductometric detection. *Analyt. Chem.*, **55**, 1617-1619.

Watson, J.G. (1979). Chemical element balance receptor model methodology for assessing the sources of fine and total suspended particulate matter in Portland, Oregon. Ph.D. Dissertation, Oregon Graduate Center, Beaverton, Oregon.

Watson, J.G., and Chow, J.C. (1994). Clear Sky Visibility as a Challenge for Society, *Annu. Rev. Energy. Environ.*, **19**, 241-266.

Weisel, C.P., Duce, R.A., Fosching, J.L., Heaton, R.W. (1984). Estimates of the transport of trace metals from the ocean to the atmosphere. *J. Geophys. Res.*, **89**, 11607-11618.

Wolff, G.T. (1987). Characteristics and consequences of soot in the atmosphere. *Envir. Int.*, **11**, 259-269.

Wolff, G.T., Church, T.M., Galloway, J.N., Knap, A.H. (1987). An examination of SO_x, NO_x and trace metal washout ratios over the Western Atlantic Ocean. *Atmos. Environ.*, **21**, 2623-2628.

Yaalon, D.H. and E. Ganor (1973). The Influence of Dust on Soils During the Quaternary. *Soil Science*, **116(3)**, 146-155.

Yaalon, D.H. and E. Ganor (1979). East Mediterranean Trajectories of Dust-Carrying Storms from the Sahara and Sinai. In: Saharan Dust, Chapter 9, (Ed by C.Morales), John Wiley and Sons, New York, 187-183.

Zeng, Y. and Hopke, P.K. (1989). A study of the sources of acid precipitation in Ontario, Canada. *Atmos. Environ.*, **23**, 1499-1509.

Zoller, W.H. and Gordon, G.E. (1970): Instrumental neutron activation analysis of atmospheric pollutants utilizing Ge(Li) detectors. *Anal.Chem.*, **42**, 257-265.

Zoller, W.H., Gladney, E.S., Duce, R.A.. (1974). Atmospheric Concentrations and Sources of Trace Metals at the South Pole., *Science*, **183**, 198-200.



VITA

Gülen Güllü was born in Ankara, on July 21, 1965. She received her B.S. in Environmental Engineering in 1987, at the Middle east Technical University. Since then, she has been a reserch assistant in the Environmental Engineering Department of the METU. She received her M.S. degree in 1989 in Environmental Engineering Department of METU. Her main areas of interest are environmental chemistry and air pollution .

